frontiers | Research Topics

In vitro transcription (IVT) reaction – the gateway to new therapeutic modalities

Edited by
Rok Sekirnik, Andreas Kuhn, Ana Margarida Azevedo and Zoltán Kis

Published in
Frontiers in Molecular Biosciences

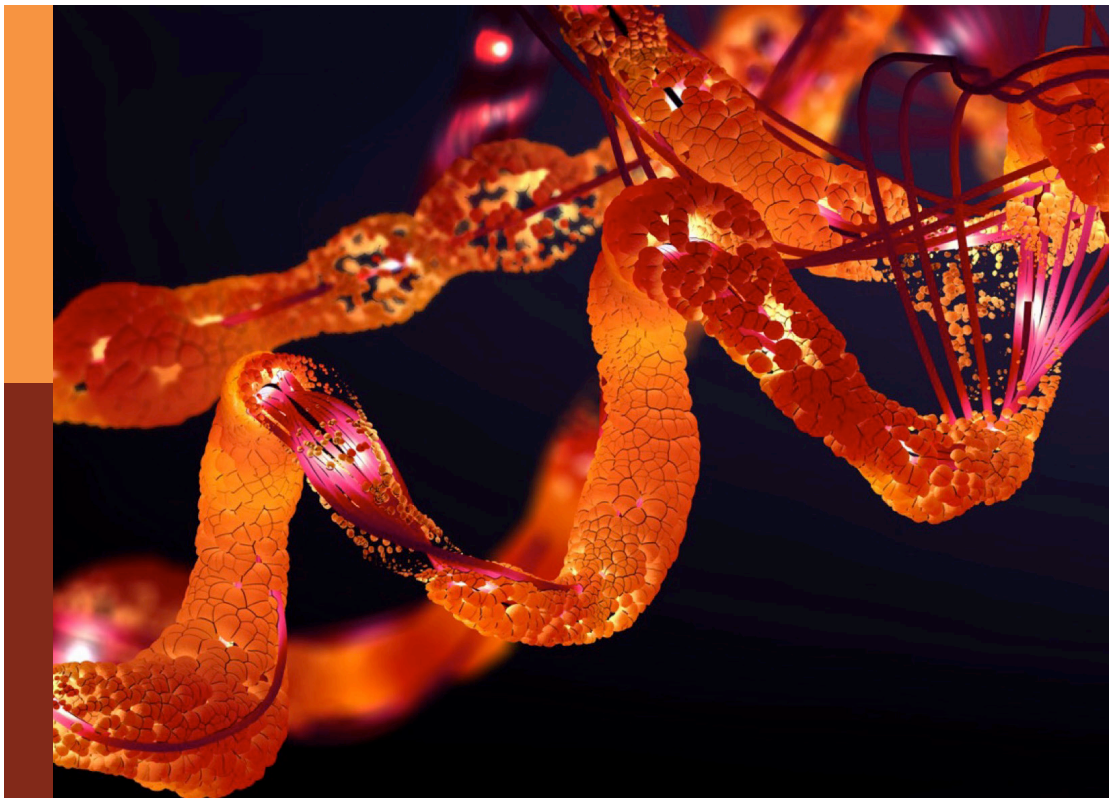

ISSN 1664-8714
ISBN 978-2-8325-7208-5
DOI 10.3389/978-2-8325-7208-5

Generative AI statement
Any alternative text (Alt text) provided alongside figures in the articles in this ebook has been generated by Frontiers with the support of artificial intelligence and reasonable efforts have been made to ensure accuracy, including review by the authors wherever possible. If you identify any issues, please contact us.

About Frontiers

Frontiers is more than just an open access publisher of scholarly articles: it is a pioneering approach to the world of academia, radically improving the way scholarly research is managed. The grand vision of Frontiers is a world where all people have an equal opportunity to seek, share and generate knowledge. Frontiers provides immediate and permanent online open access to all its publications, but this alone is not enough to realize our grand goals.

Frontiers journal series

The Frontiers journal series is a multi-tier and interdisciplinary set of open-access, online journals, promising a paradigm shift from the current review, selection and dissemination processes in academic publishing. All Frontiers journals are driven by researchers for researchers; therefore, they constitute a service to the scholarly community. At the same time, the *Frontiers journal series* operates on a revolutionary invention, the tiered publishing system, initially addressing specific communities of scholars, and gradually climbing up to broader public understanding, thus serving the interests of the lay society, too.

Dedication to quality

Each Frontiers article is a landmark of the highest quality, thanks to genuinely collaborative interactions between authors and review editors, who include some of the world's best academicians. Research must be certified by peers before entering a stream of knowledge that may eventually reach the public - and shape society; therefore, Frontiers only applies the most rigorous and unbiased reviews. Frontiers revolutionizes research publishing by freely delivering the most outstanding research, evaluated with no bias from both the academic and social point of view. By applying the most advanced information technologies, Frontiers is catapulting scholarly publishing into a new generation.

What are Frontiers Research Topics?

Frontiers Research Topics are very popular trademarks of the *Frontiers journals series*: they are collections of at least ten articles, all centered on a particular subject. With their unique mix of varied contributions from Original Research to Review Articles, Frontiers Research Topics unify the most influential researchers, the latest key findings and historical advances in a hot research area.

Find out more on how to host your own Frontiers Research Topic or contribute to one as an author by contacting the Frontiers editorial office: frontiersin.org/about/contact

In vitro transcription (IVT) reaction – the gateway to new therapeutic modalities

Topic editors
Rok Sekirnik — Sartorius, Germany
Andreas Kuhn — BioNTech, Germany
Ana Margarida Azevedo — University of Lisbon, Portugal
Zoltán Kis — The University of Sheffield, United Kingdom

Citation
Sekirnik, R., Kuhn, A., Azevedo, A. M., Kis, Z., eds. (2025). *In vitro transcription (IVT) reaction – the gateway to new therapeutic modalities*. Lausanne: Frontiers Media SA. doi: 10.3389/978-2-8325-7208-5

Dr Sekirnik and Dr Kuhn are employees of Sartorius BIA Separations and BioNTech, respectively. All other editors declare no conflict of interest

Table of contents

frontiers | Frontiers in Molecular Biosciences

TYPE Editorial
PUBLISHED 17 November 2025
DOI 10.3389/fmolb.2025.1730880

OPEN ACCESS

EDITED AND REVIEWED BY
Matteo Becatti,
University of Firenze, Italy

*CORRESPONDENCE
Rok Sekirnik,
rok.sekirnik@biaseparations.com

RECEIVED 23 October 2025
ACCEPTED 24 October 2025
PUBLISHED 17 November 2025

CITATION
Sekirnik R, Kuhn AN, Azevedo AM and Kis Z (2025) Editorial: *In vitro* transcription (IVT) reaction – the gateway to new therapeutic modalities.
Front. Mol. Biosci. 12:1730880.
doi: 10.3389/fmolb.2025.1730880

Editorial: *In vitro* transcription (IVT) reaction – the gateway to new therapeutic modalities

Rok Sekirnik[1]*, Andreas N. Kuhn[2], Ana Margarida Azevedo[3] and Zoltán Kis[4,5]

[1]Sartorius BIA Separations d.o.o., Ajdovščina, Slovenia, [2]BioNTech SE, Mainz, Germany, [3]Instituto Superior Técncio, University of Lisbon, Lisbon, Portugal, [4]School of Chemical, Materials and Biological Engineering, University of Sheffield, Sheffield, United Kingdom, [5]Department of Chemical Engineering, Imperial College London, London, United Kingdom

KEYWORDS

IVT (*in vitro* transcription), mRNA, PAT (process analytical technologies), Quality by Design (QbD), pDNA chromatography

Editorial on the Research Topic
In vitro transcription (IVT) reaction – the gateway to new therapeutic modalities

The so-called *in vitro* transcription (IVT) reaction, the enzymatic process in which a DNA template is converted into RNA using bacteriophage RNA polymerases, has become a defining gateway to a new class of medicines. By enabling the scalable production of synthetic mRNA, IVT laid the foundation for the rise of mRNA vaccines, which received an incredible amount of public and scientific attention due to their role in mitigating the risks of the COVID-19 pandemic. Since then, mRNA technology has entered a renaissance, reflected in the steep increase in clinical trials—rising from fewer than 200 in 2021 to approximately 450 by the summer of 2025—and in the approval of the first non-COVID-19 vaccine (the RSV vaccine). Therapeutic areas have broadened to individualized cancer treatment (neoantigen therapies, Rojas et al., 2023) and gene therapies targeting genetic diseases such as cystic fibrosis (Bai et al., 2024) and sickle cell anemia (Breda et al., 2024).

mRNA manufacturing involves mRNA sequence design, synthesis, and purification for therapeutic applications. The synthesis step is performed through *in vitro* transcription of a linear DNA template, typically a linearized plasmid DNA (pDNA). This process requires the preparation of pure linearized pDNA which, in addition to the promoter required to initiate the transcription reaction, contains key sequence elements required for functional mRNA: 5′ and 3′ untranslated regions (UTRs), a coding region, and a poly(A) tail. Contrary to plasmid DNA, which is generally produced in *E. coli*, the subsequent IVT reaction is carried out in a completely cell-free environment. This reaction minimally requires the above-described DNA template, an RNA polymerase, nucleoside triphosphates (NTPs), and Mg^{2+}. A 5′ cap structure on the mRNA can improve mRNA stability by protecting against exonucleases and being recognized by initiation factors to promote translation. Therefore, a 5′ cap can be added to the mRNA during the *in vitro* transcription either co-transcriptionally ("co-capping") by adding a suitable cap-analogue to be incorporated as the initiating nucleotide building block or post-transcriptionally ("post-capping") using a capping enzyme. Improvements in capping strategies can enhance translation efficiency and mRNA stability. Chemical modifications of the cap structure, e.g., within the triphosphate

linkage, can further improve mRNA stability and enhance ribosome recruitment. The poly(A) tail length also affects both mRNA stability and translation efficiency. Increasing the tail length increases protein expression but, beyond an optimal range, translation efficiency plateaus as additional adenosine residues provide no further benefit. UTRs from various genes, including globin and genes from tobacco etch virus, are often used to enhance translation and stability.

The Research Topic "*In Vitro* Transcription (IVT) Reaction–The Gateway to New Therapeutic Modalities" brings together eight complementary contributions that collectively advance our molecular, analytical, and process-engineering understanding of IVT. These works span topics from enzyme and substrate design to real-time analytics and impurity control, reflecting the maturation of IVT from a bench-top reaction to an industrially relevant, quality-by-design-enabled manufacturing process for diverse RNA modalities, including mRNA, self-amplifying RNA (saRNA), circular RNA (circRNA), and transfer RNA (tRNA) therapeutics.

As editors, we were amazed to observe the progress reported across most of these fronts and beyond. Contributions to the Research Topic include not only the science of mRNA but also studies on DNA as a critical raw material for IVT. For example, the Research Topic published the first report on the impact of DNA template purity on the quality of IVT product (Martinez et al.), which demonstrated that impurities in a linearized DNA template can lead to production of aberrant RNA, including dsRNA, if impurities are recognized as a template by RNA polymerase. The latter received much attention. Nair and Kis examined the phylogenetic and structure-function relationship of T7 RNA polymerase and its engineered mutants designed to reduce immunogenic impurities, linking enzyme activity to the quality attributes of the mRNA product. This Research Topic was further explored by Lenk et al., who provided a comprehensive analysis of product- and process-related contaminants arising from IVT, systematically categorizing nucleotide-based impurities (such as dsRNA, abortive transcripts, and RNA:DNA hybrids) and non-nucleotide contaminants (including RNAse, endotoxins, and metal ions). Their work highlights how these impurities can activate pattern-recognition receptors and underscores the interplay between reaction design, template engineering, and purification strategy in achieving high-purity, clinically efficacious mRNA.

mRNA capping received due attention in this Research Topic, reflecting its tremendous impact on the cost-of-goods for mRNA synthesis. Kurpijewski et al. reported the synthesis of cap analogues modified at the N2 position of 7-methylguanosine and demonstrated their dual application as translation inhibitors and as capping reagents. This work is likely to spur further research into improved capping structures.

To be optimally utilized in IVT reaction, reagents including cap analogues, NTPs, and mRNA can be monitored at-line or in-line. The minireview by Lee et al. explored available analytical approaches for monitoring IVT, including light-up RNA aptamer and fluorescent dye pairs, fluorophore-labelled antisense probes, and HPLC methods. Welbourne et al. further advanced this area by developing an HPLC-based method for at-line monitoring of IVT progression, providing near-real-time information on the concentration of both building blocks (NTPs) and product (mRNA). A related analytical technique was used by Megušar et al. to investigate factors affecting transfer RNA (tRNA) synthesis, a less explored IVT-derived modality, showing that chromatographic monitoring had the potential to increase yields by at least two-fold compared to previous reports.

IVT can be performed either as a batch reaction, where all reagents are added at once, or as a fed-batch reaction, in which selected reagents are added in boluses to minimize concentrations of reagents or co-substrates that could negatively impact the yield or quality of the product or to maximize utilization of the enzyme and template. Ziegenhals et al. reported an innovative use of fed-batch strategy that maintained low steady-state concentrations of GTP and UTP with high capping and low levels of dsRNA by preventing backward transcription at the 3′ end of the DNA template.

Collectively, the contributions in this Research Topic illustrate how the IVT reaction is evolving from a simple laboratory tool into a multi-variable, data-rich biomanufacturing process. Advances in reaction monitoring (Lee et al.; Welbourne et al.; Megušar et al.), impurity mitigation (Martinez et al.; Ziegenhals et al.), enzyme and cap engineering (Nair and Kis; Kurpijewski et al.), and systems-level analysis of by-products (Lenk et al.) collectively chart the course toward predictable, high-yield, low-immunogenic RNA production. The inclusion of tRNA synthesis (Megušar et al.) broadens the scope beyond mRNA to encompass other therapeutic RNAs, foreshadowing a convergent "RNA foundry" landscape where multiple RNA species may be produced on unified IVT platforms.

This Research Topic highlights how interdisciplinary advances in enzymology, chemistry, analytics, and process engineering are transforming IVT into a controllable and automated synthesis platform for next-generation RNA therapeutics. Looking ahead, we expect that continuous innovation will focus on three interrelated frontiers: 1) polymerase engineering for enhanced fidelity, modified-nucleotide tolerance, and compatibility with new RNA architectures such as circular and self-amplifying RNA; 2) real-time digital control and automatization through soft sensors, kinetic modelling, and the use of AI in sequence design; and 3) the establishment of truly continuous mRNA production processes that integrate synthesis, capping, and purification. Together, these advances will further redefine IVT from a laboratory reaction into an enabling technology for scalable, automated, and globally accessible RNA manufacturing, paving the way for the next-generation of RNA therapeutics and decentralized production for rapid vaccine responses.

Author contributions

RS: Writing – review and editing, Writing – original draft, Conceptualization. AK: Writing – original draft, Writing – review and editing, Conceptualization. AA: Conceptualization, Writing – review and editing, Writing – original draft. ZK: Conceptualization, Writing – review and editing, Writing – original draft.

Funding

The author(s) declare that no financial support was received for the research and/or publication of this article.

Conflict of interest

Author RS was employed by Sartorius BIA Separations d.o.o. Author AK was employed by BioNTech SE. Author ZK is a co-founder and advisor at RNA Forge Ltd. (UK company number: 16612680).

The remaining author declares that the research was conducted in the absence of any commercial or financial relationships that could be construed as a potential conflict of interest.

Generative AI statement

The author(s) declare that no Generative AI was used in the creation of this manuscript.

Any alternative text (alt text) provided alongside figures in this article has been generated by Frontiers with the support of artificial intelligence and reasonable efforts have been made to ensure accuracy, including review by the authors wherever possible. If you identify any issues, please contact us.

Publisher's note

References

Bai, X., Chen, Q., Li, F., Teng, Y., Tang, M., Huang, J., et al. (2024). Optimized inhaled LNP formulation for enhanced treatment of idiopathic pulmonary fibrosis via mRNA-mediated antibody therapy. *Nat. Commun.* 15, 6844. doi:10.1038/s41467-024-51056-8

Breda, L., Papp, T. E., Triebwasser, M. P., Yadegari, A., Fedorky, M. T., Tanaka, N., et al. (2023). In vivo hematopoietic stem cell modification by mRNA delivery. *Sci.* 381, 436–443. doi:10.1126/science.ade6967

Rojas, L. A., Sethna, Z., Soares, K. C., Olcese, C., Pang, N., Patterson, E., et al. (2023). Personalized RNA neoantigen vaccines stimulate T cells in pancreatic cancer. *Nature* 618, 144–150. doi:10.1038/s41586-023-06063-y

frontiers | Frontiers in Molecular Biosciences

TYPE Mini Review
PUBLISHED 11 September 2023
DOI 10.3389/fmolb.2023.1229246

OPEN ACCESS

EDITED BY
Rok Sekirnik,
Sartorius, Germany

REVIEWED BY
Yoshihiro Shimizu,
RIKEN, Japan
Zoltán Kis,
The University of Sheffield,
United Kingdom

*CORRESPONDENCE
Kyung Hyun Lee,
khlee@rznomics.com
Seong-Wook Lee,
swl0208@rznomics.com,
swl0208@dankook.ac.kr

RECEIVED 26 May 2023
ACCEPTED 16 August 2023
PUBLISHED 11 September 2023

CITATION
Lee KH, Song J, Kim S, Han SR and Lee S-W (2023), Real-time monitoring strategies for optimization of *in vitro* transcription and quality control of RNA. *Front. Mol. Biosci.* 10:1229246. doi: 10.3389/fmolb.2023.1229246

Real-time monitoring strategies for optimization of *in vitro* transcription and quality control of RNA

Kyung Hyun Lee[1]*, Jaehwi Song[1], Seongcheol Kim[1], Seung Ryul Han[1] and Seong-Wook Lee[1,2]*

[1]R&D Center, Rznomics Inc., Seongnam, Republic of Korea, [2]Department of Bioconvergence Engineering, Research Institute of Advanced Omics, Dankook University, Yongin, Republic of Korea

RNA-based therapeutics and vaccines are opening up new avenues for modern medicine. To produce these useful RNA-based reagents, *in vitro* transcription (IVT) is an important reaction that primarily determines the yield and quality of the product. Therefore, IVT condition should be well optimized to achieve high yield and purity of transcribed RNAs. To this end, real-time monitoring of RNA production during IVT, which allows for fine tuning of the condition, would be required. Currently, light-up RNA aptamer and fluorescent dye pairs are considered as useful strategies to monitor IVT in real time. Fluorophore-labeled antisense probe-based methods can also be used for real-time IVT monitoring. In addition, a high-performance liquid chromatography (HPLC)-based method that can monitor IVT reagent consumption has been developed as a powerful tool to monitor IVT reaction in near real-time. This mini-review briefly introduces some strategies and examples for real-time IVT monitoring and discusses pros and cons of IVT monitoring methods.

KEYWORDS

***in vitro* transcription, IVT, transcription, real-time monitoring, RNA**

Introduction

Since the global COVID-19 pandemic, RNA vaccines have been hailed as new vaccines to quickly respond to infectious diseases (Dolgin, 2021). Furthermore, RNA is now considered as a feasible modality for therapeutic applications as well as vaccine application (Huang et al., 2022). In addition to linear RNA modality, circular RNA (circRNA) (Liu and Chen, 2022) and self-replicating RNA (Dailey et al., 2022) are also considered as promising RNA modalities.

For efficient translation and *in vivo* stability of linear mRNA vaccine as an example, 5′-capping (Ramanathan et al., 2016) and poly(A) tail (Eckmann et al., 2011) are required for linear mRNA. 5′-capping reaction can be accomplished during *in vitro* transcription (IVT) (Contreras et al., 1982) by co-transcriptional capping using dinucleotide such as Anti-Reverse Cap Analog (ARCA) system (Peng et al., 2002) or after IVT through additional enzymatic reaction using an enzyme such as vaccinia capping enzyme and related reagents for cap-0 (Shuman, 1990) and cap 2′-O-methyltransferase for cap-1 and cap-2 structures at the 5′end of the RNA with a cap-0 as substrate (Lockless et al., 1998). Poly(A) tail can be directly transcribed from DNA template or can be added by enzymatic reaction after IVT using poly(A) polymerase such as *E. coli* poly(A) polymerase (Cao and Sarkar, 1992). IVT

reagents such as NTPs and Mg^{2+} are also important for IVT efficiency and product yield (Pregeljc et al., 2023). In addition, modified nucleotides such as m1ψ (*N1*-methylpseudouridine-5′-triphosphate) are required for linear mRNAs to have efficient translation (Svltkin et al., 2017) and avoid unwanted innate immune responses (Mu and Hur, 2021) for *in vivo* applications.

As an example of other RNA modalities, circRNA also can be generated by IVT (Petkovic and Müller, 2015; Lee et al., 2022a) using group I intron ribozyme-based strategy such as permuted intron-exon method (Puttaraju and Been, 1992). In contrast, chemical- or ligase-based circRNA preparation methods require an additional step after precursor RNA preparation by IVT (Lee et al., 2022a). For circRNA in general, 5′-capping is not necessary for translation and poly(A) is optional to improve expression mediated by internal ribosome entry site (IRES) possibly through polyadenylate binding proteins (Wesselhoeft et al., 2018). Interestingly, nucleotide modifications are not compulsory for circRNA to avoid unwanted innate immunity (Wesselhoeft et al., 2018), and this observation needs to be demonstrated by clinical trials in the near future.

Therefore, IVT process would be fundamental for determining the yield and purity of RNA products. To produce large amounts of RNA-based vaccines and therapeutics with high purities, useful IVT monitoring methods are needed to understand molecular mechanisms and to monitor target RNA production, efficacy of the aforementioned enzymatic reactions, and reagent consumption.

Traditionally, oligonucleotides and polynucleotides including RNAs have been routinely analyzed by various analytical techniques such as polyacrylamide gel electrophoresis (PAGE, Loening, 1967), agarose gel electrophoresis (Koontz, 2013), capillary electrophoresis (Wei et al., 2022), and high-performance liquid chromatography (HPLC) (Thayer et al., 1996). However, those methods are neither real-time or near real-time methods for IVT monitoring. They are generally used for endpoint analysis. Real-time IVT monitoring methods would be ideal to better understand the IVT reaction progress and/or to adjust the IVT condition immediately during IVT process. Here, we briefly review reported real-time or near real-time IVT monitoring methods and discuss their strengths and weaknesses.

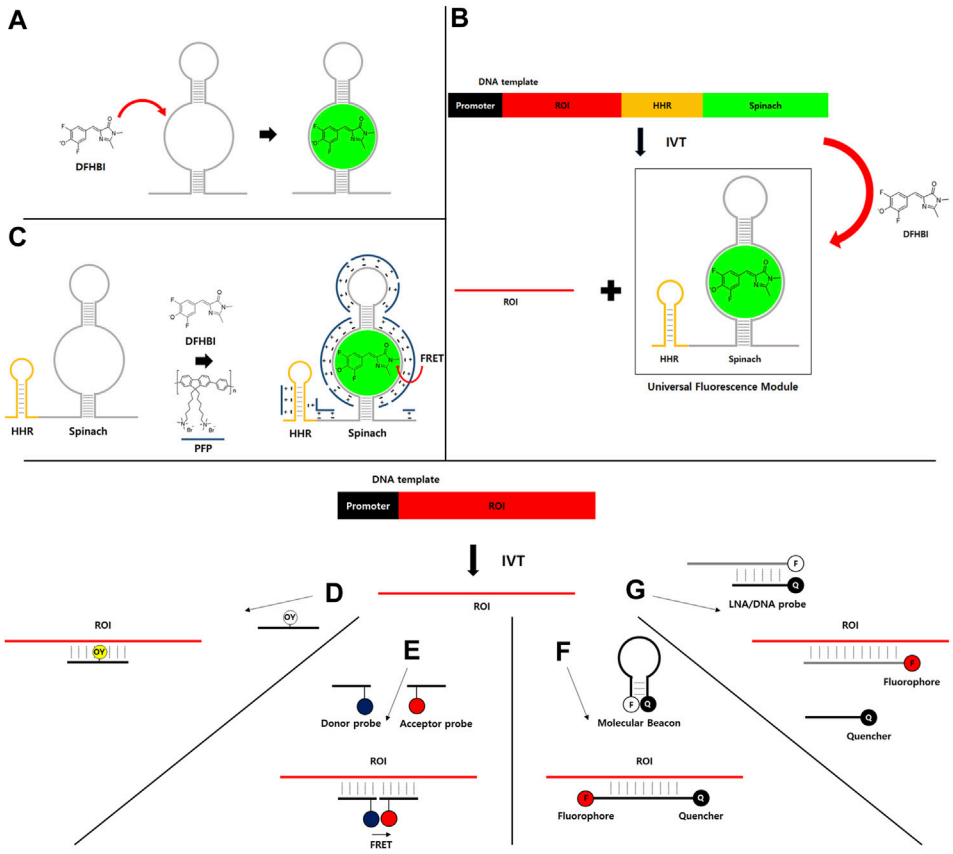

FIGURE 1
(A–C) Light-up RNA aptamer and fluorescence dye pair for real-time IVT monitoring. **(A)** An example of light-up RNA aptamer (Spinach) and fluorescence dye (DFHBI) pair. DFHBI dye is nonfluorescent due to subtle movement. However, its nonfluorescent form can switch to a fluorescent form when it binds to a specific RNA aptamer such as Spinach. **(B)** DNA template containing promoter and a universal fluorescence module (UFM) consisting of a highly active hammerhead ribozyme (HHR) and Spinach RNA aptamer can be used to monitor the synthesis of RNA of interest (ROI) during IVT in the presence of DFHBI dye. **(C)** FRET between water-soluble conjugated polymer (PFP, blue line) that binds to RNA by nonspecific electrostatic interaction as a FRET donor and RNA aptamer/DFHBI complex as a FRET acceptor. **(D–G)** Fluorophore-labeled antisense probe-based strategies for real-time IVT monitoring. **(D)** Fluorophore-labeled antisense probe for fluorescence turn-on. **(E)** FRET-based strategy. **(F)** Molecular beacon-based strategy. **(G)** Strategy using fluorophore-labeled and quencher-labeled probes.

Real-time IVT monitoring strategies using light-up RNA aptamer and fluorescence dye pairs

In nature, there are no green fluorescent protein (GFP)-like RNAs to visualize RNA by tagging. Therefore, RNA aptamers that can bind and turn on nonfluorescent fluorogens have been developed for RNA imaging and/or detection *in vitro* (Babendure et al., 2003), in bacteria (Lee et al., 2010), and in mammalian cells (Paige et al., 2011; Swetha et al., 2020; Figure 1A). Such light-up RNA aptamers can be selected by SELEX (Systematic Evolution of Ligands by EXponential enrichment) method (Ellington and Szostak, 1990; Tuerk and Gold, 1990), which can specifically bind to the target molecule such as light-up fluorophores. Therefore, the selected light-up RNA aptamer that is genetically encodable can be used for tagging of RNA of interest.

Generally, nonfluorescent dye for the light-up aptamer strategy has extremely low quantum yield due to vibrational de-excitation (Oster and Nishijima, 1956). However, RNA aptamer can bind and stabilize the nonfluorescent dye in a more fluorescent conformation by restricting the vibration, resulting in fluorescence light-up (Babendure et al., 2003). Therefore, RNA aptamer can be tagged to RNA of interest (ROI) like GFP tagging strategy. It is then incubated with a light-up fluorescence dye for the detection and/or visualization of ROI similar to the detection of protein of interest by fluorescence intensity of GFP.

Among various light-up aptamer and fluorescence dye pairs developed so far, Spinach (Paige et al., 2011) and related RNA aptamers such as Broccoli (Filonov et al., 2014), Mango (Dolgosheina et al., 2014), Corn (Song et al., 2017), and Pepper (Chen et al., 2019) are being widely used by researchers (Swetha et al., 2020). Some light-up fluorescence dyes such as DFHBI (Paige et al., 2011), DFHBI-1T (Song et al., 2014), and DFHO (Song et al., 2017) are commercially available.

For the application of light-up RNA aptamer strategy, the signal from the real-time IVT monitoring method should be independent from the polymerase, ROI, and other components to accurately monitor the transcription activity. To this end, a simple, robust, and universal method has been developed to analyze the quality and quantity of transcribed RNA during IVT (Höfer et al., 2013). In this strategy, Spinach RNA aptamer and DFHBI dye are used in a high-throughput manner (Figure 1A). A universal fluorescence module (UFM) consisting of a highly active hammerhead ribozyme (HHR) and light-up RNA aptamer is independent of ROI sequences. Thus, UFM can be used as a universal platform for real-time IVT monitoring of any ROI. As HHR is introduced behind the ROI to cleave the RNA aptamer part from the ROI, UFM can be released during IVT. Released RNA aptamer parts and fluorescence dyes can be efficiently purified out by the purification method such as HPLC as the sizes will be generally much smaller than ROI. Therefore, only ROI can be obtained as the final product without extraneous sequences for further applications (Figure 1B). As HHR generates a homogenous 3′end by removing the aptamer portion comprising of heterogenous 3′ends generated by the addition of untemplated nucleotide by T7 polymerase activity (Akoopie and Müller, 2018), poly(A) tailing reaction with the purified IVT RNA would provide a narrower distribution of poly(A) compared to reactions with RNAs comprising of heterogenous 3′ends.

Detection speed with real-time IVT monitoring using light-up aptamer and fluorescent dye pair is at least 100 times faster than conventional polyacrylamide gel electrophoresis (PAGE) method (Valentini et al., 2022), whereas PAGE method shows RNA bands that can provide purity information of RNA transcripts. Although the light-up aptamer-based method cannot provide quality information of IVT, eventually the purity of RNA products can be checked during compulsory HPLC purification process (Karikó et al., 2011) and/or by other endpoint analytical methods for applications in cells and *in vivo*.

If transcribed RNAs will not be used for further applications after real-time IVT monitoring using light-up aptamer and dye pair, in other words, if IVT is only monitored to check transcription activity itself for IVT optimization, introduction of ribozyme domain would be unnecessary (Valentini et al., 2022). For example, effects of IVT components have been investigated using Broccoli aptamer-based (Kartje et al., 2021) or iSpinach aptamer (Autour et al., 2016)-based monitoring of transcription activity in a real-time (STAR) system (Valentini et al., 2022). An approach based on contact quenching of fluorophores linked to quenchers such as dinitroaniline and fluorophore-binding aptamer has also been used for real-time IVT monitoring (Sunbul and Jäschke, 2013). Similarly, the fluorophore-quencher conjugate is not fluorescent owing to contact quenching. It becomes fluorescent upon binding to the tagged RNA aptamer on the target RNA during IVT.

Fluorescence resonance energy transfer (FRET)-based monitoring strategy using UFM and water-soluble conjugated polymer has also been reported (Li et al., 2019; Figure 1C). Briefly, poly (9, 9-bis (6′-N, N, N,-trimethylammonium) hexyl) fluorene-co-alt-1,4-phenylene) bromide (PFP) is used as a FRET donor for DFHBI dye which could bind to RNA aptamer as a FRET acceptor. Strong electrostatic interaction between PFP and RNA aptamer/DFHBI complex allows FRET. The method can amplify fluorescence signals to improve detection sensitivity compared to a UFM strategy with intensity-based fluorescence detection. Therefore, the limit of detection (LOD) is near 10-fold lower (LOD = 0.29 nM) than that of UFM alone (LOD = 2.8 nM) as PFP does not interfere with IVT and the variation of background signal is greatly reduced by FRET measurement.

However, one concern would be fast fluorescence decay by photoconversion after illumination (Han et al., 2013; Lee et al., 2022b) during real-time monitoring which requires continuous illumination of the fluorescence dye. To resolve this issue, unnatural base pair technology has been employed for real-time IVT monitoring (Lee et al., 2022b). In that technology, DFHBI-conjugated unnatural nucleotide is incorporated into specific position in Spinach RNA during IVT for fluorescence light-up, resulting in improved photostability, thermal stability, and ion sensitivity. However, that method can only be used for IVT monitoring and optimization due to incorporated unnatural nucleotide that could be inappropriate for downstream applications, although it is much more robust for IVT monitoring than the conventional method. In addition, it is possible that RNA aptamer with stable hairpin loop structure may slow down or terminate the T7 RNA polymerase activity.

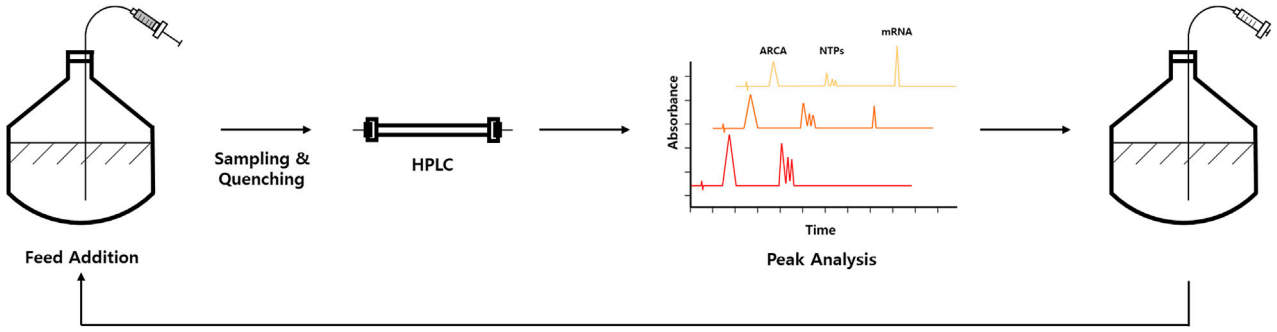

FIGURE 2
Schematic representation of at-line HPLC-based IVT optimization workflow, which allows fed-batch approach. Representative chromatograms are shown in peak analysis part. Elution peaks corresponding to anti-reverse cap analog (ARCA), NTPs, and mRNA are indicated in chromatograms.

Real-time IVT monitoring strategies using fluorophore-labeled antisense probes

Various other strategies have also been employed to monitor IVT in real time. For example, a simple strategy by directly incorporating γ-fluorophore-labeled UTP into RNA during transcription has been used to monitor IVT (Dunkak et al., 1996). However, produced RNAs with dye modification are inappropriate for downstream applications.

Instead of directly incorporating the fluorophore into RNA target, fluorophore-labeled antisense probes such as a fluorescent DNA probe that can enhance fluorescence on hybridizing with a target RNA have been developed for real-time IVT monitoring. For example, oxazole yellow (YO) is normally non-fluorescent (Ishiguro et al., 1996). However, the dye shows enhanced fluorescence by intercalation into double-stranded DNA (dsDNA). YO-linked complementary oligonucleotide can enhance the fluorescence in the presence of target RNA products in IVT reaction (Figure 1D). In addition, fluorescence correlation spectroscopy (FCS) strategy can be used for IVT monitoring using a fluorophore-labeled probe (Nomura and Kinjo, 2004). FCS can sensitively measure fluctuations in fluorescence intensity of the fluorescent molecule in solution, which is dependent on molecular weight and concentration (Maiti et al., 1997). Thus, fluorescence correlation functions were analyzed using a simple two-component model with a fast-moving component of free probe and a slow-moving component of the probe-RNA hybrid as an RNA product.

Two fluorescent DNA probes can be used for FRET-based IVT monitoring (Figure 1E). Two 15-mer DNAs with one labeled with Bodipy493/503 as the FRET donor and the other labeled with Cy5 as the acceptor have been used to generate a FRET signal when hybridized to adjacent sites of the target RNA (Sei-Iida et al., 2000). In this strategy, probes are hybridized to synthesizing RNAs before they are folded to form secondary structures. Thus, there is no need to select efficient binding sites on the target RNA for probes. In another study using Cy3 as FRET donor and Cy5 as acceptor (Niederholtmeyer et al., 2013), mRNA secondary structure and target site location are important parameters for efficient FRET (Niederholtmeyer et al., 2013). In that study, a target site located in the 3′untranslated region (UTR) was sensitive for real-time quantitation of the produced mRNA (LOD = 50 nM) by designing to reduce secondary structure. Recently, a binary fluorescence quencher (BFQ) probe consisting of two single-stranded DNA (ssDNA) probes that were modified by a donor fluorophore and a quencher fluorophore and the PBCV-1 DNA ligase were used for FRET-based real-time quantitative *in vitro* transcription assay (Zhang et al., 2023). The PBCV-1 DNA ligase ligates the two ssDNA probes hybridized to the RNA target at adjacent regions into one single DNA strand to stabilize the FRET signal. Therefore, the amount of fluorescence quenching that is proportional to the produced RNA amounts will be detected during IVT.

A simple molecular beacon (MB) strategy using a DNA probe containing a fluorophore and quencher pair has been applied for real-time IVT monitoring (Liu et al., 2002; Figure 1F). MB probe is structured as target-specific antisense oligonucleotide containing a proximate fluorophore and quencher pair. Upon binding to its target RNA during IVT, the probe undergoes a structural rearrangement, resulting in fluorescence recovery by separating the proximate fluorophore and quencher pair. 2′-*O*-methylribonucleotide backbone can be used for MB probe to increase the specificity by eliminating the background fluorescence that might be generated due to formation of duplex RNA between MB probe and its complementary RNA synthesized nonspecifically by RNA polymerase in a promoter-independent manner (Marras et al., 2004). The MB method is simple and easy by using cheap commercial oligonucleotides synthesis service for preparing fluorophore- and quencher-modified probes. However, if IVT products should be purified, how to separate antisense probes with highly complementary sequences to the target RNA should be considered.

A locked nucleic acid (LNA) (Veedu and Wengel, 2010) probe and quencher oligonucleotide pair has been used for real-time monitoring of transcription in a HeLa-based mammalian cell-free expression system (Wang et al., 2018). In that study, 21 nucleotide-long LNA probe consisting of alternating LNA/DNA monomers with Texas Red at the 5′-end and 10 nucleotide-long LNA/DNA oligonucleotides labeled with Iowa Black RQ as a quencher on the 3′-end complementary to the 5′-end of LNA probe have been designed for a double-stranded LNA probe (Figure 1G). Once the LNA probe binds to the target RNA during transcription, the binding is stabilized, preventing recombining with the quencher

strand and resulting in recovery of fluorescence intensity (LOD = 2 nM).

HPLC-based IVT monitoring strategy

HPLC is a powerful and sensitive analytical method that can monitor various reactions and provide qualitative and quantitative information for various materials including nucleic acids (Thayer et al., 1996). HPLC is also an important purification method for obtaining pure RNA products to eliminate contaminants which can induce unwanted innate immune responses (Karikó et al., 2011).

Recently, at-line HPLC strategy has been reported for IVT monitoring at a specific time point (Pregeljc et al., 2023). In this strategy, IVT sample is quenched for injection for HPLC analysis at a specific time point (Figure 2). Generally, run-time of traditional reverse-phase HPLC methods that can also resolve IVT components such as NTPs is too long (20–30 min). To overcome this issue, Pregeljc et al. have developed a high-throughput HPLC assay for simultaneous quantification of IVT components such as NTPs, plasmid, capping agent, and RNA (Korenč et al., 2021) and applied this method to follow IVT reactions at-line with a minimal lag (Pregeljc et al., 2023).

By using at-line HPLC method, IVT reaction conditions (e.g., Mg^{2+}, plasmid, and NTP concentrations) can be optimized by monitoring NTP consumption and RNA production in near real-time. More interestingly, a fed-batch approach for IVT that can extend time and yields by continuously adding IVT components to the reaction mixture for therapeutically relevant mRNA has been demonstrated (Pregeljc et al., 2023; Figure 2). Quantification of mRNA is also coupled with exonuclease digestion to monitor capping efficiency of the produced mRNA. Briefly, 5′polyphosphatase is used to remove phosphates from 5′-triphosphate of uncapped RNA. In contrast, the capped RNA is resistant to this enzyme. Next, Terminator™ 5′-phosphate-dependent exonuclease was treated to digest 5′-monophosphorylated RNA. Therefore, the capping efficiency can be calculated by comparing with control sample without exonuclease digestion (Chiron and Jais, 2017; Pregeljc et al., 2023).

As for future directions, Pregeljc et al. foresee a coupling of at-line HPLC-based IVT monitoring strategy with multi-parallel automated bioreactor systems, enabling controlled and continuous addition of IVT components such as NTP and Mg^{2+} by monitoring consumption kinetics with control of various parameters. In addition, quantitative information obtained by HPLC-based IVT monitoring could reduce uncertainty in RNA quantification before downstream purification process (Pregeljc et al., 2023).

Spectroscopic methods to improve IVT monitoring strategy

Spectroscopic methods also would be applied to strengthen the real-time IVT monitoring methods in the near future. For examples, raman spectroscopy is likely to be applied for RNA manufacturing also by measuring NTP consumption (Matuszczyk et al., 2023). Circular dichroism (CD) that sensitively probes the chirality of nucleic acids would be useful to analyze nucleotide modifications and functional structure of RNA (Valentini et al., 2022) during IVT and the database is currently available as a public repository (Zhang et al., 2023). Time-resolved infrared spectroscopy would also be an option to analyze RNA folding that affects the function of RNA such as aptamer (Brauns and Dyer, 2005).

Conclusion

In this mini review, we briefly introduced real-time IVT monitoring strategies. Among various strategies briefly explained above, light-up aptamer-based method is widely being used for RNA detection and various applications (Swetha et al., 2020). At-line HPLC-based strategy has been recently reported as a powerful tool for IVT monitoring, which can even monitor IVT reagents' consumption and allow fed-batch approach (Pregeljc et al., 2023). Although this method is near real-time rather than real-time, the strength of the HPLC-based strategy is that all components of the IVT reaction can be monitored, whereas other methods can only monitor the final RNA product. Spectroscopic methods would be also helpful to strengthen the real-time IVT monitoring strategies.

Each method has its own pros and cons for IVT monitoring. Researchers need to wisely choose an appropriate method for their research purposes. Real-time IVT monitoring would be more useful for RNA manufacturing by IVT if fluorescence-based strategies and HPLC-based methods are used complementarily. As research on RNA therapeutic and RNA vaccine is receiving a lot of attention, real-time IVT monitoring methods are expected to be rapidly advanced.

Author contributions

KHL and S-WL conceptualized this mini-review. All authors contributed to the article and approved the submitted version.

Funding

This research was supported by the Bio & Medical Technology Development Program of the National Research Foundation (NRF), funded by the Korean government (MSIT) (No. 2022M3E5F1017657).

Conflict of interest

KHL, JS, SK, and SRH are employee of Rznomics Inc. S-WL is CEO of Rznomics Inc.

Publisher's note

References

Akoopie, A., and Müller, U. F. (2018). Cotranscriptional 3′-end processing of T7 RNA polymerase transcripts by a smaller HDV ribozyme. *J. Mol. Evol.* 86 (7), 425–430. doi:10.1007/s00239-018-9861-9

Autour, A., Westhof, E., and Ryckelynck, M. (2016). iSpinach: a fluorogenic RNA aptamer optimized for *in vitro* applications. *Nucleic Acids Res.* 44 (6), 2491–2500. doi:10.1093/nar/gkw083

Babendure, J. R., Adams, S. R., and Tsien, R. Y. (2003). Aptamers switch on fluorescence of triphenylmethane dyes. *J. Am. Chem. Soc.* 125 (48), 14716–14717. doi:10.1021/ja037994o

Brauns, E. B., and Dyer, R. B. (2005). Time-resolved infrared spectroscopy of RNA folding. *Biophys. J.* 89 (5), 3523–3530. doi:10.1529/biophysj.105.061531

Cao, G. J., and Sarkar, N. (1992). Identification of the gene for an *Escherichia coli* poly(A) polymerase. *Proc. Natl. Acad. Sci. U. S. A.* 89 (21), 10380–10384. doi:10.1073/pnas.89.21.10380

Chen, X., Zhang, D., Su, N., Bao, B., Xie, X., Zuo, F., et al. (2019). Visualizing RNA dynamics in live cells with bright and stable fluorescent RNAs. *Nat. Biotechnol.* 37 (11), 1287–1293. doi:10.1038/s41587-019-0249-1

Chiron, S., and Jais, P. H. (2017). Non-radioactive monitoring assay for capping of messenger RNA. *Trans. Genet. Genom.* 1, 46–49.

Contreras, R., Cheroutre, H., Degrave, W., and Fiers, W. (1982). Simple, efficient *in vitro* synthesis of capped RNA useful for direct expression of cloned eukaryotic genes. *Nucleic Acids Res.* 10 (20), 6353–6362. doi:10.1093/nar/10.20.6353

Dailey, G. P., Crosby, E. J., and Hartman, Z. C. (2022). Cancer vaccine strategies using self-replicating RNA viral platforms. *Cancer Gene Ther.* 30, 794–802. doi:10.1038/s41417-022-00499-6

Dolgin, E. (2021). The tangled history of mRNA vaccines. *Nature* 597 (7876), 318–324. doi:10.1038/d41586-021-02483-w

Dolgosheina, E. V., Jeng, S. C. Y., Panchapakesan, S. S. S., Cojocaru, R., Chen, P. S. K., Wilson, P. D., et al. (2014). RNA mango aptamer-fluorophore: a bright, high-affinity complex for RNA labeling and tracking. *ACS Chem. Biol.* 9 (10), 2412–2420. doi:10.1021/cb500499x

Dunkak, K. S., Otto, M. R., and Beechem, J. M. (1996). Real-time fluorescence assay system for gene transcription: simultaneous observation of protein/DNA binding, localized DNA melting, and mRNA production. *Anal. Biochem.* 243 (2), 234–244. doi:10.1006/abio.1996.0511

Eckmann, C. R., Rammelt, C., and Wahle, E. (2011). Control of poly(A) tail length. *Wiley Interdiscip. Rev. RNA* 2 (3), 348–361. doi:10.1002/wrna.56

Ellington, A. D., and Szostak, J. W. (1990). *In vitro* selection of RNA molecules that bind specific ligands. *Nature* 346 (6287), 818–822. doi:10.1038/346818a0

Filonov, G. S., Moon, J. D., Svensen, N., and Jaffrey, S. R. (2014). Broccoli: rapid selection of an RNA mimic of green fluorescent protein by fluorescence-based selection and directed evolution. *J. Am. Chem. Soc.* 136 (46), 16299–16308. doi:10.1021/ja508478x

Han, K. Y., Leslie, B. J., Fei, J., Zhang, J., and Ha, T. (2013). Understanding the photophysics of the spinach-DFHBI RNA aptamer-fluorogen complex to improve live-cell RNA imaging. *J. Am. Chem. Soc.* 135 (50), 19033–19038. doi:10.1021/ja411060p

Höfer, K., Langejürgen, L. V., and Jäschke, A. (2013). Universal aptamer-based real-time monitoring of enzymatic RNA synthesis. *J. Am. Chem. Soc.* 135 (37), 13692–13694. doi:10.1021/ja407142f

Huang, X., Kong, N., Zhang, X., Cao, Y., Langer, R., and Tao, W. (2022). The landscape of mRNA nanomedicine. *Nat. Med.* 28 (11), 2273–2287. doi:10.1038/s41591-022-02061-1

Ishiguro, T., Saitoh, J., Yawata, H., Otsuka, M., Inoue, T., and Sugiura, Y. (1996). Fluorescence detection of specific sequence of nucleic acids by oxazole yellow-linked oligonucleotides. Homogeneous quantitative monitoring of *in vitro* transcription. *Nucleic Acids Res.* 24 (24), 4992–4997. doi:10.1093/nar/24.24.4992

Karikó, K., Muramatsu, H., Ludwig, J., and Weissman, D. (2011). Generating the optimal mRNA for therapy: HPLC purification eliminates immune activation and improves translation of nucleoside-modified protein-encoding mRNA. *Nucleic Acids Res.* 39 (21), e142. doi:10.1093/nar/gkr695

Kartje, Z. J., Janis, H. I., Mukhopadhyay, S., and Gagnon, K. T. (2021). Revisiting T7 RNA polymerase transcription *in vitro* with the Broccoli RNA aptamer as a simplified real-time fluorescent reporter. *J. Biol. Chem.* 296, 100175. doi:10.1074/jbc.RA120.014553

Koontz, L. (2013). Agarose gel electrophoresis. *Methods Enzymol.* 529, 35–45. doi:10.1016/B978-0-12-418687-3.00004-5

Korenč, M., Mencin, N., Puc, J., Skok, J., Nemec, K. Š., Celjar, A. M., et al. (2021). Chromatographic purification with CIMmultus™ Oligo dT increases mRNA stability. *Cell Gene Ther. Insights* 7 (9), 1207–1216. doi:10.18609/cgti.2021.161

Lee, J., Lee, K. H., Jeon, J., Dragulescu-Andrasi, A., Xiao, F., and Rao, J. (2010). Combining SELEX screening and rational design to develop light-up fluorophore-RNA aptamer pairs for RNA tagging. *ACS Chem. Biol.* 5 (11), 1065–1074. doi:10.1021/cb1001894

Lee, K. H., Kim, S., and Lee, S. W. (2022a). Pros and cons of *in vitro* methods for circular RNA preparation. *Int. J. Mol. Sci.* 23 (21), 13247. doi:10.3390/ijms232113247

Lee, K. H., Kimoto, M., Kawai, G., Okamoto, I., Fin, A., and Hirao, I. (2022b). Dye-conjugated Spinach RNA by genetic alphabet expansion. *Chem. Eur. J.* 28 (16), e202104396. doi:10.1002/chem.202104396

Li, Z., Guo, H., Xu, F., Tang, W., and Duan, X. (2019). Sensitive monitoring of RNA transcription by optical amplification of cationic conjugated polymers. *Talanta* 203, 314–321. doi:10.1016/j.talanta.2019.05.052

Liu, C. X., and Chen, L. L. (2022). Circular RNAs: characterization, cellular roles, and applications. *Cell* 185 (12), 2016–2034. doi:10.1016/j.cell.2022.04.021

Liu, J., Feldman, P., and Chung, T. D. Y. (2002). Real-time monitoring *in vitro* transcription using molecular beacons. *Anal. Biochem.* 300 (1), 40–45. doi:10.1006/abio.2001.5446

Lockless, S. W., Cheng, H. T., Hodel, A. E., Quiocho, F. A., and Gershon, P. D. (1998). Recognition of capped RNA substrates by VP39, the vaccinia virus-encoded mRNA cap-specific 2′-O-methyltransferase. *Biochemistry* 37 (23), 8564–8574. doi:10.1021/bi980178m

Loening, U. E. (1967). The fractionation of high-molecular-weight ribonucleic acid by polyacrylamide-gel electrophoresis. *Biochem. J.* 102 (1), 251–257. doi:10.1042/bj1020251

Maiti, S., Haupts, U., and Webb, W. W. (1997). Fluorescence correlation spectroscopy: diagnostics for sparse molecules. *Proc. Natl. Acad. Sci. U. S. A.* 94 (22), 11753–11757. doi:10.1073/pnas.94.22.11753

Marras, S. A. E., Gold, B., Kramer, F. R., Smith, I., and Tyagi, S. (2004). Real-time measurement of *in vitro* transcription. *Nucleic Acids Res.* 32 (9), e72. doi:10.1093/nar/gnh068

Matuszczyk, J. C., Zijlstra, G., Ede, D., Ghaffari, N., Yuh, J., and Brivio, V. (2023). Raman spectroscopy provides valuable process insights for cell-derived and cellular products. *Curr. Opin. Biotechnol.* 81, 102937. doi:10.1016/j.copbio.2023.102937

Mu, X., and Hur, S. (2021). Immunogenicity of *in vitro*-transcribed RNA. *Acc. Chem. Res.* 54 (21), 4012–4023. doi:10.1021/acs.accounts.1c00521

Niederholtmeyer, H., Xu, L., and Maerkl, S. J. (2013). Real-time mRNA measurement during an *in vitro* transcription and translation reaction using binary probes. *ACS Synth. Biol.* 2 (8), 411–417. doi:10.1021/sb300104f

Nomura, Y., and Kinjo, M. (2004). Real-time monitoring of *in vitro* transcriptional RNA by using fluorescence correlation spectroscopy. *ChemBioChem* 5 (12), 1701–1703. doi:10.1002/cbic.200400046

Oster, G., and Nishijima, Y. (1956). Fluorescence and internal rotation: their dependence on viscosity of the medium[1]. *J. Am. Chem. Soc.* 78 (8), 1581–1584. doi:10.1021/ja01589a021

Paige, J. S., Wu, K., and Jaffrey, S. R. (2011). RNA mimics of green fluorescent protein. *Science* 333 (6042), 642–646. doi:10.1126/science.1207339

Peng, Z. H., Sharma, V., Singleton, S. F., and Gershon, P. D. (2002). Synthesis and application of a chain-terminating dinucleotide mRNA cap analog. *Org. Lett.* 4 (2), 161–164. doi:10.1021/ol0167715

Petkovic, S., and Müller, S. (2015). RNA circularization strategies *in vivo* and *in vitro*. *Nucleic Acids Res.* 43 (4), 2454–2465. doi:10.1093/nar/gkv045

Pregeljc, D., Skok, J., Vodopivec, T., Mencin, N., Krušič, A., Ličen, J., et al. (2023). Increasing yield of *in vitro* transcription reaction with at-line high pressure liquid chromatography monitoring. *Biotechnol. Bioeng.* 120 (3), 737–747. doi:10.1002/bit.28299

Puttaraju, M., and Been, M. D. (1992). Group I permuted intron-exon (PIE) sequences self-splice to produce circular exons. *Nucleic Acids Res.* 20 (20), 5357–5364. doi:10.1093/nar/20.20.5357

Ramanathan, A., Robb, G. B., and Chan, S. H. (2016). mRNA capping: biological functions and applications. *Nucleic Acids Res.* 44 (16), 7511–7526. doi:10.1093/nar/gkw551

Sei-lida, Y., Koshimoto, H., Kondo, S., and Tsuji, A. (2000). Real-time monitoring of *in vitro* transcriptional RNA synthesis using fluorescence resonance energy transfer. *Nucleic Acids Res.* 28 (12), E59. doi:10.1093/nar/28.12.e59

Shuman, S. (1990). Catalytic activity of vaccinia mRNA capping enzyme subunits coexpressed in *Escherichia coli*. *J. Biol. Chem.* 265 (20), 11960–11966. doi:10.1016/S0021-9258(19)38494-7

Song, W., Filonov, G. S., Kim, H., Hirsch, M., Li, X., Moon, J. D., et al. (2017). Imaging RNA polymerase III transcription using a photostable RNA-fluorophore complex. *Nat. Chem. Biol.* 13 (11), 1187–1194. doi:10.1038/nchembio.2477

Song, W., Strack, R. L., Svensen, N., and Jaffrey, S. R. (2014). Plug-and-play fluorophores extend the spectral properties of Spinach. *J. Am. Chem. Soc.* 136 (4), 1198–1201. doi:10.1021/ja410819x

Sunbul, M., and Jäschke, A. (2013). Contact-mediated quenching for RNA imaging in bacteria with a fluorophore-binding aptamer. *Angew. Chem. Int. Ed.* 52 (50), 13401–13404. doi:10.1002/anie.201306622

Svltkin, Y. V., Cheng, Y. M., Chakraborty, T., Presnyak, V., John, M., and Sonenberg, N. (2017). N1-methyl-pseudouridine in mRNA enhances translation through eIF2α-dependent and independent mechanisms by increasing ribosome density. *Nucleic Acids Res.* 45 (10), 6023–6036. doi:10.1093/nar/gkx135

Swetha, P., Fan, Z., Wang, F., and Jiang, J. H. (2020). Genetically encoded light-up RNA aptamers and their applications for imaging and biosensing. *J. Mat. Chem. B* 8 (16), 3382–3392. doi:10.1039/c9tb02668a

Thayer, J. R., McCormick, R. M., and Avdalovic, N. (1996). High-resolution nucleic acid separations by high-performance liquid chromatography. *Methods Enzymol.* 271, 147–174. doi:10.1016/s0076-6879(96)71009-1

Tuerk, C., and Gold, L. (1990). Systematic evolution of ligands by exponential enrichment: RNA ligands to bacteriophage T4 DNA polymerase. *Science* 249 (4968), 505–510. doi:10.1126/science.2200121

Valentini, P., Pierattini, B., Zacco, E., Mangoni, D., Espinoza, S., Webster, N. A., et al. (2022). Towards SINEUP-based therapeutics: design of an *in vitro* synthesized SINEUP RNA. *Mol. Ther. Nucleic Acids* 27, 1092–1102. doi:10.1016/j.omtn.2022.01.021

Veedu, R. N., and Wengel, J. (2010). Locked nucleic acids: promising nucleic acid analogs for therapeutic applications. *Chem. Biodivers.* 7 (3), 536–542. doi:10.1002/cbdv.200900343

Wang, S., Majumder, S., Emery, N. J., and Liu, A. P. (2018). Simultaneous monitoring of transcription and translation in mammalian cell-free expression in bulk and in cell-sized droplets. *Synth. Biol.* 3 (1), ysy005. doi:10.1093/synbio/ysy005

Wei, B., Goyon, A., and Zhang, K. (2022). Analysis of therapeutic nucleic acids by capillary electrophoresis. *J. Pharm. Biomed. Anal.* 219, 114928. doi:10.1016/j.jpba.2022.114928

Wesselhoeft, R. A., Kowalski, P. S., and Anderson, D. G. (2018). Engineering circular RNA for potent and stable translation in eukaryotic cells. *Nat. Commun.* 9, 2629. doi:10.1038/s41467-018-05096-6

Zhang, F., Wang, Y., Wang, X., Dong, H., Chen, M., Du, N., et al. (2023). RT-IVT method allows multiplex real-time quantification of *in vitro* transcriptional mRNA production. *Commun. Biol.* 6 (1), 453. doi:10.1038/s42003-023-04830-1

frontiers | Frontiers in Molecular Biosciences

TYPE Original Research
PUBLISHED 29 September 2023
DOI 10.3389/fmolb.2023.1248511

OPEN ACCESS

EDITED BY
Ana Margarida Azevedo,
University of Lisbon, Portugal

REVIEWED BY
Ana Rita Santos,
University of Lisbon, Portugal
Urh Cernigoj,
BIA Separations, Slovenia

*CORRESPONDENCE
Diego Casabona,
dcasabona@certest.es

RECEIVED 27 June 2023
ACCEPTED 19 September 2023
PUBLISHED 29 September 2023

CITATION
Martínez J, Lampaya V, Larraga A, Magallón H and Casabona D (2023), Purification of linearized template plasmid DNA decreases double-stranded RNA formation during IVT reaction. *Front. Mol. Biosci.* 10:1248511. doi: 10.3389/fmolb.2023.1248511

Purification of linearized template plasmid DNA decreases double-stranded RNA formation during IVT reaction

Juan Martínez, Verónica Lampaya, Ana Larraga, Héctor Magallón and Diego Casabona*

RNA Synthesis and Development Department, Certest Pharma, Certest Biotec, Zaragoza, Spain

After the COVID-19 pandemic, messenger RNA (mRNA) has revolutionized traditional vaccine manufacturing. With the increasing number of RNA-based therapeutics, valuable new scientific insights into these molecules have emerged. One fascinating area of study is the formation of double-stranded RNA (dsRNA) during *in vitro* transcription (IVT) which is considered a significant impurity, as it has been identified as a major trigger in the cellular immune response pathway. Therefore, there is a growing importance placed to develop and optimize purification processes for the removal of this by-product. Traditionally, efforts have primarily focused on mRNA purification after IVT through chromatographic separations, with anion exchange and reverse phase chromatography emerging as effective tools for this purpose. However, to the best of our knowledge, the influence and significance of the quality of the linearized plasmid have not been thoroughly investigated. Plasmids production involves the growth of bacterial cultures, bacterial harvesting and lysis, and multiple filtration steps for plasmid DNA purification. The inherent complexity of these molecules, along with the multitude of purification steps involved in their processing, including the subsequent linearization and the less-developed purification techniques for linearized plasmids, often result in inconsistent batches with limited control over by-products such as dsRNA. This study aims to demonstrate how the purification process employed for linearized plasmids can impact the formation of dsRNA. Several techniques for the purification of linearized plasmids based on both, resin filtration and chromatographic separations, have been studied. As a result of that, we have optimized a chromatographic method for purifying linearized plasmids using monolithic columns with C4 chemistry (butyl chains located in the surface of the particles), which has proven successful for mRNAs of various sizes. This chromatographic separation facilitates the generation of homogeneous linearized plasmids, leading to mRNA batches with lower levels of dsRNA during subsequent IVT processes. This finding reveals that dsRNA formation is influenced not only by RNA polymerase and IVT conditions but also by the quality of the linearized template. The results suggest that plasmid impurities may contribute to the production of dsRNA by providing additional templates that can be transcribed into sequences that anneal with the mRNA molecules. This highlights the importance of considering the quality of plasmid purification in relation to dsRNA generation during transcription. Further investigation is needed to fully understand the mechanisms and implications of plasmid-derived dsRNA. This discovery could shift the focus in mRNA vaccine

production, placing more emphasis on the purification of linearized plasmids and potentially saving, in some instances, a purification step for mRNA following IVT.

KEYWORDS

dsRNA, chromatography, polishing, IVT, immunogenicity, vaccines, mRNA

1 Introduction

In recent years, mRNA-based therapies have emerged as highly promising tools in combating infectious diseases, correcting malfunctioning genes, and offering new approaches to tackle pathogens and tumors. The SARS-CoV-2 pandemic has served as a catalyst, propelling advancements in this technology and necessitating the development of production techniques with stringent timelines to address a global health crisis. (Schlake et al., 2012; Kis et al., 2020; Whitley et al., 2020; Ouranidis et al., 2021; Park et al., 2021; Sousa et al., 2021; Verbeke et al., 2021).

Due to the urgent need for mRNA production, IVT processes were developed at a rapid pace, often surpassing the understanding of the molecule itself and the by-products that arise during the transcription process. The transcription of DNA templates into mRNA is facilitated by phage RNA polymerases, such as T7 RNA polymerase (T7 RNAP), which exhibit high fidelity in RNA synthesis. However, the biological process is not entirely efficient, resulting in the generation of certain by-products, albeit at a low frequency. Common non-target molecules include abortive sequences, short transcripts, and dsRNA. (Mu and Hur, 2021).

From the above described, dsRNA moieties have special interest due to inherent immunogenicity that is not desirable in mRNA therapeutic applications. The innate cellular response to dsRNA byproducts, recognized by receptors like TLR3, can adversely affect mRNA therapy efficacy. TLR3 activation by dsRNA involves multiple steps, including dimerization and activation upon dsRNA recognition. This recruits cytoplasmic adapter TRIF, initiating downstream signaling with adaptors like TRAF3 and RIP1. This leads to intracellular signaling events, activating transcription factors IRF3 and NF-κB, which promote immune gene transcription. Additionally, a Src-mediated, adapter-independent TLR3 branch influences cellular properties. In summary, TLR3 activation by dsRNA initiates a complex cascade involving TRIF and transcription factors, inducing immune genes. Src's adapter-independent branch modulates cellular properties beyond gene induction (Mu and Hur, 2021).

Origin of this double stranded molecule is being studied and is not very well stablished yet. Most of the authors described a great dependence of the T7 RNAP enzyme. It has been described during the initiation of transcription; 5- to 11-nt-long RNA by-products are generated as the enzyme aborts the synthesis with a certain probability (Milligan et al., 1987; Dousis et al., 2022).

Several mechanisms have been described to explain the different pathways that lead to these kinds of molecules. One of them, explains that RNA transcript that has been synthesized by the T7 RNAP serves as a template for the RNA-dependent RNA polymerase activity of the T7 RNAP in subsequent rounds of transcription (Roy and Wu, 2019). If the 3′-end of the runoff transcript has sufficient complementarity (in cis), it will fold back and result in extension of the runoff transcript (Figure 1A). Another explanation claims that T7 RNAP might use the resulting RNA molecule as template to synthesize the complementary strand in a promoter-independent manner (Figure 1B) (Triana-Alonso et al., 1995; Gholamalipour et al., 2018). Another mechanism considers that T7 RNAP also has subjacent RNA-dependent as well as template-independent RNA polymerase activity (Konarska and Sharp, 1989; Krupp, 1989; Cazenave and Uhlenbeck, 1994; Triana-Alonso et al., 1995; Biebricher and Luce, 1996; Arnaud-Barbe, 1998; Nacheva and Berzal-Herranz, 2003; Gholamalipour et al., 2018). Indeed, the short abortive RNA fragments and the 3'-end of the full-length RNA can prime complementary RNA synthesis from the primary transcripts that leads to the generation of dsRNA contaminant (Figure 1C). However, it is crucial to acknowledge that dsRNA is not a precisely defined individual molecule, but rather a diverse population of molecules with varying sizes and annealing levels.

The permissible thresholds of dsRNA content exhibit variability contingent upon the designated application, whether within investigative, preclinical, or clinical contexts. Furthermore, these thresholds are inherently contingent upon the inherent characteristics of the mRNA in question. Presently, regulatory entities are diligently engaged in the endeavor to attain a harmonious consensus regarding the precise delineation of specifications governing mRNA vaccines. In accordance with prevailing conventions, it is widely acknowledged that dsRNA content should ideally remain below 0.5% for applications within clinical settings. However, the attainment of such modest dsRNA levels may prove to be a formidable undertaking through mere refinement of IVT conditions. As such, the implementation of supplementary purification protocols invariably becomes imperative to surmount this challenge effectively.

The presence of dsRNA impurities, which share similar physicochemical properties with single-stranded RNA (ssRNA) molecules, poses challenges in their removal during purification processes. Conventional purification methods such as lithium chloride precipitation, size exclusion chromatography, affinity chromatography, or diafiltration are not effective in eliminating dsRNA moieties. Anion exchange chromatography has emerged as good option for dsRNA removal in mRNA polishing (Levanova and Poranen, 2018; Baiersdörfer et al., 2019; Romanovskaya et al., 2013). However, scaling up these chromatographic purifications for industrial production is problematic. Recently, cellulose-based matrix purification methods have been proposed as suitable and simple approaches for dsRNA removal, irrespective of length and nucleoside composition (Baiersdörfer et al., 2019). Another strategy focuses on optimizing the transcription reaction conditions to minimize the production of dsRNA contaminants during IVT instead of relying solely on additional purification steps. Parameters such as reducing

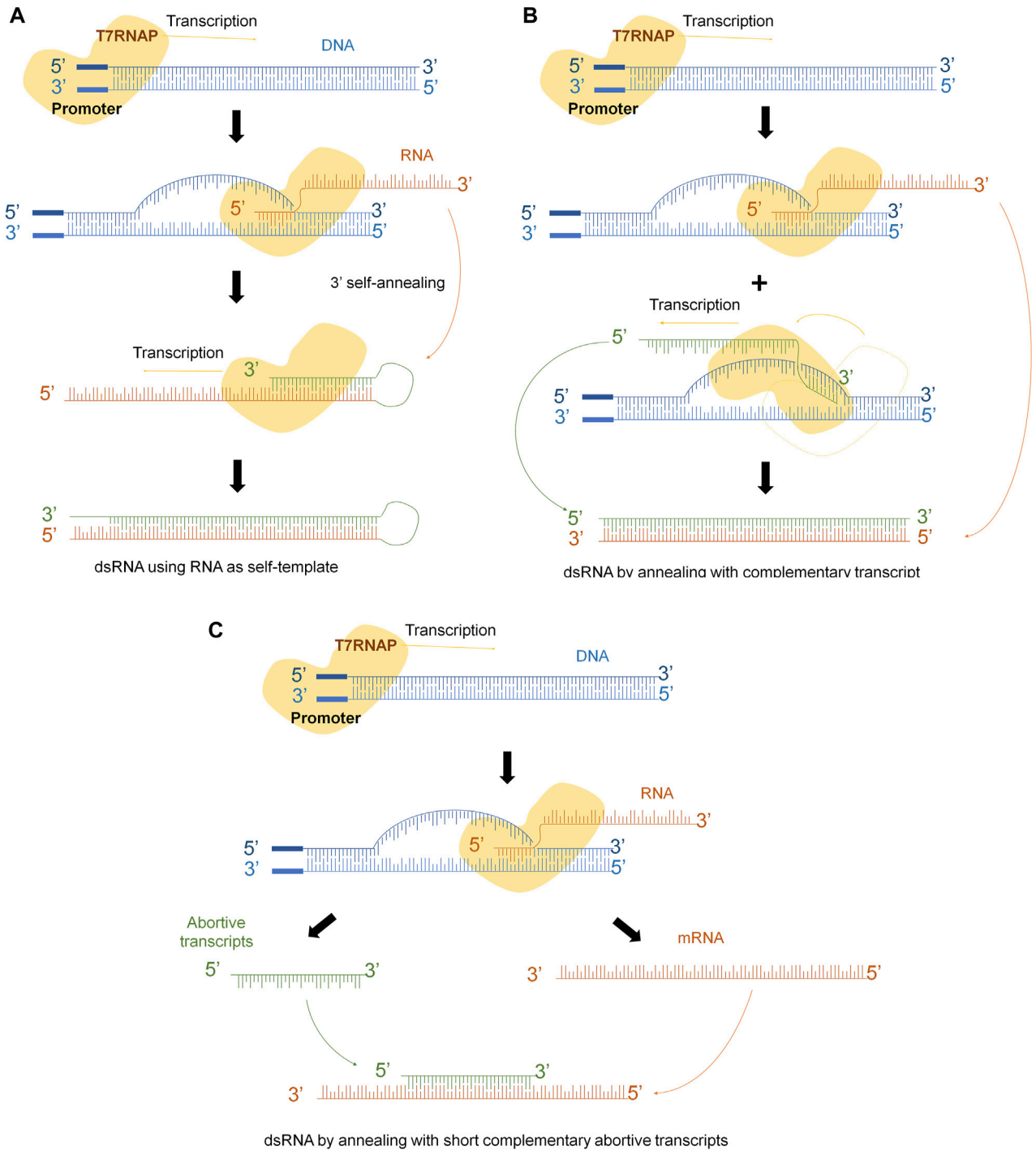

FIGURE 1
dsRNA generation mechanisms during IVT. **(A)** Template strand of DNA is transcribed into mRNA, 3'-extreme loops due to complementarity and T7RNAP uses mRNA as template to continue transcription. **(B)** Polymerase might switch to the non-template strand and generate the complementary strand of the original mRNA. **(C)** Abortive fragments during IVT with complementary sequences anneals with the run-off transcript.

Mg2+ concentration (below 10 mM), using modified nucleosides, employing thermally stable T7 RNAP or mutated T7 RNAP, sequence optimization with depletion of U-rich sequences, or RNAse III treatment have been explored to address this issue (Wu et al., 2020; Cavac et al., 2021). It is important to note that the DNA template used in IVT also plays a crucial role, and the generation of dsRNA by-products could be influenced by the quality of the linearized DNA template in addition to the transcription enzyme.

In this study, we have successfully produced a wide range of constructs encompassing different sizes and scales. Additionally, we have thoroughly investigated various reaction conditions and

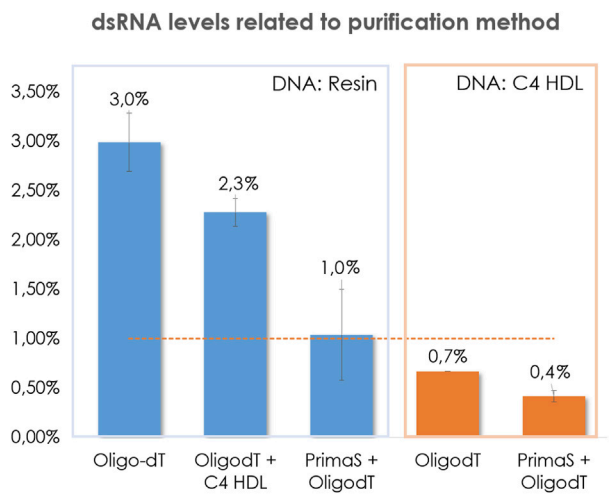

FIGURE 2
Comparison of the influence of the template purification method in the content of dsRNA in COVID transcripts. Pointed line represents threshold 1%.

purification methodologies. Commercially available plasmids are manufactured to meet specific customer requirements, and therefore, it is advisable to assess their compliance with specifications and determine the isoform status before commencing work with a new plasmid. The quality of plasmids directly impacts the quality of the resulting linearized template following the digestion step. Throughout our development process, we have observed significant heterogeneity in linearized plasmids, which appears to be dependent on the specific plasmid used. Interestingly, we have discovered a noteworthy correlation between the quality of linearized plasmids and the production of dsRNA. To the best of our knowledge, this study represents the first evidence linking plasmid quality to dsRNA generation during IVT.

2 Results

One of the primary objectives of optimization is to obtain RNA constructs of exceptionally high quality, with a specific focus on reducing levels of dsRNA. Initially, our efforts were directed towards the purification and refinement of mRNA, as many RNA producers and researchers have done in recent years.(Dickman and Hornby, 2006; Jacoby, 2006; Mccarthy and Gilar, 2008; Karikó et al., 2011; Weissman et al., 2013; Azarani and Hecker, 2021).

Various purification methodologies were combined for both linearized templates and mRNA to determine the optimal combination that would result in the lowest levels of dsRNA. Additionally, considering that dsRNA generation may be influenced by the length of the RNA, we investigated the impact of different construct sizes encoding three different proteins: Green Fluorescence Protein (GFP, 1,000 NTPs long aprox.), Firefly Luciferase (FLuc, 2000 NTPs long aprox.), and the Spike protein for SARS-CoV-2 (COV, 4,000 NTPs long aprox.). To minimize variables in the study and due to therapeutic mRNAs commonly contains modified nucleosides, we chose to employ N1-Me-ψUTP as the modified UTP for the production of all mRNA in this study (Knezevic et al., 2021; Kim et al., 2022).

At the first stage, our purification efforts were focused on mRNA that encoded COVID spike protein. After plasmid linearization, IVT crudes were purified by affinity chromatography (Oligo-dT) and levels of dsRNA were measured. It was founded that dsRNA contents were always above 2% and that most of them were higher than 3% (Figure 2). These impurity contents are unacceptable for therapy application, so it was mandatory to set up an additional step of polishing to reduce these amounts.

On this regard, it was deemed interesting to compare dsRNA levels when an additional specific dsRNA removing polishing step was added after the DNA resin purification. Typically, tandem affinity (capture step) and anion exchange chromatography (polishing step) is very well known and accepted as a good path to obtain mRNA constructs with low levels of dsRNA and high purity (Gagnon, 2020). It is important to point out, that separation of dsRNA in AEX is usually performed by pH gradient, from 7.2 to 11. It is widely recognized that basic pH enhances RNA degradation by means of internal nucleophilic attack of 2' hydroxyl to the nearest electrophilic phosphorus breaking the phosphodiester bond (Chatterjee et al., 2022; Fang et al., 2022). For this reason, the prompt neutralization of the collected fractions becomes crucially important. However, despite these efforts, a certain degree of degradation was observed. In an attempt to mitigate this degradation during our research, it was discovered that by reversing the order of these steps, improvements in purity were achieved as a result of reduced degradation. (Figure 3).

In order to prevent the loss of integrity, the decision was made to reverse the order of the purification process, starting with anion exchange chromatography (AEX) followed by affinity chromatography. Another commonly employed polishing strategy involves incorporating hydrophobic interaction chromatography (HIC) after affinity purification. Consequently, two additional polishing methods were employed: anion exchange chromatography using either the CIMmultus® PrimaS® 1 mL Monolithic Column (2 µm) or the CIMmultus® C4HLD - 1 mL (2 µm). Both methods have been recognized for their effectiveness in removing dsRNA (Dickman and Hornby, 2006; Jacoby, 2006; Mccarthy and Gilar, 2008; Karikó et al., 2011; Weissman et al., 2013; Gagnon, 2020; Azarani and Hecker, 2021) (Urbas, 2015) (Mccarthy and Gilar, 2008; Podgornik et al., 2013; Lee and Barton, 2015; Separations, 2020).

By implementing the purification and polishing steps as mentioned earlier, we were able to reduce degradation in the final isolated constructs (Figure 2). As anticipated, the additional AEX step resulted in lower levels of dsRNA, with some cases falling below the 1% threshold, thus confirming its efficacy in removing such impurities. However, it was quite surprising to find that HIC was not as effective as AEX in reducing dsRNA levels.

2.1 Influence of purification of linear plasmids in dsRNA content

At this juncture, it is pertinent to recall that the prevailing methodologies employed for dsRNA removal primarily focus on the

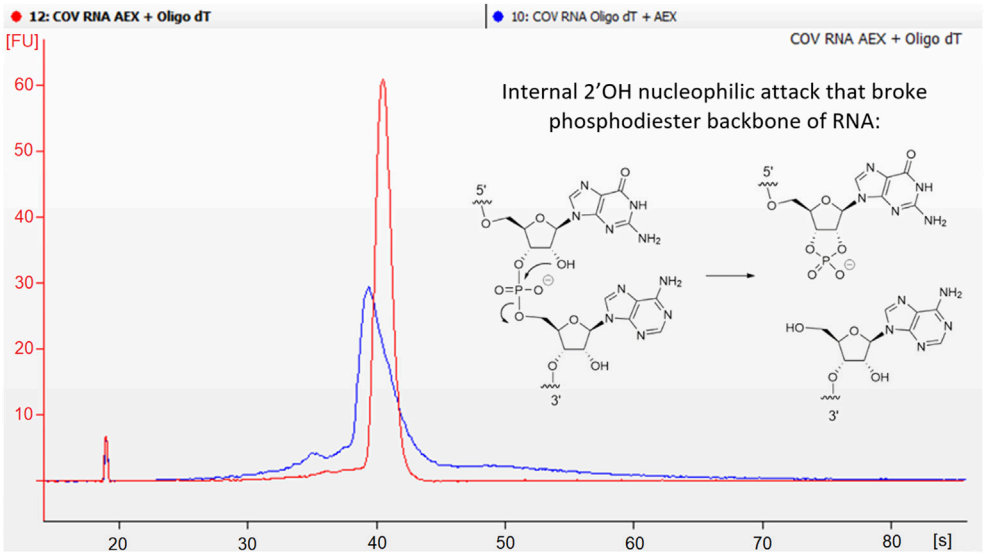

FIGURE 3
Degradation of mRNA is influenced by the type of purification method employed. Electropherogram comparison between tandem Oligo-dT + AEX (blue line) vs. AEX + Oligo-dT (red line). Blue line shows more degraded profiles. Mechanism of intramolecular hydrolysis of RNA phosphodiester bond.

purification and polishing of mRNA post IVT, often overlooking the significance of purifying the initial linearized plasmid. However, we emphasize the importance of obtaining linear templates with high purity and quality, as they directly impact the levels of dsRNA. In order to investigate this, several batches of linear plasmids were isolated using a resin filtration method employing silica resin (Wizard® Megapreps DNA Purification Resin, Promega, Cat#A7361) or by hydrophobic chromatography (CIMmultus® C4HLD—1 mL (2 µm), Sartorius, Cat# 311.8136-2). Then IVT was carried out and the resulting crudes were purified and polished in some cases by Affinity (Oligo-dT) and AEX.

Surprisingly, the linearized plasmids isolated through chromatographic purification exhibited dsRNA levels below the 1% threshold. As anticipated, the subsequent polishing steps further reduced the presence of dsRNA. However, the tandem Oligo-dT/C4 HIC method was not as effective as the Prima S Oligo-dT method in removing double-stranded impurities, as demonstrated in Figure 2. These findings highlight the significant impact of template purification, which appears to have more influence than previously acknowledged.

These results suggest that based on a good purification method of the starting linearized plasmids, such as hydrophobic chromatography, it is possible to obtain mRNA transcripts that does not require any further polishing step to obtain less percentage of dsRNA.

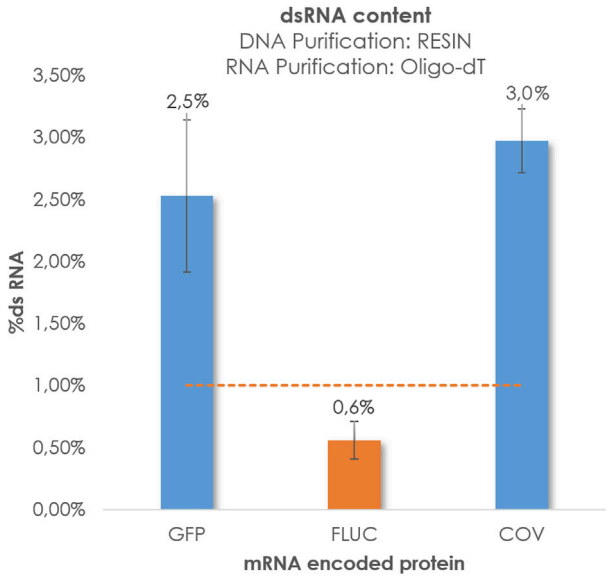

FIGURE 4
%dsRNA obtained for GFP, Fluc and COV. Linearized DNA was isolated by Wizard® Megapreps DNA Purification Resin, Promega, Cat#A7361 and RNA crudes were purified by POROS™ Oligo (dT) 25 Affinity column. Pointed line represents threshold 1%.

3 Discussion

The primary objective of this study was to optimize our internal purification methods in order to reduce the presence of dsRNA and enhance the quality of the mRNA. As mentioned previously, significant efforts were dedicated to the polishing step following IVT. Until now, the generation of dsRNA has been largely attributed to the transcription process itself, with a substantial reliance on the polymerase enzyme. (Konarska and Sharp, 1989; Krupp, 1989; Cazenave and Uhlenbeck, 1994; Triana-Alonso et al., 1995; Biebricher and Luce, 1996; Arnaud-Barbe, 1998; Nacheva and Berzal-Herranz, 2003; Gholamalipour et al., 2018). According to this theory, it is suggested that pre-IVT processes, such as plasmid linearization, do not have an impact on dsRNA levels

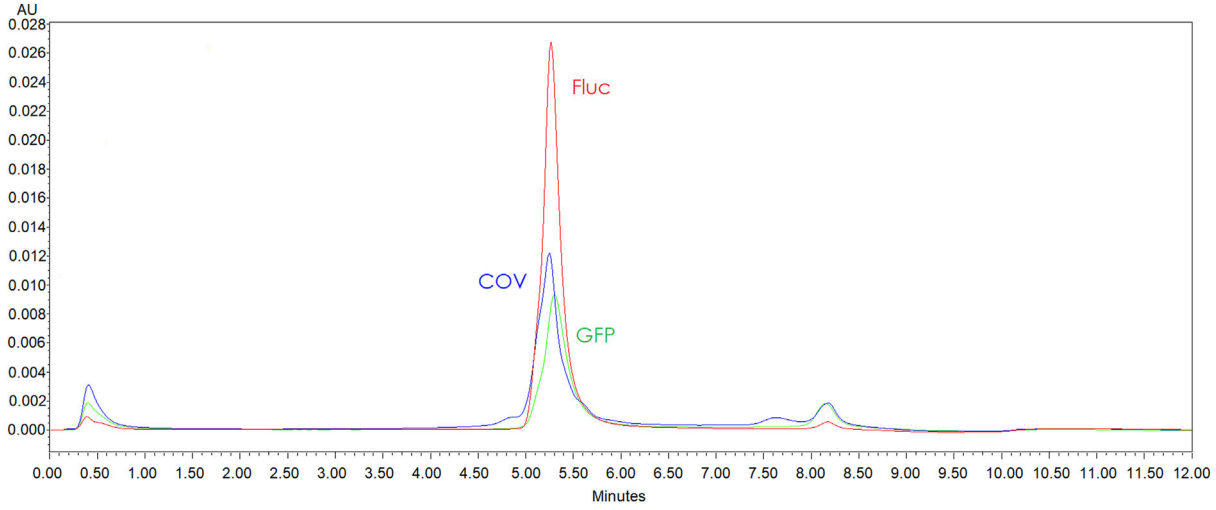

FIGURE 5
AEX-HPLC (CIMac™ pDNA 0.3 mL Analytical Column (1.4 µm)) profile comparison GFP (green line), Fluc (red line) and COV (blue line) linearized plasmids purified by resin (0.5ug each template injected). Chromatogram shows more intense impurity peaks for COV and GFP.

Nevertheless, we decided to explore also how pre-IVT factors such as plasmid linearization isolation methods could affect to the production of this important impurity. The recent findings regarding COVID have been highly informative, prompting us to investigate whether the purification of linearized plasmids using hydrophobic C4 columns could also reduce the dsRNA content in transcripts of various lengths or sizes. It is well-known that AEX chromatography has proven to be an effective technique for removing dsRNA. However, we aimed to determine if chromatographic purification of DNA templates alone could achieve dsRNA levels below 1% without the need for an additional mRNA polishing step, relying solely on Oligo-dT purification for the transcripts. In this study, our objective was to establish baseline levels of dsRNA generated without the inclusion of supplementary purification steps aimed at its removal or mitigation. To achieve this, we initiated the synthesis of respective mRNA strands for three designated protein targets from their corresponding linearized templates, followed by template purification utilizing the Wizard® Megapreps DNA Purification Resin or chromatographic methodologies involving the CIMmultus® C4HLD matrix. After the purification of templates, an Oligo-dT affinity chromatography process was employed to refine the mRNA constructs, ultimately leading to the acquisition of purified mRNA entities. Subsequently, dsRNA quantification was performed using Dot Blot analysis, as depicted in Figure 4.

We observed that the constructs encoding GFP and COV displayed elevated levels of dsRNA, whereas Fluc exhibited more favorable levels around 1%. As previously mentioned, in the absence of a polishing step, the RNA transcripts for GFP and COV exhibited higher dsRNA values compared to Fluc. These findings captured our attention, as the capillary electrophoresis, HPLC, and AGE analyses revealed linearized plasmids targeting COV and GFP with decreased purity and an increased number of peaks that do not correspond with target mRNA. (Figure 5). This observation led us to speculate about a potential relationship between the impurities of the initial template and the production of endogenous dsRNA during IVT.

To assess the impact of linearized template quality, we sought to employ a more specific and reliable purification technique instead of depending solely on simple filtration or resin retention methods. While several options exist for the chromatographic purification of circular plasmids, limited information is available regarding the purification of linearized plasmids. In this study, we investigated the efficacy of CIMmultus C4 HLD columns, which utilize hydrophobic interactions to fractionate proteins from nucleic acids, commonly applied in the polishing of purified mRNA.

To evaluate the performance of C4 columns, we enzymatically opened several circular plasmids of varying lengths using BspQI enzyme, followed by purification using this monolithic column. One example of purification is described in (Supplementary Figure S1). In the supplementary image, the chromatogram depicts a multi-stage process. Initially, during the loading phase, no breakthrough is observed, indicating that all components of the loaded sample (linearized DNA + restriction enzyme) adhere tightly to the column. The elution of the restriction enzyme only occurs after a final treatment involving CIP with 0.1M NaOH. Subsequent to the loading phase, a washing phase with buffer A is employed, followed by elution using a 100% B. This elution process yields a primary peak alongside a minor tail consisting of highly diluted fractions. It is noteworthy that the UV signal within these dilute fraction's ranges from 20 to 0 mAU. Our extensive experience has shown that the quantity of DNA present in these extremely diluted fractions is negligible compared to the total content of the primary peak, rendering them unsuitable for further analysis and thus necessitating their exclusion. The presence of this tailing-off effect in the chromatogram is attributed to residual components firmly bound to the column, which ultimately detach due to the decreasing conductivity values as the elution progresses. To further investigate these tail fractions, they were consolidated, concentrated,

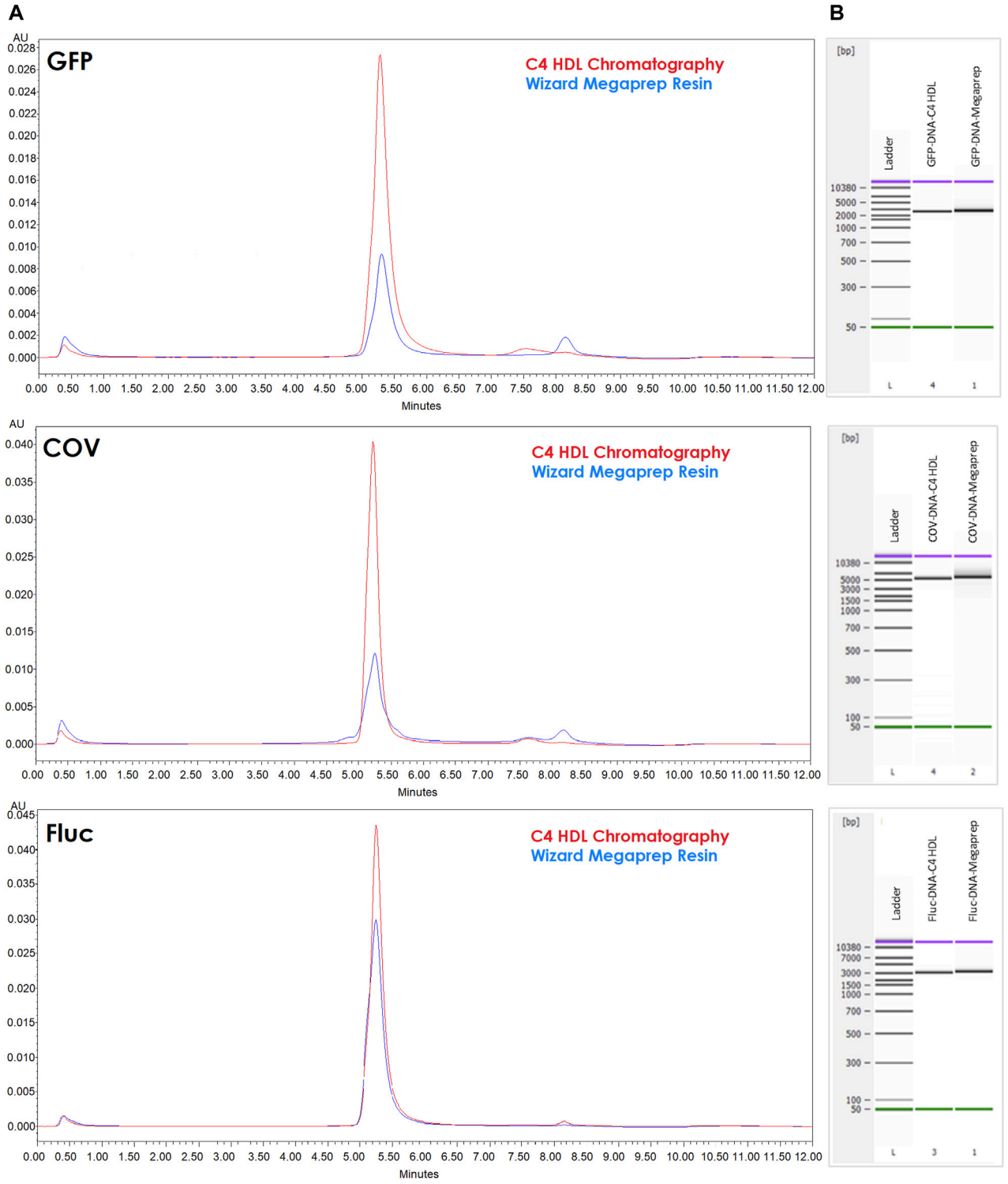

FIGURE 6
Template characterization. **(A)** AEX-HPLC (CIMac™ pDNA) analytical profile of linear DNA profiles for encoded GFP, Fluc and COV purified by Megapreps DNA Resin (blue lines) and CIMmultus C4 HLD column (red lines) (0.5ug each template injected). **(B)** Capillary electrophoresis for the same samples.

and subjected to preliminary analysis using HPLC CIMac pDNA. This analysis revealed an overlap with the target linear DNA, leading us to conclude that the main peak and the tail were essentially identical (Supplementary Figure S2). However, the mass obtained from these tail fractions constituted less than 5% of the total, prompting their exclusion from further analysis.

When comparing the purified fractions to templates purified using Megapreps DNA Resin, it became evident that C4 provided

10.3389/fmolb.2023.1248511

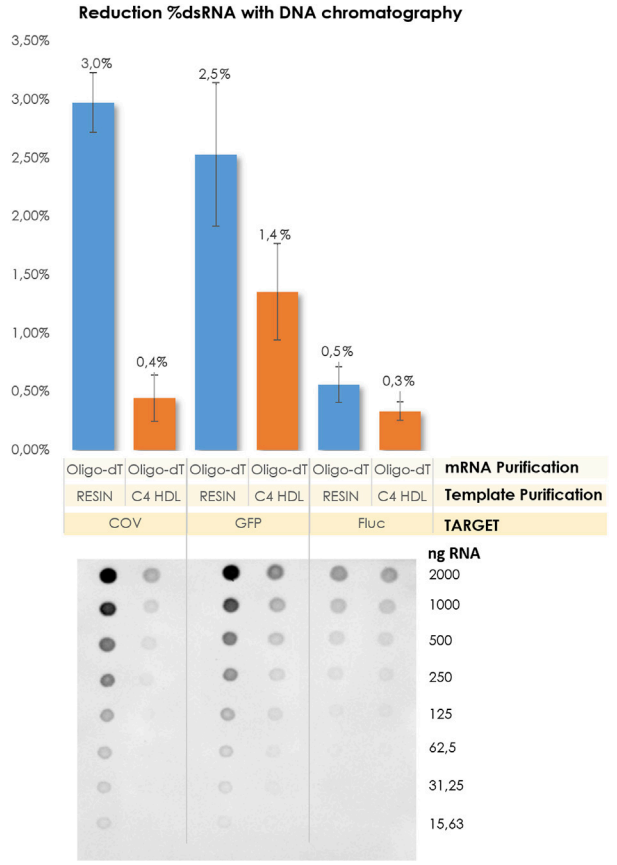

FIGURE 7
Comparison of dsRNA content related to the template purification method and transcript size. Corresponding dot blot membranes.

superior results. Capillary electrophoresis (CE) profiles exhibited reduced tailing (smearing in the simulated gel) at the right side and higher intensity, indicating improved template purity. Furthermore, HPLC analysis using ClMac™ pDNA demonstrated more prominent main peaks corresponding to the template and decreased impurities (Figure 6).

To further characterize the purified templates, we subjected them to AEX-HPLC and capillary electrophoresis (Figure 6). Comparative analysis revealed improved profiles for the chromatographically purified templates, with reduced degradation and fewer impurity peaks. Notably, the profiles of Fluc templates exhibited greater similarity and lower impurity levels, aligning with the lower dsRNA values observed in the corresponding transcripts.

These results highlight the importance of template purification in obtaining high-quality linearized plasmids. The use of C4 columns offers significant advantages in terms of template integrity and purity, ultimately contributing to the production of mRNA transcripts with reduced levels of impurities, such as dsRNA.

The purified linearized plasmids obtained through C4 chromatography were used as the starting material for the subsequent IVT reactions. Following IVT, mRNA crudes were isolated exclusively using affinity chromatography. As anticipated, the levels of dsRNA were significantly reduced, regardless of the size of the resulting mRNA molecules. Notably, the most substantial reduction in dsRNA content was observed for the COVID construct (Figure 7).

To the best of our knowledge, our findings represent the first direct evidence of a correlation between the plasmid purification method and the levels of dsRNA generated during the subsequent IVT process. While it is evident that the use of high-quality linearized plasmids leads to a significant reduction in double-stranded impurities, the underlying explanation for this phenomenon remains unclear.

As previously mentioned, two main mechanisms have been proposed to explain the origin of dsRNA. The first mechanism is associated with the occasional mispriming of the T7 RNA polymerase (T7RNAP) (Triana-Alonso et al., 1995; Gholamalipour et al., 2018; Mu et al., 2018; Mu and Hur, 2021), and the second one in which the antisense strand can be transcribed in a promoter-independent manner, leading to the generation of a complete complementary sequence that anneals to the sense strand (Mu and Hur, 2021) (Figure 1). However, until now, no studies have investigated the influence of impurities on dsRNA generation.

While our study does not aim to elucidate the specific mechanisms or origins of dsRNA, it highlights the critical role of the quality of linearized templates in obtaining transcripts with reduced levels of dsRNA. Importantly, our results suggest that the poor purification of the starting plasmid results in the presence of impurities that the T7 RNAP can potentially use as alternative templates for transcription (Figure 8). Each of these alternative templates could generate RNA fragments that are complementary to different regions of the properly transcribed mRNA sequence. Consequently, a heterogeneous population of dsRNA transcripts would coexist with the dsRNA produced through the aforementioned mechanisms.

The significant reduction of dsRNA observed during the purification of linearized plasmids highlights the substantial contribution of this impurity from the DNA fragments themselves. This finding emphasizes the importance of employing effective purification techniques for linearized templates. The data presented in this study demonstrate the successful application of chromatography, specifically using C4 columns, for this purpose.

In conclusion, our study demonstrates the importance of implementing both purification and polishing steps in the production of mRNA constructs. The use of AEX chromatography proved to be highly effective in reducing dsRNA levels, with some constructs achieving levels below the recommended threshold. However, it was observed that HIC was not as efficient in reducing dsRNA content compared to AEX. The results suggest that by employing a robust purification method for the initial linearized plasmids, such as hydrophobic chromatography, it is possible to obtain mRNA transcripts with lower dsRNA percentages without the need for additional polishing steps. This highlights the importance of optimizing the purification process of the starting linearized plasmid to achieve high-quality mRNA constructs with reduced dsRNA impurities. Further investigations should focus on understanding the underlying mechanisms and factors influencing dsRNA formation, as well as exploring alternative purification strategies for even more efficient removal of dsRNA.

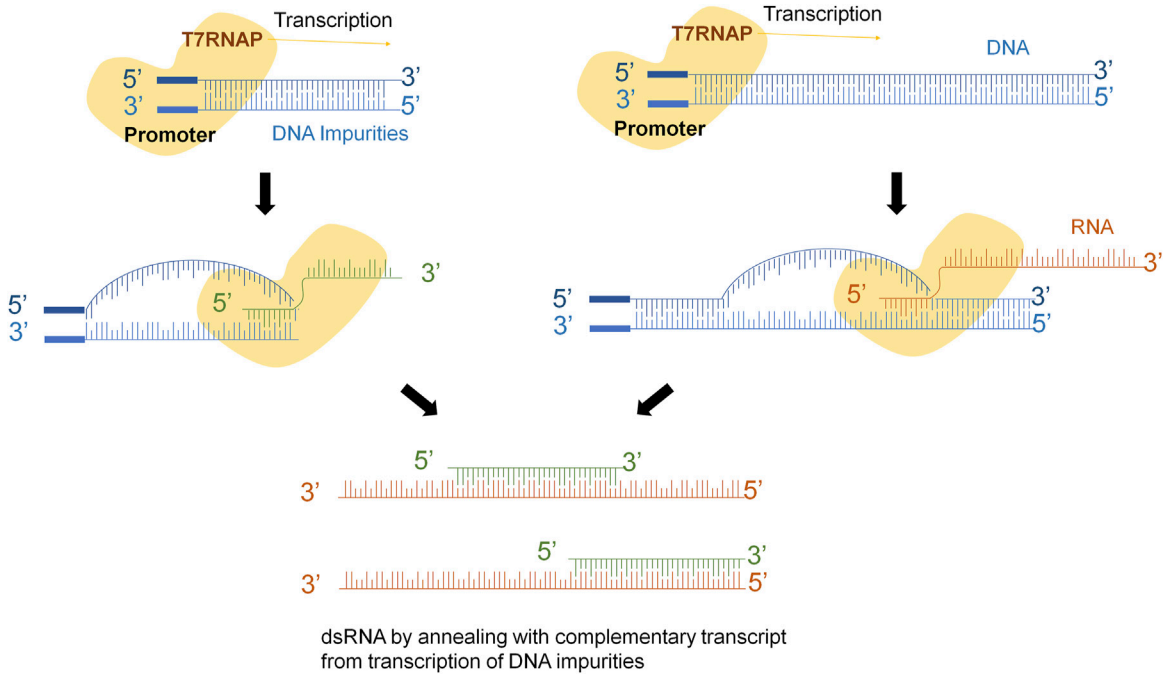

FIGURE 8
dsRNA generation mechanisms during IVT. Not removed impurities of DNA might be treated as the linearized complete plasmid producing sequences of RNA that could anneal with the original transcript. That might lead to a population of different dsRNA species.

TABLE 1 Components for upstream production.

Synthesis step	Component	Reaction conditions
Template DNA Linearization	Plasmid	50°C for 1 h
	BspQI enzyme	
	10X Dig. buffer	
	Nuclease free water	
Transcription (IVT)	NTPs (ATP, CTP, GTP)	37°C for 3 h
	N-Methyl-Pseudouridine	
	Linearized plasmid	
	CleanCap™	
	10X IVT buffer	
	T7 RNAP	
	Pyrophosphatase	
	RNAse inhibitor	
	Nuclease free water	
Template DNA Digestion	DNase	37°C for 15 min
	10X Dnase buffer	
Quenching	EDTA	N/A

4 Materials and methods

4.1 Synthetic methods

4.1.1 Plasmid linearization

Prior to RNA IVTs, pDNAs encoding firefly luciferase (pTLuc), spike 2p SARS-CoV-2 (pTCOV01), and green fluorescent protein (pTGFP) were linearized using BspQI (NEB) enzyme, according to the manufacturer's instructions.

4.1.2 IVT mRNA synthesis

Triphosphate-derivatives of *N*-methylpseudouridine (Hongene) were used to generate modified nucleoside containing RNA. All RNAs were capped using Cleancap™ (Trilink Biotechnologies). All IVT reagents except enzymes listed in (Table 1) were preheated to 37°C, mixed in a 1.5 mL plastic tube in Thermomixer™C (Eppendorf) and incubated at 37°C with shaking at 300 rpm. The reaction was quenched after 180 min by addition of 5 mM EDTA, pH 8.0 for its subsequent purification by the different methods.

4.2 Purification methods

4.2.1 Purification of linearized plasmids with silica resin

The Wizard® Plus Maxipreps DNA Purification System provides a rapid resin-based batch column method for purification of plasmid DNA. The purification procedure was carried out following the manufacturer's protocol.

4.2.2 Hydrophobic interaction chromatography of linearized plasmids

Chromatographic purification was performed on the ÄKTA Start (GE Healthcare) FPLC system composed of two pumps and a multiwavelength UV-Vis detector (2 mm flow cell path length). Unicorn software (GE Healthcare) was used for instrument control and data acquisition. DNA template linearized was diluted once in sample loading buffer (75 mM Tris + 15 mM EDTA + 3.75 M SA (ammonium sulphate) pH = 7.2 and loaded onto CIMmultus C4 HDL 1 mL column (Sartorius) equilibrated in mobile phase containing 50 mM Tris + 10 mM EDTA + 2.5 M SA pH = 7.2. After the UV 260 nm signal and conductivity was stabilized, an elution step was performed with 50 mM Tris + 10 mM EDTA pH = 7.2 DNA content from desired fractions was concentrated and desalted using Amicon Ultra-15 centrifugal filter units (30K membrane) (Millipore) by successive centrifugation at 1,000 g for 10 min RT in a 5804R centrifuge (Eppendorf).

4.2.3 Purification of mRNA by lithium chloride precipitation

RNA precipitation is an easy and cost-effective method for the concentration of RNA, leaving a pellet that can be resuspended in the buffer of choice. An equal volume of LiCl 7.5 M solution was added, and the resulting solution was stored at −80°C overnight. Next day, it was centrifuged at top speed for 20 min and the supernatant was discarded. The pellet was washed twice with ice-cold 70% ethanol to remove residual salt and dried with SpeedVac for 5 min. The pellet was then resuspended in a suitable buffer and stored at −80°C.

4.2.4 Affinity chromatography of mRNA

The ssRNA fraction from CIMmultus PrimaS was purified by affinity chromatography using POROS Oligo (dT)25 (ThermoFisher) as polishing step.

Buffer A contained 50 mM sodium phosphate, 0.5 M NaCl, 5 mM EDTA, pH = 7.0 and Buffer B contained 50 mM sodium phosphate, 5 mM EDTA, pH = 7.0. Column was equilibrated with 100% Buffer A, loaded with RNA, washed with buffer B, and finally eluted by step elution of polyadenylated mRNA with double-deionized water.

4.2.5 RNA isolation from column fractions

RNA content from desired fractions was concentrated and desalted using Amicon Ultra-15 centrifugal filter units (30K membrane) (Millipore) by successive centrifugation at 2,100 g for 10 min in a 5804R centrifuge (Eppendorf), and dilution with nuclease free water.

4.2.6 Anion exchange chromatography of mRNA

CIMmultus PrimaS is used for one-step purification of research grade of ssRNA, to process *in vitro* transcription mixtures. Purification performance is enhanced by a high-salt wash that removes the majority of dsRNA, DNA, and proteins in advance of elution. IVT mixture was diluted once in sample loading/equilibrate buffer A (20 mM Tris, 20 mM BTP, 20 mM glycine, 50 mM NaCl, 10 mM EDTA, pH = 8.0) and loaded onto CIMmultus PrimaS (BIA Separations). After unbound IVT components eluted in flow-through, a wash 1 with equilibration buffer was necessary, followed by a high-salt wash with 50 mM Tris, 3.0 M guanidine-HCl, 20 mM EDTA, pH 8.0. DNA, dsRNA, and proteins typically elute on the ascending side of the guanidine-EDTA peak. And after a wash 3 with buffer A until UV returns to baseline, a step elution was performed with buffer C (20 mM Tris, 20 mM BTP, 20 mM glycine, 50 mM NaCl, 10 mM EDTA, pH = 11.0). Fractions were neutralized immediately after elution.

4.3 Analytical methods

4.3.1 HPLC analysis of pDNA

Linear pDNA was analyzed by HPLC using a CIMac™ pDNA-0.3 Analytical Column (Pores 1.4 µm) (BIA Separations) connected to an HPLC WATERS e2695.

The separations of the isoforms were performed in a linear gradient of NaCl with the temperature of the whole system controlled to 15.0+/- 0.5°C. Using the followed mobile phases in standard protocol for the column (MPA: 100 mM Tris-HCl, 0.6 M NaCl, pH = 8, MPB: 100 mM Tris-HCl, 1 M NaCl, pH = 8). A linear gradient was performed, 5% MPB to 30% MPB in 6 min at a flow rate 1 mL/min. The column was eluted with 100% MPB for 1 min before re-equilibration in 5% MPB.

4.3.2 Dot blot

Purified IVT RNA samples were spotted onto positively charged nylon membranes (Nytran SC, Sigma Aldrich). The membranes were blocked with 5% (w/v) non-fat dried milk in TBS-T buffer (20 mM Tris-HCl, 150 mM NaCl, 0.1% [v/v] Tween-20, pH 7.4), and incubated with dsRNA-specific mAb J2 (Jena Bioscience) 4°C ON. Membranes were washed three times with TBS-T and reacted with HRP-conjugated goat anti-mouse Ig (Abcam), washed three times, and detected with ECL Plus Western blot detection reagent (Amersham). Images were captured on an iBright 750 digital imaging system.

dsRNA Ladder (Biolabs) (25 ng) was used as a positive control.

4.3.3 Capillary electrophoresis

DNA and RNA samples were loaded into the corresponding kits; Agilent DNA 12000 Kit and Agilent RNA 6000 Nano Kit, both designed for use with the Agilent 2,100 Bioanalyzer instrument, according to guide instructions. Results were analyzed with the 2,100 Expert Software.

Data availability statement

The raw data supporting the conclusion of this article will be made available by the authors, without undue reservation.

Author contributions

VL, AL, and HM, designed, performed and analyzed the experiments. DC and JM supervised the project and DC wrote the manuscript. All authors contributed to the article and approved the submitted version.

Acknowledgments

The authors would like to express their sincere appreciation to Elena Mata and her dedicated team for their invaluable assistance in performing the mRNA transfections in cell lines and providing us with crucial protein expression results. Their expertise and commitment have greatly contributed to the success of this study. The authors thanks Gobierno de Aragón (Spain) for financial funding through project IDMF/2021/0009 (Nuevas tecnologías para el diseño y obtención de vacunas de ARN en Aragón).

Conflict of interest

JM, VL, AL, HM, and DC were employed by the Company Certest Pharma, Certest Biotec.

Publisher's note

Supplementary material

The Supplementary Material for this article can be found online at: https://www.frontiersin.org/articles/10.3389/fmolb.2023.1248511/full#supplementary-material

References

Arnaud-Barbe, N., Cheynet-Sauvion, V., Oriol, G., Mandrand, B., and Mallet, F. (1998). Transcription of RNA templates by T7 RNA polymerase. *Nucleic Acids Res.* 26, 3550–3554. doi:10.1093/nar/26.15.3550

Azarani, A., and Hecker, K. H. (2021). RNA analysis by ion-pair reversed-phase high performance liquid chromatography. *Nucleic Acids Res.* 29, E7–E9. doi:10.1093/nar/29.2.e7

Biebricher, C. K., and Luce, R. (1996). Template-free generation of RNA species that replicate with bacteriophage T7 RNA polymerase. *EMBO J.* 15, 3458–3465. doi:10.1002/j.1460-2075.1996.tb00712.x

Cazenave, C., and Uhlenbeck, O. C. (1994). RNA template-directed RNA synthesis by T7 RNA polymerase. *Proc. Natl. Acad. Sci.* 91, 6972–6976. doi:10.1073/pnas.91.15.6972

Chatterjee, S., Shioi, R., and Kool, E. T. (2022). Sulfonylation of RNA 2′-OH groups. *ACS Cent. Sci.* 9, 531–539. doi:10.1021/acscentsci.2c01237

Dickman, M. J., and Hornby, D. P. (2006). Enrichment and analysis of RNA centered on ion pair reverse phase methodology. *Rna* 12, 691–696. doi:10.1261/rna.2278606

Dousis, A., Ravichandran, K., Hobert, E. M., Moore, M. J., and Rabideau, A. E. (2022). An engineered T7 RNA polymerase that produces mRNA free of immunostimulatory byproducts. *Nat. Biotechnol.* 41, 560–568. doi:10.1038/s41587-022-01525-6

Fang, L., Xiao, L., Jun, Y. W., Onishi, Y., and Kool, E. T. (2022). Reversible 2'-OH acylation enhances RNA stability. *Res. Sq.*, 0–20. doi:10.1038/s41557-023-01246-6

Gagnon, P. (2020). Purification of nucleic acids: a handbook for purification of plasmid DNA and mRNA for gene therapy and vaccines - Sartorius BIA separations. Available at: https://www.biaseparations.com/en/products/monolithic-columns/books/226/purification-of-nucleic-acids-a-handbook-for-purification-of-plasmid-dna-and-mrna-for-gene-therapy-and-vaccines.

Gholamalipour, Y., Karunanayake Mudiyanselage, A., and Martin, C. T. (2018). 3' end additions by T7 RNA polymerase are RNA self-templated, distributive and diverse in character-RNA-Seq analyses. *Nucleic Acids Res.* 46, 9253–9263. doi:10.1093/nar/gky796

Jacoby, M. (2006). Monolithic chromatography. *Chem. Eng. News* 84, 14–19. doi:10.1021/cen-v084n050.p014

Karikó, K., Muramatsu, H., Ludwig, J., and Weissman, D. (2011). Generating the optimal mRNA for therapy: HPLC purification eliminates immune activation and improves translation of nucleoside-modified, protein-encoding mRNA. *Nucleic Acids Res.* 39, e142. doi:10.1093/nar/gkr695

Kim, K. Q., Burgute, B. D., Tzeng, S. C., Jing, C., Jungers, C., Zhang, J., et al. (2022). N1-methylpseudouridine found within COVID-19 mRNA vaccines produces faithful protein products. *Cell Rep.* 40, 111300. doi:10.1016/j.celrep.2022.111300

Kis, Z., Kontoravdi, C., Dey, A. K., Shattock, R., and Shah, N. (2020). Rapid development and deployment of high-volume vaccines for pandemic response. *J. Adv. Manuf. Process.* 2, 100600–e10110. doi:10.1002/amp2.10060

Knezevic, I., Liu, M. A., Peden, K., Zhou, T., and Kang, H. N. (2021). Development of mRNA vaccines: scientific and regulatory issues. *Vaccines* 9, 81–11. doi:10.3390/vaccines9020081

Konarska, M. M., and Sharp, P. A. (1989). Replication of RNA by the DNA-dependent RNA polymerase of phage T7. *Cell* 57, 423–431. doi:10.1016/0092-8674(89)90917-3

Krupp, G. (1989). Unusual promoter-independent transcription reactions with bacteriophage RNA polymerases. *Nucleic Acids Res.* 17, 3023–3036. doi:10.1093/nar/17.8.3023

Lee, B. L., and Barton, G. M. (2015). *Trafficking of endosomal Toll-like receptors*, 360–369. S0962-8924(13)00226-2.pdf. 24. doi:10.1016/j.tcb.2013.12.002

Mccarthy, S. M., and Gilar, M. (2008). *Semi-preparative scale single-stranded RNA purification. 2–4.*

Milligan, J. F., Groebe, D. R., Witherell, G. W., and Uhlenbeck, O. C. (1987). Oligoribonucleotide synthesis using T7 RNA polymerase and synthetic DNA templates. *Nucleic Acids Res.* 15, 8783–8798. doi:10.1093/nar/15.21.8783

Mu, X., Greenwald, E., Ahmad, S., and Hur, S. (2018). An origin of the immunogenicity of *in vitro* transcribed RNA. *Nucleic Acids Res.* 46, 5239–5249. doi:10.1093/nar/gky177

Mu, X., and Hur, S. (2021). Immunogenicity of *in vitro* -transcribed RNA. *Acc. Chem. Res.* 54, 4012–4023. doi:10.1021/acs.accounts.1c00521

Nacheva, G. A., and Berzal-Herranz, A. (2003). Preventing nondesired RNA-primed RNA extension catalyzed by T7 RNA polymerase. *Eur. J. Biochem.* 270, 1458–1465. doi:10.1046/j.1432-1033.2003.03510.x

Ouranidis, A., Davidopoulou, C., Tashi, R. K., and Kachrimanis, K. (2021). Pharma 4.0 continuous mRNA drug products manufacturing. *Pharmaceutics* 13, 1371. doi:10.3390/pharmaceutics13091371

Park, J. W., Lagniton, P. N. P., Liu, Y., and Xu, R.-H. (2021). mRNA vaccines for COVID-19: what, why and how. *Int. J. Biol. Sci.* 17, 1446–1460. doi:10.7150/ijbs.59233

Podgornik, A. Š., Yamamoto, S., Peterka, M. Ž., and Krajnc, N. L. (2013). Fast separation of large biomolecules using short monolithic columns. *J. Chromatogr. B Anal. Technol. Biomed. Life Sci.* 927, 80–89. doi:10.1016/j.jchromb.2013.02.004

Roy, B., and Wu, M. Z. (2019). Understanding and overcoming the immune response from synthetic mRNAs. *Genet. Eng. Biotechnol. News* 39, 56–58. doi:10.1089/gen.39.12.15

Schlake, T., Thess, A., Fotin-mleczek, M., and Kallen, K. (2012). Developing mRNA-vaccine technologies. *RNA Biol.* 9 (11), 1319–1330. doi:10.4161/rna.22269

Separations, B. I. A. (2020). *Purification of single-stranded mRNA: The toolbox for the next generation*.

Sousa, S., Prazeres, D. M. F., Azevedo, A. M., and Marques, M. P. C. (2021). mRNA vaccines manufacturing: challenges and bottlenecks. *Vaccine* 39, 2190–2200. doi:10.1016/j.vaccine.2021.03.038

Triana-Alonso, F. J., Dabrowski, M., Wadzack, J., and Nierhaus, K. H. (1995). Self-coded 3'-extension of run-off transcripts produces aberrant products during *in vitro* transcription with T7 RNA polymerase. *J. Biol. Chem.* 270, 6298–6307. doi:10.1074/jbc.270.11.6298

Verbeke, R., Lentacker, I., De Smedt, S. C., and Dewitte, H. (2021). The dawn of mRNA vaccines: the COVID-19 case. *J. Control. Release* 333, 511–520. doi:10.1016/j.jconrel.2021.03.043

Weissman, D., Pardi, N., Muramatsu, H., and Karikó, K. (2013). HPLC purification of *in vitro* transcribed long RNA. *Methods Mol. Biol.* 969, 43–54. doi:10.1007/978-1-62703-260-5_3

Whitley, J., Zwolinski, C., Denis, C., Maughan, M., Hayles, L., Clarke, D., et al. (2020). Development of mRNA manufacturing for vaccines and therapeutics: mRNA platform requirements and development of a scalable production process to support early phase clinical trials. *Transaltional Res.* 242, 38–55. doi:10.1016/j.trsl.2021.11.009

frontiers | Frontiers in Molecular Biosciences

TYPE Original Research
PUBLISHED 11 December 2023
DOI 10.3389/fmolb.2023.1291045

OPEN ACCESS

EDITED BY
Xin Zhang,
Jiangmen Central Hospital, China

REVIEWED BY
Renata Grzela,
University of Warsaw, Poland
Subha Ranjan Das,
Carnegie Mellon University, United States
Tracy Nissan,
Stockholm University, Sweden
Ambadas Rode,
Regional Centre for Biotechnology (RCB), India

*CORRESPONDENCE
Thomas Ziegenhals,
thomas.ziegenhals@biontech.de

RECEIVED 08 September 2023
ACCEPTED 27 November 2023
PUBLISHED 11 December 2023

CITATION
Ziegenhals T, Frieling R, Wolf P, Göbel K, Koch S, Lohmann M, Baiersdörfer M, Fesser S, Sahin U and Kuhn AN (2023), Formation of dsRNA by-products during *in vitro* transcription can be reduced by using low steady-state levels of UTP. *Front. Mol. Biosci.* 10:1291045. doi: 10.3389/fmolb.2023.1291045

Formation of dsRNA by-products during *in vitro* transcription can be reduced by using low steady-state levels of UTP

Thomas Ziegenhals*, Ronja Frieling, Philipp Wolf, Katharina Göbel, Stina Koch, Mia Lohmann, Markus Baiersdörfer, Stephanie Fesser, Ugur Sahin and Andreas N. Kuhn

BioNTech SE, Mainz, Germany

Introduction: Exogeneous messenger ribonucleic acid (mRNA) can be used as therapeutic and preventive medication. However, during the enzymatic production process, commonly called *in vitro* transcription, by-products occur which can reduce the therapeutic efficacy of mRNA. One such by-product is double-stranded RNA (dsRNA). We therefore sought to limit the generation of dsRNA by-products during *in vitro* transcription.

Materials and methods: *In vitro* transcription was performed with a DNA template including a poly(A)-tail-encoding region, dinucleotide or trinucleotide cap analogs for cotranscriptional capping, and relevant nucleoside triphosphates. Concentrations of UTP or modified UTP (m1ΨTP) and GTP were reduced and fed over the course of the reaction. mRNA was analyzed for dsRNA contamination, yield of the reaction, RNA integrity, and capping efficiency before translational activity was assessed.

Results: Limiting the steady-state level of UTP or m1ΨTP during the enzymatic reaction reduced dsRNA formation, while not affecting mRNA yield or RNA integrity. Capping efficiency was optimized with the use of a combined GTP and UTP or m1ΨTP feed, while still reducing dsRNA formation. Lower dsRNA levels led to higher protein expression from the corresponding mRNAs.

Discussion: Low steady-state concentrations of UTP and GTP, fed in combination over the course of the *in vitro* transcription reaction, produce mRNA with high capping and low levels of dsRNA formation, resulting in high levels of protein expression. This novel approach may render laborious purification steps to remove dsRNA unnecessary.

KEYWORDS

mRNA-based therapeutics, *in vitro* transcription, double-stranded RNA, RNA capping, mRNA translatability

1 Introduction

The pre-clinical and clinical advancement of messenger ribonucleic acid (mRNA)-based therapeutics and vaccines have received a major boost since the successful use of mRNA vaccines in the fight against the COVID-19 pandemic. mRNA-based therapies have huge therapeutic potential in many areas of high unmet medical need, including cancer and

infectious diseases, and are under rapid development (Sahin et al., 2014; Sahin et al., 2020; Dousis et al., 2023).

mRNA-based therapies work by translating exogeneous mRNA into the active protein (Wolff et al., 1990). Exogenous mRNA is produced using a cell-free process called *in vitro* transcription, whereby a linear DNA template is transcribed into the corresponding mRNA using a single-subunit phage RNA polymerase (Konarska et al., 1984)—most commonly the RNA polymerase from the T7 phage is used (Chamberlin and Ring, 1973; Cheetham et al., 1999). For efficient translation, and to increase mRNA stability, the mRNA is capped at the 5′ end and a poly(A)-tail is included at the 3′end (Gao et al., 2000; Galloway and Cowling, 2019). For capping, cap analogs can be added to the *in vitro* transcription reaction that are co-transcriptionally incorporated (Konarska et al., 1984; Pasquinelli et al., 1995; Stepinski et al., 2001).

mRNA synthesis using *in vitro* transcription gives rise to by-products that can have unwanted side effects. One of the major by-products of concern is double-stranded RNA (dsRNA) which can cause immunogenic reactions by inducing type I interferons and reduce protein expression (Kariko et al., 2011). Run-off transcription at the 3′ end of the DNA template, which can lead to prolonged RNA extension in the form of "loop back RNA" or "backward transcribed" RNA, is a significant source of dsRNA during *in vitro* transcription (Triana-Alonso et al., 1995; Gholamalipour et al., 2018; Dousis et al., 2023): While dsRNA can be reduced in subsequent purification steps (Kariko et al., 2011; Baiersdorfer et al., 2019), this typically leads to a decrease in mRNA yield and can impact mRNA integrity. Therefore, altering the manufacturing process to reduce formation of dsRNA may be more efficient. This has previously been achieved by increasing the temperature (Wu et al., 2020), adapting the Mg^{2+} concentration (Mu et al., 2018), adding chaotropic agents to the reaction (Piao et al., 2022), or using a mutated T7 RNA polymerase (Dousis et al., 2023).

When using DNA templates that encode a poly(A)-tail, extension of the transcribed RNA in the reverse orientation starts with a poly(A)-tail. Therefore, we hypothesized that reducing the concentration of UTP in the reaction [or a corresponding modified nucleotide, such as N1-methyl-pseudouridine triphosphate (m1ΨTP)] would negatively impact the backward reaction, leading to less dsRNA by-products. Here, we show that limiting UTP via stepwise addition of UTP over the course of the *in vitro* transcription reaction reduces dsRNA formation. Furthermore, combining a UTP and GTP feed reduces dsRNA formation while keeping the capping efficiency high. Importantly, the lower dsRNA levels obtained in this manner led to higher protein expression from the corresponding mRNAs.

2 Material and methods

2.1 mRNA synthesis

In vitro transcription was performed in the presence of a DNA template (linearized plasmid DNA or PCR product) including the coding region for a poly(A)-tail ($A_{30}L_{10}A_{70}$), either a dinucleotide ($m^{2,7,3'-O}$GppSpG, denoted beta-S-ARCA(D1) (Kuhn et al., 2010) or a trinucleotide ($m^{2,7,2'-O}$Gppp ($m^{2'-O}$)ApG, sold as CleanCap® by TriLink BioTechnologies) cap analog for co-transcriptional capping, and relevant nucleoside triphosphates (GTP, ATP, UTP or m1ΨTP, CTP, Thermo Fisher Scientific) with a final concentration of 9 mM each. The starting concentrations of GTP and/or UTP/m1ΨTP were reduced to 0.5 mM and fed-in 4 or 11 times in equal amounts over the course of the transcription reaction until the final concentration was reached with an additional incubation time of 30 min after the last feed. The transcribed RNAs code for the sequences listed in Supplementary Table S1. The reaction was performed at 37°C with HEPES buffer (40 mM pH 8,3) containing magnesium acetate (40 mM), dithiothreitol (10 mM), and spermidine (2 mM) in the presence of a T7 RNA polymerase, RNase inhibitor (Ribolock, Thermo Fisher Scientific) and inorganic pyrophosphatase (Thermo Fisher Scientific). After *in vitro* transcription, the DNA template was hydrolyzed via DNase I digestion (Thermo Fisher Scientific) and the RNA was purified using magnetic beads for immobilization (Berensmeier, 2006). RNA was eluted in H_2O. Purified RNA was used for further analysis. Concentration was analyzed by UV spectroscopy and the yield as an indicator for the efficiency of the reaction was calculated in µg RNA per µl of *in vitro* transcription reaction. RNA integrity was analyzed using fragment analyzer (Agilent). Further, the RNA was analyzed for dsRNA contamination and capping efficiency. If indicated, RNA translation was analyzed using a luciferase assay.

2.2 Double-stranded (ds)RNA

To determine the amount of dsRNA, 1 µg of RNA was spotted onto a nylon blotting membrane [Nytran SuPerCharge Nylon Blotting Membrane (GE Healthcare Life Sciences, Cat #10416216)] in triplicates, which was then blocked for 1 h in TBS-T buffer containing 5% (w/v) skimmed milk powder. For detection of dsRNA the membrane was incubated for 1 h with J2 dsRNA-specific mouse monoclonal antibody (English and Scientific Consulting, Szirák, Hungary). After washing with TBS-T the membrane was incubated for 1 h with HRP-conjugated donkey anti-mouse IgG (Jackson ImmunoResearch, Cat #715-035-150) washed with TBS-T and developed using Amersham ECL Prime Western Blotting Detection Reagent (Fisher Scientific, Cat # RPN2232) and the ChemiDoc MP Imaging system (Bio-Rad Laboratories, Inc.). Signal intensities were quantified by densitometry using Image Lab 5.1 software (Bio-Rad Laboratories, Inc.). A standard covering the range of 0–1,280 pg dsRNA/µg RNA was part of the dotblot. Densitometric values were evaluated using a standard curve fit in sigma blot.

2.3 Capping

To test capping efficiency, the RNA was digested by a P1 3′ exonuclease. The resulting nucleotides were separated with high-performance liquid chromatography and measured by mass spectrometry (Shimadzu Prominence LC-20). Of interest are the 5′-end nucleotides. Capped RNA will leave an NpppN dinucleotide while uncapped RNA will leave a triphosphate-nucleotide (pppN).

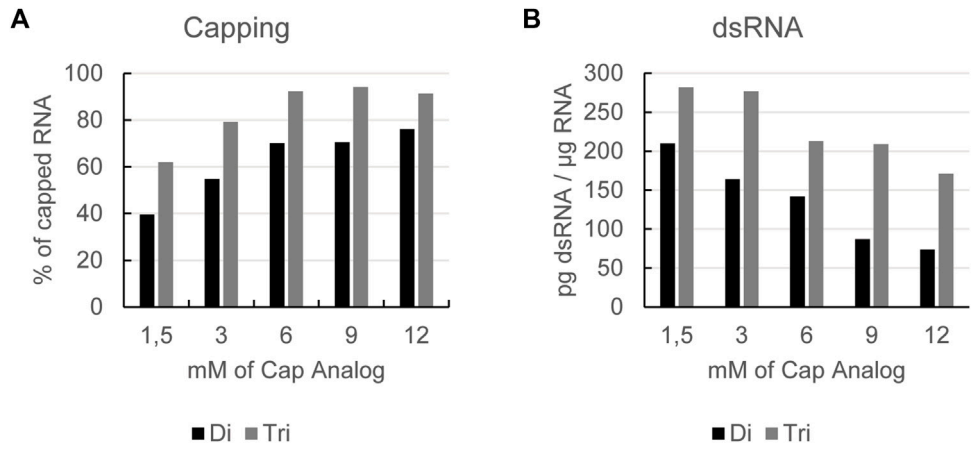

FIGURE 1
Increasing cap analog concentration leads to higher capping efficiency **(A)** and a reduction in dsRNA formation **(B)**: RNAs produced by *in vitro* transcription with increasing concentrations of either a dinucleotide (Di) or a trinucleotide (Tri) cap analog using a GTP fed-batch reaction were analyzed for capping efficiency **(A)** and dsRNA levels **(B)**. Representative example of several experiments with similar outcomes.

Capping efficiency was calculated as the ratio of NpppN and the sum of NpppN and pppN.

2.4 Cell culture

For generation of human immature DCs (hiDCs), PBMCs were isolated from Buffy Coats by Ficoll gradient and $CD14^+$ cells were selected via human CD14 Microbeads (130-050-201, Miltenyi). $CD14^+$ cells were incubated for 5 days with 0.2 ng/µL IL4 (130-093-924, Miltenyi) and GM-CSF (130-093-868, Miltenyi). Differentiation into DCs was controlled via FACS with a double CD83 (551073, BD Pharmingen) and CD209 (551265, BD Pharmingen) staining.

2.5 Luciferase assay

To prepare lipoplexes for transfection, reporter firefly luciferase (Luc)-encoding RNA was incubated with liposomes following proprietary inhouse protocols. RNA was provided as a HEPES-buffered solution and diluted with 1.5 M NaCl and water to a concentration of 150 mM NaCl and an RNA concentration of 0.1 mg/mL, which results in a molar charge ratio of 0.65:1.00 (positive:negative) upon incubation with liposomes. The charge ratio was calculated from the number of positive charges present in lipid head groups and the number of negative charges derived from the number of RNA nucleotides (330 Da per nucleotide was assumed). Liposomes were in-house generated containing (R)-N,N,N-trimethyl-2-3-dioleyloxy-1-propanammonium chloride (DOTMA) and 1,2-dioleoyl-sn-glycero-3-phosphoethanolamine (DOPE) in a molar ratio of 2:1 (DOTMA:DOPE). Lipoplexes were then mixed with hiDCs, and the transfected cells were seeded in 96-well plates with a density of 5 × 10^4 cells and 0.5 µg RNA per well, in media containing 0.4 ng/µL IL4 and GM-CSF. Luciferase assays were conducted at 6, 24, 48 and 72 h after transfection using the Promega BrightGlo Kit according to manufacturer's instructions.

3 Results

3.1 Increasing the cap analog concentration reduces formation of dsRNA

When performing co-transcriptional capping, the cap analog should be kept in excess over the competing nucleoside triphosphate for initiation (most commonly GTP) to obtain a high capping efficiency. To achieve a high yield from the reaction, i.e., to not be limited by a low concentration of GTP, we perform a so-called fed-batch reaction. Here, we start with a low concentration of GTP and then feed in more GTP over the course of the reaction. To optimize capping efficiency of *in vitro* transcribed mRNA, we tested increasing concentrations of cap analogs. This was done with both dinucleotide and trinucleotide cap analogs. As expected, we observed that increasing the cap analog concentration led to higher capping efficiency (Figure 1A). Under these conditions, capping efficiency was higher for the trinucleotide cap analog versus the dinucleotide cap analog (Figure 1A). For both the di- and tri-nucleotide cap analogs, a plateau was reached at a concentration of 6 mM with respect to the capping degree of the obtained mRNA.

Further analysis of the mRNA showed that cap concentration had no impact on reaction yield or RNA integrity (Supplementary Table S1). However, when analyzing the dsRNA level, we observed that by increasing either cap analog concentration, the formation of dsRNA was reduced (Figure 1B). This was the case for cap concentrations of up to 12 mM, i.e., beyond the levels shown to have an impact on the capping efficiency of *in vitro* transcribed mRNA.

3.2 *In vitro* transcription with a UTP feed lowers dsRNA formation in poly(A)-carrying transcripts

For poly(A)-encoding DNA templates, where backwards transcription at the 3′ end of the DNA template would start with a poly(U)-stretch, we reasoned that a lower concentration of UTP

10.3389/fmolb.2023.1291045

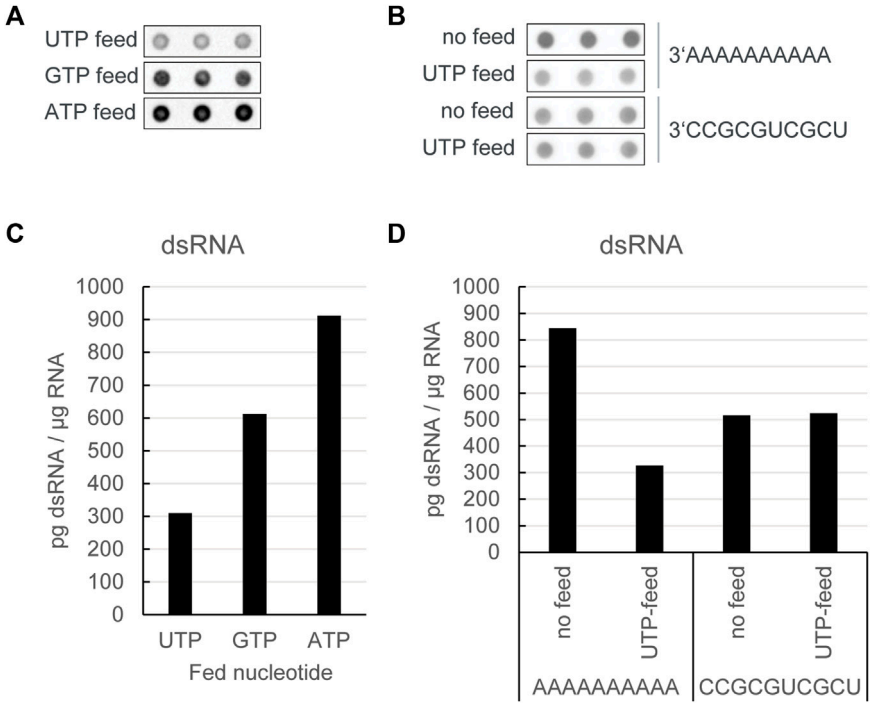

FIGURE 2
In vitro transcription reactions with a UTP feed resulted in production of mRNA with the lowest level of dsRNA. **(A)** J2 dotblot of *in vitro* transcription reactions with a dinucleotide cap analog and a DNA template encoding a poly(A)-tail at the 3′ end, in which different nucleotide triphosphates as indicated were fed over time: **(B)** J2 dotblot of dsRNA levels from *in vitro* transcription RNA from DNA templates encoding different 3′ ends either with no nucleotide triphosphate feed or with a UTP feed: Quantification of dsRNA levels as shown in **(C, D)**. Representative example of several experiments with similar outcomes.

might limit the number of backward reactions, leading to lower dsRNA levels.

To test this hypothesis, we performed an *in vitro* transcription of an unmodified RNA using the dinucleotide cap analog reaction with a low starting concentration of UTP. To reduce the impact on the reaction yield, we then fed UTP into the reaction over time at a rate similar to the GTP feed. Reactions with a GTP feed or an ATP feed were used as controls. Overall, *in vitro* transcription reactions with a UTP feed resulted in production of mRNA with the lowest level of dsRNA, while limitation of ATP was shown to increase dsRNA formation versus the GTP feed as control (Figure 2A and Figure 2C). Notably, the reduction in dsRNA was only seen if the DNA template encoded a poly(A)-tail at the 3′ end, and not with templates ending with a more random nucleotide distribution (Figure 2B and Figure 2D), thereby corroborating our hypothesis that limiting UTP reduces the occurrence of a backward reaction, thus giving rise to lower levels of dsRNA by-products.

3.3 A combined feed of GTP and UTP reduces dsRNA formation while keeping capping efficiency high

As already shown, lowering the steady-state concentration of UTP during *in vitro* transcription leads to lower levels of dsRNA formation. However, as the GTP concentration is not lowered, as expected, capping is suboptimal in reactions applying a UTP feed with dinucleotide co-transcriptional capping (Figure 3A). We subsequently tested whether we could optimize capping while still reducing dsRNA formation by using a combined feed of GTP and UTP. The capping of mRNAs obtained from a combined GTP/UTP feed was similar to that from a GTP feed alone (Figure 3A), thus indicating that the lower UTP concentration had no negative impact on capping. Additionally, the GTP/UTP feed also lowered formation of dsRNA, albeit not as much as the UTP feed alone (Figure 3B).

For the experiments shown in Figures 2, 3, we used as indicated a dinucleotide cap analog and non-modified UTP. To check if the positive effect of lower steady-state levels of UTP, alone or in combination with GTP, on dsRNA levels also held true for trinucleotide cap analogs and/or modified UTPs, we performed a set of reactions in which we used all four combinations: a dinucleotide or a trinucleotide cap analog with either UTP or N1-methyl-pseudouridine triphosphate (m1ΨTP). In each case, we fed either GTP, UTP or m1ΨTP alone, or GTP together with either UTP or m1ΨTP, and analyzed capping efficiency and dsRNA levels of the resulting mRNAs. For the reactions with a GTP feed, reaction conditions were adapted to give similar levels of capping for both the di- and tri-nucleotide cap analogs. In this set of experiments, the RNAs were coding for luciferase, which allowed to also test their translatability (see below).

Lowering the steady-state concentration of UTP or m1ΨTP led to a reduction of dsRNA formation for all four combinations (Figures 4A–D). Similarly, capping efficiency was not affected by feeding either UTP or m1ΨTP in combination with GTP, as capping levels obtained with combined feeds were similar to levels

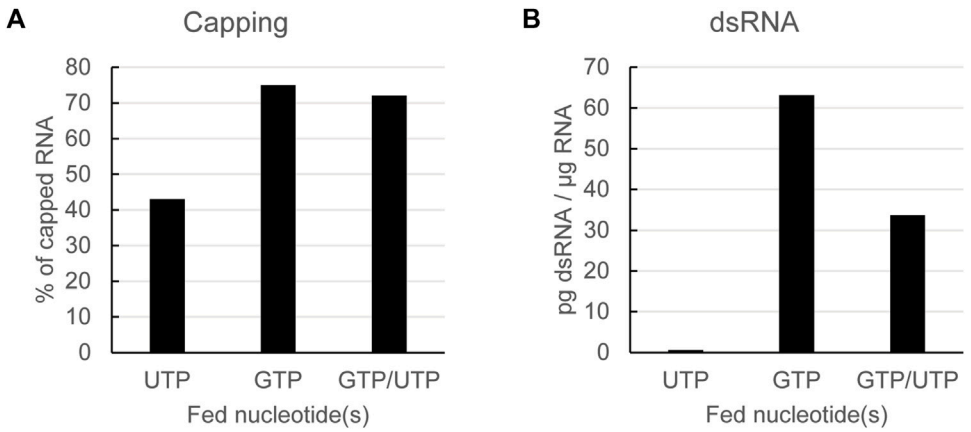

FIGURE 3
Using a combined GTP and UTP feed keeps capping efficiency high while still reducing dsRNA formation. Analysis of *in vitro* transcribed RNA with a dinucleotide cap analog fed with the indicated nucleotides. Capping efficiency is reduced using a UTP feed, but can be rescued to GTP feed levels with a combined GTP/UTP feed **(A)**: dsRNA is reduced using UTP feed or GPT/UTP dual feed **(B)**: Representative example of several experiments with similar outcomes.

obtained with GTP-only feeds (Figures 4E–H). As already shown for a dinucleotide cap with UTP (Figure 3), in all four combinations combined feeds reduced levels of dsRNA to a lesser extent than single feeds with only UTP or m1ΨTP (Figures 4A–D). Lastly, we observed that dsRNA levels were higher for the reactions with a trinucleotide cap analog. This is more pronounced for reactions with UTP than m1ΨTP. In summary, optimized mRNA production—with high capping and low levels of dsRNA—can be obtained by using a combined feed of GTP and (modified) UTP, independent of the type of cap analog.

To further demonstrate the advantages of the dual feed, we performed the same experiment with RNAs coding for eGFP (Supplementary Figure S1). The effect of the different nucleotide feeds as seen for the luciferase RNA could also be observed for the RNAs encoding eGFP, showing that this is a general effect independent of the mRNA sequence.

3.4 Translational activity is increased for mRNAs produced with a combined feed of GTP and UTP

For mRNAs with a high capping efficiency and low levels of dsRNA, high protein expression was expected because: (i) more mRNAs would be expected to be translated and (ii) less type I interferons should be induced, therefore reducing repression of translation. To verify this, we analyzed the same set of mRNAs coding for luciferase as described above for translatability in cell culture.

For each of the four combinations (di- or tri-nucleotide, with UTP or m1ΨTP), maximal protein expression was observed for the mRNAs produced with the combined feed, GTP and UTP or m1ΨTP (Figure 5). This demonstrated—as expected—that high capping efficiency and low levels of dsRNA increase the translational activity of mRNAs. However, some differences were still observed between the four combinations. For unmodified mRNAs using a dinucleotide cap analog, the single feeds of GTP or UTP yielded about the same level of protein expression (Figure 5A). This suggests that the higher capping with the GTP feed has a similar impact on translation as the lower dsRNA amount with the UTP feed.

As previously shown the combination of unmodified RNA with a trinucleotide cap analog yielded the highest levels of dsRNA (Figure 4A). This might be the reason why with each of the three feeds, protein expression is lowest for the mRNAs capped with a trinucleotide versus those capped with a dinucleotide cap analog (Figures 5A, B). With the trinucleotide cap analog, the UTP feed alone yielded slightly higher protein expression compared with the GTP feed alone (Figure 5C). For the modified mRNAs, i.e., transcribed using m1ΨTP, the dsRNA levels were low for the mRNAs capped with either a di- or a tri-nucleotide cap structure, even with the GTP feed. However, protein expression was still higher for mRNAs transcribed with a combined GTP and m1ΨTP feed. Interestingly, luciferase activity for an mRNA produced with a m1ΨTP feed compared with a combined feed is higher with a dinucleotide cap structure (Figures 5C, D), which may be due to differences in cap structure, as the capping efficiencies for the pairs of mRNAs with the same feed are approximately equal.

Overall, our data show that formation of dsRNA by-products during *in vitro* transcription can be reduced for mRNAs with a poly(A)-tail at the 3′ end by keeping the steady-state concentration of UTP (or m1ΨTP) low. When this is combined with a GTP feed for high capping efficiency, the corresponding mRNAs exhibit increased protein expression in cell culture, in line with the expected effect of highly capped mRNA containing less dsRNA.

4 Discussion

mRNAs used as therapeutics or vaccines need to be translated with high efficiency, while at the same time inducing low reactogenicity. Therefore, reducing production of by-products,

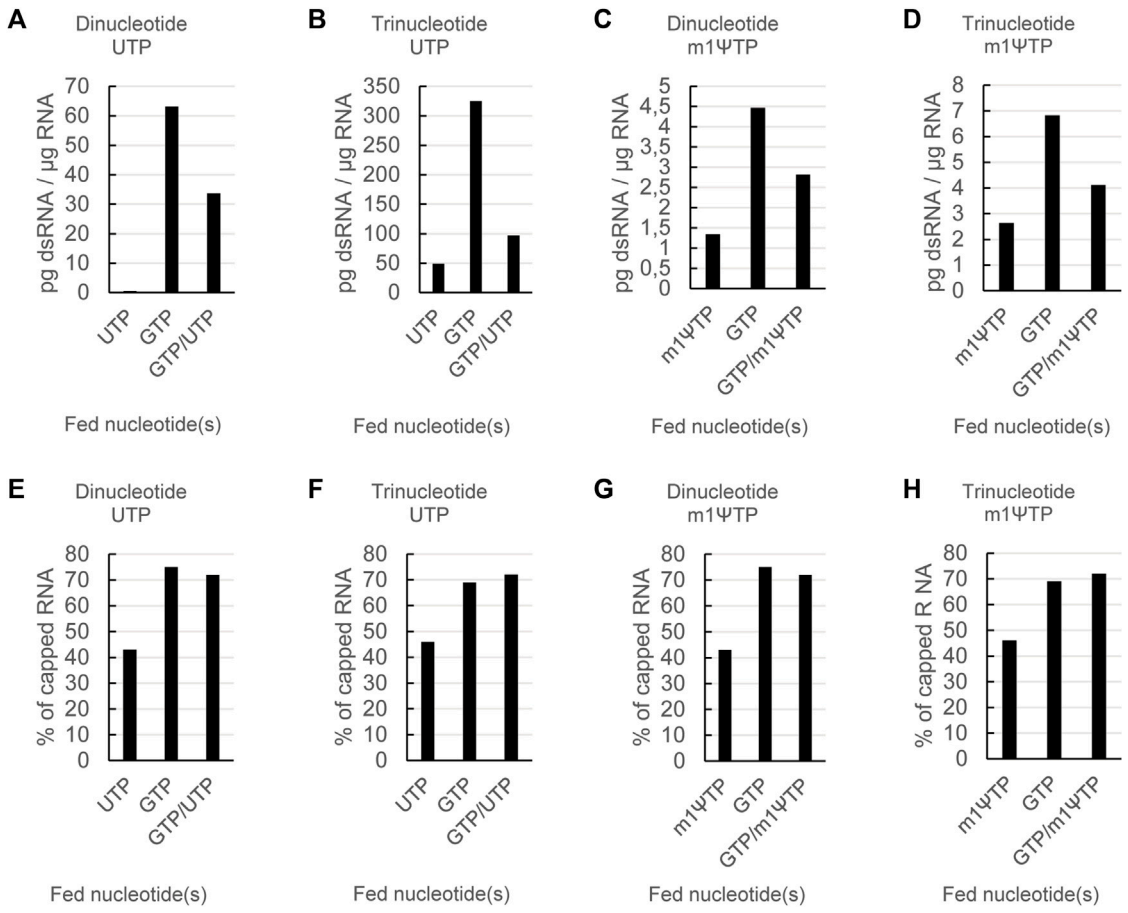

FIGURE 4
The effects of nucleotide feeds on dsRNA and capping are independent of the type of cap analog and whether modified or unmodified UTP is used. RNAs were *in vitro* transcribed either in the presence of a dinucleotide or a trinucleotide cap analog and either using UTP or m1ΨTP with feeding of the indicated nucleotide triphosphates. The resulting RNAs were then analyzed for dsRNA levels **(A)** and capping **(B)**. Please note the different scales for the dsRNA levels in **(A)**.

that can cause immunogenic reactions, such as dsRNA, while retaining translational efficiency is desirable (Kariko et al., 2011). In this study we found that increasing the di- or tri-nucleotide cap analog concentration reduced dsRNA formation and limiting UTP over the course of the *in vitro* transcription reaction led to reduced dsRNA formation in poly(A)-carrying transcripts. Additionally, by combining UTP and GTP feeds, high capping efficiency with reduced dsRNA formation was achieved. Lower dsRNA levels led to higher protein expression from the corresponding mRNAs.

Mechanistically, it is difficult to reason why increasing cap analog concentration results in reduced formation of dsRNA. One possible explanation is that initiation of the reaction is more efficient because higher amounts of cap analog leads to more free promotor sequences, which are available to be bound by T7 RNA polymerase. This in turn might favor the release of T7 RNA polymerases from the DNA templates upon reaching the 3′ end, as all these processes would be expected to happen in equilibrium to a certain extent.

As previously mentioned, during *in vitro* transcription, a major source of dsRNA formation is backward transcription once the RNA polymerase reaches the 3′ end of the DNA template rather than termination (Gholamalipour et al., 2018; Dousis et al., 2023). For DNA templates with an encoded poly(A)-tail these backward transcription events start with a poly(U)-stretch. Here we showed that starting *in vitro* transcription with a low concentration of UTP or m1ΨTP, and then feeding additional UTP or m1ΨTP over the course of the reaction, reduced levels of dsRNA independent of the type of cap analog and regardless of whether UTP or m1ΨTP was used. As expected, this effect was specific for DNA templates encoding a poly(A)-tail at the 3′ end.

Reaching a satisfactory capping efficiency with co-transcriptional capping is a challenge because the cap analog competes with the starting nucleotide for the initiation of a new mRNA. T7 RNA polymerase favors starting transcription with a G (Chamberlin and Ring, 1973) therefore GTP is used at a lower concentration and then fed to the reaction when using dinucleotide cap analogs. As T7 RNA polymerase also has a tendency to skip the first base when transcribing, it is still recommended to have the ratio of cap to GTP as high as possible during the reaction also for the use of AG starting trinucleotides. However, cap analogs are expensive and therefore reducing the GTP concentration is a less expensive way to achieve a ratio in favor of the cap analog rather than further increasing the concentration of the cap analog, with GTP being replenished over the course of the reaction via a GTP feed. Importantly, we observed a reduction in dsRNA formation when UTP

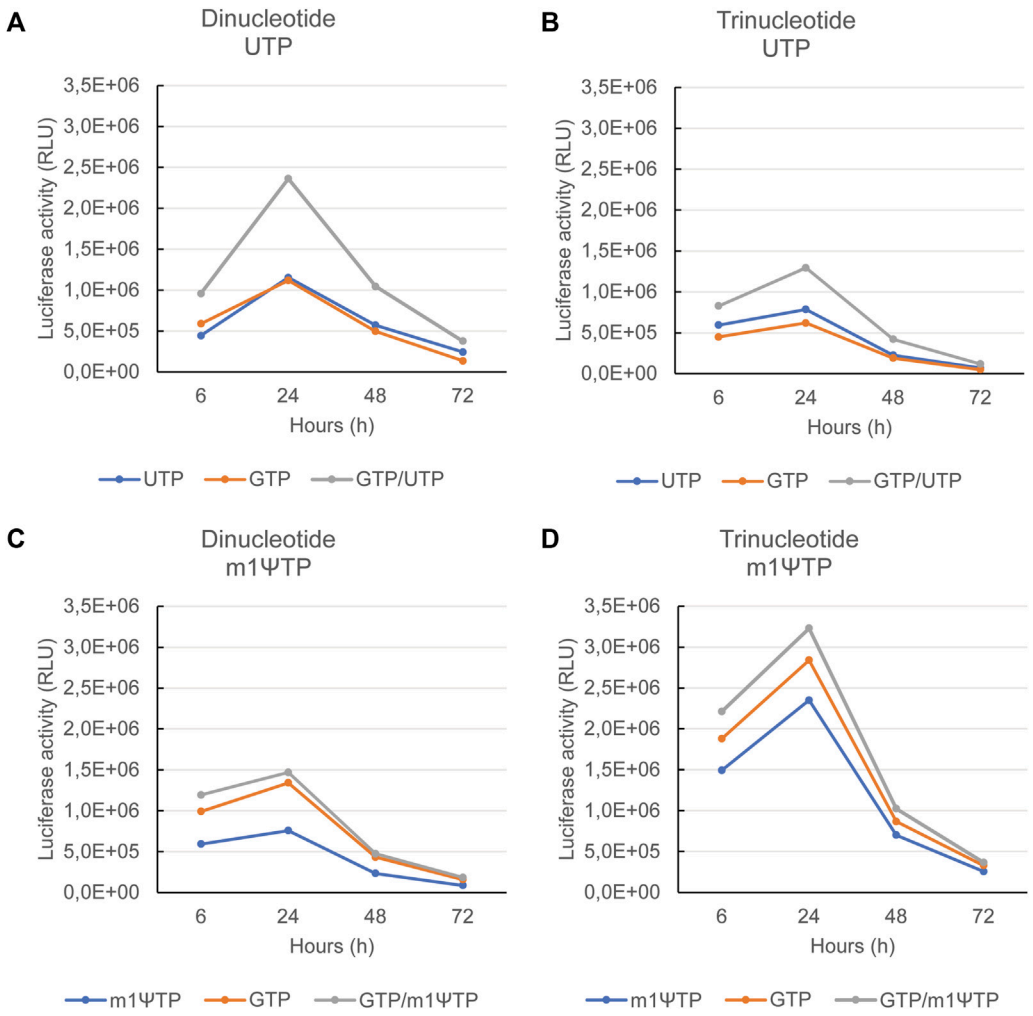

FIGURE 5
Maximal protein expression is observed with mRNAs transcribed using a combined feed of GTP and UTP or m1ΨTP. The mRNAs as also used for the experiments in Figure 4, all coding for luciferase, were transfected into human immature dendritic cells. Upon transfection, luciferase activity was measured 6, 24, 48, and 72 h after transfection. The luciferase activity is depicted for mRNAs capped with a dinucleotide cap analog and using UTP in **(A)**, capped with a trinucleotide cap analog and using UTP in **(B)**, capped with a dinucleotide cap analog and using m1ΨTP in **(C)**, and capped with a trinucleotide cap analog and using m1ΨTP in **(D)**. In each panel, the corresponding feeds are indicated at the bottom. Representative example of several experiments with similar outcomes.

and GTP feeds were combined to ensure a high capping efficiency. However, dsRNA reduction was not as pronounced with the combined feed versus the singular UTP or m1ΨTP feeds. This may be because the low steady-state concentration of GTP leads to impaired transcription initiation. Consequently, this may have partially counteracted the effect of using lower steady-state levels of UTP or m1ΨTP on dsRNA formation. Capping efficiency was improved with both dinucleotide and trinucleotide analogs. Capping efficiency is further improved by keeping the GTP concentration low and this can save costs with respect to expensive cap analogs.

Testing mRNAs produced with different nucleoside triphosphate feeds also allowed us to gain some insight into how capping and dsRNA formation impact protein expression, which may be informative for both pre-clinical and clinical research. Importantly, we showed that mRNAs produced using a combined feed gave the highest levels of protein expression versus singular feeds. This indicates that reducing dsRNA formation during *in vitro* transcription, by lowering the steady-state concentration of UTP, increases protein expression. The impact of reducing dsRNA levels on protein expression is more pronounced for mRNA transcribed with UTP (non-modified mRNA) compared with mRNA transcribed with m1ΨTP (modified mRNA), which is reflected in the absolute amount of dsRNA.

While higher levels of capping appear to correlate with higher levels of protein expression, the correlation may be weaker with trinucleotide versus dinucleotide cap analogs. However, it is difficult to determine whether this may be due to differences between the cap analogs themselves or the effect of different cap structures, i.e., cap0 versus cap1. High capping and low levels of dsRNA formation led to increased translational activity for non-modified and modified mRNAs transcribed in the presence of dinucleotide or trinucleotide cap analogs. The potential benefit of a cap1 structure (Kumar et al., 2014), as obtained with the trinucleotide cap analog, is apparently counteracted by the higher

amounts of dsRNA observed with trinucleotide cap analogs compared with dinucleotide analogs, as the corresponding mRNAs all showed lower protein expression. However, it remains unknown why trinucleotide cap analogs lead to higher levels of dsRNA. Notably, the capping assay we used cannot differentiate between capped mRNA species that have aberrantly initiated and nucleotides that have been added or missed by T7 RNA polymerase. Thus, further work—which is beyond the scope of this study—will be needed to better understand the effects of different cap structures and dsRNA formation on mRNA in reactions with different nucleotide triphosphate feeds.

With the increasing interest in mRNA-based therapies, improved manufacturing processes are needed to allow this technology to reach its full potential. *In vitro* transcription reactions should be optimized when synthesizing exogenous mRNAs. Here, we have shown that low steady-state concentrations of UTP and GTP, fed in combination over the course of the *in vitro* transcription reaction, produces mRNA with high capping and low levels of dsRNA formation, resulting in high levels of protein expression. This novel approach may render laborious purification steps to remove dsRNA unnecessary.

Data availability statement

The raw data supporting the conclusion of this article will be made available by the authors, without undue reservation.

Ethics statement

Ethical approval was not required for the studies involving humans because the *in vitro* studies were performed using dendritic cells generated from human blood buffy coats. The studies were conducted in accordance with the local legislation and institutional requirements. The human samples used in this study were acquired from an external vendor located in Mainz. Written informed consent to participate in this study was not required from the participants or the participants' legal guardians/next of kin in accordance with the national legislation and the institutional requirements.

Author contributions

TZ: Conceptualization, Formal Analysis, Investigation, Methodology, Visualization, Writing–original draft. RF: Formal Analysis, Investigation, Methodology, Visualization, Writing–review and editing. PW: Formal Analysis, Investigation, Methodology, Visualization, Writing–review and editing. KG: Investigation, Methodology, Visualization, Writing–review and editing. SK: Formal Analysis, Investigation, Methodology, Visualization, Writing–review and editing. ML: Formal Analysis, Investigation, Methodology, Visualization, Writing–review and editing. MB: Formal Analysis, Investigation, Methodology, Visualization, Writing–review and editing. SF: Conceptualization, Supervision, Writing–review and editing. US: Conceptualization, Supervision, Writing–review and editing. AK: Conceptualization, Supervision, Writing–original draft.

Funding

The author(s) declare financial support was received for the research, authorship, and/or publication of this article. This work was funded by BioNTech SE.

Acknowledgments

We thank all current and former members of the RNA Synthesis Unit, Elena Böhm, Rekia Sinderwald, Franziska Kraft, Christin Berger, Fabrizio Santangelo, Shahrzad Karimzadeh, Sergey Bessonov, Veronika Georgieva; as well as the whole RNA Biochemistry and Protein Replacement departments and Madeleine Nowak (BioNTech SE) for medical writing and editorial assistance.

Conflict of interest

Authors TZ, RF, PW, KG, SK, ML, MB, SF, US, and AK were employed by BioNTech SE.

Publisher's note

Supplementary material

The Supplementary Material for this article can be found online at: https://www.frontiersin.org/articles/10.3389/fmolb.2023.1291045/full#supplementary-material

References

Baiersdorfer, M., Boros, G., Muramatsu, H., Mahiny, A., Vlatkovic, I., Sahin, U., et al. (2019). A facile method for the removal of dsRNA contaminant from *in vitro*-Transcribed mRNA. *Mol. Ther. Nucleic Acids* 15, 26–35. doi:10.1016/j.omtn.2019.02.018

Berensmeier, S. (2006). Magnetic particles for the separation and purification of nucleic acids. *Appl. Microbiol. Biotechnol.* 73 (3), 495–504. doi:10.1007/s00253-006-0675-0

Chamberlin, M., and Ring, J. (1973). Characterization of T7-specific ribonucleic acid polymerase. *J. Biol. Chem.* 248 (6), 2235–2244. doi:10.1016/S0021-9258(19)44211-7

Cheetham, G. M. T., Jeruzalmi, D., and Steitz, T. A. (1999). Structural basis for initiation of transcription from an RNA polymerase–promoter complex. *Nature* 399 (6731), 80–83. doi:10.1038/19999

Dousis, A., Ravichandran, K., Hobert, E. M., Moore, M. J., and Rabideau, A. E. (2023). An engineered T7 RNA polymerase that produces mRNA free of immunostimulatory byproducts. *Nat. Biotechnol.* 41 (4), 560–568. doi:10.1038/s41587-022-01525-6

Galloway, A., and Cowling, V. H. (2019). mRNA cap regulation in mammalian cell function and fate. *Biochim. Biophys. Acta Gene Regul. Mech.* 1862 (3), 270–279. doi:10.1016/j.bbagrm.2018.09.011

Gao, M., Fritz, D. T., Ford, L. P., and Wilusz, J. (2000). Interaction between a poly(A)-specific ribonuclease and the 5' cap influences mRNA deadenylation rates *in vitro*. *Mol. Cell* 5 (3), 479–488. doi:10.1016/s1097-2765(00)80442-6

Gholamalipour, Y., Karunanayake Mudiyanselage, A., and Martin, C. T. (2018). 3' end additions by T7 RNA polymerase are RNA self-templated, distributive and diverse in character-RNA-Seq analyses. *Nucleic Acids Res.* 46 (18), 9253–9263. doi:10.1093/nar/gky796

Kariko, K., Muramatsu, H., Ludwig, J., and Weissman, D. (2011). Generating the optimal mRNA for therapy: HPLC purification eliminates immune activation and improves translation of nucleoside-modified, protein-encoding mRNA. *Nucleic Acids Res.* 39 (21), e142. doi:10.1093/nar/gkr695

Konarska, M. M., Padgett, R. A., and Sharp, P. A. (1984). Recognition of cap structure in splicing *in vitro* of mRNA precursors. *Cell* 38 (3), 731–736. doi:10.1016/0092-8674(84)90268-X

Kuhn, A. N., Diken, M., Kreiter, S., Selmi, A., Kowalska, J., Jemielity, J., et al. (2010). Phosphorothioate cap analogs increase stability and translational efficiency of RNA vaccines in immature dendritic cells and induce superior immune responses *in vivo*. *Gene Ther.* 17 (8), 961–971. doi:10.1038/gt.2010.52

Kumar, P., Sweeney, T. R., Skabkin, M. A., Skabkina, O. V., Hellen, C. U., and Pestova, T. V. (2014). Inhibition of translation by IFIT family members is determined by their ability to interact selectively with the 5'-terminal regions of cap0-cap1- and 5'ppp-mRNAs. *Nucleic Acids Res.* 42 (5), 3228–3245. doi:10.1093/nar/gkt1321

Mu, X., Greenwald, E., Ahmad, S., and Hur, S. (2018). An origin of the immunogenicity of *in vitro* transcribed RNA. *Nucleic Acids Res.* 46 (10), 5239–5249. doi:10.1093/nar/gky177

Pasquinelli, A. E., Dahlberg, J. E., and Lund, E. (1995). Reverse 5' caps in RNAs made *in vitro* by phage RNA polymerases. *RNA* 1 (9), 957–967.

Piao, X., Yadav, V., Wang, E., Chang, W., Tau, L., Lindenmuth, B. E., et al. (2022). Double-stranded RNA reduction by chaotropic agents during *in vitro* transcription of messenger RNA. *Mol. Ther. Nucleic Acids* 29, 618–624. doi:10.1016/j.omtn.2022.08.001

Sahin, U., Kariko, K., and Tureci, O. (2014). mRNA-based therapeutics--developing a new class of drugs. *Nat. Rev. Drug Discov.* 13 (10), 759–780. doi:10.1038/nrd4278

Sahin, U., Muik, A., Derhovanessian, E., Vogler, I., Kranz, L. M., Vormehr, M., et al. (2020). COVID-19 vaccine BNT162b1 elicits human antibody and T(H)1 T cell responses. *Nature* 586 (7830), 594–599. doi:10.1038/s41586-020-2814-7

Stepinski, J., Waddell, C., Stolarski, R., Darzynkiewicz, E., and Rhoads, R. E. (2001). Synthesis and properties of mRNAs containing the novel "anti-reverse" cap analogs 7-methyl(3'-O-methyl)GpppG and 7-methyl (3'-deoxy)GpppG. *RNA* 7 (10), 1486–1495.

Triana-Alonso, F. J., Dabrowski, M., Wadzack, J., and Nierhaus, K. H. (1995). Self-coded 3'-extension of run-off transcripts produces aberrant products during *in vitro* transcription with T7 RNA polymerase. *J. Biol. Chem.* 270 (11), 6298–6307. doi:10.1074/jbc.270.11.6298

Wolff, J. A., Malone, R. W., Williams, P., Chong, W., Acsadi, G., Jani, A., et al. (1990). Direct gene transfer into mouse muscle *in vivo*. *Science* 247 (4949 Pt 1), 1465–1468. doi:10.1126/science.1690918

Wu, M. Z., Asahara, H., Tzertzinis, G., and Roy, B. (2020). Synthesis of low immunogenicity RNA with high-temperature *in vitro* transcription. *RNA* 26 (3), 345–360. doi:10.1261/rna.073858.119

frontiers | Frontiers in Molecular Biosciences

TYPE Brief Research Report
PUBLISHED 06 February 2024
DOI 10.3389/fmolb.2023.1269028

OPEN ACCESS

EDITED BY
Andreas Kuhn,
BioNTech, Germany

REVIEWED BY
Mateusz Wilamowski,
Jagiellonian University, Poland
Umesh Kalathiya,
University of Gdańsk, Poland

*CORRESPONDENCE
Renata Grzela,
rgrzela@fuw.edu.pl
Marzena Jankowska-Anyszka,
marzena@chem.uw.edu.pl

RECEIVED 28 July 2023
ACCEPTED 13 December 2023
PUBLISHED 06 February 2024

CITATION
Kurpiejewski K, Stankiewicz-Drogon A, Piecyk K, Rajkowska E, Skrzypczyk P, Geng J, Darzynkiewicz E, Grzela R and Jankowska-Anyszka M (2024), The potential of N2-modified cap analogues for precise genetic manipulation through mRNA engineering.
Front. Mol. Biosci. 10:1269028.
doi: 10.3389/fmolb.2023.1269028

The potential of N2-modified cap analogues for precise genetic manipulation through mRNA engineering

Karol Kurpiejewski[1], Anna Stankiewicz-Drogon[2], Karolina Piecyk[1], Eliza Rajkowska[1], Paulina Skrzypczyk[1], Jingping Geng[3], Edward Darzynkiewicz[3], Renata Grzela[2]* and Marzena Jankowska-Anyszka[1]*

[1]Faculty of Chemistry, University of Warsaw, Warsaw, Poland, [2]Division of Biophysics, Institute of Experimental Physics, Faculty of Physics, University of Warsaw, Warsaw, Poland, [3]Centre of New Technologies, University of Warsaw, Warsaw, Poland

The technology of mRNA-based drugs is currently being intensively developed and implemented. Medical products of this type are already being used as viral vaccines and could potentially find application in a wide range of diseases. The tremendous interest in mRNA is due to the relatively easy production process, which can be quickly adapted to meet societal needs. The properties of this molecule depend on the structure of its individual components, such as the structure of the cap at the 5′ end. Modifications of the cap significantly affect the translational potential and lifespan of the whole mRNA. In the current work, we present the synthesis of derivatives of cap analogues modified at the N2 position of 7-methylguanosine. In addition to the substituent at the N2 position, the derivatives had either an extended triphosphate chain, a thiophosphate modification, an added cap1-modified nucleotide or an extended linker between the substituent and 7-methylguanosine. The compounds were tested for use as translation inhibitors and as components for mRNA preparation and appeared of interest for both applications.

KEYWORDS

cap analogues, mRNA engineering, mRNA-based drugs, mRNA therapeutics, mRNA technology

1 Introduction

Before 2020, few would have considered mRNA vaccines could become so quickly a "game-changer" in the fight against serious health and life-threatening diseases. The turning point in the perception of mRNA-based technology in medical application came with the SARS-CoV-2 virus pandemic. One of the greatest advantages of mRNA is that it can be easily modified. The improvement of stability and translational efficiency of mRNA is often achieved by modifications of the cap structure at the 5′ end.

The cap structure is a natural modification that consists of a 7-methylguanosine linked by a 5′–5′ triphosphate bridge to the first transcribed nucleotide (Supplementary Figure S1A) (Furuichi, 2015). Cap plays a key role in many aspects of mRNA metabolism providing protection against nucleolytic degradation and allowing mRNA recruitment to ribosome by eIF4E (Furuichi, 2015). In cells, there are three types of caps, cap0, 1 and 2. Cap0 is the

simplest possible structure, bearing no additional methylation on the first transcribed nucleotide within the ribose. In mammalian cells, mRNAs are usually terminated by m^7GpppN_m or $m^7GpppN1_mN2_m$ called cap1 and cap2, respectively, where N_m is the 2′-*O*-methylated nucleotide (Züst et al., 2011) and the role of this modification is to differentiate between "self" and "non-self" RNA during viral infection.

It is known that factor eIF4E, when overexpressed, contributes to increased translation of proteins associated with cell division which leads to tumorigenesis (Lazaris-Karatzas et al., 1990). Modified cap analogues, most often in the form of mono- or dinucleotides, that have a high affinity for eIF4E, can act as potential translation inhibitors. Additionally, dinucleotides can be effectively used to prepare mRNA transcripts with high translational activity (Shanmugasundaram et al., 2022). Attractive analogues, which showed several times higher affinity for eIF4E, turned out to be those with aliphatic, cyclic and aromatic substituents within the exocyclic N2-amino group of N7-methylated guanine (Cai et al., 1999; Piecyk et al., 2012; 2014). It is also known that elongation of the phosphate bridge usually leads to better inhibitory properties of cap analogue. This is explained by a stronger interaction with eIF4E due to the formation of additional water-mediated hydrogen bonds and salt bridges (Rydzik et al., 2009).

Currently, the most common method for preparation of capped mRNA is incorporation of a dinucleotide by an RNA polymerase during the *in vitro* transcription (IVT) reaction. However, the existence of two free 3′-OH groups on both guanosine moieties allows transcription elongation on both sides, resulting in a translationally active product with cap structure introduced in the correct orientation of $m^7GpppG(pN)_n$ but also translationally inactive mRNA with cap in the reverse orientation of $Gpppm^7G(pN)_n$ (Pasquinelli et al., 1995). The solution to this problem came with the discovery of ARCA-type analogues (Anti-Reverse Cap Analogues) bearing an O-methyl group at the C2′ or C3′ position of 7-methylguanosine. These were the first dinucleotide cap analogues to enable incorporation almost exclusively in the correct orientation (Supplementary Figure S1B) (Grudzien-Nogalska et al., 2007a). Subsequent modifications of ARCA within the phosphate bridge showed that β-modification in the form of a thiophosphate (β-S-ARCA) increased mRNA stability while ensuring similar or increased translation efficiency (Grudzien-Nogalska et al., 2007a). Moreover, enrichment of ARCA with a benzyl substituent at the N2 position yielded mRNA with increased translational properties and higher stability *in vivo* compared to m^7GpppG- or ARCA-capped transcripts (Kocmik et al., 2018). In our previous studies, we presented a series of N2-modified dinucleotide cap analogues without a methyl group at the 2′-*O* or 3′-*O* position, that were both efficiently and mostly in correct orientation incorporated into mRNA chain and resulted in a highly efficient translation (Grzela et al., 2022). Such dinucleotides have become an alternative to ARCA-type analogues.

Obtaining mRNA transcripts by IVT using dinucleotide analogues has some limitations. First, to ensure a high transcription yield, purine must be present as the first transcribed nucleotide. Second, the 2′-*O* modification of the first transcribed nucleotide (cap1) prevents the incorporation of such an analogue during IVT. The novel idea of using trinucleotide analogues of cap containing such modification (m^7GpppN_mpN) avoids these limitations and has been already used to obtain Pfizer-BioNTech's mRNA vaccine against SARS-CoV-2 (Ishikawa et al., 2009).

In this work, we continued our research on cap analogues modified within the exocyclic amino group. We synthesized a series of N2-modified dinucleotide analogues: triphosphate, β-S triphosphate and tetraphosphate compounds as well as three trinucleotides, bearing aromatic N2 substitution (on the m^7G side), and evaluated their properties in biological experiments.

2 Methods

2.1 Synthesis

All presented compounds were obtained according to synthetic procedures described in detail in Supplementary Material.

2.2 Synthesis of luciferase encoding mRNAs

A PCR product encompassing the firefly luciferase coding sequence under the T7 RNA polymerase promoter was used as the template for the IVT reaction. Transcription buffer, 25 ng/μL dsDNA template, 0.5 mM ATP/CTP/UTP, 0.1 mM GTP, 0.5 mM dinucleotide analogue of cap (cap:GTP molar ratio was 5:1), 0.5 U/μL Ribolock ribonuclease inhibitor and 1 U/μL RNA polymerase T7 (Thermo Fisher Scientific) were added to the reaction mix (Strenkowska et al., 2016). The transcription reaction was incubated for 1 h at 37°C, followed by the addition of 0.025 U/μL DNaseI (Thermo Scientific) and incubation for 20 min at 37°C. The prepared transcripts were purified using NucleoSpin® RNA Clean-Up (Macherey-Nagel) according to the manufacturer's instructions. The integrity of the transcripts was tested on a non-denaturing 1% agarose gel and the concentration was measured spectrophotometrically.

2.3 Translation measurement in the RRL system

The expression level of luciferase mRNA bearing the synthesized cap analogues was measured in the Flexi Rabbit Reticulocyte Lysate System, Promega, (Strenkowska et al., 2016). The reaction mixture contained 40% Flexi RRL lysate, 0.01 mM amino acid mixture, 0.9 mM magnesium acetate (1.8 mM endogenous magnesium concentration in the lysate) and 190 mM potassium acetate. Samples were preincubated for 60 min at 30°C before the addition of mRNA. The translation reaction was carried out under the same conditions for another 60 min. The activity of the synthesized luciferase was measured using a Glomax luminometer.

2.4 Translation inhibition

The inhibitory activities of the new cap analogues were tested using Flexi Rabbit Reticulocyte Lysate, Promega, under

10.3389/fmolb.2023.1269028

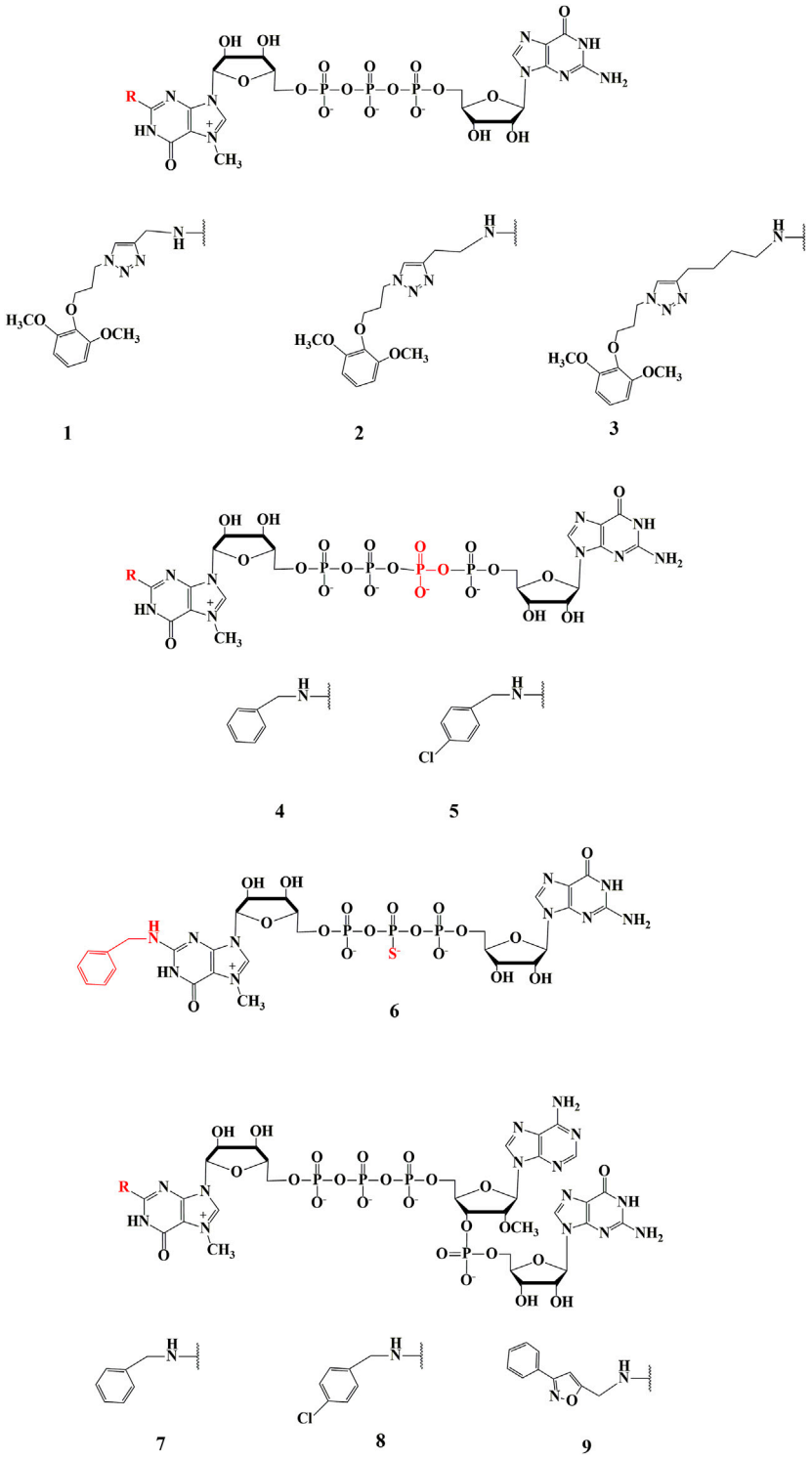

FIGURE 1
Structure of new cap analogues, modified at N2 position of m7-guanosine. **1**—(4-(diOCH$_3$-bn)-tz-CH$_2$)^{2}m^{7}GpppG, **2**—(4-(diOCH$_3$–bn)-tz-(CH$_2$)$_2$)^{2}m^{7}GpppG, **3**—(4-(diOCH$_3$–bn)-tz-(CH$_2$)$_4$)^{2}m^{7}GpppG, **4**—(bn^{2}m^{7}GppppG, **5**—(4-Cl-bn)^{2}m^{7}GppppG, **6**—bn^{2}m^{7}Gpp$_s$pG, **7**—bn^{2}m^{7}GpppA$_m$pG, **8**—(4-Cl-bn)^{2}m^{7}GpppA$_m$pG, **9**—(4-bn-isx)^{2}m^{7}GpppA$_m$pG.

conditions specified for cap-dependent translation (Kowalska et al., 2009). Briefly, the reaction mixture was pre-incubated for 60 min at 30°C, followed by the addition of a mixture of ARCA-mRNA encoding the firefly luciferase and the cap analogue under study. Samples were incubated for further 60 min at 30°C. Luciferase activity was measured using a Glomax luminometer (Promega). IC_{50} values were determined by non-linear regression analysis of the experimental data using

GraphPad Prism 8. IC_{50} values are mean ± SD from at least three independent replicates.

2.5 Synthesis of short RNAs and cap hydrolysis with hNudt16

The annealing product of two complementary primers: 5′ CAG TAATACGACTCACTATA**G**GGAAGCGGGCATGCGGCCAGC CATAGCCGATCA 3′ and 5′ TGATCGGCTATGGCTGGCCGC ATGCCCGCTTCC**C**TATAGTGAGTCGTATTACTG 3′ was used as a template for short RNA synthesis. Thus obtained dsDNA contained the sequence of T7 promoter and G at position +1 (bold). Capping was performed co-transcriptionally during IVT. Transcripts were purified on Oligo Clean-Up and Concentration columns (Norgen Biotek) followed by DNAzyme trimming and subsequent purification (Grzela et al., 2022). 100 ng of analogue-capped RNA was digested with 2.5 μM hNudt16 and loaded onto 15% polyacrylamide/7 M urea TBE gel as described previously (Grzela et al., 2022). To assess both capping efficiency and the amount of decapped product, a densitometric analysis with the use of Image Lab software (Bio-Rad) was applied. Decapping was calculated as the per cent loss in the capped band after addition of the enzyme. The data represent the means ± SD from three experiments.

2.6 Statistical analysis

All statistical analyses were performed with GraphPad Prism 8 software. One-way ANOVA with *post hoc* Turkey test was used. Statistical significance in *p*-value is denoted in asterixes $^{****}p < 0.0001$, $^{***}p < 0.001$, and $^{**}p < 0.01$ and the data are shown as mean ± SD.

3 Results

3.1 Chemistry

Our current research concerns the synthesis and biological studies of three groups of N2-modified cap analogues. The first group consists of dinucleotides modified only within the exocyclic amino group of the m^7G moiety (Figure 1A) with a modified triazole ring attached to N2 position via aliphatic linkers of different lengths. The second group consists of dinucleotide analogues modified both at the N2 position of 7-methylguanosine with aromatic substituents and within the 5′-5′ bridge in the form of tetraphosphate or β-thiophosphate (Figures 1B, C). The last group consists of trinucleotides containing modified m^7G moiety in the N2 position with aromatic substituents (benzyl, p-chlorobenzyl and isoxazole) and 2′-O-methylated adenosine as the first transcribed nucleotide (characteristic for cap1) connected via 3′,5′-phosphodiester bond to guanosine ($R^2m^7GpppA_mpG$ shown in Figure 1D).

The synthesis of N2-modified dinucleotide cap analogues has already been described (Piecyk et al., 2015; Grzela et al., 2022). Therefore, compounds 1-3 were obtained in an analogous procedure, with compound 1 synthesized again as a reference for biological studies.

Tetraphosphate analogues (4–5) were obtained using a method for the synthesis of a simpler analogue such as $m^7GppppN$ (Rydzik et al., 2009). This method requires the preparation of two 5′-diphosphate subunits (GDP and m^7GDP), one of which must be converted to an imidazole derivative using Mukaiyama method (Mukaiyama and Hashimoto, 1972) to increase the susceptibility to nucleophilic attack of the second subunit in the coupling reaction with a $ZnCl_2$ catalyst under anhydrous conditions (Kadokura et al., 1997). In the course of our research, N2-substituted 7-methylguanosine 5′ diphosphate (7) (R^2m^7GDP) and an imidazole derivative of guanosine 5′ diphosphate (im-GDP), were synthesized and subjected to a coupling reaction to obtain a series of tetraphosphate N2-modified dinucleotides.

Compound (6) was obtained analogous to the procedure reported for the synthesis of m^7Gpp_spG (Kowalska et al., 2008). In the first step, 5′ monophosphate of N2-benzyl, 7-methylguanosine (bn^2m^7GMP), was obtained and converted to its imidazole derivative (im-bn^2m^7GMP). Thus prepared compound was subjected to a coupling reaction using triethylammonium thiophosphate in the presence of $ZnCl_2$ catalyst to obtain the diphosphate derivative $bn^2m^7Gpp_S$, which was further subjected to the coupling reaction with an imidazole derivative of GMP yielding the product in the form of two diastereoisomers. Since attempts to separate each isomer were unsuccessful, a mixture of diastereoisomers was used for biological experiments.

Trinucleotide analogues of cap (7–9) were obtained in a multistep synthesis, where in the final reaction, the two nucleotide subunits of im-R^2m^7GDP and pA_mpG were linked together in a coupling reaction analogous to the one used for preparation of dinucleotides. The im-R^2m^7GDP subunit was prepared according to previously described methods. The pA_mpG dinucleotide was synthesized in three steps using the amidophosphite method (Senthilvelan et al., 2021). In the first step, coupling reactions of the commercially available 5′-O-dimetoxytrityl-N-benzoyl-2′-O-methyladenosine 3′-cyanoethyl phosphoramidite with N2-iso butyryl-2′,3′-isopropylideneguanosine were carried out according to the protocol (Eisenführ et al., 2003). The coupling reactions were conducted in acetonitrile and the presence of 5-(benzylthio)-1H-tetrazolium as activator while the oxidation was carried out using iodine to obtain the appropriately protected A_mpG dinucleotide. In a subsequent step, the protecting group was removed from the 5′-OH position using dichloroacetic acid while the ketal protection was removed using trifluoroacetic acid. Thus the indirectly deprotected dinucleotide was phosphorylated at 5′-OH position by the Yoshikawa method (Yoshikawa et al., 1969), and finally deprotection was performed using an aqueous ammonia solution to obtain the desired dinucleotide pA_mpG.

All dinucleotides and trinucleotides were isolated from the reaction mixtures and purified by ion-exchange chromatography described in Methods (Supplementary Material). The structure and homogeneity of each compound was confirmed by HPLC, high-resolution mass spectrometry with positive electrospray ionisation (HRMS-ESI) and ^1H and ^{31}P NMR.

10.3389/fmolb.2023.1269028

TABLE 1 Biological proprieties of novel cap analogues and analogue-capped mRNA.

Cap analogue	IC50 ± SD (μM)	Relative translation efficiency ±SD	Relative cap-dependent translation efficiency	Capping ±SD (%)	Decapping ±SD (%)	References
m^7GpppG	8.94 ± 0.86	1	1	74.30	45.74 ± 3.42	Grzela et al. (2018)
bn^2m^7GpppG	0.61 ± 0.04	3.30 ± 0.77	3.52 ± 0.82	80.50	29.05 ± 3.72	Grzela et al. (2022)
(4-Cl-bn)$^2m^7$GpppG	0.98 ± 0.13	3.29 ± 0.74	3.52 ± 0.73	88.20	26.45 ± 7.34	Grzela et al. (2018)
(4-bn-isx)$^2m^7$GpppG	0.57 ± 0.06	3.37 ± 0.84	3.51 ± 0.82	88.50	33.25 ± 7.16	Grzela et al. (2022)
Newly Synthesized Derivatives						
m^7GpppG	12.98 ± 5.07	1	1	70.60 ± 4.91	52.77 ± 10.82	this work
ARCA	nd	1.51 ± 0.08	1.56 ± 0.10	61.87 ± 3.60	6.70 ± 1.85	this work
ApppG	nd	0.08 ± 0.03	0	94.57 ± 1.78 (GpppG)	87.87 ± 4.69 (GpppG)	this work
$bn^2m^7GpppA_mpG$ (7)	1.38 ± 1.02	3.25 ± 0.32	3.43 ± 0.40	90.22 ± 7.65	7.62 ± 2.48	this work
(4-Cl-bn) $^2m^7GpppA_mpG$ (8)	2.66 ± 1.73	3.72 ± 0.28	3.94 ± 0,36	91.51 ± 3.81	6.73 ± 4.20	this work
(4-bn-isx) $^2m^7GpppA_mpG$ (9)	1.57 ± 0.95	3.31 ± 0.25	3.49 ± 0.32	nd	nd	this work
bn^2m^7GppppG (4)	0.43 ± 0.28	2.68 ± 0.34	2.82 ± 0.41	88.55 ± 4.60	37.40 ± 14.99	this work
(4-Cl-bn)$^2m^7$GppppG (5)	0.60 ± 0.50	2.91 ± 0.52	3.07 ± 0.58	92.00 ± 7.21	55.07 ± 6.73	this work
(4-(diOCH$_3$-bn)-tz-CH$_2$) $^2m^7$GpppG (1)	2.61 ± 1.74	2.27 ± 0.20	2.36 ± 0.25	85.63 ± 2.10	11.50 ± 1.50	this work
(4-(diOCH$_3$-bn)-tz-(CH$_2$)$_2$)$^2m^7$GpppG (2)	0.85 ± 0.51	2.49 ± 0.16	2.60 ± 0.17	85.77 ± 7.00	29.70 ± 5.40	this work
(4-(diOCH$_3$-bn)-tz-(CH$_2$)$_4$)$^2m^7$GpppG (3)	1.73 ± 1.37	2.66 ± 0.09	2.83 ± 0.10	82.13 ± 2.72	12.40 ± 2.42	this work
bn^2m^7GppspG (6)	0.45 ± 0.11	2.58 ± 0.28	2.75 ± 0.31	78.00 ± 4.70	2.60 ± 1.39	this work

3.2 Inhibition

The protein biosynthesis process depends on the delivery of the information encoded on the mRNA to ribosomes by the eIF4E protein. The efficiency of this process is related to the affinity of eIF4E to the cap structure located at the 5′ end of the mRNA. The addition of a free cap analogue with high affinity for eIF4E impairs protein synthesis. Therefore, new compounds are routinely tested for their ability to inhibit translation. For this purpose, we used an extracellular translation system from rabbit reticulocytes (RRL). We added the ARCA-bearing mRNA encoding firefly luciferase to an RRL extract containing all factors necessary for protein synthesis and measured the bioluminescence level. To the subsequent sample, we added increasing amounts of newly synthesized cap analogues and observed changes in bioluminescence relative to the control sample without free cap analogue. Compounds bn^2m^7GppppG (4) and (4-Cl-bn)$^2m^7$GppppG (5) turned out to be the most effective inhibitors, with IC_{50} of 0.43 ± 0.16 and 0.60 ± 0.29, respectively (Table 1; Figure 2A). These compounds are tetraphosphates of the derivatives described previously (Grzela et al., 2022), that have shown strong inhibition of protein biosynthesis. Here, an even stronger inhibitory effect was observed. This can be explained by the presence of an additional phosphate in the triphosphate chain that enhance the interaction between cap and eIF4E.

Compound $bn^2m^7Gpp_spG$ (6) appeared as potent translational inhibitor as bn^2m^7GppppG (4) with an IC_{50} of 0.45 ± 0.05 (Table 1; Figure 2A). For the trinucleotide analogues ($bn^2m^7GpppA_mpG$ (7), (4-Cl-bn)$^2m^7GpppA_mpG$ (8), (4-bn-isx)$^2m^7GpppA_mpG$ (9)), the IC_{50} values ranged from 1.38 ± 0.59 to 2.66 ± 1.0, while for compounds with longer linkers [(4-(diOCH$_3$-bn)-tz-CH$_2$)$^2m^7$GpppG (1), (4-(diOCH$_3$-bn)-tz-(CH$_2$)$_2$)$^2m^7$GpppG (2), (4-(diOCH$_3$-bn)-tz-(CH$_2$)$_4$) $^2m^7$GpppG (3)] from 0.85 ± 0.30 to 2.61 ± 1.0 (Table 1; Figure 2A). Although these scores are higher, still the studied compounds represent more potent inhibitors of translation than m^7GppppG.

3.3 Translational properties of mRNA capped with newly synthesized cap analogues

An extracellular translation system from RRL was used to assess the translational properties of mRNAs containing newly synthesized

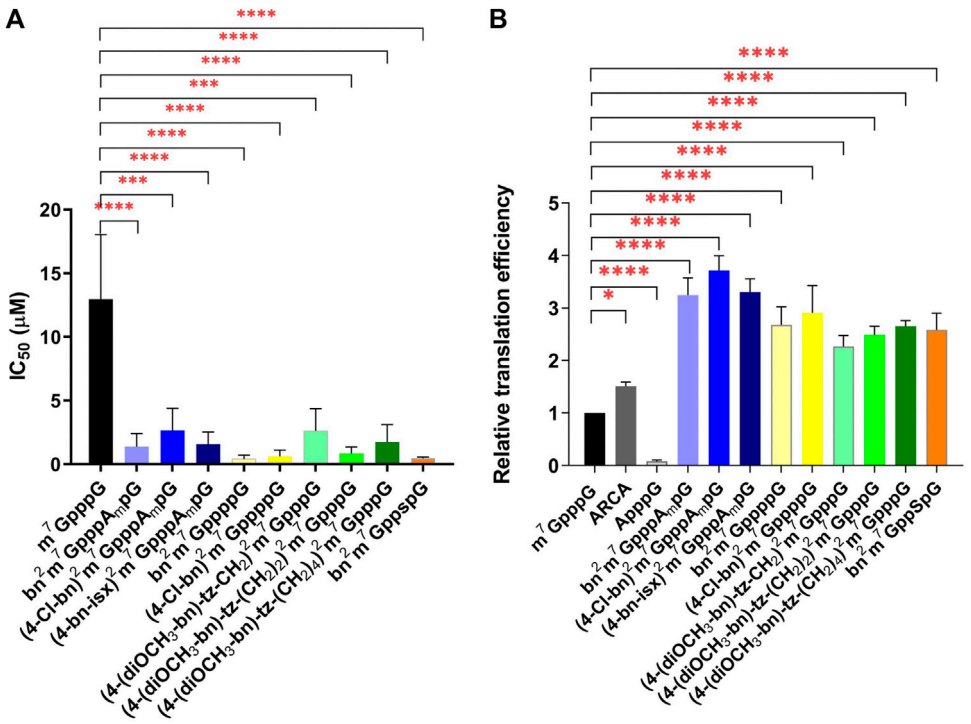

FIGURE 2
Properties of new N2-modified cap analogues in RRL. **(A)** Cap analogues as translational inhibitors. The graph represents inhibition of translation of ARCA-capped mRNA encoding firefly luciferase in RRL upon addition of cap analogues. IC_{50} stands for the cap analogue concentration that inhibits luciferase activity by 50%. IC_{50} values were determined by non-linear regression analysis of the experimental data using GraphPad Prism 8 and are presented as mean ± SD of at least three independent replicates. **(B)** Translational properties of mRNAs capped with N2-modified analogues. Luciferase activity presented in the graph reflects the level of translation in RRL of analogue-capped mRNA encoding firefly luciferase. Data are presented as mean ± SD of at least three independent experiments.

cap analogues. Analogue-capped mRNAs encoding luciferase were added to the extracts and protein activity was measured. The highest levels of luciferase synthesis were provided by mRNAs with trinucleotide derivatives $bn^2m^7GpppA_mpG$ (7), $(4\text{-Cl-bn})^2m^7GpppA_mpG$ (8), and $(4\text{-bn-isx})^2m^7GpppA_mpG$ (9). The translation level of mRNA capped with these derivatives was 3.31, 3.25 and 3.72 times higher than that of m^7GpppG-mRNA, respectively (Table 1; Figure 2B).

Transcripts bearing derivatives with a tetraphosphate bridge, $bn^2m^7GppppG$ (4) and $(4\text{-Cl-bn})^2m^7GppppG$ (5), showed lower translational properties compared to their initial compounds bn^2m^7GpppG and $(4\text{-Cl-bn})^2m^7GpppG$ (Table 1). RNA capped with compounds that differ in linker length $(4\text{-(diOCH}_3\text{-bn)-tz-CH}_2)^2m^7GpppG$ (1), $(4\text{-(diOCH}_3\text{-bn)-tz-(CH}_2)_2)^2m^7GpppG$ (2), $(4\text{-(diOCH}_3\text{-bn)-tz-(CH}_2)_4)^2m^7GpppG$ (3) show very similar level of translation, e.g., around 2.2–2.6 times higher than observed for m^7GpppG-RNA (Table 1). RNA bearing cap analogue with a thiophosphate modification $bn^2m^7GppspG$ (6) showed 2.6 times higher translation than m^7GpppG-RNA (Table 1; Figure 2B).

3.4 Capping efficiency of RNA

To assess the incorporation of cap analogues, we used short RNAs that, after synthesis, were visualized on a UREA-PAGE gel. Such gels have a high capacity to separate products that differ in length by one nucleotide. The mRNA chain without the cap analogue has a length of 24 nt and is denoted by NC in Figure 3. When the cap analogue is attached, the short RNA migrates higher depending on whether a dinucleotide (25 nt) or a trinucleotide (26 nt) is attached. Residual products are also visible on the gel, which is due to the properties of the RNA polymerase, which has the ability to fall off the template before the product is completed or to further attach nucleotides off-template. Control caps: GpppG, m^7GpppG, and ARCA showed expected incorporation efficiencies (Grzela et al., 2022) of 94.57%, 70.60% and 61.87%, respectively (Figure 3; Table 1). The trinucleotides ($bn^2m^7GpppA_mpG$ (7) and $(4\text{-Cl-bn})^2m^7GpppA_mpG$ (8)) had a very high incorporation efficiency of 90.22% and 91.51%, similarly $bn^2m^7GppppG$ (4) and $(4\text{-Cl-bn})^2m^7GppppG$ (5) (88.55% and 92.00%, respectively) while the percentage of incorporation of remaining dinucleotide caps into mRNA ranged from 78.00% to 85.77% (Figure 3; Table 1).

3.5 Orientation of incorporation

Next, we estimated the orientation of cap incorporation into RNA. For this purpose, we used an assay we developed with the enzyme hNudt16 (Grzela et al., 2022). In a certain concentration range, this enzyme performs the hydrolytic reaction only when the RNA at the 5′ end exposes unmethylated guanosine (Grzela et al., 2018; Chrabąszczewska et al., 2021). Given that the cap is

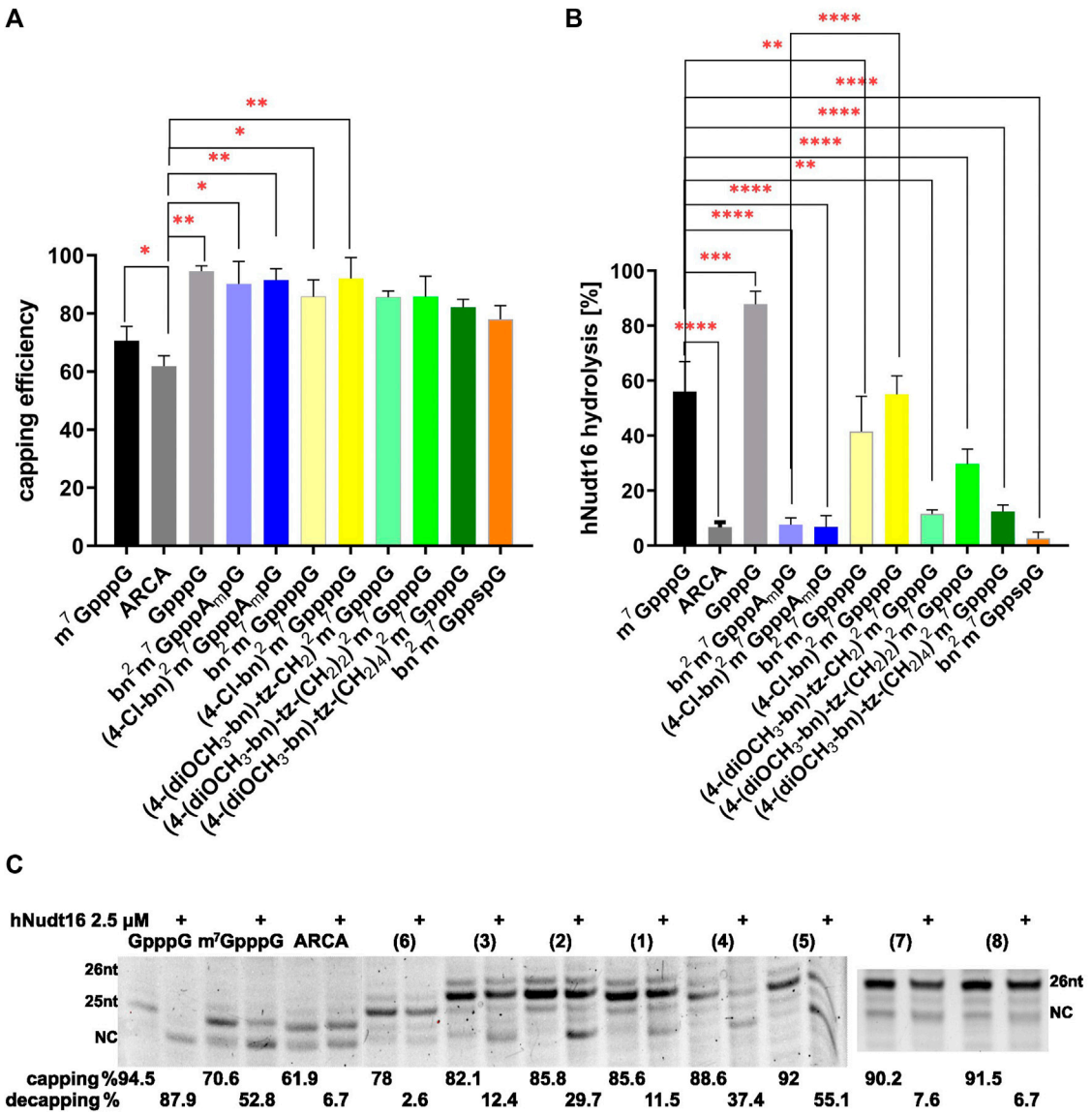

FIGURE 3
Efficiency and orientation of incorporation of N2-modified cap analogues into RNA. **(A)** The level of RNA 5′ capping with new cap analogues. The graph represents the percentage of capped RNA obtained during IVT reaction, calculated from densitometric analysis. Capping was calculated as percent of capped product in samples not subjected to hydrolysis. **(B)** The level of cap hydrolysis with hNudt16. The graph represents the per cent loss in the capped fraction of the sample after 30 min hydrolysis with hNudt16. Data represent mean ± SD of three independent experiments and were analyzed using GraphPad Prism 8 (GraphPad Software, San Diego California, United States) statistical analysis software. Statistical analysis were performed using ordinary one-way ANOVA with Turkey test. Statistical significance between the RNA with modified caps and m^7GpppG-capped RNA is denoted by a value of ****$p < 0.0001$, ***$p < 0.001$, and **$p < 0.01$. Otherwise, the differences are not statistically significant. **(C)** Exemplary gel electrophoretic analysis of 5′ cap hydrolysis with hNudt16. NC denotes product without the cap (not capped and/or decapped). Capping and decapping levels were estimated by densitometric analysis of bands using ImageLab software (Bio-Rad). The data represent mean ± SD of three independent experiments.

asymmetric concerning methylation at position 7 of guanosine, the rate of hydrolysis reflects its orientation of incorporation.

Among the tested analogues, only 7.62% of the $bn^2m^7GpppA_mpG$-capped RNA and 6.73% of the $(4\text{-Cl-bn})^2m^7GpppA_mpG$-capped RNA was hydrolyzed by the hNudt16 (Figure 3; Table 1). Such a result indicates the incorporation of the analogue only in the correct orientation. A similar level of hydrolysis was observed for $bn^2m^7Gpp_spG$-capped RNA (Figure 3; Table 1). However, the orientation of this compound incorporation cannot be assessed, since the presence of a thiophosphate modification in the triphosphate bridge prevents the hydrolysis reaction from proceeding. RNAs capped with compounds $(4\text{-(diOCH}_3\text{-bn)-tz-CH}_2)^2m^7GpppG$ (1) and $(4\text{-(diOCH}_3\text{–bn)-tz-(CH}_2)_4)^2m^7GpppG$ (3) undergo hNudt16 hydrolysis to a small extent (11.5%–12.4%), leading to the conclusion that these analogues are built into RNA mostly in the correct orientation, while capping with $(4\text{-(diOCH}_3\text{–bn)-tz-(CH}_2)_2)^2m^7GpppG$ (2) is incorrect in about 30% (Figure 3; Table 1).

Given that the hNudt16 hydrolysis assay was developed for triphosphate-chain dinucleotides, we checked its fidelity for control

tetraphosphate-chain dinucleotides. We used m^7GppppG and m^7Gppppm^{7}G for the reaction. Hydrolysis of the first analogue showed the presence of GMP and m^7GTP products. The second of studied analogues, m^7Gppppm^{7}G, did not undergo hydrolysis at the hNudt16 concentration tested. This confirms the validity of the statement that the enzyme preferentially attacks unmethylated guanosine. Therefore, we can conclude that the hydrolysis of dinucleotides with a tetraphosphate bridge proceeds in the same way as for triphosphate compounds.

The hydrolysis of RNA capped with analogues bearing tetraphosphate chain (bn^{2}m^{7}GppppG (4) - and (4-Cl-bn)^{2}m^{7}GppppG (5)) proceeded at a similar rate as that for m^7GpppG-RNA, indicating two possible orientations of incorporation of these analogues into RNA chain (Figure 3; Table 1).

4 Discussion

Despite the many drugs available on the pharmaceutical market, we are still unable to cure many serious diseases. Efficacy, safety and short time to market are important criteria for drug development. Response time to an emerging threat is particularly important in the case of viral diseases, that can take on a pandemic spread. Given global temperatures rise, melting glaciers releasing old pathogens or the increasing transmission of pathogens from animals to humans, the danger of new diseases emerging is high (Alempic et al., 2023). Therapeutic mRNA molecule has brought new hope, as its production process is quick and easily adjustable for many different therapeutic applications (Li et al., 2023; Yu et al., 2023). By changing the sequence, any protein of therapeutic interest can be obtained. As a result, the waiting time for a new medicine, or a medicine tailored to the patient, is significantly reduced.

For the efficient production of a protein encoded on mRNA, the individual components of the carrier molecule such as the cap structure, 5′ and 3′ UTRs, modified nucleotides or poliA are important. The cap structure is a 7-methyloguanosine attached via a triphosphate bond to the RNA chain. Intensive research work has led to the introduction into the biotechnology market of several synthetic analogues of particular interest: m^7GpppG, ARCA, β-S-ARCA, and CleanCap (Grudzien-Nogalska et al., 2007a; Grudzien-Nogalska et al., 2007b; Henderson et al., 2021).

However, this does not exhaust the possible modifications that can give the cap structure a new quality. New analogues modified at the N2 position of 7-methylguanosine have recently been synthesized (Grzela et al., 2022). The positioning of benzene substituents at the N2 7-methylguanosine allowed efficient synthesis of protein from modified mRNA at levels more than three times higher than in the case of RNA bearing the standard m^7GpppG analogue. The new caps also had an extremely interesting feature, since some substituents at the N2 position of 7-methylguanosine prevented the polymerase from attacking the methylated guanosine. This resulted in the elongation of the RNA chain from the unmethylated guanosine only, so that the entire transcript had cap incorporated in the correct orientation.

The aim of this study was the small-scale synthesis of new cap analogues that would simultaneously carry N2 modifications of 7-methylguanosine and the following other modifications: a) added adenine with 2′-*O* ribose methylation at position +1, b) triphosphate chain extended by one phosphate, c) added thiophosphate modification in the triphosphate chain, d) altered linker between 7-methylguanosine and the substituent. The addition of these modifications is known to provide the following features: recognition of the mRNA molecule as a "self" (Vladimer et al., 2014; Miedziak et al., 2020), enhanced affinity for eIF4E (Strenkowska et al., 2010), protection against the activity of decapping enzymes and in consequence extended lifespan of mRNA in the cell (Grudzien-Nogalska et al., 2007a), and different structural arrangement of the derivative relative to binding pocket of eIF4E. Since synthesizing compounds with the described modifications is difficult and challenging, we aimed at a small-scale synthesis, that would allow for initial characterization of the analogues and selection of most promising ones for further studies.

Caps are being investigated as translation inhibitors and as a component of mRNA molecule. We characterized the newly obtained compounds in terms of their inhibitory properties using an *in vitro* translation system. Among the analogues tested, there were three that showed very strong inhibitory properties. The results obtained are as expected, since these compounds are derivatives of the analogues described in (Grzela et al., 2022), which have already shown strong inhibitory properties on protein biosynthesis. In the case of aforementioned new derivatives, the inhibitory potential was even stronger than in the case of the initial compounds. Two of these compounds: bn^{2}m^{7}GppppG (4) and (4-Cl-bn)^{2}m^{7}GppppG (5) had, in addition to the modification at N2 7-methylguanosine, the triphosphate chain extended to four phosphates, that is known to enhance the interaction between cap and eIF4E. The third analogue was bn^{2}m^{7}Gpp$_s$pG, a compound with modification at N2 7-methylguanosine and with a thiophosphate group in the triphosphate chain. This result is very important, as an analogue of this type is characterized by its resistance to decapping enzymes and can therefore be stable for long periods of time. However, it should be noted, that we studied the compound 6 as a mixture of stereoisomers due to the difficulty in separating them. All these compounds deserve special attention in the development of anticancer drugs based on inhibitors of the translation process.

We then focused on the characterization of caps as components of the mRNA molecule. We assessed their incorporation efficiency into mRNA. Trinucleotide analogues had the highest incorporation efficiency, exeeding 90%. All other compounds modified at the N2 position of 7-methylguanosine had a fairly high percentage of incorporation into mRNA. As in the previous study (Grzela et al., 2022), compound (4-(diOCH$_3$–bn)-tz-CH$_2$)^{2}m^{7}GpppG (1) showed low levels of hydrolysis by the hNudt16 enzyme, indicating its correct incorporation orientation. We observed a similar low level of decapping for a derivative of this compound, analogue (4-(diOCH$_3$–bn)-tz-(CH$_2$)$_4$)^{2}m^{7}GpppG (3). The result for RNA containing trinucleotide derivatives was even better. In contrast, derivatives with an extended triphosphate chain behaved similarly to the standard compound m^7GpppG, which incorporates into mRNA in two orientations. This indicates that these derivatives should be developed into inhibitors rather than mRNA elements. Considering both the incorporation efficiency and its orientation, trinucleotide derivatives are ideal compounds for the preparation of therapeutic mRNA. During IVT reaction with these compounds, fewer by-products are formed due to incomplete cap incorporation or the

presence of an RNA fraction with a reversibly attached cap. These factors have a significant impact on the quality of the therapeutic RNA molecule and on the subsequent cellular response to the introduced transcript.

Finally, we tested the functionality of the new derivatives attached to 5′ end of mRNA in an *in vitro* translation assay. The highest values were achieved by mRNAs containing trinucleotide caps. However, these values were almost the same as for the initial dinucleotide compounds modified at the N2 position of 7-methylguanosine ($bn^2m^7GpppA_mpG$ (7) vs. bn^2m^7GpppG, (4-Cl-bn)$^2m^7GpppA_mpG$ (8) vs. (4-Cl-bn)$^2m^7GpppG$, (4-bn-isx)$^2m^7GpppA_mpG$ (9) vs. (4-bn-isx)$^2m^7GpppG$). Only one of these compounds, (4-Cl-bn)$^2m^7GpppA_mpG$ (8), presented more effective translation than its original counterpart. It is well known, the 2′-*O* ribose modification present in the trinucleotide analogues is important for proper mRNA recognition by the immune system, while the extracellular assay is not apt to evaluate the cellular response (Züst et al., 2011). Unfortunately, we were unable to perform experiments in the cells due to the small-scale of compounds synthesis. Still, the set of basic experiments we performed, allowed us to select trinucleotide derivatives modified at the N2 position of 7-methylguanosine as promising components for the preparation of mRNA. In the near future, we plan to optimize the process of synthesis of these analogues to obtain quantities that would allow tests in a cellular system and further administration of modified transcripts to animals.

Data availability statement

All relevant data is included in the article. There is no data that should be deposited in any repository. Any further questions can be directed to the respective authors, as indicated in the article.

Ethics statement

Ethical approval was not required for the studies on animals in accordance with the local legislation and institutional requirements because only commercially available established cell lines were used.

Author contributions

KK: Data curation, Investigation, Writing–original draft, Writing–review and editing. AS-D: Data curation, Investigation, Methodology, Writing–review and editing. KP: Conceptualization, Data curation, Investigation, Methodology, Writing–review and editing. ER: Investigation, Writing–review and editing. PS: Investigation, Writing–review and editing. JG: Investigation, Writing–review and editing. ED: Conceptualization, Funding acquisition, Writing–review and editing. RG: Conceptualization, Data curation, Methodology, Project administration, Supervision, Writing–original draft, Writing–review and editing. MJ-A: Conceptualization, Data curation, Funding acquisition, Methodology, Project administration, Supervision, Writing–original draft, Writing–review and editing.

Funding

The author(s) declare financial support was received for the research, authorship, and/or publication of this article. Financial support for this work was provided by the National Science Centre, Poland grant nos. UMO/2018/31/B/ST5/03544 (MJ-A), UMO/2019/33/B/NZ1/01322 (ED) and with funds from the University of Warsaw the "Excellence Initiative—Research University Program" action No. II.2.1–Tandems for Excellence (RG and AS-D)

Conflict of interest

The authors declare that the research was conducted in the absence of any commercial or financial relationships that could be construed as a potential conflict of interest.

Publisher's note

All claims expressed in this article are solely those of the authors and do not necessarily represent those of their affiliated organizations, or those of the publisher, the editors and the reviewers. Any product that may be evaluated in this article, or claim that may be made by its manufacturer, is not guaranteed or endorsed by the publisher.

Supplementary material

The Supplementary Material for this article can be found online at: https://www.frontiersin.org/articles/10.3389/fmolb.2023.1269028/full#supplementary-material

References

Alempic, J. M., Lartigue, A., Goncharov, A. E., Grosse, G., Strauss, J., Tikhonov, A. N., et al. (2023). An update on eukaryotic viruses revived from ancient permafrost. *Viruses* 15, 564. doi:10.3390/v15020564

Cai, A., Jankowska-Anyszka, M., Centers, A., Chlebicka, L., Stepinski, J., Stolarski, R., et al. (1999). Quantitative assessment of mRNA cap analogues as inhibitors of *in vitro* translation. *Biochemistry* 38, 8538–8547. doi:10.1021/bi9830213

Chrabąszczewska, M., Winiewska-Szajewska, M., Ostrowska, N., Bojarska, E., Stępiński, J., Łukaszewicz, M., et al. (2021). Insight into the binding and hydrolytic preferences of hNudt16 based on nucleotide diphosphate substrates. *Int. J. Mol. Sci.* 22, 10929. doi:10.3390/ijms222010929

Eisenführ, A., Arora, P. S., Sengle, G., Takaoka, L. R., Nowick, J. S., and Famulok, M. (2003). A ribozyme with michaelase activity: synthesis of the substrate precursors. *Bioorg Med. Chem.* 11, 235–249. doi:10.1016/s0968-0896(02)00311-5

Furuichi, Y. (2015). Discovery of m(7)G-cap in eukaryotic mRNAs. *Proc. Jpn. Acad. Ser. B Phys. Biol. Sci.* 91, 394–409. doi:10.2183/pjab.91.394

Grudzien-Nogalska, E., Jemielity, J., Kowalska, J., Darzynkiewicz, E., and Rhoads, R. E. (2007a). Phosphorothioate cap analogs stabilize mRNA and increase translational efficiency in mammalian cells. *RNA* 13, 1745–1755. doi:10.1261/rna.701307

Grudzien-Nogalska, E., Stepinski, J., Jemielity, J., Zuberek, J., Stolarski, R., Rhoads, R. E., et al. (2007b). Synthesis of anti-reverse cap analogs (ARCAs) and their applications

in mRNA translation and stability. *Methods Enzymol.* 431, 203–227. doi:10.1016/S0076-6879(07)31011-2

Grzela, R., Nasilowska, K., Lukaszewicz, M., Tyras, M., Stepinski, J., Jankowska-Anyszka, M., et al. (2018). Hydrolytic activity of human Nudt16 enzyme on dinucleotide cap analogs and short capped oligonucleotides. *RNA* 24, 633–642. doi:10.1261/rna.065698.118

Grzela, R., Piecyk, K., Stankiewicz-Drogon, A., Pietrow, P., Lukaszewicz, M., Kurpiejewski, K., et al. (2022). N2 modified dinucleotide cap analogs as a potent tool for mRNA engineering. *RNA* 29, 200–216. doi:10.1261/rna.079460.122

Henderson, J. M., Ujita, A., Hill, E., Yousif-Rosales, S., Smith, C., Ko, N., et al. (2021). Cap 1 messenger RNA synthesis with Co-transcriptional CleanCap® analog by *in vitro* transcription. *Curr. Protoc.* 1, e39. doi:10.1002/cpz1.39

Ishikawa, M., Murai, R., Hagiwara, H., Hoshino, T., and Suyama, K. (2009). Preparation of eukaryotic mRNA having differently methylated adenosine at the 5′-terminus and the effect of the methyl group in translation. *Nucleic Acids Symp. Ser. (Oxf)* 129–130, 129–130. doi:10.1093/nass/nrp065

Kadokura, M., Wada, T., Urashima, C., and Sekine, M. (1997). Efficient synthesis of γ-methyl-capped guanosine 5′-triphosphate as a 5′-terminal unique structure of U6 RNA via a new triphosphate bond formation involving activation of methyl phosphorimidazolidate using ZnCl2 as a catalyst in DMF under anhydrous conditions. *Tetrahedron Lett.* 38, 8359–8362. doi:10.1016/s0040-4039(97)10263-5

Kocmik, I., Piecyk, K., Rudzinska, M., Niedzwiecka, A., Darzynkiewicz, E., Grzela, R., et al. (2018). Modified ARCA analogs providing enhanced translational properties of capped mRNAs. *Cell Cycle* 15384101, 1486164. doi:10.1080/15384101.2018.1486164

Kowalska, J., Lewdorowicz, M., Zuberek, J., Grudzien-Nogalska, E., Bojarska, E., Stepinski, J., et al. (2008). Synthesis and characterization of mRNA cap analogs containing phosphorothioate substitutions that bind tightly to eIF4E and are resistant to the decapping pyrophosphatase DcpS. *RNA* 14, 1119–1131. doi:10.1261/rna.990208

Kowalska, J., Lukaszewicz, M., Zuberek, J., Ziemniak, M., Darzynkiewicz, E., and Jemielity, J. (2009). Phosphorothioate analogs of m^7GTP are enzymatically stable inhibitors of cap-dependent translation. *Bioorg Med. Chem. Lett.* 19, 1921–1925. doi:10.1016/j.bmcl.2009.02.053

Lazaris-Karatzas, A., Montine, K. S., and Sonenberg, N. (1990). Malignant transformation by a eukaryotic initiation factor subunit that binds to mRNA 5′ cap. *Nat* 345, 544–547. doi:10.1038/345544a0

Li, D., Liu, C., Li, Y., Tenchov, R., Sasso, J. M., Zhang, D., et al. (2023). Messenger RNA-based therapeutics and vaccines: what's beyond COVID-19? *ACS Pharmacol. Transl. Sci.* 6, 943–969. doi:10.1021/acsptsci.3c00047

Miedziak, B., Dobiezyńska, A., Darzynkiewicz, Z. M., Bartkowska, J., Miszkiewicz, J., Kowalska, J., et al. (2020). Kinetic analysis of IFIT1 and IFIT5 interactions with different native and engineered RNAs and its consequences for designing mRNA-based therapeutics. *RNA* 26, 58–68. doi:10.1261/rna.073304.119

Mukaiyama, T., and Hashimoto, M. (1972). Synthesis of oligothymidylates and nucleoside cyclic phosphates by oxidation–reduction condensation. *J. Am. Chem. Soc.* 94, 8528–8532. doi:10.1021/ja00779a039

Pasquinelli, A. E., Dahlberg, J. E., and Lund, E. (1995). Reverse 5′ caps in RNAs made *in vitro* by phage RNA polymerases. *RNA* 1, 957–967. Available at: https://pubmed.ncbi.nlm.nih.gov/8548660/(Accessed July 15, 2022).

Piecyk, K., Davis, R. E., and Jankowska-Anyszka, M. (2012). Synthesis of N^2-modified 7-methylguanosine 5'-monophosphates as nematode translation inhibitors. *Bioorg. Med. Chem.* 20, 4781–4789. doi:10.1016/j.bmc.2012.05.078

Piecyk, K., Lukaszewicz, M., Darzynkiewicz, E., and Jankowska-Anyszka, M. (2014). Triazole-containing monophosphate mRNA cap analogs as effective translation inhibitors. *RNA* 20, 1539–1547. doi:10.1261/rna.046193.114

Piecyk, K., Niedzwiecka, A., Ferenc-Mrozek, A., Lukaszewicz, M., Darzynkiewicz, E., and Jankowska-Anyszka, M. (2015). How to find the optimal partner--studies of snurportin 1 interactions with U snRNA 5′ TMG-cap analogues containing modified 2-amino group of 7-methylguanosine. *Bioorg Med. Chem.* 23, 4660–4668. doi:10.1016/j.bmc.2015.05.054

Rydzik, A. M., Lukaszewicz, M., Zuberek, J., Kowalska, J., Darzynkiewicz, Z. M., Darzynkiewicz, E., et al. (2009). Synthetic dinucleotide mRNA cap analogs with tetraphosphate 5′,5′ bridge containing methylenebis(phosphonate) modification. *Org. Biomol. Chem.* 7, 4763–4776. doi:10.1039/b911347a

Senthilvelan, A., Vonderfecht, T., Shanmugasundaram, M., Pal, I., Potter, J., and Kore, A. R. (2021). Trinucleotide cap analogue bearing a locked nucleic acid moiety: synthesis, mRNA modification, and translation for therapeutic applications. *Org. Lett.* 23, 4133–4136. doi:10.1021/acs.orglett.1c01037

Shanmugasundaram, M., Senthilvelan, A., and Kore, A. R. (2022). Recent advances in modified cap analogs: synthesis, biochemical properties, and mRNA based vaccines. *Chem. Rec.* 22, e202200005. doi:10.1002/tcr.202200005

Strenkowska, M., Grzela, R., Majewski, M., Wnek, K., Kowalska, J., Lukaszewicz, M., et al. (2016). Cap analogs modified with 1,2-dithiodiphosphate moiety protect mRNA from decapping and enhance its translational potential. *Nucleic Acids Res.* 44, 9578–9590. doi:10.1093/nar/gkw896

Strenkowska, M., Kowalska, J., Lukaszewicz, M., Zuberek, J., Su, W., Rhoads, R. E., et al. (2010). Towards mRNA with superior translational activity: synthesis and properties of ARCA tetraphosphates with single phosphorothioate modifications. *New J. Chem.* 34, 993–1007. doi:10.1039/b9nj00644c

Vladimer, G. I., Górna, M. W., and Superti-Furga, G. (2014). IFITs: emerging roles as key anti-viral proteins. *Front. Immunol.* 5, 94. doi:10.3389/fimmu.2014.00094

Yoshikawa, M., Kato, T., and Takenishi, T. (1969). Studies of phosphorylation. III. Selective phosphorylation of unprotected nucleosides. *Bull. Chem. Soc. Jpn.* 42, 3505–3508. doi:10.1246/bcsj.42.3505

Yu, M. Z., Wang, N. N., Zhu, J. Q., and Lin, Y. X. (2023). The clinical progress and challenges of mRNA vaccines. *Wiley Interdiscip. Rev. Nanomed Nanobiotechnol* 15, e1894. doi:10.1002/wnan.1894

Züst, R., Cervantes-Barragan, L., Habjan, M., Maier, R., Neuman, B. W., Ziebuhr, J., et al. (2011). Ribose 2′-O-methylation provides a molecular signature for the distinction of self and non-self mRNA dependent on the RNA sensor Mda5. *Nat. Immunol.* 12, 137–143. doi:10.1038/ni.1979

frontiers | Frontiers in Molecular Biosciences

TYPE Original Research
PUBLISHED 07 March 2024
DOI 10.3389/fmolb.2024.1250833

OPEN ACCESS

EDITED BY
Artur Slomka,
Nicolaus Copernicus University in Toruń, Poland

REVIEWED BY
Daniel Gilbert Bracewell,
University College London, United Kingdom
Lyne Josse,
University of Kent, United Kingdom

*CORRESPONDENCE
Mark J. Dickman,
m.dickman@sheffield.ac.uk

RECEIVED 30 June 2023
ACCEPTED 15 February 2024
PUBLISHED 07 March 2024

CITATION
Welbourne EN, Loveday KA, Nair A, Nourafkan E, Qu J, Cook K, Kis Z and Dickman MJ (2024), Anion exchange HPLC monitoring of mRNA *in vitro* transcription reactions to support mRNA manufacturing process development. *Front. Mol. Biosci.* 11:1250833. doi: 10.3389/fmolb.2024.1250833

Anion exchange HPLC monitoring of mRNA *in vitro* transcription reactions to support mRNA manufacturing process development

Emma N. Welbourne[1], Kate A. Loveday[1], Adithya Nair[1], Ehsan Nourafkan[1], Jixin Qu[1], Ken Cook[2], Zoltán Kis[1,3] and Mark J. Dickman[1]*

[1]Department of Chemical and Biological Engineering, University of Sheffield, Sheffield, United Kingdom, [2]ThermoFisher Scientific, Hemel Hempstead, United Kingdom, [3]Department of Chemical Engineering, Imperial College London, London, United Kingdom

mRNA technology has recently demonstrated the ability to significantly change the timeline for developing and delivering a new vaccine from years to months. The potential of mRNA technology for rapid vaccine development has recently been highlighted by the successful development and approval of two mRNA vaccines for COVID-19. Importantly, this RNA-based approach holds promise for treatments beyond vaccines and infectious diseases, e.g., treatments for cancer, metabolic disorders, cardiovascular conditions, and autoimmune diseases. There is currently significant demand for the development of improved manufacturing processes for the production of mRNA therapeutics in an effort to increase their yield and quality. The development of suitable analytical methods for the analysis of mRNA therapeutics is critical to underpin manufacturing development and the characterisation of the drug product and drug substance. In this study we have developed a high-throughput, high-performance liquid chromatography (HPLC) workflow for the rapid analysis of mRNA generated using *in vitro* transcription (IVT). We have optimised anion exchange (AEX) HPLC for the analysis of mRNA directly from IVT. Chromatography was performed in under 6 min enabling separation of all of the key components in the IVT, including nucleoside triphosphates (NTPs), Cap analogue, plasmid DNA and mRNA product. Moreover, baseline separation of the NTPs was achieved, which facilitates accurate quantification of each NTP such that their consumption may be determined during IVT reactions. Furthermore, the HPLC method was used to rapidly assess the purification of the mRNA product, including removal of NTPs/Cap analogue and other contaminants after downstream purification, including solid phase extraction (SPE), oligo deoxythymidine (oligo-dT) affinity chromatography and tangential flow filtration (TFF). Using the developed method excellent precision was obtained with calibration curves for an external mRNA standard and NTPs giving correlation coefficients of 0.98 and 1.0 respectively. Intra- and inter-day studies on retention time stability of NTPs, showed a relative standard deviation ≤ 0.3% and ≤1.5% respectively. The mRNA retention time variability was ≤0.13%. This method was then utilised to monitor

the progress of an IVT reaction for the production of Covid spike protein (C-Spike) mRNA to measure the increasing yield of mRNA alongside the consumption of NTPs during the reaction.

KEYWORDS

mRNA, anion exchange HPLC, *In vitro* transcription, mRNA vaccines/therapeutics, process development

1 Introduction

mRNA has recently emerged as a new class of therapeutic, as demonstrated by the development and approval of two highly efficacious vaccines based on mRNA sequences encoding for a modified version of the SARS-CoV-2 spike protein (Corbett et al., 2020; Polack et al., 2020). Furthermore, RNA-based approaches have potential for treatments beyond vaccines and infectious diseases as treatments for cancer, metabolic disorders, cardiovascular conditions, and autoimmune diseases. During the enzymatic manufacturing process of mRNA vaccines/therapeutics, incomplete mRNA products are generated in conjunction with other potential impurities such as double stranded (ds)RNA. Furthermore, during manufacturing and storage, RNA and RNA therapeutics can be degraded by exposure to heat, hydrolysis, oxidation, light and ribonucleases. The development of analytical methods for the analysis of mRNA therapeutics is critical to underpin manufacturing development. Analytical methods are also required to assess batch to batch manufacture and process repeatability, as well as the quality of mRNA produced. Furthermore, validated analytical methods are required to support the relevant phase of clinical development, regulatory submission requirements or to support ongoing quality control of the approved product. Current analytical methods available to characterise RNA therapeutics are limited and the development of methods for the analysis of large RNA (>1,000 nucleotides), including mRNA vaccines, is challenging. Therefore, there is currently significant demand for the development of new and improved analytical methods for the characterization of mRNA therapeutics.

The mRNA manufacturing process centres on the synthesis of the mRNA drug substance. Typically, mRNA can be synthesized using both chemical and enzymatic methods. Baronti el al. have reviewed the most suitable methods for RNA preparation, presenting their advantages, disadvantages and their latest advances (Baronti et al., 2018). Chemical synthesis of RNA is routinely performed using solid phase synthesis, with an upper size chain limit of approximately 100 nucleotides after repetitive yields of >99%, while physiological mRNAs are typically 1,000–10,000 nucleotides. Although mRNA's length is restrictive for its chemical synthesis, enzymatic *in vitro* transcription (IVT) is considered a simple and inexpensive procedure for mRNA synthesis, which can yield products of variable sizes in Gram quantities (Beckert et al., 2011; Sahin et al., 2014). In a commercial manufacturing process, sufficient amounts of functional pharmaceutical mRNA are typically synthesized in a cell-free system by IVT.

Plasmid DNA (pDNA), isolated and purified from bacterial cells and subsequently linearised by an appropriate restriction enzyme is commonly used as the DNA template for IVT reactions. Typical plasmid vectors contain a T7 promoter sequence upstream of multiple cloning sites. Furthermore, a poly(A) tail sequence, 5′ and 3′ untranslated regions are included in the DNA template design (Hadas et al., 2019; Tusup et al., 2019). In addition, a DNA template can be generated using a PCR product consisting of a T7 promoter at the 5′ end (Hadas et al., 2019). Typically, the poly(A) tail is incorporated in the initial DNA plasmid to be transcribed (Grier et al., 2016; To and Cho, 2021). Alternatively, mRNAs can be generated without a 3' poly(A) tail using "tailless" pDNA template and a further poly(A) tailing step is performed post-transcriptionally. Under these conditions a poly(A) polymerase can be used to add poly(A) tails of approximately 80–160 nucleotides.

IVT reactions are commonly performed using highly processive, single-subunit, bacteriophage DNA dependent RNA polymerases, and have been widely established as a cost-effective and scalable mRNA manufacturing process (McNamara et al., 2015). Bacteriophage T3, T7, and SP6 DNA dependent RNA polymerases are single polypeptide chains that require only Mg^{2+} as a cofactor and run off the DNA template after several transcription reactions (Sahin et al., 2014; Baronti et al., 2018). In the IVT reaction the linearized pDNA template, containing an RNA polymerase promoter sequence, is typically incubated with the DNA dependent RNA polymerase, nucleoside triphosphates (NTPs), RNase inhibitor and inorganic pyrophosphatase. This method has been widely employed for large scale IVT mRNA manufacturing. Furthermore, a variety of mutant DNA dependent RNA polymerases have been used in an approach to incorporate modified nucleotides (Meyer et al., 2015; Duffy et al., 2020) and reduce the synthesis of dsRNA impurities (Dousis et al., 2023). Optimisation of the IVT reactions and mRNA manufacturing process enables significant increases in mRNA yield and quality of the mRNA drug substance (e.g., reduced impurities and increases integrity of the mRNA). High quantities of mRNA can be produced in a few hours.

The application of high-performance liquid chromatography (HPLC) has previously been focussed on the purification of RNA generated using IVT reactions, including short RNA transcripts (<40 nt) synthesised for nuclear magnetic resonance structural studies (Anderson et al., 1996). The addition of the hammerhead ribozyme into the sequence has allowed workers to overcome the length limitation of short RNAs in HPLC purification (Shields et al., 1999). RNA transcription reaction mixtures have been directly purified by weak anion exchange (AEX) fast protein liquid chromatography (FPLC) to remove free nucleotides, short abortive transcripts, linearized plasmids, and enzymes from the desirable transcripts within 4 h (Easton et al., 2010). Strong AEX (Mono Q) FPLC for transcript purification and in the studies of transcription reactions has also been demonstrated (Koubek et al.,

2013). Analysis of oligonucleotides (OGNs) and RNA under denaturing conditions in conjunction with AEX HPLC has been performed in a variety of different systems in an approach to remove secondary/tertiary structures in OGNs and RNA (Thayer et al., 2005; Cook and Thayer, 2011; Kanavarioti, 2019; Sun et al., 2020).

Optimisation of the mRNA manufacturing process enables significant increases in mRNA yield and quality of the mRNA drug substance (e.g., reduced impurities and increased integrity of the mRNA). Rapid analysis of the mRNA generated in the manufacturing process, using on-line or near at-line analytical methods, is key to underpin process optimisation. In this study we have developed a rapid method for the analysis of IVT reactions using AEX HPLC. This method enables quantification of NTPs/Cap analogue, mRNA and residual DNA with separations performed in <6 min. This method has been successfully used to measure mRNA yield, NTPs (consumption) and mRNA purification for high throughput studies providing important information to support mRNA manufacturing process development and downstream processing.

2 Materials and methods

2.1 *In vitro* transcription

mRNA transcripts were prepared using *in vitro* transcription. eGFP and C-Spike plasmid DNA was provided by Genscript, NLuc plasmid DNA was provided by Aldevron. *In vitro* transcription reactions utilised template DNA (linearised plasmid), at 2. E−05 mM. DNA-dependent RNA polymerase of T7 bacteriophage (Roche) and ATP, CTP, GTP and UTP (Roche) in an equimolar ratio at 10 mM concentration were added to the reaction mixture. The reaction was further supplemented with the standard reaction buffer provided by the enzyme manufacturer. Inorganic pyrophosphatase (Roche) at 2.9E-03 mM was added to the reaction mixture to prevent magnesium pyrophosphate precipitation. RNase inhibitor (Roche) was added at 2.1E-04 mM to maintain RNase free environment in the reaction mixture. The reaction was incubated at 37°C for 2 hours. After incubation, the reaction was quenched by adding 200 mM EDTA. Following IVT, RNA was purified by solid phase extraction using silica columns as previously described (Nwokeoji et al., 2017). RNA concentrations were determined using a NanoDrop™ 2000c spectrophotometer (ThermoFisher Scientific) by absorbance at 260 nm normalized to a 1.0 cm (10.0 mm) path.

2.2 Tangential flow filtration (TFF)

A benchtop cross-flow TFF system (KrosFlo® KR2i, Repligen) and hollow fiber (HF) filter modules (300 kDa mPES, 20 cm^2) were used to separate the mRNA from unreacted NTPs in the IVT reaction mixture. All experiments were carried out at a feed flowrate of 10 mL/min and room temperature of 20.0°C ± 0.5°C. Crude IVT samples were diluted 16 times in 40 mM HEPES buffer (pH 7), before feeding through the TFF. The mRNA separation was accomplished by 4X concentration followed by 5X dia-filtration volumes of fresh buffer. At the end of process, the HF filter was washed with 20 mL of fresh buffer followed by 20 mL RNase-free water to recover any remaining mRNA from the TFF system.

2.3 mRNA oligo-dT chromatography purification

mRNA of interest in crude IVT was isolated and purified by oligo-dT chromatography using a 1 mL monolithic column (CIMmultus Oligo dT18; Sartorius, Gottingen, Germany) on an AKTA PCC (Cytiva, Uppsala, Sweden). All steps were performed at room temperature and UV sensors at 280 nm were used for all stages. The column was equilibrated in 20 mL loading buffer (250 mM NaCl, 50 mM sodium phosphate, 5 mM EDTA, pH 7.0) at a flow rate of 2 mL/min and the samples were loaded at 1 mL/min in 10 mL loading buffer. This was followed by a wash step in 20 mL loading buffer at 2 mL/min. The column bound fraction was eluted using 10 mL nuclease-free water at 2 mL/min. Chromatograms were generated with the UNICORN software (Cytiva, Uppsala, Sweden).

2.4 Anion exchange high-performance liquid chromatography (AEX HPLC)

IVT reaction samples (20 µL) were quenched by addition of 2 µL of 200 mM EDTA. Quenched samples were diluted 100–500 fold with RNase-free water to reach the final mRNA concentration 0.2–100 ng/µL. Injection volume was 5 µL. Samples were analysed by AEX on a U3000 HPLC system using a DNAPac PA200 column (50 mm × 2.1 mm I.D. Thermo Fisher Scientific). Chromatograms were generated using UV detection at a wavelength of 260 nm. The chromatographic analysis was performed using the following conditions: 10 mM NaOH in mobile phase A and 10 mM NaOH, 2 M NaCl in mobile phase B. Samples were analysed using the following gradient: 0%–15% mobile phase B over 2 min, 15%–55% mobile phase B over 1 min, 55%–65% mobile phase B over 1 min and 65%–100% over 1 min. This was performed at a flow rate of 0.5 mL/min and a temperature of 25°C. Standard curves for individual NTPs were prepared by a serial dilution of each reagent from 100 mM stock in RNase-free water to a final concentration range of 0.5–100 µM (NTPs). A standard curve for mRNA was prepared by a serial dilution from 1 mg/mL stock to a final concentration range of 0.2–100 ng/µL. The slope and intercept of the standard curve were calculated by fitting with a linear regression function. Limits of detection (LOD) and limits of quantification (LOQ) were determined using the Chromeleon ICH LOD LOQ (SN) processing method in Chromeleon 7.2. The following variables were chosen in the method Component Table: Cal. Type = Lin. WithOffset, Measure_Noise = Current, LOQ_Ratio = 10, LOD_Ratio = 3, Noise_Start = 5.5 min and Noise_End = 7.5 min.

3 Results and discussion

3.1 Optimisation of AEX HPLC

Initial work focussed on the optimisation of the mobile phases utilised in conjunction with AEX HPLC to enable the rapid

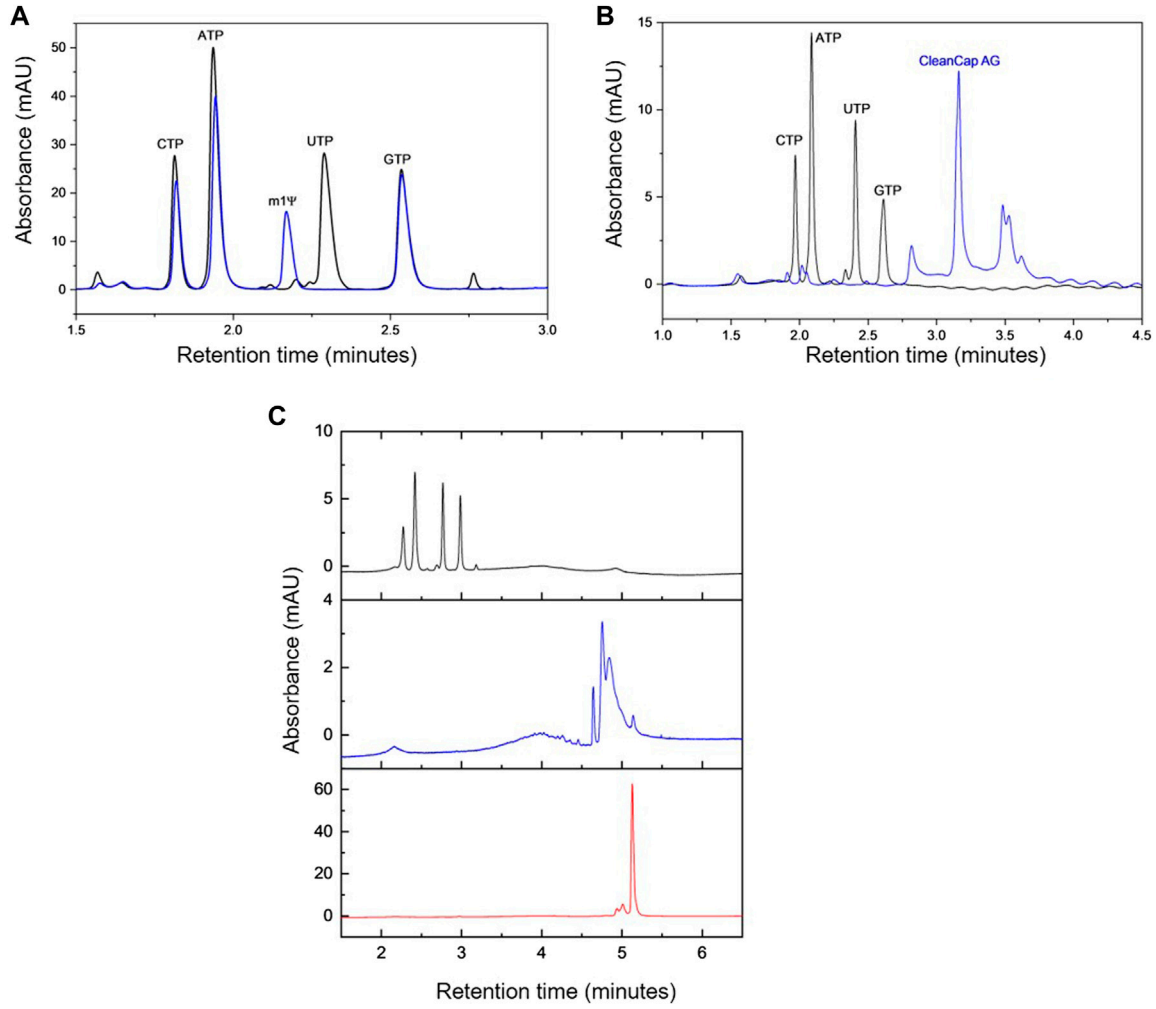

FIGURE 1
AEX HPLC analysis. **(A)** AEX chromatograms generated from a mixture of NTPs (black) and a mixture of NTPs where UTP is replaced by N1-methylpseudo-UTP (m1Ψ, blue). **(B)** AEX chromatograms produced by a mixture of NTPs (black) and CleanCap® AG (m7G (5′)ppp (5′) (2′OMeA)pG) (blue). **(C)** Comparative analysis of AEX chromatograms from a mixture of NTPs (black), eGFP plasmid DNA (blue) and eGFP mRNA (red).

separation of NTPs, mRNA and plasmid DNA in a single analysis. AEX chromatography was performed on DNAPac PA200 (2.1 mm × 50 mm) to facilitate the use of short gradients and enable high throughput analysis of mRNA from IVT reactions. A number of different mRNA sequences were synthesised using IVT, including eGFP (~930 nt), COVID spike protein (C-Spike ~4,300 nt) and NanoLuc (NLuc, ~870 nt). Following IVT and purification of the mRNA, further characterisation was performed using capillary electrophoresis for sizing of the mRNA and analysis of mRNA integrity (see Supplementary Figure S1). The results confirm the expected size of the mRNAs and purification of intact mRNA. Furthermore direct RNA sequence mapping using LC MS in conjunction with partial RNase T1 digests was performed to confirm the sequence of the mRNAs [Vanhinsbergh et al., 2021]. The results show >90% sequence coverage was obtained based on unique oligoribonucleotides. These results confirm the sequence, size and integrity of the mRNAs used in this study.

Initial work was performed using mobile phases at pH 8.0 (buffering with 25 mM Tris-HCl), in conjunction with increasing sodium chloride concentration for elution. This resulted in the incomplete separation of all of the NTPs (see Supplementary Figure S2A). Moreover, under these conditions incomplete and variable elution of the mRNA was observed from the stationary phase. Therefore, in an approach to further optimise the AEX HPLC, mobile phases were prepared at pH ≈ 11.95 using 10 mM sodium hydroxide. The resulting chromatogram demonstrating the baseline separation of the NTPs, including N1-methylpseudo-UTP (m1Ψ-UTP), is shown in Figure 1A. By performing the separation at pH 11.95, the ionisation state of the nucleobases of guanosine and uridine is changed (deprotonated at N1 and N3 respectively) as pH is increased from 8.0 to 11.95. Furthermore, by moving to pH 11.95, this resulted in complete and consistent elution of mRNA and no mRNA was retained on the column. Previously, AEX at high pH has been used to analyse RNA (sgRNA, tRNA and mRNA) and demonstrated the improved resolution of RNA under these conditions by removing the secondary/tertiary structures present and maintaining stability of the RNA under these chromatographic

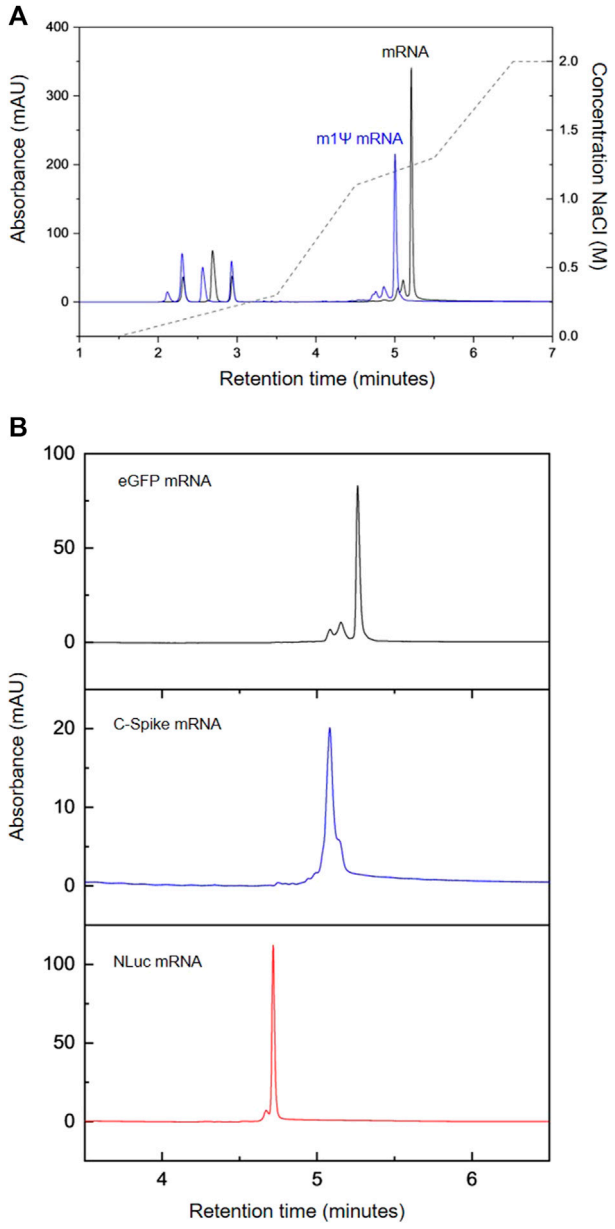

FIGURE 2
AEX HPLC analysis of IVT mRNA. **(A)** AEX analysis of IVT reactions producing modified eGFP mRNA (m1Ψ, blue) and unmodified eGFP mRNA (black) **(B)** AEX analysis of a range of different mRNA. eGFP (black), C-Spike (blue) NLuc (red).

conditions (Kanavarioti, 2019). Following mobile phase optimisation, further work was performed to optimise the AEX gradient and enable rapid separation of the NTPs, cap analogue, mRNA and pDNA in a single analysis (see Figures 1B, C). The results show that separation of the NTPs, cap analogue, mRNA and pDNA can be achieved <6 min using the optimised gradient.

mRNA vaccines/therapeutics are typically manufactured using chemically modified UTP such as m1Ψ-UTP. Therefore, further work was performed to enzymatically synthesise mRNA containing N1-methylpsuedouridine instead of uridine. The chromatograms are shown in Figure 1A and demonstrate that the AEX HPLC separates all 4 NTPs including the m1Ψ-UTP and the chemically

TABLE 1 Retention time stability and linearity data.

Analyte	Retention time, RSD/%		Calibration curve, R^2
	Intra-day	Inter-day	
CTP	0.30	1.5	0.9997
ATP	0.24	1.3	0.9995
UTP	0.13	1.3	0.9996
GTP	0.09	1.2	0.9997
eGFP mRNA	0.02	0.11	0.9845
No. reps	9	3	3
No. days	1	3	3
Tot. reps	9	9	9

modified mRNA. It is interesting to note that even on the rapid gradient used in this study, a change in retention time of the m1Ψ-UTP mRNA from the unmodified mRNA is observed (see Figure 2A), highlighting an alteration in the overall charge or hydrophilicity of the mRNA. This is consistent with the earlier elution of the m1Ψ-UTP compared to UTP (see Figure 1A) and demonstrates the influence of sequence on the separation of large RNA molecules using AEX.

In addition to testing how the inclusion of m1Ψ-UTP affects the mRNA peak in the chromatography, a variety of mRNAs with different lengths were assessed. Figure 2B shows the comparison between the peaks produced by mRNAs for eGFP (~930 nt), COVID spike protein (C-Spike ~4,300 nt) and NanoLuc (NLuc, ~870 nt). The results show that all three mRNAs exhibit a peak within the 1.1–1.3 M NaCl window designed for elution of IVT products. Consistent with previous data shown for the different retention times of unmodified and modified (m1Ψ) mRNA, the order of elution of the mRNA is not related to the length of the mRNA and reflects the overall hydrophilicity of the RNA which is influenced by the sequence, potential secondary structure and charge density of the mRNA.

3.2 Quantification of mRNA and NTPs

Quantification of the mRNA and NTPs was performed in conjunction with external calibration curves. The linearity of the AEX HPLC assay was evaluated using a standard calibration curve with concentrations of NTPs ranging from 0.5–100 µM and amount of eGFP mRNA ranging from 1–530 ng. LOD and LOQ for eGFP mRNA were determined as 7.8 ng and 25.9 ng respectively. LOD for each of the individual NTPs ranged from 4.0–7.6 pmoles and LOQ ranged from 13.2–25.2 pmoles. These standards were prepared in triplicate and evaluated over the course of 3 days. In addition, the method robustness was tested by assessing the relative standard deviation (RSD) of the retention time for 100 µM NTPs and 530 ng eGFP mRNA. Intra- and inter-day RSDs were calculated for nine separate measurements over one or 3 days respectively. The results are summarised in Table 1.

Figure 3A shows the HPLC analysis of the dilution series used to generate the calibration curve for eGFP mRNA, which is shown in

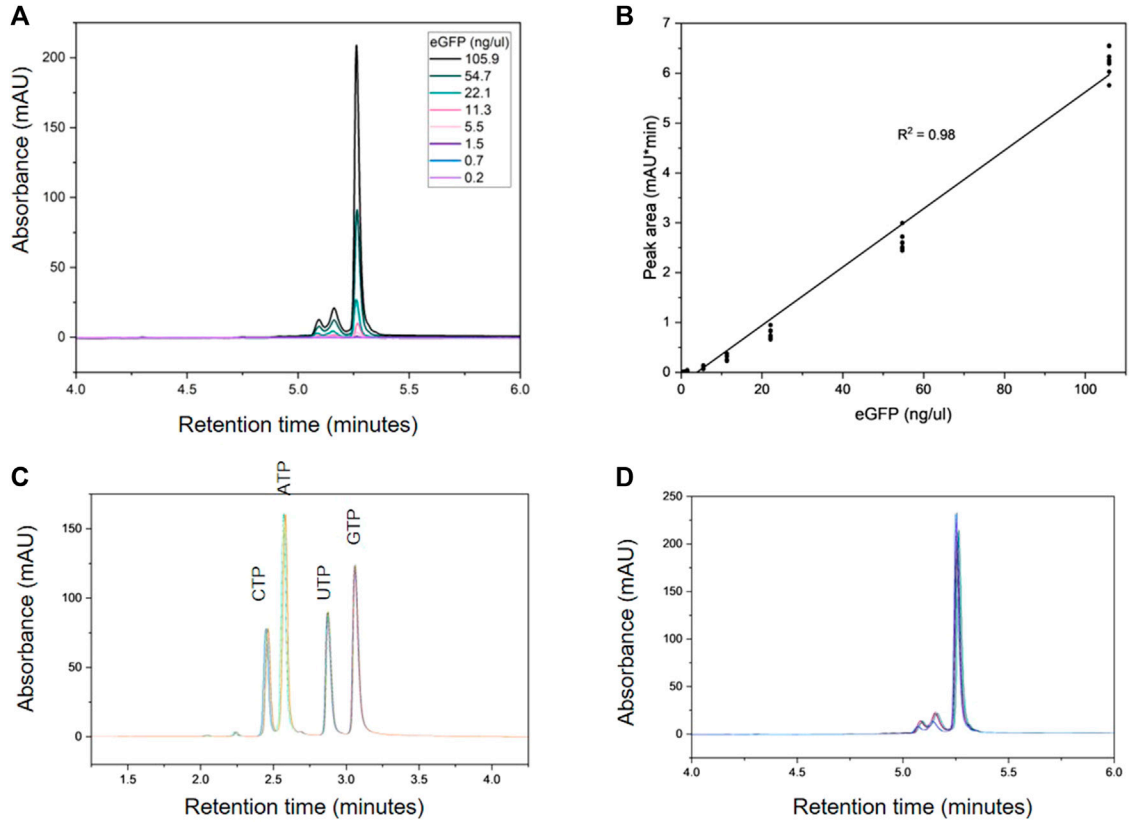

FIGURE 3
Quantification of mRNA and NTPs using AEX HPLC. **(A)** AEX chromatograms produced by a series dilution of eGFP mRNA (0.2–105.9 ng). **(B)** Calibration curve produced from the eGFP dilution series in triplicate over 3 days. Overlays of the intra-day analyses of 100 μM NTPs and 530 ng eGFP (n = 9) are shown in **(C)** and **(D)** respectively.

Figure 3B. The slope demonstrates good linearity with a correlation coefficient (R^2) of 0.98. Each of the NTPs produced a calibration curve with an R^2 of 1.0; the dilution series and resulting calibration curves for the NTPs are shown in Supplementary Figure S3. Intra-day variability of retention times for NTPs and mRNA was ≤0.3%. Inter-day variability was higher for the retention time of the NTPs at ≤1.5% however the mRNA retention time variability remained at 0.11%.

3.3 Analysis of IVT reactions using AEX HPLC to determine mRNA yield and NTP consumption

Recent studies have demonstrated the application of HPLC monitoring of consumption of NTPs with concomitant production of mRNA, to optimise the yield of mRNA production (batch and fed batch processes) (Pregeljc et al., 2023). However, under the HPLC conditions employed no separation of CTP/UTP was observed, preventing accurate quantification of CTP/UTP consumption. Following optimisation of the AEX HPLC method for the analysis of IVT reactions, further work was performed to enable high throughput analysis and quantification of mRNA and NTPs directly from the IVT reactions. Quantification of the mRNA and NTPs was performed using external standards (C-Spike mRNA and separately NTPs) to generate separate calibration curves from both mRNA and NTPs–the dilution series and curve for C-Spike is shown in Supplementary Figure S4.

The AEX HPLC enables direct analysis of the IVT reaction mixture with no sample preparation or purification required. To demonstrate the application of IVT analysis, samples were taken from selected time points (every 10 min, 0–2 h) from an IVT reaction producing C-Spike mRNA. The resulting chromatograms are shown in Figure 4A and corresponding quantification of the mRNA and NTPs is shown in Figure 4B. The results show the increase in synthesis of mRNA overtime and corresponding consumption of NTPs during the IVT reaction. The results show that the IVT reactions reached a maximum mRNA yield within approximately 70 min, furthermore, the results show that this plateau in mRNA production coincided with a significant drop of NTP concentration to approximately 10%–20% of the starting value for ATP/CTP/GTP. However, the concentration of UTP remained higher at approximately 50% of the starting value. The results also show that by 90 min all the CTP from the IVT reaction was essentially depleted. These results are consistent with the nucleotide composition of the C-Spike mRNA (31% C, 26% A, 19% U, 25% G) reflecting the demand for the corresponding NTPs during the synthesis of the mRNA. The ability to rapidly quantify all NTPs can be used to ensure mRNA synthesis is not inhibited by consumption or depletion of specific NTPs during the IVT reaction.

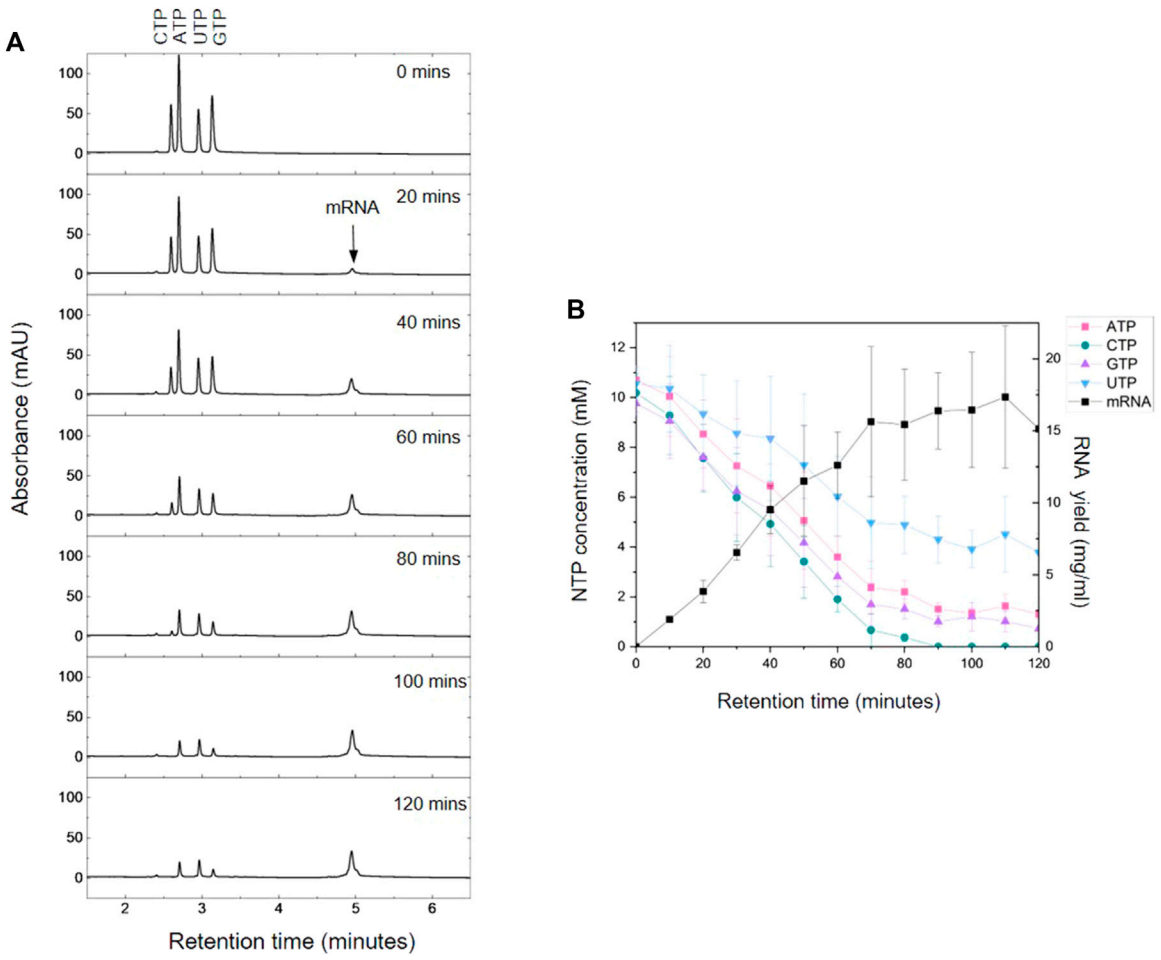

FIGURE 4
AEX HPLC analysis of the kinetics of mRNA production. **(A)** AEX chromatograms produced by time points taken every 20 min during an IVT reaction for C-Spike mRNA. **(B)** NTP concentration and mRNA yields determined using HPLC analysis in conjunction with standard curves for NTPs and mRNA. Mean and SD are plotted of n = 3 biological replicates.

This allows optimisation of the NTP ratios based on the target sequence to increase yield and reduce the frequency of miss-incorporation of NTPs. Efficient use of NTPs (especially m1Ψ-UTP) and capping analogues can substantially reduce manufacturing costs (Kis et al., 2022).

3.4 Monitoring mRNA purification using AEX HPLC

In addition to the quantification of mRNA synthesis and NTP consumption direct from IVT reactions, the developed AEX HPLC method was also used to monitor mRNA purification, in particular NTP/Clean Cap removal during the purification process. Prior to downstream applications and LNP formulation it is essential to remove IVT reaction components such as NTPs/Cap reagents, salts, proteins, *etc.*, which is required for accurate quantification using UV spectrophotometry of the purified mRNA drug substance. Therefore, the AEX HPLC method utilised in this study offers a rapid approach to monitor NTP/Cap analogue removal and mRNA yield during downstream purifications.

To demonstrate the application of the AEX HPLC method, a variety of downstream purification methods were used to purify the mRNA prior to analysis. This included solid phase extraction (SPE) using silica membranes, TFF and oligo-dT affinity chromatography. The small scale purification using SPE is shown in Figure 5A and demonstrates the effective removal (>99%) of NTPs. Larger scale purification, *via* TFF in diafiltration mode and oligo-dT chromatography is demonstrated in Figures 5B, C respectively. The results also show the successful purification and removal of residual NTPs (>96% and >99.9% respectively).

This AEX HPLC method provides valuable information for developing kinetic models of the IVT unit operation and mass-balance models for downstream purification unit operations (van de Berg et al., 2021). These models can lay the foundations for establishing digital-twins and soft sensors, and for promoting accelerated production process development and automation of the final manufacturing process. Moreover, these models can be integrated into a Quality by Digital Design framework. Based on this, a design space can be defined for developing and manufacturing a wide range of RNA vaccines and therapeutics using the same platform process (Daniel et al., 2022).

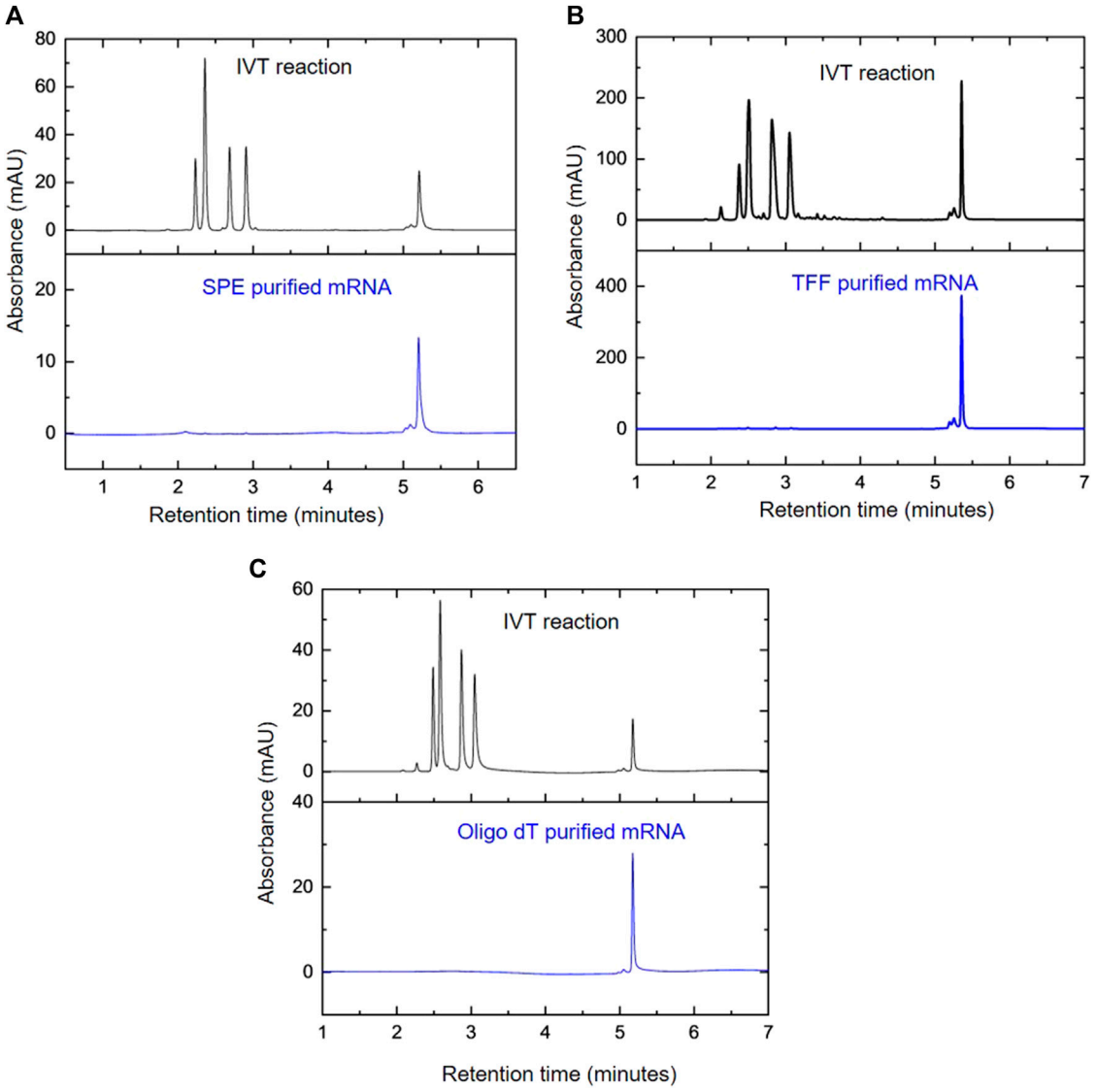

FIGURE 5
Monitoring mRNA purifications using AEX HPLC. AEX chromatograms comparing the IVT products before and after purification using; **(A)** SPE, **(B)** TFF diafiltration and **(C)** oligo-dT affinity chromatography.

4 Conclusion

mRNA has emerged as an important new class of therapeutic. Optimisation of the mRNA manufacturing process enables significant increases in mRNA yield and quality of the mRNA drug substance produced. Rapid analysis of IVT reactions and the mRNA generated during manufacturing, including downstream processing, using on-line or at-line analytical methods provides critical information for the optimisation of the mRNA manufacturing process. In this study we have developed a rapid method for the analysis of IVT reactions using AEX HPLC. This method enables quantification of each individual NTP, Cap analogue, mRNA and residual DNA, with separations achieved in <6 min. This method has been successfully used to measure mRNA yield, NTP consumption and mRNA purification in high throughput studies. This method was then utilised to monitor the progress of an IVT reaction for the production of mRNA. Here, it was possible to quantify the production of mRNA alongside the consumption of NTPs demonstrating that under the conditions used the IVT reaction, mRNA synthesis was complete at 70 min, in conjunction with significant consumption of NTPs (80%–90% for ATP/GTP/CTP) at this time. Furthermore, the AEX HPLC analysis was used to provide impurity analysis of the mRNA product following downstream purifications using SPE, TFF and oligo-dT affinity chromatography. The application of at-line analytics can provide the critical insight required for optimisation of the mRNA manufacturing process, enabling optimization of individual IVT reaction components, such as concentration of Mg2+, plasmid, NTP concentration, as well as adjusting the reaction parameters in near real-time. Therefore, this AEX HPLC method provides valuable information for developing

kinetic models of the IVT unit operation and mass-balance models for downstream purification unit operations.

Data availability statement

The raw data supporting the conclusion of this article will be made available by the authors, without undue reservation.

Author contributions

EW: Methodology, Validation, Investigation, Formal Analysis, Data curation, Visualization, Writing–original draft preparation. KL: Investigation, Formal Analysis, Data curation. AN: Investigation, Formal Analysis. EN: Investigation, Formal Analysis. JQ: Investigation, Formal Analysis. KC: Conceptualization, Review and Editing. ZK: Supervision, Review and Editing, Project administration, Funding acquisition. MD: Conceptualization, Supervision, Writing–original draft preparation, Review and Editing, Project administration, Funding acquisition. All authors contributed to the article and approved the submitted version.

Funding

This work was supported by funding from the Wellcome Leap R3 Program.

Acknowledgments

MD acknowledges further support from Biotechnology and Biological Sciences Research Council UK (BBSRC) (BB/M012166/1). The authors acknowledge Rebecca Ryan for procuring the NLuc plasmid DNA.

Conflict of interest

The authors declare that the research was conducted in the absence of any commercial or financial relationships that could be construed as a potential conflict of interest.

Publisher's note

Supplementary material

The Supplementary Material for this article can be found online at: https://www.frontiersin.org/articles/10.3389/fmolb.2024.1250833/full#supplementary-material

References

Anderson, A. C., Scaringe, S. A., Earp, B. E., and Frederick, C. A. (1996). HPLC purification of RNA for crystallography and NMR. *RNA N. Y. N.* 2 (2), 110–117.

Baronti, L., Karlsson, H., Marušič, M., and Petzold, K. (2018). A guide to large-scale RNA sample preparation. *Anal. Bioanal. Chem.* 410 (14), 3239–3252. doi:10.1007/s00216-018-0943-8

Beckert, B., and Masquida, B. (2011). "Synthesis of RNA by *in vitro* transcription," in *RNA: methods and protocols*. Editor H. Nielsen (Totowa, NJ: Humana Press), 29–41. Methods in Molecular Biology). doi:10.1007/978-1-59745-248-9_3

Cook, K., and Thayer, J. (2011). Advantages of ion-exchange chromatography for oligonucleotide analysis. *Bioanalysis* 3 (10), 1109–1120. doi:10.4155/bio.11.66

Corbett, K. S., Edwards, D. K., Leist, S. R., Abiona, O. M., Boyoglu-Barnum, S., Gillespie, R. A., et al. (2020). SARS-CoV-2 mRNA vaccine design enabled by prototype pathogen preparedness. *Nature* 586 (7830), 567–571. doi:10.1038/s41586-020-2622-0

Daniel, S., Kis, Z., Kontoravdi, C., and Shah, N. (2022). Quality by Design for enabling RNA platform production processes. *Trends Biotechnol.* 40 (10), 1213–1228. doi:10.1016/j.tibtech.2022.03.012

Dousis, A., Ravichandran, K., Hobert, E. M., Moore, M. J., and Rabideau, A. E. (2023). An engineered T7 RNA polymerase that produces mRNA free of immunostimulatory byproducts. *Nat. Biotechnol.* 41 (4), 560–568. doi:10.1038/s41587-022-01525-6

Duffy, K., Arangundy-Franklin, S., and Holliger, P. (2020). Modified nucleic acids: replication, evolution, and next-generation therapeutics. *BMC Biol.* 18 (1), 112. doi:10.1186/s12915-020-00803-6

Easton, L. E., Shibata, Y., and Lukavsky, P. J. (2010). Rapid, nondenaturing RNA purification using weak anion-exchange fast performance liquid chromatography. *RNA N. Y. N.* 16 (3), 647–653. doi:10.1261/rna.1862210

Grier, A. E., Burleigh, S., Sahni, J., Clough, C. A., Cardot, V., Choe, D. C., et al. (2016). pEVL: a linear plasmid for generating mRNA IVT templates with extended encoded poly(A) sequences. *Mol. Ther. Nucleic Acids* 5 (4), e306. doi:10.1038/mtna.2016.21

Hadas, Y., Sultana, N., Youssef, E., Sharkar, M. T. K., Kaur, K., Chepurko, E., et al. (2019). Optimizing modified mRNA *in vitro* synthesis protocol for heart gene therapy. *Mol. Ther. Methods Clin. Dev.* 14, 300–305. doi:10.1016/j.omtm.2019.07.006

Kanavarioti, A. (2019). HPLC methods for purity evaluation of man-made single-stranded RNAs. *Sci. Rep.* 9 (1), 1019. doi:10.1038/s41598-018-37642-z

Kis, Z., Tak, K., Ibrahim, D., Papathanasiou, M. M., Chachuat, B., Shah, N., et al. (2022). Pandemic-response adenoviral vector and RNA vaccine manufacturing. *Npj Vaccines* 7 (1), 29–10. doi:10.1038/s41541-022-00447-3

Koubek, J., Lin, K. F., Chen, Y. R., Cheng, R. P., and Huang, J. J. T. (2013). Strong anion-exchange fast performance liquid chromatography as a versatile tool for preparation and purification of RNA produced by *in vitro* transcription. *RNA N. Y. N.* 19 (10), 1449–1459. doi:10.1261/rna.038117.113

McNamara, M. A., Nair, S. K., and Holl, E. K. (2015). RNA-based vaccines in cancer immunotherapy. *J. Immunol. Res.* 2015, 794528. doi:10.1155/2015/794528

Meyer, A. J., Garry, D. J., Hall, B., Byrom, M. M., McDonald, H. G., Yang, X., et al. (2015). Transcription yield of fully 2'-modified RNA can be increased by the addition of thermostabilizing mutations to T7 RNA polymerase mutants. *Nucleic Acids Res.* 43 (15), 7480–7488. doi:10.1093/nar/gkv734

Nwokeoji, A. O., Kung, A. W., Kilby, P. M., Portwood, D. E., and Dickman, M. J. (2017). Purification and characterisation of dsRNA using ion pair reverse phase chromatography and mass spectrometry. *J. Chromatogr. A* 1484, 14–25. doi:10.1016/j.chroma.2016.12.062

Polack, F. P., Thomas, S. J., Kitchin, N., Absalon, J., Gurtman, A., Lockhart, S., et al. (2020). Safety and efficacy of the BNT162b2 mRNA covid-19 vaccine. *N. Engl. J. Med.* 383 (27), 2603–2615. doi:10.1056/NEJMoa2034577

Pregeljc, D., Skok, J., Vodopivec, T., Mencin, N., Krušič, A., Ličen, J., et al. (2023). Increasing yield of *in vitro* transcription reaction with at-line high pressure liquid chromatography monitoring. *Biotechnol. Bioeng.* 120 (3), 737–747. doi:10.1002/bit.28299

Sahin, U., Karikó, K., and Türeci, Ö. (2014). mRNA-based therapeutics — developing a new class of drugs. *Nat. Rev. Drug Discov.* 13 (10), 759–780. doi:10.1038/nrd4278

Shields, T. P., Mollova, E., Ste Marie, L., Hansen, M. R., and Pardi, A. (1999). High-performance liquid chromatography purification of homogenous-length RNA produced by trans cleavage with a hammerhead ribozyme. *RNA* 5 (9), 1259–1267. doi:10.1017/s1355838299990945

Sun, J., Joshi, D., Betancourt, F., Solodinin, A., Woodland, B., and Yan, H. (2020). Anion exchange chromatography of oligonucleotides under denaturing conditions. *Nucleosides Nucleotides Nucleic Acids* 39 (6), 818–828. doi:10.1080/15257770.2019.1706096

Thayer, J. R., Barreto, V., Rao, S., and Pohl, C. (2005). Control of oligonucleotide retention on a pH-stabilized strong anion exchange column. *Anal. Biochem.* 338 (1), 39–47. doi:10.1016/j.ab.2004.11.013

To, K. K. W., and Cho, W. C. S. (2021). An overview of rational design of mRNA-based therapeutics and vaccines. *Expert Opin. Drug Discov.* 16 (11), 1307–1317. doi:10.1080/17460441.2021.1935859

Tusup, M., French, L. E., De Matos, M., Gatfield, D., Kundig, T., and Pascolo, S. (2019). Design of *in vitro* transcribed mRNA vectors for research and therapy. *Chimia* 73 (6), 391–394. doi:10.2533/chimia.2019.391

van de Berg, D., Kis, Z., Behmer, C. F., Samnuan, K., Blakney, A. K., Kontoravdi, C., et al. (2021). Quality by design modelling to support rapid RNA vaccine production against emerging infectious diseases. *Npj Vaccines* 6 (1), 65–10. doi:10.1038/s41541-021-00322-7

frontiers | Frontiers in Molecular Biosciences

TYPE Review
PUBLISHED 10 July 2024
DOI 10.3389/fmolb.2024.1426129

OPEN ACCESS

EDITED BY
Zoltán Kis,
The University of Sheffield, United Kingdom

REVIEWED BY
Bharathikumar Vellalore Maruthachalam,
Janssen Research and Development,
United States
Craig Martin,
University of Massachusetts Amherst,
United States

*CORRESPONDENCE
Irena Vlatkovic,
irena.vlatkovic@biontech.de

†These authors have contributed equally to this work and share the first authorship

RECEIVED 30 April 2024
ACCEPTED 14 June 2024
PUBLISHED 10 July 2024

CITATION
Lenk R, Kleindienst W, Szabó GT, Baiersdörfer M, Boros G, Keller JM, Mahiny AJ and Vlatkovic I (2024), Understanding the impact of *in vitro* transcription byproducts and contaminants. *Front. Mol. Biosci.* 11:1426129.
doi: 10.3389/fmolb.2024.1426129

Understanding the impact of *in vitro* transcription byproducts and contaminants

Robin Lenk†, Werner Kleindienst†, Gábor Tamás Szabó, Markus Baiersdörfer, Gábor Boros, Jason M. Keller, Azita J. Mahiny and Irena Vlatkovic*

BioNTech SE, Mainz, Germany

The success of messenger (m)RNA-based vaccines against SARS-CoV-2 during the COVID-19 pandemic has led to rapid growth and innovation in the field of mRNA-based therapeutics. However, mRNA production, whether in small amounts for research or large-scale GMP-grade for biopharmaceutics, is still based on the *In Vitro* Transcription (IVT) reaction developed in the early 1980s. The IVT reaction exploits phage RNA polymerase to catalyze the formation of an engineered mRNA that depends on a linearized DNA template, nucleotide building blocks, as well as pH, temperature, and reaction time. But depending on the IVT conditions and subsequent purification steps, diverse byproducts such as dsRNA, abortive RNAs and RNA:DNA hybrids might form. Unwanted byproducts, if not removed, could be formulated together with the full-length mRNA and cause an immune response in cells by activating host pattern recognition receptors. In this review, we summarize the potential types of IVT byproducts, their known biological activity, and how they can impact the efficacy and safety of mRNA therapeutics. In addition, we briefly overview non-nucleotide-based contaminants such as RNases, endotoxin and metal ions that, when present in the IVT reaction, can also influence the activity of mRNA-based drugs. We further discuss current approaches aimed at adjusting the IVT reaction conditions or improving mRNA purification to achieve optimal performance for medical applications.

KEYWORDS

***in vitro* transcription reaction (IVT), double-stranded RNA (dsRNA), abortive transcripts, IVT byproducts, IVT contaminants, mRNA purification**

Introduction

Following the success of the first clinically approved mRNA-based vaccines during the COVID-19 pandemic, mRNA therapeutics hold tangible promise as safe and effective biologics of the future, expected to prevent, improve, or cure a variety of diseases with unmet medical need. The active substance and basis of this new class of drugs is a designed, synthetic single-stranded messenger RNA (mRNA) molecule. In mammalian cells, endogenous mRNA is normally transcribed from DNA in the nucleus by RNA polymerase II, in the form of a pre-mRNA transcript, then it is 5′ capped,

Abbreviations: dsRNA, double-stranded RNA; LPS, lipopolysaccharide; mRNA, messenger RNA; NTP, nucleoside-triphosphates; ssRNA, single-stranded RNA.

3′ polyadenylated, spliced to remove introns, and finally transported to the cytoplasm where it can be translated into a specific protein. The synthetic mRNA used for therapeutics is instead produced enzymatically in solution, purified, packaged into a formulated lipid carrier, and delivered to the cytoplasm by way of endocytosis. To artificially generate mRNA in solution under cell-free conditions, the technique of *in vitro* transcription (IVT) was developed and utilizes a phage RNA polymerase that can recognize diverse types of DNA templates. However, due to the properties and components of the IVT reaction, distinct nucleotide-based byproducts may be formed in addition to the full-length mRNA molecule templated by the DNA. Moreover, depending on the starting materials or equipment used at different stages of the production and purification processes, other types of process related, non-nucleotide-based contaminants may be introduced. Any of the product or process related contaminants that reach the formulated drug can potentially activate pattern recognition receptors (PRRs), causing a host immune response that may negatively impact mRNA-encoded protein expression. Thus, several aspects of mRNA production are necessary to implement, and they are under continuous development: (1) optimizing the IVT reaction components and conditions; (2) purification procedures; and (3) stringent quality control using analytical methods that can detect and characterize byproducts and contaminants. Previous reviews and assessment reports have already discussed in detail the specific analytical methods and quality controls currently used for mRNA-based drug manufacturing (European Medicines Agency, 2021; Schoenmaker et al., 2021; Daniel et al., 2022; European Medicines Agency, 2022; BioPhorum Operations Group Ltd, 2023). In this review, we will highlight the various types of IVT reaction byproducts and contaminants as well as their mechanisms of action that may influence the quality and performance of mRNA-based therapeutics.

In vitro transcription reaction

A synthetic mRNA is typically produced in a cell-free enzymatic IVT reaction consisting of a DNA template to guide the sequence, free nucleoside triphosphate (NTP) monomers, a DNA-dependent RNA polymerase that transcribes the mRNA directly from the template, and an optimized buffer. The quality of the components and their stoichiometric ratios in the reaction mixture, physical parameters of the process such as duration, pH or temperature, and the design of the mRNA encoded on the template can highly influence the yield and quality of the final product (Triana-Alonso et al., 1995; Mu et al., 2018). The design of the encoded mRNA, particularly its length, the sequence of the untranslated regions (UTR) and open reading frame, the number of repetitive sequences and homogenic parts, and the templated poly(A) tail, can directly influence the performance of the IVT process (Conrad et al., 2020; Leppek et al., 2022). Most commonly, circular plasmid DNA (pDNA) containing the specific RNA polymerase promoter sequence is linearized and used as the template for IVT reactions. How the plasmid is linearized, including the selected type and concentration of restriction enzymes, the buffer used, duration of the reaction, and the downstream purification process, can influence the quality of the DNA template and consequently the final mRNA product. A chemically synthesized 'doggybone' DNA (dbDNA™) vector, which is a linear, closed-end molecule produced entirely in a cell-free process, can also be used (Touchlight Genetics Ltd, 2024). Similarly, synthetic linear DNA with either two open 5′ and 3′ ends (oeDNA™) or one open and one hairpin end (opDNA™) are available whereby the open ends can be chosen to include a blunt end or an overhang (4basebio PLC, 2024). Such synthetic DNA templates for IVT reactions, however, are still in development. Alternatively, PCR amplified DNA can serve as an effective template for the IVT reaction (Brunelle and Green, 2013). As necessary building blocks of mRNA, the IVT reaction contains adenine (A), guanine (G), cytosine (C) and uridine (U), and/or their isomers or modified derivatives. The choice of nucleotides and their starting ratios, or changing their ratios during IVT respectively ("feeding" strategy), can influence the transcription efficiency and the amount and types of byproducts produced during the reaction (Skok et al., 2022; Ziegenhals et al., 2023). Currently, the most widely used RNA polymerase is the bacteriophage T7 RNA polymerase. Selection of the RNA polymerase might significantly influence the IVT reaction. Ideally, the RNA polymerase should have a high transcriptional yield and fidelity, full activity under variable reaction conditions, and the ability to incorporate modified NTPs with high fidelity. 5′ cap analogs can be added to the reaction mixture for co-transcriptional capping, which reduces the need for later purification steps and also increases the yield of full-length mRNA (Ramanathan et al., 2016; Henderson et al., 2021). If co-transcriptional capping is not performed, a 5′ cap can be enzymatically added post-transcriptionally using RNA triphosphatase, guanylyl-transferase and guanine methyltransferase to first form Cap0 and then with the subsequent addition of mRNA Cap 2′-O-Methyltransferase to form Cap1 (Ensinger et al., 1975). Similarly, while a poly(A) tail is often directly encoded by the template, it can also be added or extended post transcriptionally using Poly(A) polymerase. mRNA yields and quality, including the amounts of byproducts, are significantly influenced by the stoichiometric ratios of the ingredients, the physical parameters of the reaction such as pH and temperature, and the duration of the reaction. To select optimal conditions, the sequence and the length of the mRNA and the selected RNA polymerase must be considered. With optimization of the IVT reaction, a dramatic reduction of unwanted byproducts can be achieved. Moreover, non-obligatory ingredients can be added to enhance yield and quality or reduce downstream purification steps. Such auxiliary reagents can be used to enhance transcription (e.g., spermidine, DMSO, urea) (Moruzzi et al., 1975; Chen and Zhang, 2005; Francis et al., 2024), to support polymerase enzymatic activity (e.g., dithiothreitol) (Kartje et al., 2021) or to reduce mRNA degradation (e.g., RNase inhibitors) and byproduct formation (e.g., denaturing agents; pyrophosphatase) (Cunningham and Ofengand, 1990; Piao et al., 2022).

IVT byproducts and their biological impacts

The major forms of IVT byproducts are short or long ssRNA, dsRNA or RNA:DNA hybrids (Figure 1). Since many viruses rely on RNA to carry their genetic information, the uptake of such

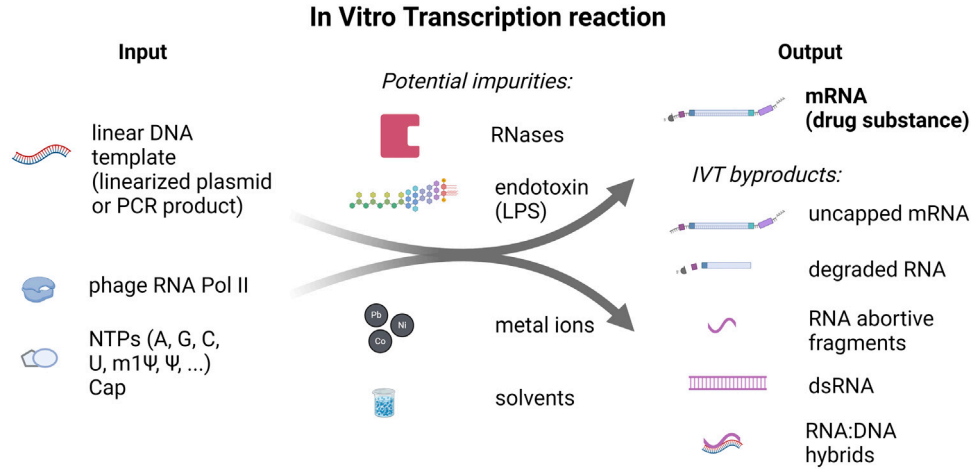

FIGURE 1
In vitro transcription reaction input and output components and potential impurities. On the left side, linear DNA template (linearized plasmid and PCR product) and nucleoside-triphosphates (NTPs), including N1-Methylpseudouridine-5′-Triphosphate (m1Ψ), and RNA Polymerase (RNA Pol II) are listed as inputs to the IVT reaction. On the right side, outputs of the IVT reaction: mRNA (drug substance) and IVT byproducts are shown. In addition, potential impurities that can be introduced to the reaction through the raw materials or during the production process are listed in the middle.

material has been determined through evolution to be a potential danger signal for the cell. The nucleotide-based byproducts are sensed by a multitude of immune pathways leading to inflammation, growth inhibition or even cell death (Figure 2) (Sahin et al., 2014; Devoldere et al., 2016; Vlatkovic, 2021). Even the purest single-stranded, uridine containing mRNA products show a certain degree of immunogenicity mediated through Toll-like receptor (TLR) 7 and 8 (Heil et al., 2004). However, by incorporating modified nucleotides and removing the byproducts from the final mRNA transcription reaction, it is possible to create a therapeutic product that is nearly immune silent (Karikó et al., 2005; Karikó et al., 2008; Karikó et al., 2011; Andries et al., 2015). For certain applications where relatively high doses under repetitive intravenous administration would be required without causing an unwanted immune response, mRNA-based therapeutics are being further improved (Vlatkovic, 2021). Some critical elements serving as the basis for such improvements are a better understanding of the types of byproducts that can be produced in the IVT reaction, tactics to control their quantities, and clarifying their potential biological impacts. Below we summarize progress that has been made in this regard.

Abortive transcripts

The first evidence that RNA polymerases can produce short, abortive transcripts derived from the transcription start site was given by Bellamy et al. (1972) when they sequenced short RNA oligonucleotides in the virions of reoviruses. Later, a steady-state release of di-nucleotide RNA oligos in the presence of only two species of RNA nucleotides (ATP and UTP) was described using λb2 DNA and *Escherichia coli* RNA polymerase (Johnston and McClure, 1976). More importantly, the authors also showed that in the presence of all four RNA nucleotides, ≤10% of the total RNA synthesized resembled abortive products (i.e., RNA dinucleotides).

As stated above, T7 RNA polymerase is commonly used for industrial production of RNA therapeutics because of its high fidelity and processivity. In 1987, the first RNA using T7 RNA polymerase and synthetic DNA templates was synthesized (Milligan et al., 1987). As reported previously for *E. coli* RNA polymerase (Johnston and McClure, 1976; McClure et al., 1978), Milligan et al. found that T7 RNA polymerase also produces numerous shorter sequences resembling the 5′-end of the template strand. The amounts and specific sequences of abortive products varied but depended on the +1 to +6 sequence of the synthetic DNA template (Milligan et al., 1987).

To date, many studies have contributed to our understanding of the complex mechanism by which T7 RNA polymerase initiates RNA transcription. Briefly, after the T7 RNA polymerase binds its promoter (Rosa, 1979), bending the DNA strand and thereby opening it (Ujvári and Martin, 2000; Tang and Patel, 2006a; 2006b; Tang et al., 2008), the enzyme starts synthesizing the first nucleotides of the RNA strand. The growing RNA:DNA hybrid pushes against the promoter-bound region of the T7 RNA polymerase and causes a 40° rotation after 3 to 7 nt have been synthesized. (Brieba and Sousa, 2001; Mukherjee et al., 2002; Tahirov et al., 2002; Ma et al., 2005; Bandwar et al., 2007; Durniak et al., 2008). Only after the synthesis of 9 to 12 nt does a drastic 220° rotation occur, which releases the upstream promoter interactions and thus enables the transition of the T7 RNA polymerase into a stable elongation complex (EC) for full-length RNA synthesis (Brieba and Sousa, 2001; Mukherjee et al., 2002; Tahirov et al., 2002; Ma et al., 2005; Bandwar et al., 2007; Durniak et al., 2008; Tang et al., 2009; Ramírez-Tapia and Martin, 2012). During the entire initiation process, abortive byproducts with a length of 2 to 13 nt can be released (Martin et al., 1988; Brieba and Sousa, 2001; Ikeda and Richardson, 1986; Jia and Patel, 1997; Tang et al., 2008).

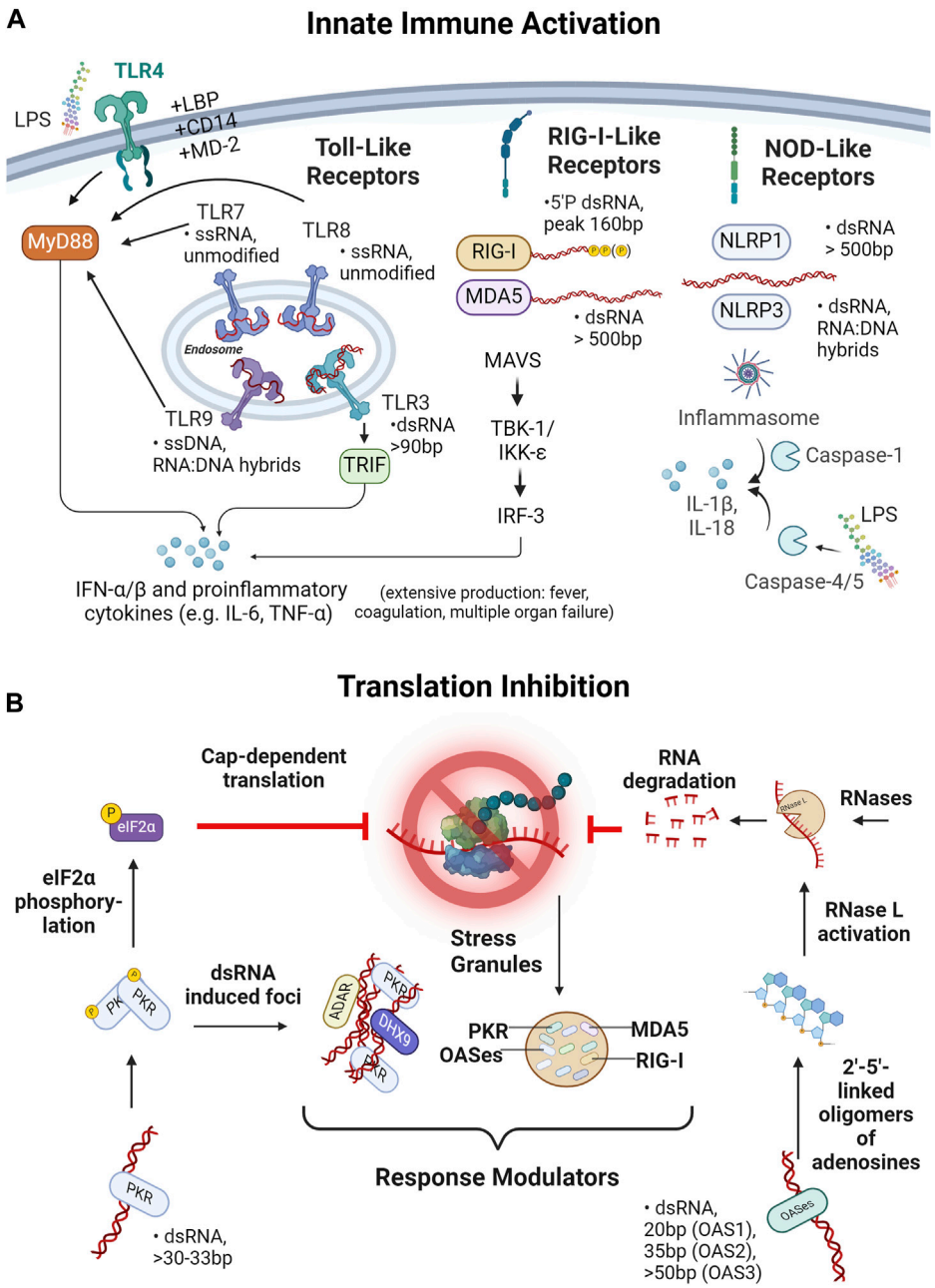

FIGURE 2
IVT reaction byproducts and contaminants and their impact in transfected cells. **(A)** Impact of IVT reaction byproducts and contaminants on innate immune activation is shown. Depicted are three receptor families, namely, Toll-like receptors (TLRs), retinoic acid inducible gene I-like receptors (RIG-I-like receptors) and NOD-like receptors (NLRs) known to detect ssRNA, dsRNA and RNA:DNA hybrids of various lengths. Activation of TLR4, 7, 8 or 9 leads via the MyD88-pathway and TLR3 via TRIF to the secretion of IFN- α/β and proinflammatory cytokines such as IL-6 or IFN-γ. Likewise, the RIG-I-like receptors, MDA5 and RIG-I lead via MAVS, TBK-1/IKK-ε and IRF-3 to a secretion of proinflammatory cytokines. In contrast, the NOD-like receptors NLRP1 and NLRP3 trigger inflammasome assembly and via caspase-1 lead to IL-1β and IL-18 release. Apart from the immunostimulatory activity of IVT byproducts of "nucleic nature", detection of bacterial lipopolysaccharide (LPS) via TLR4 or caspase-4/5 and subsequent inflammasome activation triggers innate immune activation. **(B)** Mechanisms of translational inhibition due to effects of dsRNA byproducts are depicted. dsRNA can be recognized by protein kinase R (PKR) or 2′–5′ Oligoadenylate synthetases (OASes). Two PKR-molecules can autophosphorylate upon dsRNA binding, allowing phosphorylation of eIF2 transcription initiation factor. eIF2 plays a central role in initiating translation, thus, phosphorylation of eIF2 inhibits cap-dependent translation of RNA. OASes, on the other hand, act through linkage and oligomerization of ATP leading to activation of RNase L and, in turn, to the degradation of ssRNA (i.e., the drug product). Both PKR and OASes, as well as the RIG-I,-like receptors MDA5 and RIG-I participate in the formation of dsRNA-induced foci, so called stress granules which are thought to amplify or control dsRNA sensing responses.

Koh et al. (2018) were able to resolve the transcription initiation process at near base-pair resolution enabling a thorough understanding of abortive cycling and processive RNA synthesis, respectively. They found two distinct pathways that can lead to the release of abortive products. Either the T7 RNA polymerase remains bound to the DNA and re-starts RNA synthesis after a release of

abortive products ('RNA polymerase recycling') or, secondly, T7 RNA polymerase dissociates with or after RNA release and the next round of RNA synthesis starts only after binding of a new T7 RNA polymerase molecule ('RNA polymerase exchange'). Moreover, in the same study, the authors were able to develop a probabilistic model for the three possible outcomes of T7 RNA polymerase mediated transcription (on DNA templates bearing a class III consensus promoter) that are: elongation, dissociation, and abortive initiation (Koh et al., 2018). Interestingly, they could show that the majority (about 56%) of total initiation events with T7 RNA polymerase molecules result in elongation (i.e., full-length RNA synthesis) without generating abortive byproducts. The remaining initiation events lead to the generation of abortive byproducts whereby the T7 RNA polymerase molecules can either still produce the full-length product after 're-starting' the transcription or completely fail to undergo the transition into the elongation complex. Those molecules that completely fail to transition into the elongation phase account for about six-times as many abortive byproducts as those molecules that can still proceed with full-length RNA synthesis. This underscores that failed transitions into the elongation complex not only reduce the productive capacity of RNA polymerase but are also a major contributor to byproduct formation (Koh et al., 2018).

Of note, abortive initiation can be regarded as a universal feature of RNA polymerases (Alhadid et al., 2017) occurring in prokaryotic (Hsu, 2002), viral (e.g., T7 phage as described, reovirus (Bellamy et al., 1972; Farsetta et al., 2000) or brome mosaic virus (Sun et al., 1996)) and eukaryotic RNA polymerases (e.g., shown for yeast by Bhargava and Kassavetis, 1999). Recently, abortive transcripts were also shown to occur in (yeast) mitochondria (Goovaerts et al., 2023) and in mouse serum and liver (Qin et al., 2024). From an evolutionary perspective, abortive RNA byproducts might have served as the first primers for DNA replication (Matsumoto, 1994). Interestingly, abortive products can exert anti-termination activity by interfering with RNA terminator hairpin formation (Lee et al., 2010) and thus regulate the activation of the late genes of viral replication after accumulating during transcription of earlier genes. Moreover, very short RNAs (2–4 nt in length, termed nanoRNAs) are thought to prime transcription in bacteria, thereby regulating gene expression (Goldman et al., 2011; Nickels and Dove, 2011; Vvedenskaya et al., 2012). Assuming abortive byproducts reach the cytosol of transfected cells, there might occur yet to be defined interactions with intrinsic RNAs or PRRs underlining the need for further research on IVT byproducts.

Double-stranded RNA (dsRNA)

Even though RNA itself inherently has a certain immunogenicity, the immunogenicity associated with IVT products can be induced by dsRNA (Karikó et al., 2011) (Figure 2A). Two main pathways for how dsRNA byproducts arise during IVT have been identified. One is by way of a promoter-independent, DNA-dependent transcription of the nontemplate strand (Mu et al., 2018) and the other is by RNA-dependent 3′ end additions (Cazenave and Uhlenbeck, 1994; Triana-Alonso et al., 1995). With regard to 3′ end additions, it was shown by Gholamalipour et al. that most 3′ additions arise via a *cis* mechanism, whereby the end of the RNA folds back onto itself and the T7 RNA polymerase rebinds to this dsRNA hairpin and starts extending it with the nontemplate sequence (Gholamalipour et al., 2018). This rebinding and extension of the RNA by the T7 RNA polymerase is independent of the DNA template and can even be observed on chemically produced run-off RNAs (Gholamalipour et al., 2018). Double-stranded RNA can also form when the T7 RNA polymerase switches strands at the end of the DNA template and thereby transcribes a complimentary mRNA strand. This mechanism was shown, although promoter-independent, to have a certain sequence specificity for the 3′ end of the DNA template (Sequence: GTGGAA TACCCATTCGACATTCTCCC) even though the mechanism underlying this effect has not been investigated yet (Mu et al., 2018; Wu et al., 2020). In both cases, the 3′ extension as well as the promoter-independent transcription initiation, the exact mechanism of how the T7 RNA polymerase impacts the formation of dsRNA byproducts remains elusive. In general, upon binding to the T7 promoter, the T7 RNA polymerase forms an initiation complex (IC) that transitions into the more stable elongation complex (EC) after transcription of ~10 nucleotides (Cheetham and Steitz, 1999). It has been hypothesized that the dsRNA byproducts mentioned above are driven by the EC of the T7 RNA polymerase, which is either directly binding to the nontemplate strand or to the run-off product that folds into a hairpin and starts producing the undesired nontemplate RNA strand. This suggests that stabilizing the IC or decreasing the IC to EC transition barrier might decrease the formation of dsRNA (Dousis et al., 2023) but further investigation is needed.

Once inside a cell, dsRNA can be detected by several sensor proteins that lead to different response cascades. One class of well-known dsRNA sensors are the cytosolic RIG-I (retinoic acid inducible gene I)-like receptors (RLRs): RIG-I, melanoma differentiation-associated protein 5 (MDA5) and LGP2 (Rehwinkel and Gack, 2020) (Table 1; Figure 2A). While RIG-I and MDA5 are direct activators of pathways leading to the release of type I interferons, LGP2 is hypothesized to be a regulator of RIG-I and MDA5 (Satoh et al., 2010; Kato et al., 2011; Childs et al., 2013). RIG-I and MDA5 both activate the MAVS pathway upon filamentation and the subsequent ubiquitination and oligomerization of their two N-terminal CARD domains (Peisley et al., 2012; Peisley et al., 2013). MAVS recruits TRAF3/6 which subsequently activates the kinase complexes TBK1 and IKK, which in turn leads to activation of IRF3/7 and NF-κB, respectively (Wu et al., 2023). While the downstream signaling cascades of the two receptors are very similar, the dsRNA species that they each recognize are distinct. MDA5 forms a filament by binding multiple monomers to one dsRNA. The downstream signal strength increases with the length of the dsRNA duplex but requires a minimum length of ~500–1000bp to initiate and is sequence independent (Peisley et al., 2011; Peisley et al., 2012). Since most RNAs produced with IVT for clinical applications are longer than 500bp and can even be significantly longer, dsRNA byproducts of these RNAs would have the potential to trigger MDA5. RIG-I, on the other hand, is triggered by dsRNA species with a di- or triphosphate on the 5′end, and where the 2′-O position of the terminal nucleotide is unmethylated (Hornung et al., 2006; Schmidt et al., 2009; Goubau et al., 2014; Schuberth-Wagner et al., 2015).

TABLE 1 Impacts of IVT reaction byproducts on immune signaling sensors and dsRNA-dependent enzymes in the cell.

	Family name	Name	Recognition species	Evading RNA modifications
Immune Signaling Sensors	RLR	RIG-I	di-, triphosphate 5′end, peak activity 160bp	Ψ, m1 Ψ, m6A
		MDA5	>500bp	none
	NLR	NLPR1	ND	ND
		NLRP3	>500bp	ND
	TLR	TLR3	>90bp	m6a, s2u
dsRNA-dependent Enzymes	PKR	PKR	>30 – 33bp	Ψ
	OAS	OAS1	~20bp	Ψ, m6a, s2u
		OAS2	~35bp	
		OAS3	>50bp	

Abbreviations: RLR, RIG-I (retinoic acid inducible gene I)-like receptors; MDA5, melanoma differentiation-associated protein 5; NLR, NOD-like receptors; TLR, Toll-like receptor; PKR, protein kinase R; OAS, 2′-5′-oligoadenylate synthetase; ND, not determined.

Length-dependent activation of RIG-I seems to follow a bell-shaped curve with an apparent peak at ~160bp (Cadena et al., 2019). The IVT byproducts that would fit this size profile and activate RIG-I are uncapped dsRNAs. However, it is possible that when T7 RNA polymerase switches strands, it effectively leaves a triphosphate at the 5′ end of the nontemplated RNA strand, even on an initially capped transcript, and this may also activate RIG-I. While RNA modifications like m6-adenosine (m6A), pseudouridine (Ψ) and 1-methylpseudouridine (m1Ψ) have been shown to strongly reduce the downstream activity of RIG-I, the same effect has not been observed for MDA5 (Table 1) (Peisley et al., 2013; Durbin et al., 2016; Mu et al., 2018).

Another class of sensors capable of detecting dsRNA are the NOD-like receptors (NLRs) (Table 1; Figure 2A). While there are about 20 known representatives of this type in humans, only NLRP1 and NLRP3 have been shown to be activated by RNA duplexes (Allen et al., 2009; Bauernfried et al., 2021). These two receptors both have a pyrin domain (PYD), through which they interact with apoptosis-associated speck-like protein containing a CARD (ASC) and form the inflammasome to activate caspase1. Caspase1 leads to the activation of the proinflammatory cytokines IL-1β and IL-18 (Kienes et al., 2021; Ohto, 2022; Xu and Núñez, 2023). For NLRP1 it has been shown that a dsRNA duplex length >500bp is needed for activation, while for NLRP3 the precise nature of the stimulatory dsRNA species remains to be identified (Table 1) (Allen et al., 2009; Bauernfried et al., 2021). Thus, NLRP1 appears to sense the same species of byproducts as MDA5. If and how RNA modifications influence recognition by NLR has not been investigated yet.

One of the oldest classes of PRRs in evolution are the Toll-like receptors (TLRs). In humans the TLR family comprises 10 types (TLR1-10), with only TLR3 able to sense dsRNA. In contrast to the RLRs and NLRs, TLR3 is present in the endosomal membrane and senses dsRNA inside the endosome (Figure 2A). In fact, the low pH of the early to late endosomes is crucial for dsRNA binding to TLR3 (Leonard et al., 2008). Upon binding dsRNA, TLR3 homodimerizes, forms clusters on longer dsRNA and recruits TIR-domain-containing adapter-inducing interferon (TRIF). Downstream of TRIF, TRAF3 induces activation of TBK1, again leading to the transcription of type I interferons and proinflammatory cytokines by IRF3/7 and NF-κB (Fitzgerald and Kagan, 2020; Lim et al., 2022). To activate TLR3, a minimum dsRNA duplex of 90bp is required, but the avidity of TRIF to the receptor increases as more receptors cluster together, which results in an increased signal strength on longer dsRNA (Leonard et al., 2008; Jelinek et al., 2011; Luo et al., 2012). However, the dsRNAs that are detected by TLR3 can be much shorter than dsRNA detected by MDA5 and NRLP1 (Table 1). Furthermore, TLR3 recognition is not dependent on the end structure of the dsRNAs, which makes it possible to detect dsRNA duplexes in the same range as RIG-I, but without the requirement for a tri- or diphosphate on the 5′end. However, incorporating nucleoside modifications like m6-adenosine or s2-uridine lead to reduced TLR3 activation (Karikó et al., 2005).

Protein kinase R (PKR) is a protein kinase whose enzymatic activity is dependent on dsRNA binding. Upon binding a dsRNA, two PKR proteins are stabilized by autophosphorylation and become active (Dey et al., 2005) (Figure 2B). The active kinase can then phosphorylate the eIF2 transcription initiation factor, which subsequently shuts down protein synthesis (Balachandran et al., 2000). Moreover, PKR seems to play a role in modulating other RNA sensors through its involvement in the formation of stress granules (SG) (Onomoto et al., 2012) (Figure 2B). In several studies recruitment of RIG-I, MDA5, PKR and 2′-5′-oligoadenylate synthetase (OAS) to SG has been shown (Onomoto et al., 2012; Langereis et al., 2013; Manivannan et al., 2020; Paget et al., 2023). However, it remains unclear if this recruitment has a positive or negative effect on immune signaling (Yoo et al., 2014; Paget et al., 2023). Another cell condensate that recruits PKR is dsRNA-induced foci (dRIFs) (Corbet et al., 2022; Zappa et al., 2022) (Figure 2B). These dRIFs form predominantly before protein synthesis is suppressed and contain proteins that are also involved in dsRNA sensing (NLRP1) or regulating the immune response (DHX9, ADAR1) (Corbet et al., 2022; Ren et al., 2023; Levanon et al., 2024). As with SG, the data available for dRIFs condensates do not yet provide a clear conclusion on whether these dRIFs are amplifying or controlling the dsRNA sensing response (Corbet et al., 2022; Zappa et al., 2022). In any case, to activate PKR a minimum

length of 30 – 33bp is required and the maximum level of activation positively correlates with the length of the dsRNA (Husain et al., 2012). Furthermore, it was shown that ssRNAs that form a short stem-loop were also detected by PKR, even though the activation was also dependent on the presence of 5′triphosphates (Nallagatla et al., 2007). This highlights the possibility that PKRs also detect the secondary structure of a correctly transcribed RNA product. In contrast, the presence of pseudouridine (Ψ) in the RNA has been shown to reduce PKR activation and boost translation (Anderson et al., 2010).

2′–5′ Oligoadenylate synthetases (OAS) are, like PKR, enzymes whose catalytic activity is dependent on dsRNA. In humans, the family is comprised of OAS1 – OAS3 and OASL, with OAS1 – OAS3 possessing enzymatic activity while OASL does not (Rebouillat and Hovanessian, 1999). Active OASes fuse ATP molecules together by linking the 2′ and 5′ positions of the ribose rings (2′p5′a) (Hovanessian and Justesen, 2007; Kristiansen et al., 2011). From these 2′5′- linked ATPs the OASes catalyze the formation of even longer oligomers that lead to activation of Ribonuclease L (RNase L), which degrades ssRNA (Han et al., 2014; Hornung et al., 2014) (Figure 2B). Even though OAS1 – 3 all harbor enzymatic activity, OAS3 is the prime activator of RNase L, leaving the main function and physiological role of OAS1 and OAS2 open (Ibsen et al., 2014; Sarkar et al., 2023). The minimum duplex lengths that are required for activation vary between ~20bp for OAS1 to ~35bp for OAS2 and ~50bp for OAS3, even though the mechanism of dsRNA binding and activation is still unresolved (Donovan et al., 2015; Koul et al., 2020; Wang et al., 2020). OASL, although also capable of binding dsRNA without having an enzymatic activity, is thought to influence the immune response through other pathways, like activation of RIG-I signaling, but mechanistic insights remain unclear (Rex et al., 2023). Even though the binding mechanism is unknown, it was shown that RNA with modified nucleotides like pseudouridine, m6-adenosine and s2-uridine has a reduced capability to activate OASes and is resistant to degradation by RNase L (Anderson et al., 2011).

RNA:DNA hybrids

During IVT the newly synthesized RNA strand can displace the nontemplate strand from the DNA duplex and anneal to the template strand of the DNA template, thus forming stable RNA:DNA hybrids. The amount of these hybrid byproducts depends on the sequence of the transcribed DNA template. IVT of purine-rich sequences or DNA templates containing multiple GAA repeats using T7 RNA polymerase has been demonstrated to yield significant amounts of RNA:DNA hybrids (Daniels and Lieber, 1995; Grabczyk et al., 2007). These generally underappreciated IVT contaminants can be detected by immunoblotting using established anti-RNA:DNA hybrid antibodies (Boguslawski et al., 1986; Phillips et al., 2013). There is increasing evidence that the PRRs cGAS (Mankan et al., 2014), TLR9 (Rigby et al., 2014) and NLRP3 (Kailasan Vanaja et al., 2014) can detect RNA:DNA hybrids leading to the activation of innate immune signaling pathways and the induction of cytokine, chemokine and type I interferon expression. This strongly suggests that RNA:DNA hybrid contaminants are also sensed by innate immune receptors and thus, contribute to the immunogenicity of IVT mRNA. However, studies analyzing this possibility are currently lacking. Nevertheless, effective removal of contaminating RNA:DNA hybrids from clinical grade IVT mRNA should be considered if immune activation is not desirable in a therapeutic setting.

Removal of the dsDNA template from IVT reaction mixes is usually achieved by digestion with DNase I directly after the completion of the IVT process. DNase I hydrolyzes ssDNA and dsDNA as well as the DNA strand of RNA:DNA hybrids. The specific activity of DNase I for RNA:DNA hybrids, however, is at least 100-fold below that for dsDNA (Sutton et al., 1997). Compared to the dsDNA template, DNase I therefore removes the RNA:DNA hybrid contaminants very inefficiently from IVT reactions. Residual RNA:DNA hybrids may thus be co-isolated together with the single-stranded mRNA from the IVT reaction mix by established methods like precipitation with lithium chloride or alcohol/sodium acetate, or by using nucleic acid binding silica material. In contrast to dsRNA, RNA:DNA hybrids are also not removed by cellulose-based chromatography (Baiersdörfer et al., 2019). Therefore, there is a need to establish methods for efficient elimination of RNA:DNA hybrids from IVT mRNA like HPLC (high-performance liquid chromatography) purification or optimized conditions for enzymatic digestion.

IVT reaction contaminants/impurities of non-nucleotide nature and their biological effects

In addition to the intrinsic biochemical nucleotide-based byproducts produced during IVT, other types of exogenous contaminants or impurities that may be present in the final product could have a biological impact. Examples of these potential contaminants are residual solvents, enzymes such as RNases, endotoxins and metal ions. The source of these contaminants may be from the starting materials or the associated procedures such as template production, IVT reaction, purification, filtration, formulation, and packaging. Generally, GMP drug production relies on strict quality control of both the starting materials and the final drug substance. Special attention should be given to all possible extractables/leachables for all materials with liquid product contact. Since these contaminants, similar to nucleotide-based byproducts, may lead to significant biological effects, there is a necessity for strict mRNA production and quality assessments covering all types of potential contaminants and impurities not only for clinical studies but also for any research or preclinical studies.

Ribonucleases (RNases)

RNase-free conditions are an absolute necessity for successful RNA production independent of the scale or downstream application. RNases can have diverse intrinsic cellular roles in relation to tRNA and rRNA maturation, quality control, mRNA decay and RNA metabolism in bacteria and eukaryotic cells (reviewed in Cerritelli and Crouch, 2009; Cook et al., 2013; Bechhofer and Deutscher, 2019). However, contamination with

TABLE 2 Upstream and downstream solutions to reduce IVT reaction byproducts and impurities.

Impurities	Upstream precautions	Downstream purifications
RNases	Sterile conditions, well-defined RNase-free starting materials, RNase-free consumables, reducing handling and production time, proper mRNA storage conditions, avoiding usage of templates produced in *E. coli*, usage of RNase inhibitors	Chromatography, filtration
Endotoxins	Strictly endotoxin-free starting materials and consumables, avoiding usage of templates produced in *E. coli*	Chromatography, filtration
Metal ions	Well-defined starting materials, attention to potential leachables including containers, closures, storage bags	ND
dsRNA	Improved IVT conditions (pH, temp, adding auxiliary reagents), mutated RNA Pol II, promoters, optimized DNA template	Cellulose chromatography, oligo(dT) bead purification, HPLC
Abortive RNAs	Pyrophosphorolysis, mutated RNA Pol II, transcription start site/sequence optimized DNA template	HPLC
Degraded RNA	RNase inhibitors, lower IVT reaction temperature	HPLC
RNA:DNA hybrids	DNAse I treatment	HPLC

Abbreviations: HPLC, high-performance liquid chromatography; IVT, *in vitro* transcription; mRNA, messenger RNA.

endo- or exoribonucleases can be a major cause of IVT mRNA degradation, impacting its integrity and compromising its drug activity. For example, RNA interferases are endonucleases belonging to the bacterial toxin-antitoxin (TA) systems and have a major role in degrading mRNA and inhibiting mRNA translation, thus preventing bacterial growth (Cook et al., 2013). Culviner et al. used template switching libraries in combination with RNA-seq and found that a number of *E.coli* endoribonucleases cleave mRNA at short low-complexity cleavage motifs exemplified by ACA for MazF and UAC for ChpB mRNA interferases (Culviner et al., 2021). Moreover, the authors found that three interferases from the ReIE family cleave before a G, showing minimal specificity (Culviner et al., 2021). In addition to interferases, a number of other RNase subtypes exist that can contaminate mRNA production (reviewed in Bechhofer and Deutscher, 2019): (1) endonucleases such as RNase III, RNase HII and RNase P; (2) 5′exonucleases such as RNase J1 and J2; and (3) 3′endonucleases such as PNPase, RNase PH and RNase R. In all cases using contaminant-free starting materials, RNase-free consumables, reducing handling and production time, proper mRNA storage conditions, and in the future, avoiding usage of templates produced in *E. coli* (Table 2), may significantly contribute to the prevention of RNase contamination in the IVT reaction or the formulated drug.

Endotoxin

Endotoxin contamination of mRNA-based therapeutics might originate from linearized plasmids produced in *E. coli* used as templates for IVT reactions, or from any of the raw materials including water. Endotoxins originate from the outer membrane of Gram-negative bacteria. They are composed of lipopolysaccharide (LPS), consisting of an acylated backbone (lipid A) responsible for the induction of a proinflammatory immune response, a chain of repeated sugar units (O-antigen) and an oligosaccharide core (O'Neill et al., 2013; Cavaillon, 2018; Sondhi et al., 2024). If present, LPS contaminants can interact with LPS-binding protein (LBP), Myeloid differentiation protein 2 (MDA2), CD14 and Toll-Like Receptor 4 (TLR4), thereby leading to signal transduction through the TRIF and MyD88 pathways, resulting in the secretion of proinflammatory cytokines such as IL-6, TNF-α, and IL-1 (O'Neill et al., 2013; Sondhi et al., 2024). In addition, LPS can interact with caspase-4 in mice or caspase-4/5 in humans, leading to inflammasome activation and IL-1α and IL-1β release (Kayagaki et al., 2011; Viganò et al., 2015). Endotoxin is extremely potent, where even amounts as low as 0.1–0.5 ng/kg can lead to cytokine release, and dose-dependent side effects such as fever, chills, nausea, hypotension, tissue damage, sepsis, and death might occur (Elin et al., 1981; Sondhi et al., 2024). Thus, the upper limits and acceptance criteria as well as analytical methods for measuring endotoxin are strictly defined per USP chapter <85> Bacterial Endotoxins Test 3 (BET) based on dose, application route and type (Dawson, 2017). In addition to endotoxin, bioburden and sterility are part of the critical quality attributes (CQAs) ensuring the safety of mRNA products with regard to microbiological contamination (BioPhorum Operations Group Ltd, 2023).

Metal ions

The potential impact of metal ions on mRNA-based drugs is not fully understood. At high concentrations, heavy metal ions can bind with varying affinities to specific motifs in RNA. They can modify its secondary or tertiary structure and influence folding, potentially negatively affecting RNA stability (Pyle, 2002; Draper, 2004). Searching for specific RNA-ion interactions, Ciesiolka et al. performed Zn^{2+} affinity selection of a large RNA pool and detected GC cluster, the augmented GC cluster (two adjacent helical GC base pairs) and E element (consisting of AUG and AAC triads) as motifs, which together with conserved flanking G:C and C:G pairs, bind Zn^{2+} (Ciesiolka and Yarus, 1996). Hofmann et al. proposed that small, asymmetric, purine-rich loops containing G-A interactions may represent binding sites for divalent metal cations (Hofmann et al., 1997). For example, they used *in vitro* selection and amplification with a polymer matrix that contains Ni^{2+}-nitrilo-tri-acetic-acid and showed binding of Ni^{2+} to such specific conserved RNA motifs present in their screen

(Hofmann et al., 1997). Furukawa et al. discovered a riboswitch czc motif RNA that forms specific binding pockets which interacted strongly with Co^{2+} and Ni^{2+}, and weakly with Mn^{2+} (Furukawa et al., 2015). Interestingly, in-line probing analysis of the same sequence resulted in spontaneous RNA degradation when La^{3+}, Os^{3+}, Sn^{2+}, Hg^{2+} and Pb^{2+} were tested. Sequence-specific Pb^{2+}-induced hydrolysis of RNA was already described in model RNA oligomers and further noted as potentially useful for interpreting the cleavage of large mRNAs (Ciesiołka et al., 1998). Kiliszek et al. recently found that a UGG motif can bind up to two metal ions (Ba^{2+}, Cs^{+} and Sr^{+}) (Kiliszek et al., 2022). The presence of Ba^{2+} was associated with two G · U and G · G wobble noncanonical pairs formed by a UGG/UGG motif that significantly impacted the structure of the RNA. While in the majority of cases the ion-binding motifs in RNA were examined in the context of ribozymes and riboswitches, where ions play important roles in their activity, the potential impact on the folding and stability of mRNA drugs by excess ion contaminants binding to structural motifs is still unknown. In addition, the dual role of some cations (e.g., Mg^{2+}) in: 1) intrinsic in-line mRNA hydrolysis and 2) increasing the activity of certain RNases, may promote RNA instability (AbouHaidar and Ivanov, 1999; Sun et al., 2005). Therefore, regarding undesirable metal ion contaminants, special attention should be given to potential leachables including containers, closures, storage bags, etc. (Table 2) early in process development as well as in the research laboratory for small scale mRNA production.

Overcoming or depleting nucleotide-based byproducts and contaminants/impurities from IVT reaction

Strategies to prevent the formation of abortive byproducts

To reduce the generation of abortive byproducts during IVT reactions several parts of the reaction can be altered, including using mutant forms of the T7 RNA polymerase, changing the T7 promoter sequence, optimizing the sequence of the transcription start site or adding pyrophosphatase (Table 2).

Mutating the T7 RNA polymerase

Using *E. coli* expressing a combination of a mutant version of the T7 RNA polymerase (I810S mutant) and the lacZ enzyme with an unfavorable transcription start site, Guillerez et al. were able to abolish productive transcription of the T7 RNA polymerase and 'trap' the enzyme in abortive cycling (Guillerez et al., 2005). After hydroxylamine-mediated mutagenesis of the plasmid encoding T7 RNA polymerase, they screened for restoration of productive transcription based on the expression of lacZ and identified the P266L mutation as a potent way of reducing the generation of abortive products while increasing synthesis rate and maximum yield. Guillerez et al. proposed weakened promoter interactions to be causal for the reduced amount of abortive products (Guillerez et al., 2005).

Later it was found that the P266L mutant leads to a reduction of very short abortive byproducts (4–7 nt in length) since it is transitioning at longer length into the elongation phase (onset of transition is 2 nt later than for the WT polymerase) (Ramírez-Tapia and Martin, 2012; Tang et al., 2014). As described above, the newly synthesized RNA in form of a growing RNA:DNA hybrid 'pushes' against the promoter-bound (N-terminal) region of the RNA polymerase and the promoter-bound region due to the promoter binding affinity *vice versa* "pushes" against the RNA:DNA hybrid, which "destabilizes" the RNA:DNA hybrid and eventually leads to the release of abortive byproducts. The P266L mutation is thought to decrease the rigidity of the rotation of the N-terminal domain, allowing a longer and thus more stable RNA:DNA hybrid pushing against the promoter-bound region and thereby decreasing the probability of an abortive release (Ramírez-Tapia and Martin, 2012; Tang et al., 2014).

Although the P266L mutant drastically reduces the amount of abortive byproducts 4 to 7 nt in length, it should be noted that the mutant generates abortive byproducts of longer length (9–11 nt) which might show different effects in transfected cells than shorter byproducts. The beneficial effect of the later transition into the elongation complex, which significantly reduces very short abortive byproducts, comes at the expense of a less favorably positioned 5' end of the RNA which needs to find its way into the RNA-exit channel of the RNA polymerase (the previously promoter-bound region of the enzyme contributes to the formation of an RNA-exit channel after its rotation). As a result, RNA synthesis is (slightly) more likely to stop after 11–13 nt.

Using the P266L mutant in combination with a mutated promoter known to weaken upstream promoter interactions (cytosine instead of adenosine (A-15C) in the φ9 promoter), all species of abortive byproducts could be reduced–shorter ones due to the use of the P266L mutant, longer ones due to the φ9(A-15C) promoter–as it allows the P266L mutant to undergo the transition from initiation to elongation 'already' at 9 nt, similar to the WT enzyme. This results in a more efficient release from the promoter and fewer long abortive byproducts (Tang et al., 2014). Consequently, the combination of the P266L mutant enzyme with the φ9(A-15C) promoter yields a significantly higher proportion of productive vs. abortive synthesis compared to the WT enzyme. These results suggest that this combination could represent a valuable tool for large-scale mRNA production.

Pyrophosphorolysis

An increasing amount of diphosphate (PPi) occurring through the incorporation of NTPs can shift productively cycling *E. coli* RNA polymerase complexes to abortive cycling, leading to an increase of primarily short 3 to 5 nt byproducts (Plaskon et al., 2022). Thus, when including pyrophosphatase during the IVT reaction (as reported first by Sampson and Uhlenbeck, 1988) using T7 RNA polymerase, it not only increases the general yield of the reaction (Cunningham and Ofengand, 1990), but might also lower the number of abortive byproducts.

Nicks, gaps and truncated promoters

Abortive byproducts can arise due to the instability of the initially generated RNA:DNA hybrid that needs to 'loosen' the promoter-bound subdomain of the enzyme by causing the drastic 220° rotation of the enzyme into the elongation conformation. Thus, it was hypothesized that weakening the promoter interactions of the T7 RNA polymerase might facilitate the promoter release, thereby

stabilizing the RNA:DNA hybrid and finally leading to less abortive byproducts. Truncated promoters were shown to yield successful and normal levels of transcription, but also comparable levels of abortive byproducts, when the DNA in the nontemplate strand was removed at position −17 to −14 and −3 to +6 (Milligan et al., 1987). Similarly, a mismatch at position −10 or a truncation of the nontemplate strand upstream of position −14 were described to result in only slight changes in the rate of abortive byproducts formation despite having an order of magnitude lower affinity (Km) (Martin et al., 1988).

In a study by Jiang et al. a variety of promotor topologies were tested: non-complementary nontemplate strands in position −4 to +5, insertion of six non-complementary nucleotides in the nontemplate strand (between −5 and −4), and deletion downstream of −5 (Jiang et al., 2001). Also nicks in the template strand between −5 and −4 or gapped strands (deletion of −3 and −4) were tested. Moreover, they introduced 6 nt insertions (between −5 and −4) in the template strand whereby the nontemplate strand was either fully complementary (including the insertion), complementary except for the insertion (non-complementary insertion), or was lacking an insertion or was non-complementary from position −5 to +5. For those templates that resulted in the production of a relevant amount of run-off products, only the nicked DNA template strand at position −5 not only reduced the formation of abortive products significantly but also the overall yield of the reaction (Jiang et al., 2001). Thus, reducing the amount of abortive byproducts using nicked, gapped or truncated promoters seems to be unsuitable for a large-scale production of RNA therapeutics.

Transcription start site/sequence optimization

Incorporation of uridine monophosphate (UMP) in the first eight transcribed nucleotides was shown to result in the highest probability of abortive initiation whereas guanosine monophosphate (GMP) incorporation had the least probability for generating abortive byproducts (Martin et al., 1988). Consistent with this finding, Imburgio et al. noted that all natural T7 promoters/transcription start sites do not encode for an UMP incorporation until position +6 (Imburgio et al., 2000). Incorporation of UMP at position +3, however, increased the number of abortive products (Imburgio et al., 2000).

Strategies to prevent the formation of dsRNA and 3′ nucleotide addition

Optimizing IVT reaction conditions

To avoid the emergence of dsRNA byproducts during IVT, many reaction parameters have been tested, including the concentration of ions, chaotropic agents, nucleotides and temperature (Table 2). Lowering the ion concentrations of Mg^{2+} from 30 mM to 5 mM led to a reduced amount of dsRNA (Mu et al., 2018). Even though the precise mechanism is unclear, one hypothesis is that a high Mg^{2+} concentration stabilizes the EC which keeps the T7 RNA polymerase transcriptionally active thereby generating elevated levels of dsRNA (Mu and Hur, 2021). Another approach to prevent the production of dsRNA is to add chaotropic agents like urea or formamide to the IVT to weaken undesired binding of the poly(A) tail to the product and thereby prevent backwards transcription. With this strategy a reduction of the dsRNA content of about 60%–70% could be achieved (Piao et al., 2022). As an alternative to chaotropic agents to prevent the backfolding of the product, the reaction temperature during IVT can be increased. Interestingly, studies with thermostable T7 RNA polymerase showed that temperatures of up to 50°C were effective to reduce dsRNA by 3′ extension, but failed to reduce dsRNA formation by strand switching of the T7 RNA polymerase (Wu et al., 2020). Apart from that, the backfolding of the RNA product can also be prevented by adding a capture DNA complementary to the 3′end of the RNA product (Gholamalipour et al., 2019). To effectively reduce 3′extension the capture DNA needs to be longer than 14 nucleotides and has to be present in excess compared to the RNA product (Gholamalipour et al., 2019). Instead of preventing the backfolding of the RNA, the backward transcription can also be avoided by limiting the amount of uridine excess. This applies in particular to mRNAs with a poly(A) tail, since their backward transcription starts with a poly(U). Ziegenhals et al. were able to design a fed batch process in which the limited steady-state concentration of UTP or m1ΨTP led to reduced dsRNA production during IVT (Ziegenhals et al., 2023). Furthermore, they found that di-nucleotide caps had an improved dsRNA profile compared to tri-nucleotide caps. In addition to the excess of certain nucleotides, the nucleoside modification also plays a role. The use of Ψ, m1Ψ and m5C nucleosides led to lower dsRNA production (Baiersdörfer et al., 2019; Mu and Hur, 2021).

Mutating or switching RNA polymerase

Next to optimizing reaction conditions, a viable option is also to mutate the T7 RNA polymerase or change the polymerase altogether. The carboxy-terminal domain (CTD) of the T7 RNA polymerase has been shown to have an influence on 3′ homogeneity, as well as enzyme productivity. The homogeneity of the 3′end is higher the larger the amino acid that is added to the end, while the productivity decreases with increasing size (Gardner et al., 1997; Dousis et al., 2023). Since the EC has been proposed as the driving force behind the dsRNA byproducts, stabilizing the IC might be favorable to reduce dsRNA. The mutation G47A has been identified to reduce dsRNA production without loss of yield and computational analysis suggests that it favors the IC over the EC, even though the equilibrium studies are still ongoing (Dousis et al., 2023). While T7 is by far the best optimized and characterized RNA polymerase, several other phage RNA polymerases have surfaced in recent years. All of them emerged from the subfamily of the short-tailed phage *Autographiviridae*, which was also the origin of the T7 RNA polymerase (Lu et al., 2019). The characterized polymerases include T3, SP6, Syn5 and KP34 polymerases (Butler and Chamberlin, 1982; Zhu et al., 2013; Lu et al., 2019). Even though claims of higher yield and lower byproducts have been announced for most of them, it remains to be shown that these polymerases are valid competitors for T7 under high yield conditions in an industrial setting (Zhu et al., 2014; Lu et al., 2019). The latest candidate that emerged is the VSW-3 polymerase from the psychrophilic bacteriophage VSW-3 (Xia et al., 2022). In laboratory scale under VSW-3-optimized conditions VSW-3 polymerase shows a higher 3′ homogeneity and comparable yield to T7, while it has a lower optimal reaction temperature of 25°C, which would reduce RNA

degradation during the IVT (Wang et al., 2022). Interestingly, the lower temperature leads in this study to lower dsRNA byproducts, contrary to the other study that depleted dsRNA with a thermostable T7 RNA polymerase and higher temperature (Wu et al., 2020). These results leave open the question of the fundamental mechanisms driving the formation of dsRNA byproducts by this new polymerase. Additionally, it should be noted that since the mechanism of 3′extension is dependent on the concentration of the run-off product, lower yield reaction will always lead to less dsRNA byproducts, making it difficult to draw conclusions about high yield conditions from these studies (Gholamalipour et al., 2018; Mu et al., 2018).

Optimization of the DNA template

Lastly, not only the IVT itself and its components and reaction conditions have an influence on dsRNA formation, but also the DNA template from which the RNA is produced. Especially the preparation and the purity of the linearized template has an impact on dsRNA. It was demonstrated with monolithic columns with butyl chains, which are normally used to fractionate nucleic acids from proteins by hydrophobic interactions, that the purity of the linearized plasmid influences dsRNA content (Martínez et al., 2023). Moreover, it has long been known that the DNA template end structure has an influence on byproducts (Schenborn and Mierendorf, 1985). This was confirmed recently when Mu et al. found that a 3′ overhang at the end of the template led to significantly more dsRNA and a 5′ overhang can reduce the dsRNA content (Mu et al., 2018). In another approach, a DNA template which is single-stranded, except in the T7 promoter region, yielded significantly less dsRNA (Mu et al., 2018). High salt concentrations have been known to reduce protein-nucleic acid interactions. In the case of the T7 RNA polymerase this leads to weaker binding of the T7 RNA polymerase to the RNA product, which prevents undesired 3′extension but also weakens the binding to the T7 promoter and results in decreased yield (Cavac et al., 2021). To overcome the loss in yield, the T7 RNA polymerase needs to be forced into close proximity to the T7 promoter or have an improved binding affinity to the T7 promoter. The latter can be achieved by a small manipulation of the DNA template (Malagoda Pathiranage et al., 2023). By introducing a nick to the −4 position into the DNA template the binding affinity from the T7 to the promoter is enhanced. This has been explained by the T7 RNA polymerase using parts of the available energy from the T7 RNA polymerase–promoter complex to drive melting of the DNA downstream of the promoter (Bandwar and Patel, 2002; Martin et al., 2005). The nicked template in combination with high salt concentration has been shown as a promising approach to deplete 3′ extensions without disrupting yields (Malagoda Pathiranage and Martin, 2023).

Depleting byproducts and impurities by purification

Another option to remove byproducts from IVT is purification and filtration following IVT, where the full-length mRNA is separated from all diverse types of impurities and contaminants (Table 2). There are several methods to ensure purified, high-quality mRNA, and they are proven to remove both process related impurities (plasmid DNA fragments, enzymes, unused NTPs or cap analogs, and additive ingredients) and product-related impurities (truncated ssRNA, DNA-RNA hybrids and dsRNA). Since mRNA can be sensitive and degrades easily under certain conditions, rapid and selective purification is required. During purification procedures, the elimination of product-related impurities imposes specific challenges since those species share similar physicochemical properties with the final mRNA product.

In the laboratory under small scale production conditions, mRNA is typically precipitated using alcohol and sodium or ammonium salts or by using lithium chloride alone (Walker and Lorsch, 2013). Large-scale mRNA production may however integrate diverse non-chromatography or chromatography-based mRNA purification methods (as previously and extensively reviewed in Baronti et al., 2018; Zhang et al., 2023), and these can be combined as well. Among the combined methods, the “sandwich” method is widely used, where a chromatography-based purification is flanked both before and after by tangential flow filtration (TFF) steps. During TFF, through tangential continuous flow, the mRNA is separated from impurities in the IVT mixture by filtration through a membrane, and subsequently the mRNA solution can also be concentrated (Table 2). In the chromatography step, molecules are separated based on their physicochemical properties, e.g., charge, size and hydrodynamic radius, affinity to specific ligands or differences in hydrophobicity (Karikó et al., 2011; Linares-Fernández et al., 2021; Szabó et al., 2022). Affinity chromatography in the case of mRNA purification utilizes a resin functionalized with oligo-deoxythymidylic acid (oligo-dT) to capture mRNA by forming bonds with its poly(A) tail. There are diverse ways to implement this purification strategy, e.g., by using magnetic oligo (dT) beads (Jacobsen et al., 2004; Green and Sambrook, 2019; Korenč et al., 2021). Despite these purification methods, the solution still may contain dsRNA, and thus consequently may need to be combined with further downstream purifications. For example, high-performance liquid chromatography (HPLC) (Karikó et al., 2011) and cellulose-based columns (Baiersdörfer et al., 2019) have been proven to significantly mitigate dsRNA contamination (Table 2).

Conclusions and future perspectives

In vitro transcription (IVT) is the fundamental process used to generate synthetic mRNA transcripts at scale for therapeutics. All mRNA-based vaccines and drugs currently on the market or in clinical trials rely on the IVT reaction to be produced. Despite the advancements made to the IVT reaction, in the majority of cases it still produces byproducts and there are persistent challenges in scalability and mRNA purification. In the future, IVT might be replaced by new technologies. One such strategy is cell-based mRNA manufacturing, which is currently being exploited in publicly funded and commercial projects. While these efforts aim to develop cell-based factory platforms for large-scale and cost-effective manufacturing of mRNA therapeutics, this technology still requires its own process optimizations. Furthermore, some potential limitations of such an approach might be the inability to generate modified mRNA (such as N1-methylpseudouridine- or pseudouridine-modified mRNA) and the possibility of uncontrolled cell-based modifications and non-optimal cap structures. These issues could negatively impact the biological activity of mRNA in human cells. Another future

strategy would aim at synthesizing long mRNAs chemically; however, new advancements are also required in that field since it is currently limited to sizes of about 100 nucleotides. In the meantime, the enzymatic IVT reaction continues to be the standard, most reliable and cost-effective mRNA manufacturing method available as it has been for more than 40 years. As discussed, numerous optimizations, including improvements to the RNA polymerase, starting materials and reaction conditions, as well as refinements to downstream purification methods, have led to an increased yield of high-grade, full-length mRNA and a decrease in byproducts, contaminants, and impurities. Consequently, this has greatly improved both the efficacy and safety of mRNA therapeutics. Further engineering of the RNA polymerase and IVT reaction conditions, as well as tailoring mRNA purification to diverse medical applications is ongoing. For example, both the drug substance and byproducts can induce innate immune activation that might also impact adaptive immunity, and this may be beneficial for certain applications such as vaccines or fully undesirable for others such as RNA protein replacement therapies. These differences may necessitate specific manufacturing requirements for diverse medical applications. In addition, complete characterization of certain byproducts and impurities depends strongly on sensitive and reliable analytical methods that are also constantly under development. Here we have discussed the biological impact of some byproducts, for example, dsRNA, which in high quantities leads to cytokine and chemokine release and thus potential safety issues. However, a better understanding of the types, subclasses and quantities of all byproducts and impurities as well as defining their biological impact in different cell types, including in diverse application routes would be highly beneficial for characterizing mRNA drug activity and safety. For example, it is still challenging to detect and quantify dsRNA byproducts smaller than 50bp and therefore difficult to understand their biological effects. Moreover, the biological impact of abortive RNA byproducts originating from the IVT reaction also remains elusive in the context of RNA therapeutics. Thus, further research of the biological effects of IVT reaction byproducts and impurities, together with improved analytical methods will help in future tailoring of mRNA drug production for specific medical applications.

Author contributions

RL: Resources, Visualization, Writing–original draft, Writing–review and editing. WK: Resources, Visualization, Writing–original draft, Writing–review and editing. GS: Resources, Writing–original draft, Writing–review and editing. MB: Resources, Writing–original draft, Writing–review and editing. GB: Resources, Writing–original draft, Writing–review and editing. JK: Resources, Writing–original draft, Writing–review and editing. AM: Resources, Writing–original draft, Writing–review and editing. IV: Conceptualization, Resources, Supervision, Visualization, Writing–original draft, Writing–review and editing.

Funding

The author(s) declare that financial support was received for the research, authorship, and/or publication of this article.

Acknowledgments

We would like to thank Florian Bock of BioNTech SE for excellent scientific and medical writing support. Figures were created using BioRender.com.

Conflict of interest

RL, WK, GS, MB, GB, JK, AM, and IV are all full-time employees at BioNTech SE, Mainz, Germany, and may hold shares from BioNTech SE.

The author(s) declared that they were an editorial board member of Frontiers, at the time of submission. This had no impact on the peer review process and the final decision.

The authors declare that this study received funding from BioNTech SE. The funder had the following involvement in the study: all authors are current employees at BioNTech SE.

Publisher's note

References

AbouHaidar, M. G., and Ivanov, I. G. (1999). Non-enzymatic RNA hydrolysis promoted by the combined catalytic activity of buffers and magnesium ions. *Zeitschrift fur Naturforschung. C, J. Biosci.* 54, 542–548. doi:10.1515/znc-1999-7-813

Alhadid, Y., Chung, S., Lerner, E., Taatjes, D. J., Borukhov, S., and Weiss, S. (2017). Studying transcription initiation by RNA polymerase with diffusion-based single-molecule fluorescence. *Protein Sci. a Publ. Protein Soc.* 26, 1278–1290. doi:10.1002/pro.3160

Allen, I. C., Scull, M. A., Moore, C. B., Holl, E. K., McElvania-TeKippe, E., Taxman, D. J., et al. (2009). The NLRP3 inflammasome mediates *in vivo* innate immunity to influenza A virus through recognition of viral RNA. *Immunity* 30, 556–565. doi:10.1016/j.immuni.2009.02.005

Anderson, B. R., Muramatsu, H., Jha, B. K., Silverman, R. H., Weissman, D., and Karikó, K. (2011). Nucleoside modifications in RNA limit activation of 2'-5'-oligoadenylate synthetase and increase resistance to cleavage by RNase L. *Nucleic acids Res.* 39, 9329–9338. doi:10.1093/nar/gkr586

Anderson, B. R., Muramatsu, H., Nallagatla, S. R., Bevilacqua, P. C., Sansing, L. H., Weissman, D., et al. (2010). Incorporation of pseudouridine into mRNA enhances translation by diminishing PKR activation. *Nucleic acids Res.* 38, 5884–5892. doi:10.1093/nar/gkq347

Andries, O., Mc Cafferty, S., Smedt, S. C. de, Weiss, R., Sanders, N. N., and Kitada, T. (2015). N(1)-methylpseudouridine-incorporated mRNA outperforms pseudouridine-incorporated mRNA by providing enhanced protein expression and reduced immunogenicity in mammalian cell lines and mice. *J. Control. release official J. Control. Release Soc.* 217, 337–344. doi:10.1016/j.jconrel.2015.08.051

Baiersdörfer, M., Boros, G., Muramatsu, H., Mahiny, A., Vlatkovic, I., Sahin, U., et al. (2019). A facile method for the removal of dsRNA contaminant from *in vitro*-

Transcribed mRNA. *Mol. Ther. Nucleic acids* 15, 26–35. doi:10.1016/j.omtn.2019.02.018

Balachandran, S., Roberts, P. C., Brown, L. E., Truong, H., Pattnaik, A. K., Archer, D. R., et al. (2000). Essential role for the dsRNA-dependent protein kinase PKR in innate immunity to viral infection. *Immunity* 13, 129–141. doi:10.1016/s1074-7613(00)00014-5

Bandwar, R. P., Ma, N., Emanuel, S. A., Anikin, M., Vassylyev, D. G., Patel, S. S., et al. (2007). The transition to an elongation complex by T7 RNA polymerase is a multistep process. *J. Biol. Chem.* 282, 22879–22886. doi:10.1074/jbc.M702589200

Bandwar, R. P., and Patel, S. S. (2002). The energetics of consensus promoter opening by T7 RNA polymerase. *J. Mol. Biol.* 324, 63–72. doi:10.1016/S0022-2836(02)01034-3

Baronti, L., Karlsson, H., Marušič, M., and Petzold, K. (2018). A guide to large-scale RNA sample preparation. *Anal. Bioanal. Chem.* 410, 3239–3252. doi:10.1007/s00216-018-0943-8

4basebio, P. L. C. (2024). Applications. Available at: https://www.4basebio.com/applications/#mrnavaccines (Accessed June 13, 2024).

Bauernfried, S., Scherr, M. J., Pichlmair, A., Duderstadt, K. E., and Hornung, V. (2021). Human NLRP1 is a sensor for double-stranded RNA. *Sci. (New York, N.Y.)* 371, eabd0811. doi:10.1126/science.abd0811

Bechhofer, D. H., and Deutscher, M. P. (2019). Bacterial ribonucleases and their roles in RNA metabolism. *Crit. Rev. Biochem. Mol. Biol.* 54, 242–300. doi:10.1080/10409238.2019.1651816

Bellamy, A. R., Nichols, J. L., and Joklik, W. K. (1972). Nucleotide sequences of reovirus oligonucleotides: evidence for abortive RNA synthesis during virus maturation. *Nat. New Biol.* 238, 49–51. doi:10.1038/newbio238049a0

Bhargava, P., and Kassavetis, G. A. (1999). Abortive initiation by *Saccharomyces cerevisiae* RNA polymerase III. *J. Biol. Chem.* 274, 26550–26556. doi:10.1074/jbc.274.37.26550

BioPhorum Operations Group Ltd (2023). Defining the required critical quality attributes (CQAs) and phase requirements for mRNA/LNP product development and manufacture. Available at: https://www.biophorum.com/download/defining-the-required-critical-quality-attributes-cqas-and-phase-requirements-for-mrna-lnp-product-development-and-manufacture/ (Accessed June 26, 2024).

Boguslawski, S. J., Smith, D. E., Michalak, M. A., Mickelson, K. E., Yehle, C. O., Patterson, W. L., et al. (1986). Characterization of monoclonal antibody to DNA.RNA and its application to immunodetection of hybrids. *J. Immunol. methods* 89, 123–130. doi:10.1016/0022-1759(86)90040-2

Brieba, L. G., and Sousa, R. (2001). T7 promoter release mediated by DNA scrunching. *EMBO J.* 20, 6826–6835. doi:10.1093/emboj/20.23.6826

Brunelle, J. L., and Green, R. (2013). *In vitro* transcription from plasmid or PCR-amplified DNA. *Methods Enzymol.* 530, 101–114. doi:10.1016/B978-0-12-420037-1.00005-1

Butler, E. T., and Chamberlin, M. J. (1982). Bacteriophage SP6-specific RNA polymerase. I. Isolation and characterization of the enzyme. *J. Biol. Chem.* 257, 5772–5778. doi:10.1016/S0021-9258(19)83846-2

Cadena, C., Ahmad, S., Xavier, A., Willemsen, J., Park, S., Park, J. W., et al. (2019). Ubiquitin-dependent and -independent roles of E3 ligase RIPLET in innate immunity. *Cell.* 177, 1187–1200. doi:10.1016/j.cell.2019.03.017

Cavac, E., Ramírez-Tapia, L. E., and Martin, C. T. (2021). High-salt transcription of DNA cotethered with T7 RNA polymerase to beads generates increased yields of highly pure RNA. *J. Biol. Chem.* 297, 100999. doi:10.1016/j.jbc.2021.100999

Cavaillon, J.-M. (2018). Exotoxins and endotoxins: inducers of inflammatory cytokines. *Toxicon official J. Int. Soc. Toxinology* 149, 45–53. doi:10.1016/j.toxicon.2017.10.016

Cazenave, C., and Uhlenbeck, O. C. (1994). RNA template-directed RNA synthesis by T7 RNA polymerase. *Proc. Natl. Acad. Sci. U. S. A.* 91, 6972–6976. doi:10.1073/pnas.91.15.6972

Cerritelli, S. M., and Crouch, R. J. (2009). Ribonuclease H: the enzymes in eukaryotes. *FEBS J.* 276, 1494–1505. doi:10.1111/j.1742-4658.2009.06908.x

Cheetham, G. M., and Steitz, T. A. (1999). Structure of a transcribing T7 RNA polymerase initiation complex. *Sci. (New York, N.Y.)* 286, 2305–2309. doi:10.1126/science.286.5448.2305

Chen, Z., and Zhang, Y. (2005). Dimethyl sulfoxide targets phage RNA polymerases to promote transcription. *Biochem. biophysical Res. Commun.* 333, 664–670. doi:10.1016/j.bbrc.2005.05.166

Childs, K. S., Randall, R. E., and Goodbourn, S. (2013). LGP2 plays a critical role in sensitizing mda-5 to activation by double-stranded RNA. *PloS one* 8, e64202. doi:10.1371/journal.pone.0064202

Ciesiołka, J., Michałowski, D., Wrzesinski, J., Krajewski, J., and Krzyzosiak, W. J. (1998). Patterns of cleavages induced by lead ions in defined RNA secondary structure motifs. *J. Mol. Biol.* 275, 211–220. doi:10.1006/jmbi.1997.1462

Ciesiolka, J., and Yarus, M. (1996). Small RNA-divalent domains. *RNA (New York, N.Y.)* 2, 785–793.

Conrad, T., Plumbom, I., Alcobendas, M., Vidal, R., and Sauer, S. (2020). Maximizing transcription of nucleic acids with efficient T7 promoters. *Commun. Biol.* 3, 439. doi:10.1038/s42003-020-01167-x

Cook, G. M., Robson, J. R., Frampton, R. A., McKenzie, J., Przybilski, R., Fineran, P. C., et al. (2013). Ribonucleases in bacterial toxin-antitoxin systems. *Biochimica biophysica acta* 1829, 523–531. doi:10.1016/j.bbagrm.2013.02.007

Corbet, G. A., Burke, J. M., Bublitz, G. R., Tay, J. W., and Parker, R. (2022). dsRNA-induced condensation of antiviral proteins modulates PKR activity. *Proc. Natl. Acad. Sci. U. S. A.* 119, e2204235119. doi:10.1073/pnas.2204235119

Culviner, P. H., Nocedal, I., Fortune, S. M., and Laub, M. T. (2021). Global analysis of the specificities and targets of endoribonucleases from *Escherichia coli* toxin-antitoxin systems. *mBio* 12, e0201221. doi:10.1128/mBio.02012-21

Cunningham, P. R., and Ofengand, J. (1990). Use of inorganic pyrophosphatase to improve the yield of *in vitro* transcription reactions catalyzed by T7 RNA polymerase. *BioTechniques* 9 (6), 713–714.

Daniel, S., Kis, Z., Kontoravdi, C., and Shah, N. (2022). Quality by Design for enabling RNA platform production processes. *Trends Biotechnol.* 40, 1213–1228. doi:10.1016/j.tibtech.2022.03.012

Daniels, G. A., and Lieber, M. R. (1995). RNA: DNA complex formation upon transcription of immunoglobulin switch regions: implications for the mechanism and regulation of class switch recombination. *Nucleic acids Res.* 23, 5006–5011. doi:10.1093/nar/23.24.5006

Dawson, M. (2017). *Endotoxin Limits For Parental Drug Products*. BET White Paper, Associates of Cape Cod, Inc., Vol. 1 (2). Available at: https://www.acciusa.com/pdfs/whitepapers/EndotoxinLimits_SeanJH-PR17-012.pdf (Accessed June 25, 2024).

Devoldere, J., Dewitte, H., Smedt, S. C. de, and Remaut, K. (2016). Evading innate immunity in nonviral mRNA delivery: don't shoot the messenger. *Drug Discov. today* 21, 11–25. doi:10.1016/j.drudis.2015.07.009

Dey, M., Cao, C., Dar, A. C., Tamura, T., Ozato, K., Sicheri, F., et al. (2005). Mechanistic link between PKR dimerization, autophosphorylation, and eIF2alpha substrate recognition. *Cell.* 122, 901–913. doi:10.1016/j.cell.2005.06.041

Donovan, J., Whitney, G., Rath, S., and Korennykh, A. (2015). Structural mechanism of sensing long dsRNA via a noncatalytic domain in human oligoadenylate synthetase 3. *Proc. Natl. Acad. Sci. U. S. A.* 112, 3949–3954. doi:10.1073/pnas.1419409112

Dousis, A., Ravichandran, K., Hobert, E. M., Moore, M. J., and Rabideau, A. E. (2023). An engineered T7 RNA polymerase that produces mRNA free of immunostimulatory byproducts. *Nat. Biotechnol.* 41, 560–568. doi:10.1038/s41587-022-01525-6

Draper, D. E. (2004). A guide to ions and RNA structure. *RNA (New York, N.Y.)* 10, 335–343. doi:10.1261/rna.5205404

Durbin, A. F., Wang, C., Marcotrigiano, J., and Gehrke, L. (2016). RNAs containing modified nucleotides fail to trigger RIG-I conformational changes for innate immune signaling. *mBio* 7, e00833. doi:10.1128/mBio.00833-16

Durniak, K. J., Bailey, S., and Steitz, T. A. (2008). The structure of a transcribing T7 RNA polymerase in transition from initiation to elongation. *Sci. (New York, N.Y.)* 322, 553–557. doi:10.1126/science.1163433

Elin, R. J., Wolff, S. M., McAdam, K. P., Chedid, L., Audibert, F., Bernard, C., et al. (1981). Properties of reference *Escherichia coli* endotoxin and its phthalylated derivative in humans. *J. Infect. Dis.* 144, 329–336. doi:10.1093/infdis/144.4.329

Engel, B. J., Grindel, B. J., Gray, J. P., and Millward, S. W. (2020). Purification of poly-dA oligonucleotides and mRNA-protein fusions with dT25-OAS resin. *Bioorg. Med. Chem. Lett.* 30, 126934. doi:10.1016/j.bmcl.2019.126934

Ensinger, M. J., Martin, S. A., Paoletti, E., and Moss, B. (1975). Modification of the 5'-terminus of mRNA by soluble guanylyl and methyl transferases from vaccinia virus. *Proc. Natl. Acad. Sci. U. S. A.* 72, 2525–2529. doi:10.1073/pnas.72.7.2525

European Medicines Agency (2021). *COVID-19 vaccine moderna, INN-COVID-19 mRNA vaccine (nucleoside modified): assessment report.*

European Medicines Agency (2022). *Comirnaty, INN-tozinameran, tozinameran/riltozinameran: assessment report.*

Farsetta, D. L., Chandran, K., and Nibert, M. L. (2000). Transcriptional activities of reovirus RNA polymerase in recoated cores. Initiation and elongation are regulated by separate mechanisms. *J. Biol. Chem.* 275, 39693–39701. doi:10.1074/jbc.M004562200

Fitzgerald, K. A., and Kagan, J. C. (2020). Toll-like receptors and the control of immunity. *Cell.* 180, 1044–1066. doi:10.1016/j.cell.2020.02.041

Francis, C., Frida J, P., Thanh-Huong, B., Alicja, M., Artem, K., Jérémie, P., et al. (2024). Urea supplementation improves mRNA *in vitro* transcription by decreasing both shorter and longer RNA byproducts. *RNA Biol.* 21, 1–6. doi:10.1080/15476286.2024.2321764

Furukawa, K., Ramesh, A., Zhou, Z., Weinberg, Z., Vallery, T., Winkler, W. C., et al. (2015). Bacterial riboswitches cooperatively bind Ni(2+) or Co(2+) ions and control expression of heavy metal transporters. *Mol. Cell.* 57, 1088–1098. doi:10.1016/j.molcel.2015.02.009

Gardner, L. P., Mookhtiar, K. A., and Coleman, J. E. (1997). Initiation, elongation, and processivity of carboxyl-terminal mutants of T7 RNA polymerase. *Biochemistry* 36, 2908–2918. doi:10.1021/bi962397i

Gholamalipour, Y., Johnson, W. C., and Martin, C. T. (2019). Efficient inhibition of RNA self-primed extension by addition of competing 3'-capture DNA-improved RNA synthesis by T7 RNA polymerase. *Nucleic acids Res.* 47, e118. doi:10.1093/nar/gkz700

Gholamalipour, Y., Karunanayake Mudiyanselage, A., and Martin, C. T. (2018). 3' end additions by T7 RNA polymerase are RNA self-templated, distributive and diverse in character-RNA-Seq analyses. *Nucleic acids Res.* 46, 9253–9263. doi:10.1093/nar/gky796

Goldman, S. R., Sharp, J. S., Vvedenskaya, I. O., Livny, J., Dove, S. L., and Nickels, B. E. (2011). NanoRNAs prime transcription initiation *in vivo*. *Mol. Cell.* 42, 817–825. doi:10.1016/j.molcel.2011.06.005

Goovaerts, Q., Shen, J., Wijngaert, B. de, Basu, U., Patel, S. S., and Das, K. (2023). Structures illustrate step-by-step mitochondrial transcription initiation. *Nature* 622, 872–879. doi:10.1038/s41586-023-06643-y

Goubau, D., Schlee, M., Deddouche, S., Pruijssers, A. J., Zillinger, T., Goldeck, M., et al. (2014). Antiviral immunity via RIG-I-mediated recognition of RNA bearing 5'-diphosphates. *Nature* 514, 372–375. doi:10.1038/nature13590

Grabczyk, E., Mancuso, M., and Sammarco, M. C. (2007). A persistent RNA.DNA hybrid formed by transcription of the Friedreich ataxia triplet repeat in live bacteria, and by T7 RNAP *in vitro*. *Nucleic acids Res.* 35, 5351–5359. doi:10.1093/nar/gkm589

Green, M. R., and Sambrook, J. (2019). Isolation of Poly(A)+ messenger RNA using magnetic oligo(dT) beads. *Cold Spring Harb. Protoc.* doi:10.1101/pdb.prot101733

Guillerez, J., Lopez, P. J., Proux, F., Launay, H., and Dreyfus, M. (2005). A mutation in T7 RNA polymerase that facilitates promoter clearance. *Proc. Natl. Acad. Sci. U. S. A.* 102, 5958–5963. doi:10.1073/pnas.0407141102

Han, Y., Donovan, J., Rath, S., Whitney, G., Chitrakar, A., and Korennykh, A. (2014). Structure of human RNase L reveals the basis for regulated RNA decay in the IFN response. *Sci. (New York, N.Y.)* 343, 1244–1248. doi:10.1126/science.1249845

Heil, F., Hemmi, H., Hochrein, H., Ampenberger, F., Kirschning, C., Akira, S., et al. (2004). Species-specific recognition of single-stranded RNA via toll-like receptor 7 and 8. *Sci. (New York, N.Y.)* 303, 1526–1529. doi:10.1126/science.1093620

Henderson, J. M., Ujita, A., Hill, E., Yousif-Rosales, S., Smith, C., Ko, N., et al. (2021). Cap 1 messenger RNA synthesis with Co-transcriptional CleanCap® analog by *in vitro* transcription. *Curr. Protoc.* 1, e39. doi:10.1002/cpz1.39

Hofmann, H. P., Limmer, S., Hornung, V., and Sprinzl, M. (1997). Ni2+-binding RNA motifs with an asymmetric purine-rich internal loop and a G-A base pair. *RNA (New York, N.Y.)* 3, 1289–1300.

Hornung, V., Ellegast, J., Kim, S., Brzózka, K., Jung, A., Kato, H., et al. (2006). 5'-Triphosphate RNA is the ligand for RIG-I. *Sci. (New York, N.Y.)* 314, 994–997. doi:10.1126/science.1132505

Hornung, V., Hartmann, R., Ablasser, A., and Hopfner, K.-P. (2014). OAS proteins and cGAS: unifying concepts in sensing and responding to cytosolic nucleic acids. *Nat. Rev. Immunol.* 14, 521–528. doi:10.1038/nri3719

Hovanessian, A. G., and Justesen, J. (2007). The human 2'-5'oligoadenylate synthetase family: unique interferon-inducible enzymes catalyzing 2'-5' instead of 3'-5' phosphodiester bond formation. *Biochimie* 89, 779–788. doi:10.1016/j.biochi.2007.02.003

Hsu, L. M. (2002). Promoter clearance and escape in prokaryotes. *Biochimica biophysica acta* 1577, 191–207. doi:10.1016/s0167-4781(02)00452-9

Husain, B., Mukerji, I., and Cole, J. L. (2012). Analysis of high-affinity binding of protein kinase R to double-stranded RNA. *Biochemistry* 51, 8764–8770. doi:10.1021/bi301226h

Ibsen, M. S., Gad, H. H., Thavachelvam, K., Boesen, T., Desprès, P., and Hartmann, R. (2014). The 2'-5'-oligoadenylate synthetase 3 enzyme potently synthesizes the 2'-5'-oligoadenylates required for RNase L activation. *J. virology* 88, 14222–14231. doi:10.1128/JVI.01763-14

Ikeda, R. A., and Richardson, C. C. (1986). Interactions of the RNA polymerase of bacteriophage T7 with its promoter during binding and initiation of transcription. *Proc. Natl. Acad. Sci. U.S.A.* 83, 3614–3618. doi:10.1073/pnas.83.11.3614

Imburgio, D., Rong, M., Ma, K., and McAllister, W. T. (2000). Studies of promoter recognition and start site selection by T7 RNA polymerase using a comprehensive collection of promoter variants. *Biochemistry* 39, 10419–10430. doi:10.1021/bi000365w

Jacobsen, N., Nielsen, P. S., Jeffares, D. C., Eriksen, J., Ohlsson, H., Arctander, P., et al. (2004). Direct isolation of poly(A)+ RNA from 4 M guanidine thiocyanate-lysed cell extracts using locked nucleic acid-oligo(T) capture. *Nucleic Acids Res.* 32, e64. doi:10.1093/nar/gnh056

Jelinek, I., Leonard, J. N., Price, G. E., Brown, K. N., Meyer-Manlapat, A., Goldsmith, P. K., et al. (2011). TLR3-specific double-stranded RNA oligonucleotide adjuvants induce dendritic cell cross-presentation, CTL responses, and antiviral protection. *J. Immunol. Baltim. Md* 186, 2422–2429. doi:10.4049/jimmunol.1002845

Jia, Y., and Patel, S. S. (1997). Kinetic mechanism of transcription initiation by bacteriophage T7 RNA polymerase. *Biochem.* 36, 4223–4232. doi:10.1021/bi9630467

Jiang, M., Rong, M., Martin, C., and McAllister, W. T. (2001). Interrupting the template strand of the T7 promoter facilitates translocation of the DNA during initiation, reducing transcript slippage and the release of abortive products. *J. Mol. Biol.* 310, 509–522. doi:10.1006/jmbi.2001.4793

Johnston, D. E., and McClure, W. R. (1976). in *Abortive initiation of* in vitro *RNA synthesis on bacteriophage λ DNA*. RNA polymerase. Editors R. Losick and M. J. Chamberlin (Germany: Cold Spring Harbor Laboratory, Cold Spring Harbor), 413–428.

Kailasan Vanaja, S., Rathinam, V. A. K., Atianand, M. K., Kalantari, P., Skehan, B., Fitzgerald, K. A., et al. (2014). Bacterial RNA:DNA hybrids are activators of the NLRP3 inflammasome. *Proc. Natl. Acad. Sci. U. S. A.* 111, 7765–7770. doi:10.1073/pnas.1400075111

Karikó, K., Buckstein, M., Ni, H., and Weissman, D. (2005). Suppression of RNA recognition by Toll-like receptors: the impact of nucleoside modification and the evolutionary origin of RNA. *Immunity* 23, 165–175. doi:10.1016/j.immuni.2005.06.008

Karikó, K., Muramatsu, H., Ludwig, J., and Weissman, D. (2011). Generating the optimal mRNA for therapy: HPLC purification eliminates immune activation and improves translation of nucleoside-modified, protein-encoding mRNA. *Nucleic acids Res.* 39, e142. doi:10.1093/nar/gkr695

Karikó, K., Muramatsu, H., Welsh, F. A., Ludwig, J., Kato, H., Akira, S., et al. (2008). Incorporation of pseudouridine into mRNA yields superior nonimmunogenic vector with increased translational capacity and biological stability. *Mol. Ther. J. Am. Soc. Gene Ther.* 16, 1833–1840. doi:10.1038/mt.2008.200

Kartje, Z. J., Janis, H. I., Mukhopadhyay, S., and Gagnon, K. T. (2021). Revisiting T7 RNA polymerase transcription *in vitro* with the Broccoli RNA aptamer as a simplified real-time fluorescent reporter. *J. Biol. Chem.* 296, 100175. doi:10.1074/jbc.RA120.014553

Kato, H., Takahasi, K., and Fujita, T. (2011). RIG-I-like receptors: cytoplasmic sensors for non-self RNA. *Immunol. Rev.* 243, 91–98. doi:10.1111/j.1600-065X.2011.01052.x

Kayagaki, N., Warming, S., Lamkanfi, M., Vande Walle, L., Louie, S., Dong, J., et al. (2011). Non-canonical inflammasome activation targets caspase-11. *Nature* 479, 117–121. doi:10.1038/nature10558

Kienes, I., Weidl, T., Mirza, N., Chamaillard, M., and Kufer, T. A. (2021). Role of NLRs in the regulation of type I interferon signaling, host defense and tolerance to inflammation. *Int. J. Mol. Sci.* 22, 1301. doi:10.3390/ijms22031301

Kiliszek, A., Pluta, M., Bejger, M., and Rypniewski, W. (2022). Structure and thermodynamics of a UGG motif interacting with Ba2+ and other metal ions: accommodating changes in the RNA structure and the presence of a G(syn)-G(syn) pair. *RNA (New York, N.Y.)* 29, 44–54. doi:10.1261/rna.079414.122

Koh, H. R., Roy, R., Sorokina, M., Tang, G.-Q., Nandakumar, D., Patel, S. S., et al. (2018). Correlating transcription initiation and conformational changes by a single-subunit RNA polymerase with near base-pair resolution. *Mol. Cell.* 70, 695–706. doi:10.1016/j.molcel.2018.04.018

Korenč, M., Mencin, N., Puc, J., Skok, J., Nemec, K. Š., Celjar, A. M., et al. (2021). Chromatographic purification with CIMmultus™ Oligo dT increases mRNA stability. *Cell Gene Ther. Insights.* 7, 1207–1216. doi:10.18609/cgti.2021.161

Koul, A., Deo, S., Booy, E. P., Orriss, G. L., Genung, M., and McKenna, S. A. (2020). Impact of double-stranded RNA characteristics on the activation of human 2'-5'-oligoadenylate synthetase 2 (OAS2). *Biochem. Cell. Biol. = Biochimie Biol. Cell.* 98, 70–82. doi:10.1139/bcb-2019-0060

Kristiansen, H., Gad, H. H., Eskildsen-Larsen, S., Despres, P., and Hartmann, R. (2011). The oligoadenylate synthetase family: an ancient protein family with multiple antiviral activities. *J. interferon & cytokine Res. official J. Int. Soc. Interferon Cytokine Res.* 31, 41–47. doi:10.1089/jir.2010.0107

Langereis, M. A., Feng, Q., and van Kuppeveld, F. J. (2013). MDA5 localizes to stress granules, but this localization is not required for the induction of type I interferon. *J. virology* 87, 6314–6325. doi:10.1128/jvi.03213-12

Lee, S., Nguyen, H. M., and Kang, C. (2010). Tiny abortive initiation transcripts exert antitermination activity on an RNA hairpin-dependent intrinsic terminator. *Nucleic acids Res.* 38, 6045–6053. doi:10.1093/nar/gkq450

Leonard, J. N., Ghirlando, R., Askins, J., Bell, J. K., Margulies, D. H., Davies, D. R., et al. (2008). The TLR3 signaling complex forms by cooperative receptor dimerization. *Proc. Natl. Acad. Sci. U. S. A.* 105, 258–263. doi:10.1073/pnas.0710779105

Leppek, K., Byeon, G. W., Kladwang, W., Wayment-Steele, H. K., Kerr, C. H., Xu, A. F., et al. (2022). Combinatorial optimization of mRNA structure, stability, and translation for RNA-based therapeutics. *Nat. Commun.* 13, 1536. doi:10.1038/s41467-022-28776-w

Levanon, E. Y., Cohen-Fultheim, R., and Eisenberg, E. (2024). In search of critical dsRNA targets of ADAR1. *Trends Genet. TIG* 40, 250–259. doi:10.1016/j.tig.2023.12.002

Lim, C. S., Jang, Y. H., Lee, G. Y., Han, G. M., Jeong, H. J., Kim, J. W., et al. (2022). TLR3 forms a highly organized cluster when bound to a poly(I:C) RNA ligand. *Nat. Commun.* 13, 6876. doi:10.1038/s41467-022-34602-0

Linares-Fernández, S., Moreno, J., Lambert, E., Mercier-Gouy, P., Vachez, L., Verrier, B., et al. (2021). Combining an optimized mRNA template with a double purification

process allows strong expression of *in vitro* transcribed mRNA. *Mol. Ther. Nucleic acids* 26, 945–956. doi:10.1016/j.omtn.2021.10.007

Lu, X., Wu, H., Xia, H., Huang, F., Yan, Y., Yu, B., et al. (2019). Klebsiella phage KP34 RNA polymerase and its use in RNA synthesis. *Front. Microbiol.* 10, 2487. doi:10.3389/fmicb.2019.02487

Luo, J., Obmolova, G., Malia, T. J., Wu, S.-J., Duffy, K. E., Marion, J. D., et al. (2012). Lateral clustering of TLR3:dsRNA signaling units revealed by TLR3ecd: 3Fabs quaternary structure. *J. Mol. Biol.* 421, 112–124. doi:10.1016/j.jmb.2012.05.006

Ma, K., Temiakov, D., Anikin, M., and McAllister, W. T. (2005). Probing conformational changes in T7 RNA polymerase during initiation and termination by using engineered disulfide linkages. *Proc. Natl. Acad. Sci. U. S. A.* 102, 17612–17617. doi:10.1073/pnas.0508865102

Malagoda Pathiranage, K., Cavac, E., Chen, T.-H., Roy, B., and Martin, C. T. (2023). High-salt transcription from enzymatically gapped promoters nets higher yields and purity of transcribed RNAs. *Nucleic acids Res.* 51, e36. doi:10.1093/nar/gkad027

Malagoda Pathiranage, K., and Martin, C. T. (2023). A simple approach to improving RNA synthesis: salt inhibition of RNA rebinding coupled with strengthening promoter binding by a targeted gap in the DNA. *Methods Enzym.* 691, 209–222. doi:10.1016/bs.mie.2023.06.001

Manivannan, P., Siddiqui, M. A., and Malathi, K. (2020). RNase L amplifies interferon signaling by inducing protein kinase R-mediated antiviral stress granules. *J. virology* 94, e00205. doi:10.1128/JVI.00205-20

Mankan, A. K., Schmidt, T., Chauhan, D., Goldeck, M., Höning, K., Gaidt, M., et al. (2014). Cytosolic RNA:DNA hybrids activate the cGAS-STING axis. *EMBO J.* 33, 2937–2946. doi:10.15252/embj.201488726

Martin, C. T., Esposito, E. A., Theis, K., and Gong, P. (2005). Structure and function in promoter escape by T7 RNA polymerase. *Prog. nucleic acid Res. Mol. Biol.* 80, 323–347. doi:10.1016/S0079-6603(05)80008-X

Martin, C. T., Muller, D. K., and Coleman, J. E. (1988). Processivity in early stages of transcription by T7 RNA polymerase. *Biochemistry* 27, 3966–3974. doi:10.1021/bi00411a012

Martínez, J., Lampaya, V., Larraga, A., Magallón, H., and Casabona, D. (2023). Purification of linearized template plasmid DNA decreases double-stranded RNA formation during IVT reaction. *Front. Mol. Biosci.* 10, 1248511. doi:10.3389/fmolb.2023.1248511

Matsumoto, J. (1994). Evolutionary role of abortive transcript as a primer for DNA replication. *J. Mol. Evol.* 39, 620–624. doi:10.1007/BF00160407

McClure, W. R., Cech, C. L., and Johnston, D. E. (1978). A steady state assay for the RNA polymerase initiation reaction. *J. Biol. Chem.* 253, 8941–8948. doi:10.1016/s0021-9258(17)34268-0

Milligan, J. F., Groebe, D. R., Witherell, G. W., and Uhlenbeck, O. C. (1987). Oligoribonucleotide synthesis using T7 RNA polymerase and synthetic DNA templates. *Nucleic acids Res.* 15, 8783–8798. doi:10.1093/nar/15.21.8783

Moruzzi, G., Barbiroli, B., Moruzzi, M. S., and Tadolini, B. (1975). The effect of spermine on transcription of mammalian chromatin by mammalian deoxyribonucleic acid-dependent ribonucleic acid polymerase. *Biochem. J.* 146, 697–703. doi:10.1042/bj1460697

Mu, X., Greenwald, E., Ahmad, S., and Hur, S. (2018). An origin of the immunogenicity of *in vitro* transcribed RNA. *Nucleic acids Res.* 46, 5239–5249. doi:10.1093/nar/gky177

Mu, X., and Hur, S. (2021). Immunogenicity of *in vitro*-Transcribed RNA. *Accounts Chem. Res.* 54, 4012–4023. doi:10.1021/acs.accounts.1c00521

Mukherjee, S., Brieba, L. G., and Sousa, R. (2002). Structural transitions mediating transcription initiation by T7 RNA polymerase. *Cell.* 110, 81–91. doi:10.1016/s0092-8674(02)00815-2

Nallagatla, S. R., Hwang, J., Toroney, R., Zheng, X., Cameron, C. E., and Bevilacqua, P. C. (2007). 5'-triphosphate-dependent activation of PKR by RNAs with short stem-loops. *Sci. (New York, N.Y.)* 318, 1455–1458. doi:10.1126/science.1147347

Nickels, B. E., and Dove, S. L. (2011). NanoRNAs: a class of small RNAs that can prime transcription initiation in bacteria. *J. Mol. Biol.* 412, 772–781. doi:10.1016/j.jmb.2011.06.015

Ohto, U. (2022). Activation and regulation mechanisms of NOD-like receptors based on structural biology. *Front. Immunol.* 13, 953530. doi:10.3389/fimmu.2022.953530

O'Neill, L. A. J., Golenbock, D., and Bowie, A. G. (2013). The history of Toll-like receptors - redefining innate immunity. *Nat. Rev. Immunol.* 13, 453–460. doi:10.1038/nri3446

Onomoto, K., Jogi, M., Yoo, J.-S., Narita, R., Morimoto, S., Takemura, A., et al. (2012). Critical role of an antiviral stress granule containing RIG-I and PKR in viral detection and innate immunity. *PloS one* 7, e43031. doi:10.1371/journal.pone.0043031

Paget, M., Cadena, C., Ahmad, S., Wang, H.-T., Jordan, T. X., Kim, E., et al. (2023). Stress granules are shock absorbers that prevent excessive innate immune responses to dsRNA. *Mol. Cell.* 83, 1180–1196.e8. doi:10.1016/j.molcel.2023.03.010

Peisley, A., Jo, M. H., Lin, C., Wu, B., Orme-Johnson, M., Walz, T., et al. (2012). Kinetic mechanism for viral dsRNA length discrimination by MDA5 filaments. *Proc. Natl. Acad. Sci. U. S. A.* 109, E3340–E3349. doi:10.1073/pnas.1208618109

Peisley, A., Lin, C., Wu, B., Orme-Johnson, M., Liu, M., Walz, T., et al. (2011). Cooperative assembly and dynamic disassembly of MDA5 filaments for viral dsRNA recognition. *Proc. Natl. Acad. Sci. U. S. A.* 108, 21010–21015. doi:10.1073/pnas.1113651108

Peisley, A., Wu, B., Yao, H., Walz, T., and Hur, S. (2013). RIG-I forms signaling-competent filaments in an ATP-dependent, ubiquitin-independent manner. *Mol. Cell.* 51, 573–583. doi:10.1016/j.molcel.2013.07.024

Phillips, D. D., Garboczi, D. N., Singh, K., Hu, Z., Leppla, S. H., and Leysath, C. E. (2013). The sub-nanomolar binding of DNA-RNA hybrids by the single-chain Fv fragment of antibody S9.6. *J. Mol. Recognit. JMR* 26, 376–381. doi:10.1002/jmr.2284

Piao, X., Yadav, V., Wang, E., Chang, W., Tau, L., Lindenmuth, B. E., et al. (2022). Double-stranded RNA reduction by chaotropic agents during *in vitro* transcription of messenger RNA. *Mol. Ther. Nucleic acids* 29, 618–624. doi:10.1016/j.omtn.2022.08.001

Plaskon, D., Evensen, C., Henderson, K., Palatnik, B., Ishikuri, T., Wang, H.-C., et al. (2022). Step-by-Step regulation of productive and abortive transcription initiation by pyrophosphorolysis. *J. Mol. Biol.* 434, 167621. doi:10.1016/j.jmb.2022.167621

Pyle, A. M. (2002). Metal ions in the structure and function of RNA. *J. Biol. Inorg. Chem. JBIC a Publ. Soc. Biol. Inorg. Chem.* 7, 679–690. doi:10.1007/s00775-002-0387-6

Qin, S., Wu, H., Li, C., Yang, J., Yan, W., He, Z., et al. (2024). Detection of naturally occurring abortive transcripts by base-stacking hybridization assisted ligation and PCR amplification. *Biosens. Bioelectron.* 251, 116099. doi:10.1016/j.bios.2024.116099

Ramanathan, A., Robb, G. B., and Chan, S.-H. (2016). mRNA capping: biological functions and applications. *Nucleic acids Res.* 44, 7511–7526. doi:10.1093/nar/gkw551

Ramírez-Tapia, L. E., and Martin, C. T. (2012). New insights into the mechanism of initial transcription: the T7 RNA polymerase mutant P266L transitions to elongation at longer RNA lengths than wild type. *J. Biol. Chem.* 287, 37352–37361. doi:10.1074/jbc.M112.370643

Rebouillat, D., and Hovanessian, A. G. (1999). The human 2',5'-oligoadenylate synthetase family: interferon-induced proteins with unique enzymatic properties. *J. interferon & cytokine Res. official J. Int. Soc. Interferon Cytokine Res.* 19, 295–308. doi:10.1089/107999099313992

Rehwinkel, J., and Gack, M. U. (2020). RIG-I-like receptors: their regulation and roles in RNA sensing. *Nat. Rev. Immunol.* 20, 537–551. doi:10.1038/s41577-020-0288-3

Ren, X., Wang, D., Zhang, G., Zhou, T., Wei, Z., Yang, Y., et al. (2023). Nucleic DHX9 cooperates with STAT1 to transcribe interferon-stimulated genes. *Sci. Adv.* 9, eadd5005. doi:10.1126/sciadv.add5005

Rex, V., Stempel, M., Halle, S., and Brinkmann, M. M. (2023). The two faces of oligoadenylate synthetase-like: effective antiviral protein and negative regulator of innate immunity. *Curr. Opin. virology* 60, 101329. doi:10.1016/j.coviro.2023.101329

Rigby, R. E., Webb, L. M., Mackenzie, K. J., Li, Y., Leitch, A., Reijns, M. A. M., et al. (2014). RNA:DNA hybrids are a novel molecular pattern sensed by TLR9. *EMBO J.* 33, 542–558. doi:10.1002/embj.201386117

Rosa, M. D. (1979). Four T7 RNA polymerase promoters contain an identical 23 bp sequence. *Cell.* 16, 815–825. doi:10.1016/0092-8674(79)90097-7

Sahin, U., Karikó, K., and Türeci, Ö. (2014). mRNA-based therapeutics--developing a new class of drugs. *Nat. Rev. Drug Discov.* 13, 759–780. doi:10.1038/nrd4278

Sampson, J. R., and Uhlenbeck, O. C. (1988). Biochemical and physical characterization of an unmodified yeast phenylalanine transfer RNA transcribed *in vitro*. *Proc. Natl. Acad. Sci. U. S. A.* 85, 1033–1037. doi:10.1073/pnas.85.4.1033

Sarkar, S. N., Harioudh, M. K., Shao, L., Perez, J., and Ghosh, A. (2023). The many faces of oligoadenylate synthetases. *J. interferon & cytokine Res. official J. Int. Soc. Interferon Cytokine Res.* 43, 487–494. doi:10.1089/jir.2023.0098

Satoh, T., Kato, H., Kumagai, Y., Yoneyama, M., Sato, S., Matsushita, K., et al. (2010). LGP2 is a positive regulator of RIG-I- and MDA5-mediated antiviral responses. *Proc. Natl. Acad. Sci. U. S. A.* 107, 1512–1517. doi:10.1073/pnas.0912986107

Schenborn, E. T., and Mierendorf, R. C. (1985). A novel transcription property of SP6 and T7 RNA polymerases: dependence on template structure. *Nucleic acids Res.* 13, 6223–6236. doi:10.1093/nar/13.17.6223

Schmidt, A., Schwerd, T., Hamm, W., Hellmuth, J. C., Cui, S., Wenzel, M., et al. (2009). 5'-triphosphate RNA requires base-paired structures to activate antiviral signaling via RIG-I. *Proc. Natl. Acad. Sci. U. S. A.* 106, 12067–12072. doi:10.1073/pnas.0900971106

Schoenmaker, L., Witzigmann, D., Kulkarni, J. A., Verbeke, R., Kersten, G., Jiskoot, W., et al. (2021). mRNA-lipid nanoparticle COVID-19 vaccines: structure and stability. *Int. J. Pharm.* 601, 120586. doi:10.1016/j.ijpharm.2021.120586

Schuberth-Wagner, C., Ludwig, J., Bruder, A. K., Herzner, A.-M., Zillinger, T., Goldeck, M., et al. (2015). A conserved histidine in the RNA sensor RIG-I controls immune tolerance to N1-2'o-methylated self RNA. *Immunity* 43, 41–51. doi:10.1016/j.immuni.2015.06.015

Skok, J., Megušar, P., Vodopivec, T., Pregeljc, D., Mencin, N., Korenč, M., et al. (2022). Gram-scale mRNA production using a 250-mL single-use bioreactor. *Chem. Ing. Tech.* 94, 1928–1935. doi:10.1002/cite.202200133

Sondhi, P., Adeniji, T., Lingden, D., and Stine, K. J. (2024). Advances in endotoxin analysis. *Adv. Clin. Chem.* 118, 1–34. doi:10.1016/bs.acc.2023.11.001

Sun, J. H., Adkins, S., Faurote, G., and Kao, C. C. (1996). Initiation of (-)-strand RNA synthesis catalyzed by the BMV RNA-dependent RNA polymerase: synthesis of oligonucleotides. *Virology* 226, 1–12. doi:10.1006/viro.1996.0622

Sun, W., Pertzev, A., and Nicholson, A. W. (2005). Catalytic mechanism of *Escherichia coli* ribonuclease III: kinetic and inhibitor evidence for the involvement of two magnesium ions in RNA phosphodiester hydrolysis. *Nucleic acids Res.* 33, 807–815. doi:10.1093/nar/gki197

Sutton, D. H., Conn, G. L., Brown, T., and Lane, A. N. (1997). The dependence of DNase I activity on the conformation of oligodeoxynucleotides. *Biochem. J.* 321 (Pt 2), 481–486. doi:10.1042/bj3210481

Szabó, G. T., Mahiny, A. J., and Vlatkovic, I. (2022). COVID-19 mRNA vaccines: platforms and current developments. *Mol. Ther. J. Am. Soc. Gene Ther.* 30, 1850–1868. doi:10.1016/j.ymthe.2022.02.016

Tahirov, T. H., Temiakov, D., Anikin, M., Patlan, V., McAllister, W. T., Vassylyev, D. G., et al. (2002). Structure of a T7 RNA polymerase elongation complex at 2.9 A resolution. *Nature* 420, 43–50. doi:10.1038/nature01129

Tang, G.-Q., Nandakumar, D., Bandwar, R. P., Lee, K. S., Roy, R., Ha, T., et al. (2014). Relaxed rotational and scrunching changes in P266L mutant of T7 RNA polymerase reduce short abortive RNAs while delaying transition into elongation. *PloS one* 9, e91859. doi:10.1371/journal.pone.0091859

Tang, G.-Q., and Patel, S. S. (2006a). Rapid binding of T7 RNA polymerase is followed by simultaneous bending and opening of the promoter DNA. *Biochemistry* 45, 4947–4956. doi:10.1021/bi052292s

Tang, G.-Q., and Patel, S. S. (2006b). T7 RNA polymerase-induced bending of promoter DNA is coupled to DNA opening. *Biochemistry* 45, 4936–4946. doi:10.1021/bi0522910

Tang, G.-Q., Roy, R., Bandwar, R. P., Ha, T., and Patel, S. S. (2009). Real-time observation of the transition from transcription initiation to elongation of the RNA polymerase. *Proc. Natl. Acad. Sci. U. S. A.* 106, 22175–22180. doi:10.1073/pnas.0906979106

Tang, G.-Q., Roy, R., Ha, T., and Patel, S. S. (2008). Transcription initiation in a single-subunit RNA polymerase proceeds through DNA scrunching and rotation of the N-terminal subdomains. *Mol. Cell.* 30, 567–577. doi:10.1016/j.molcel.2008.04.003

Touchlight Genetics Ltd (2024) DNA vector and enzymatic manufacturing process. Available at: https://www.touchlight.com/platform-technology/overview/ (Accessed April 21, 2024).

Triana-Alonso, F. J., Dabrowski, M., Wadzack, J., and Nierhaus, K. H. (1995). Self-coded 3'-extension of run-off transcripts produces aberrant products during *in vitro* transcription with T7 RNA polymerase. *J. Biol. Chem.* 270, 6298–6307. doi:10.1074/jbc.270.11.6298

Ujvári, A., and Martin, C. T. (2000). Evidence for DNA bending at the T7 RNA polymerase promoter. *J. Mol. Biol.* 295, 1173–1184. doi:10.1006/jmbi.1999.3418

Viganò, E., Diamond, C. E., Spreafico, R., Balachander, A., Sobota, R. M., and Mortellaro, A. (2015). Human caspase-4 and caspase-5 regulate the one-step non-canonical inflammasome activation in monocytes. *Nat. Commun.* 6, 8761. doi:10.1038/ncomms9761

Vlatkovic, I. (2021). Non-immunotherapy application of LNP-mRNA: maximizing efficacy and safety. *Biomedicines* 9, 530. doi:10.3390/biomedicines9050530

Vvedenskaya, I. O., Sharp, J. S., Goldman, S. R., Kanabar, P. N., Livny, J., Dove, S. L., et al. (2012). Growth phase-dependent control of transcription start site selection and gene expression by nanoRNAs. *Genes. & Dev.* 26, 1498–1507. doi:10.1101/gad.192732.112

Walker, S. E., and Lorsch, J. (2013). RNA purification--precipitation methods. *Methods Enzym.* 530, 337–343. doi:10.1016/B978-0-12-420037-1.00019-1

Wang, G., Cheng, R., Chen, Q., Xu, Y., Yu, B., Zhu, B., et al. (2022). mRNA produced by VSW-3 RNAP has high-level translation efficiency with low inflammatory stimulation. *Cell. insight* 1, 100056. doi:10.1016/j.cellin.2022.100056

Wang, Y., Holleufer, A., Gad, H. H., and Hartmann, R. (2020). Length dependent activation of OAS proteins by dsRNA. *Cytokine* 126, 154867. doi:10.1016/j.cyto.2019.154867

Wu, M., Pei, Z., Long, G., Chen, H., Jia, Z., and Xia, W. (2023). Mitochondrial antiviral signaling protein: a potential therapeutic target in renal disease. *Front. Immunol.* 14, 1266461. doi:10.3389/fimmu.2023.1266461

Wu, M. Z., Asahara, H., Tzertzinis, G., and Roy, B. (2020). Synthesis of low immunogenicity RNA with high-temperature *in vitro* transcription. *RNA (New York, N.Y.)* 26, 345–360. doi:10.1261/rna.073858.119

Xia, H., Yu, B., Jiang, Y., Cheng, R., Lu, X., Wu, H., et al. (2022). Psychrophilic phage VSW-3 RNA polymerase reduces both terminal and full-length dsRNA byproducts in *in vitro* transcription. *RNA Biol.* 19, 1130–1142. doi:10.1080/15476286.2022.2139113

Xu, J., and Núñez, G. (2023). The NLRP3 inflammasome: activation and regulation. *Trends Biochem. Sci.* 48, 331–344. doi:10.1016/j.tibs.2022.10.002

Yoo, J.-S., Takahasi, K., Ng, C. S., Ouda, R., Onomoto, K., Yoneyama, M., et al. (2014). DHX36 enhances RIG-I signaling by facilitating PKR-mediated antiviral stress granule formation. *PLoS Pathog.* 10, e1004012. doi:10.1371/journal.ppat.1004012

Zappa, F., Muniozguren, N. L., Wilson, M. Z., Costello, M. S., Ponce-Rojas, J. C., and Acosta-Alvear, D. (2022). Signaling by the integrated stress response kinase PKR is fine-tuned by dynamic clustering. *J. Cell. Biol.* 221, e202111100. doi:10.1083/jcb.202111100

Zhang, J., Liu, Y., Li, C., Xiao, Q., Zhang, D., Chen, Y., et al. (2023). Recent advances and innovations in the preparation and purification of *in vitro*-Transcribed-mRNA-Based molecules. *Pharmaceutics* 15, 2182. doi:10.3390/pharmaceutics15092182

Zhu, B., Tabor, S., Raytcheva, D. A., Hernandez, A., King, J. A., and Richardson, C. C. (2013). The RNA polymerase of marine cyanophage Syn5. *J. Biol. Chem.* 288, 3545–3552. doi:10.1074/jbc.M112.442350

Zhu, B., Tabor, S., and Richardson, C. C. (2014). Syn5 RNA polymerase synthesizes precise run-off RNA products. *Nucleic acids Res.* 42, e33. doi:10.1093/nar/gkt1193

Ziegenhals, T., Frieling, R., Wolf, P., Göbel, K., Koch, S., Lohmann, M., et al. (2023). Formation of dsRNA by-products during *in vitro* transcription can be reduced by using low steady-state levels of UTP. *Front. Mol. Biosci.* 10, 1291045. doi:10.3389/fmolb.2023.1291045

frontiers | Frontiers in Molecular Biosciences

TYPE Original Research
PUBLISHED 27 September 2024
DOI 10.3389/fmolb.2024.1443917

OPEN ACCESS

EDITED BY
Alessio Branchini,
University of Ferrara, Italy

REVIEWED BY
Robin Stanley,
National Institute of Environmental Health Sciences (NIH), United States
Dylan Girodat,
University of Arkansas, United States

*CORRESPONDENCE
Louise J. Walport,
l.walport@imperial.ac.uk
Rok Sekirnik,
rok.sekirnik@biaseparations.com

†These authors have contributed equally to this work

RECEIVED 04 June 2024
ACCEPTED 10 September 2024
PUBLISHED 27 September 2024

CITATION
Megušar P, Calder EDD, Vodopivec Seravalli T, Lebar S, Walport LJ and Sekirnik R (2024) HPLC for at-line reaction monitoring and purification improves yield and purity of tRNA. *Front. Mol. Biosci.* 11:1443917. doi: 10.3389/fmolb.2024.1443917

HPLC for at-line reaction monitoring and purification improves yield and purity of tRNA

Polona Megušar[1†], Ewen D. D. Calder[2,3†], Tina Vodopivec Seravalli[1], Sergeja Lebar[1], Louise J. Walport[2,3*] and Rok Sekirnik[1*]

[1]Sartorius BIA Separations d.o.o., Ajdovščina, Slovenia, [2]Department of Chemistry, Molecular Sciences Research Hub, Imperial College London, London, United Kingdom, [3]Protein-Protein Interaction Laboratory, The Francis Crick Institute, London, United Kingdom

Engineered transfer RNA is an emerging therapeutic modality, particularly suited to treatment of diseases caused by genetic disorders based on premature termination codons, frameshifts, or missense mutations. It is also extensively used in reprogramming of *in vitro* translation systems to generate non-canonical amino acid-containing proteins and peptides, such as in mRNA display. Due to its length, chemical synthesis of tRNA is challenging and production of engineered tRNA at scale is currently limited to *in vitro* transcription from a DNA template. Previously, the highest reported *in vitro* transcription yield was 2.5 g/L, significantly below the industry standard for mRNA production of 7–10 g/L. To improve this process, we implemented monitoring of nucleoside triphosphate consumption and tRNA production during *in vitro* transcription, using at-line high-performance liquid chromatography, with a monolithic solid phase. This allowed for optimization of nucleoside triphosphate concentration, reduction of the *in vitro* transcription time to <4 h, and improvement of yield up to 4.7 g/L. A step-elution purification on a DEAE chromatographic monolith with >90% step yield was then developed. These improvements in the production and purification of tRNA represent an important step in facilitating production of tRNA for research purposes, and provide a method for purification of therapeutic tRNAs that is scalable and compatible with Good Manufacturing Practice requirements for clinical production.

KEYWORDS

tRNA, *in vitro* transcription, HPLC, chromatography, anion exchange

Introduction

Transfer RNA (tRNA) is a key component of the protein synthesis machinery, acting as the adaptor molecule that decodes mRNA into amino acid sequences. Recent advances have unveiled further tRNA roles beyond their canonical function in translation, including regulation of gene expression, involvement in disease pathogenesis, and their potential as therapeutic agents (Anastassiadis and Köhrer, 2023; Berg and Brandl, 2021; Coller and Ignatova, 2023).

The therapeutic potential of tRNAs is significant, as they can be engineered to correct genetic mutations that cause disease. Mutations within protein-coding sequences can lead to various pathologies by creating premature termination codons, frameshifts,

or missense mutations, all of which can be targeted by specifically designed tRNAs. For instance, engineered tRNAs can facilitate read-through of premature termination codons, adjust reading frames disrupted by frameshift mutations, or correct missense mutations, thereby restoring the synthesis of functional proteins (Anastassiadis and Köhrer, 2023; Coller and Ignatova, 2023).

tRNA therapeutics offer an approach to treating genetic diseases based on targeting the mutation itself rather than the affected gene. This strategy could transform the treatment landscape for patients with rare and ultrarare diseases, which often lack viable therapeutic options due to the small patient populations and the high specificity of gene-targeted treatments. Engineered tRNAs have been shown to suppress premature termination codon mutations effectively, both *in vitro* and *in vivo* (Albers et al., 2023). Moreover, the ability to deliver tRNAs directly as RNA (formulated as lipid nanoparticle or exosome) or via viral vector (e.g., AAV) expands the potential delivery options and facilitates the development of versatile therapeutic platforms (Coller and Ignatova, 2023).

Synthetic tRNA are also used extensively for genetic code reprogramming in chemical biology and drug discovery applications. A range of methods have been developed to couple non-natural amino acids to tRNA, including by chemoenzymatic synthesis, use of engineered aminoacyl tRNA synthetases or use of evolved ribozymes, known as flexizymes (Forster et al., 2003; Heckler et al., 1984; Murakami et al., 2006; Sigal et al., 2024). Introduction of these artificially aminoacylated tRNA into *in vitro* translation reactions allows synthesis of peptides and proteins containing a vast variety of non-natural amino acids that can augment their functions (Zhou and Obexer, 2024). This has been exploited extensively, both in industry and academia, through combination with mRNA display for the discovery of *de novo* cyclic peptides (Huang et al., 2019; Josephson et al., 2005; Ohta et al., 2023; Yamagishi et al., 2011).

Due to its size (70–90 nucleotides), tRNA is too long for large scale *de novo* production by chemical synthesis. Instead, it is primarily produced by an *in vitro* transcription (IVT) reaction, an RNA polymerase-catalyzed incorporation of nucleoside triphosphates (NTPs) into a nascent RNA chain guided by a DNA template (Milligan et al., 1987). Alternatively, tRNA can also be produced by *in vivo* overproduction (Perona et al., 1988). Optimizing IVT conditions for high yield, as well as developing efficient purification methods is critical for cost-effective production of mRNA, self-amplifying RNA (saRNA) and circular RNA (circRNA) therapeutics (Rosa et al., 2021). For tRNA, only few reports have addressed optimization of IVT reaction, of which the key study described optimization of *Escherichia coli* tRNATrp production by IVT to 2.5 g/L by fine-tuning the concentrations of T7 RNA polymerase, DNA template, NTPs, and magnesium, using a combination of incomplete factorial design and response surface methodology (Yin and Carter, 1996). The study used densitometry as well as a radioactive labelling approach to quantitate yield, both of which could lead to potential quantification errors. Other analytical methods have since been applied to monitor the yield of IVT reactions in real time (reviewed in Lee et al., 2023): light-up RNA aptamer coupled with fluorescent dye pairs (Höfer et al., 2013; Kartje et al., 2021; Valentini et al., 2022) and fluorophore-labeled antisense probe-based methods (Dunkak et al., 1996). High-performance liquid chromatography (HPLC)-based methods able to monitor NTP consumption as well as RNA production in near-real time have recently been developed (Pregeljc et al., 2023; Welbourne et al., 2024) with resolution-times of 3–6 min and total run-times of ~8 min, thereby enabling IVT reaction optimization based on kinetics of NTP consumption. To our knowledge, none of these methods have been applied for monitoring of IVT reactions for production of tRNA.

For *in vitro* or *in vivo* use, tRNA needs to be purified from IVT reaction mixture to remove residual NTPs, enzymes and DNA template. The most common approach to purify synthetic tRNA is by polyacrylamide gel electrophoresis and excision of the tRNA band from the gel (Avcilar-Kucukgoze et al., 2020). This method is highly selective for target tRNA, potentially allowing single-nucleotide resolution. However, PAGE gels are poorly scalable beyond laboratory scale, and require handling toxic acrylamide during preparation of gels.

A widely used scalable purification approach, which can be employed at clinical and commercial manufacturing scales under Good Manufacturing Practice compliance, is chromatography. Various chromatographic techniques have been used to purify tRNA, either IVT-derived (defined tRNA sequence) or from *E. coli* extract, including ion exchange (Guenther et al., 1988), reverse-phase HPLC (RP-HPLC) (Cayama et al., 2000) and hydrophobic interaction chromatography (HIC) (Mesters et al., 1994). More selective approaches including use of dihydroxyboryl cellulose (McCutchan et al., 1975), which bind the cis-diol group of the 3′-terminal ribose in unaminoacylated, but not aminoacylated tRNA, have also been explored, however, these are not used in practice as dihydroxyboryl cellulose is not a commercially available chromatography media. Seminal preparative scale tRNA purification from IVT was reported with weak anion exchanger (DEAE Sepharose), which suffered from broad elution peaks and was not able to fully separate DNA template from tRNA (Easton et al., 2010). Chromatographic resolution was significantly increased with a strong anion exchanger (MonoQ) enabling baseline separation of tRNA from DNA template (Koubek et al., 2013), and although quantification of tRNA in IVT mixtures was shown, NTPs could not be quantified and the separation was too slow to be useful for at-line IVT monitoring. MonoQ was reported to require multiple elutions to achieve full RNA recovery, suggesting that strong AEX could present issues for tRNA recovery (Pikovskaya et al., 2009). We reasoned that resolution and recovery of tRNA could be improved, and purification time decreased, with use of chromatographic monoliths, stationary phases consisting of a single piece of highly porous polymer with open, ligand-functionalized pores forming interconnected channels which provide binding surface for analytes (Podgornik et al., 2013). Due to their architecture, monoliths exhibit high binding capacity for large biomolecules (plasmid DNA, mRNA, virus particles) and mass transport based on convection, which results in flow-rate independent chromatographic resolution and binding capacity. Analytical anion exchange monolith can resolve a mixture of oligonucleotides with single-nucleotide resolution in 10 min (Yamamoto et al., 2009).

We recently reported how the high resolution at short run times of monoliths can be harnessed to analytically resolve NTPs from mRNA to monitor IVT reaction for production of mRNA (Pregeljc et al., 2023). In the present study we expand the scope

10.3389/fmolb.2024.1443917

TABLE 1 Reference IVT reaction conditions for tRNA production. GMP was not used in the reaction.

Reagent	Final concentration
Nuclease free water	
10x IVT buffer	1x
RNAse inhibitor 40 U/μL	1 U/μL
$MgCl_2$	22.5 mM
NTP (each)	3.75 mM
DNA template	4.3 ng/μL
Pyrophosphatase, 100 U/mL	1 U/mL
T7 RNA polymerase 50 U/μL	10 U/μL

of the analytical strategy to increase yield of IVT-produced tRNA by analyzing the consumption of NTPs and optimizing reagent concentrations and reaction times. Further, we verify that recently developed monolith chromatographic supports which showed high recovery of mRNA and saRNA at room temperature and neutral pH (Megušar et al., 2023; Miklavčič et al., 2023) can also be used to purify tRNA, and compare their purification efficiency to more traditional anion exchange ligands (e.g., diethylaminoethyl DEAE) with high (single-nucleotide) resolution for oligonucleotides at short run times (Podgornik et al., 1999; Yamamoto et al., 2007). We demonstrate that applying convective monolith stationary phases, with flow-rate independent binding capacity and resolution, could shorten tRNA purification without sacrificing tRNA purity with the potential for industrial applications in the future.

Materials and methods

At-line monitoring of *in vitro* transcription by HPLC

40 U/μL RNase inhibitor, 100 U/μL pyrophosphatase, 50 U/μL T7 RNA polymerase, ATP, UTP, CTP and GTP (100 mM stocks) were purchased from Jena Biosciences or Mebep Bioscience, China. 1 M $MgCl_2$ was purchased from Invitrogen, USA, 10 × IVT buffer (400 mM Tris, 20 mM spermidine, 10 mM DTT, pH 7.9) was prepared in-house. All IVT reagents listed except enzymes were preheated to 37°C, mixed in a 1.5 mL plastic tube in Thermomixer™C (Eppendorf, Germany) and, after addition of enzymes, incubated at 37°C with shaking at 300 rpm unless otherwise stated. For sampling, 2 μL aliquots were quenched with 2 μL of 100 mM EDTA pH 8.0 for HPLC analytics at defined timepoints. tRNA production and NTP consumption were monitored by CIMac PrimaS™ (Sartorius BIA Separations, Slovenia) every 30–60 min.

IVT reaction optimization for tRNA was based on reference protocol described in Table 1.

CIMac PrimaS analysis for determination of tRNA concentration and NTP consumption

HPLC analysis for mRNA quantification and determination of NTP consumption was performed as previously reported (Skok et al., 2022). PATfix®2.0 software (Sartorius BIA Separations, Slovenia) was used for instrument control, data acquisition and data analysis. A purified tRNA standard was used for calibration of the UV signal corresponding to tRNA. Linearity of signal responses (tRNA, UTP/CTP, GTP, ATP) is shown in Supplementary Figure S1; samples for HPLC analysis were diluted accordingly.

Purification development

In a typical chromatographic experiment, a freshly prepared IVT reaction mixture was diluted at least 10-fold with selected mobile phase A (MPA) i) 50 mM citric acid pH 5 for Swiper and ii) 100 mM Tris, 300 mM guanidine hydrochloride (GuHCl), pH 8 for DEAE) to provide pH buffering and binding conditions. Chromatographic purification was performed using PATfix system (Sartorius BIA Separations, Slovenia) equipped with quaternary pump and a multiwavelength UV-Vis detector (10 mm flow cell path length). PATfix 2.0 software (Sartorius BIA Separations) was used for instrument control and data acquisition. Column was equilibrated with at least 10 CV selected mobile phase B (MPB) [i) 50 mM citric acid, 0.3 M NaCl pH 5 for Swiper and ii) 100 mM Tris, 300 mM GuHCl, 700 mM NaCl, pH 8 for DEAE] followed by at least 10 CV of selected MPA. Sample, usually with tRNA concentration between 300 and 400 μg/mL, was loaded onto CIM discs or CIMmultus®Swiper or DEAE monolith column (0.1 or 1 mL, respectively) with 2 μm channel size (Sartorius BIA Separations, Ajdovščina, Slovenia) at 1–10 column volume per min (CV/min) and UV absorbance was monitored at 260 nm. After UV260, conductivity and pH signal stabilized, where indicated, wash and/or elution steps where performed: a) CIM Swiper: high salt wash (MPB), followed by elution step with 100 mM sodium phosphate pH 7.5 and cleaning in place step (CIP) for column sanitization with 0.1 M NaOH and 1 M NaCl; b) DEAE: elution with linear gradient from MPA to MPB in 15 min or elution in step gradient described below in spin column section.

tRNA purification with spin columns

Samples containing tRNA were diluted 10-fold in 100% MPA. Sample was then transferred onto a prototype CIM DEAE spin column (0.1 mL bed volume) and loaded by centrifuging at 1,200 rpm for 3 min. Column was then washed with 10 CV of MPA (3,000 rpm for 2 min) to remove NTPs and tRNA fragments. Permeate was collected in the collection tube and transferred to a separate tube for analytical purposes. Next, 5 CV of elution buffer 1 (70% MPA, 30% MPB) was used to wash the column. Elution was transferred to a separate tube. 5 CV of elution buffer 2 (60% MPA, 40% MPB) was used to elute the tRNA. The elution, which contained final purified tRNA, was transferred into a new tube. The column was stripped with 5 CV of 100% MPB. Spin columns were sanitised with 5 CV of 0.1 M NaOH, 1 M NaCl and regenerated with 10 CV of MPA before next use.

Aminoacylation of tRNA

Flexizyme-mediated aminoacylation reactions were performed as described previously (Goto et al., 2011a; Goto et al., 2011b). Aminoacylation was performed by mixing 5 mM amino acid cyanomethyl ester (Biotin-L-Phe-CME or D-Phe-CME) with 600 mM $MgCl_2$, 20% DMSO, 25 μM eFx and either 25 μM initiator $tRNA^{fMet}_{CAU}$, 25 μM elongator $tRNA^{AsnE2}_{CAU}$ or 25 μM elongator $tRNA^{AsnE3}_{CAU}$ in 50 mM HEPES-KOH (pH 7.5). The mixture was incubated for 2 h on ice, precipitated with sodium acetate and ethanol and resuspended in 1 mM NaOAc. Solution at 250 μM is assumed to be 50% loaded with amino acid and is used without further purification.

In vitro translation of an mRNA template for MALDI-TOF MS

mRNA templates used for *in vitro* translation experiments encoded for either MGSVSGWRLFKKISGSGSGS for initiator testing or MGSMGSVSGWRLFKKISGSGSGS for elongator testing.

Translations were performed using solution B from a PURExpress (NEB), (Δaa, ΔtRNA) kit and solA (composition described in Supplementary Material). Working on ice, the mRNA template (5 μM, 1.0 μL), 19 amino acid mix (ΔMet, 5 μM each amino acid, 0.50 μL), aminoacylated tRNA (125 μM, 1.0 μL), water (0.22 μL), solA (0.78 μL) and PURExpress (Δaa, ΔtRNA) solution B (1.5 μL) were combined. The solution was mixed by pipette and incubated with shaking at 37 °C for 1 h.

Results

IVT optimization

We aimed to develop an optimized protocol for the synthesis and purification of tRNA by IVT. Initial efforts focused on IVT optimization following an HPLC-based at-line IVT monitoring approach previously reported for mRNA. The methodology employed a rapid HPLC analytical method based on multimodal anion exchange/hydrogen bonding ligand PrimaS which separates NTPs from DNA and RNA. This method has been employed to increase IVT yield for mRNA and saRNA (Pregeljc et al., 2023; Skok et al., 2022), but has not been applied for monitoring IVT to produce shorter RNA constructs such as tRNA.

The starting point for optimization was a standard IVT protocol for tRNA production commonly used to produce tRNA (Goto et al., 2011a; Milligan and Uhlenbeck, 1989). The historical tRNA IVT protocol employs guanosine monophosphate (GMP) to incorporate a 5′-monophosphate (instead of a 5′-triphosphate incorporated by guanosine triphosphate (Milligan and Uhlenbeck, 1989; Sampson and Uhlenbeck, 1998)). Since multiple studies demonstrated that a 5′-phosphate does not have a significant impact on efficiency of tRNA aminoacylation (Fechter et al., 1998; Sampson and Uhlenbeck, 1998) or *in vitro* translation (Sprinzl and Graeser, 1980), we performed IVT optimization without GMP, using NTPs only, translating an initiator tRNA template ($tRNA^{fMet}_{CAU}$, INI).

A reference IVT reaction mixture after 3 h reaction time was separated into multiple peaks by CIMac PrimaS. Retention times (RT) corresponding to NTPs were easily identifiable, while the remaining peaks presumably corresponded to DNA and tRNA (1.4 min (E1), 1.8 min (E2) and 2.3 min (E3), Figure 1). Only the RT of E3 coincided with typical RT of mRNA. To confirm the identity of chromatographic peaks, tRNA loading on the column was increased to 50 μg to allow collection of elution fractions for analysis by RP-HPLC, PAGE gel and CIMac PrimaS (Figures 1B–E). Due to higher mass loading onto the analytical column, the resolution between peaks decreased (Figure 1B) compared to analytical loading (Figure 1A) but the order of elution was identical.

The two major elution peaks (E2 and E3) were indistinguishable by IP-RP and PAGE (Figures 1C, D), and corresponded to tRNA of target size (76 nt, determined by IP-RP). Analytical profiles of elution fractions E2 and E3 were consistent with tRNA of same length, therefore the combined integral of peak areas was used for quantification of tRNA in IVT mixtures when IVT reactions were monitored at-line for tRNA content and NTP concentrations (Figure 2) and in calibration curves (Supplementary Figure S1). E1 did not bind to IP-RP column under analytical binding conditions (Figure 1C; RNA chain length >20 nt is required for binding); PAGE band of E1 was consistent with migration of DNA template (Figure 1D); and the CIMac PrimaS elution profile was consistent with elution of DNA template or short RNA fragments (Figure 1E). We concluded that E1 corresponds to DNA template and/or short RNA fragments, but not target tRNA.

The reference IVT protocol resulted in production of 1.5 g/L tRNA after 3 h. GTP was completely consumed, indicating that GTP was limiting for tRNA production (data not shown). We increased GTP concentration in the IVT reaction, initially in batch, then in fed-batch mode (Table 2). DNA concentration was also varied based on reports that it may impact IVT productivity (Yin and Carter, 1996), as were the concentrations of other NTPs (Table 2).

An increase in GTP from 3.75 to 6 mM led to a moderate increase in yield from 1.5 to 1.8 g/L (IVT 2). Yield could also be doubled if DNA template concentration was doubled (IVT 3), though this effect is likely limited to low overall NTP concentrations. A further increase in NTP to 6 mM and GTP concentration to 12 mM (IVT 4) yielded 4.1 g/L tRNA, surpassing the highest previously reported yield of 2.5 g/L (Yin and Carter, 1996). Comparable yield (4.0 g/L) could be achieved if GTP was maintained at 12 mM while other NTPs were reduced to 4.5–5.0 mM (IVT 5). When more DNA template (5 ng/μL) and more T7 polymerase (12 U/mL) was used (IVT 6), the reaction proceeded faster and increased the yield even further: 4.7 g/L was reached after 4 h and did not increase further with overnight incubation. This result was not surpassed by fed-batch approach (IVT 7, IVT 8) which resulted in a decreased reaction rate, but not overall yield, possibly due to additional dilution of reaction components which slow the reaction; tRNA was produced more slowly after feeding but the reaction could still reach a high yield if incubated overnight. Nearly 50% higher yield was observed if fed-batch reactions were incubated overnight, whereas only a 10% yield increase was observed when leaving batch reactions overnight, which already reached >4 g/L in 3 h.

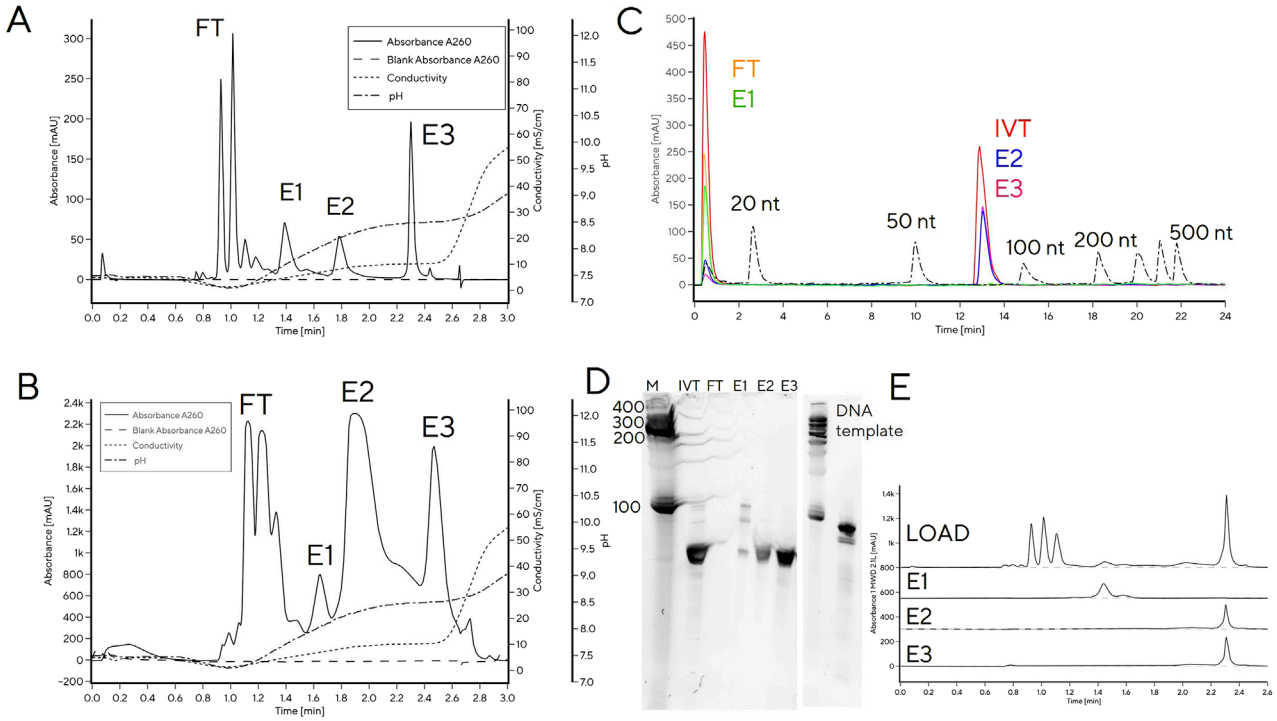

FIGURE 1
Separation of IVT mixture containing using a tRNA CIMac PrimaS analytical HPLC column. **(A)** Analytical loading (1 µg) onto CIMac PrimaS; **(B)** 50 µg loading onto CIMac PrimaS; **(C)** overlay of IP-RP analytical chromatograms of CIMac PrimaS elution fractions (FT, E1-E3) and molecular weight standards, **(D)** 10% TBE-Urea PAGE gel of CIMac PrimaS elution fractions, **(E)** CIMac PrimaS analytical chromatograms of CIMac PrimaS elution fractions. M: molecular weight marker (Small RNA ladder, Agilent), IVT: quenched IVT mixture, FT: column flow-through fraction, L: load, E1-E3 elution fractions E1-E3 from 50 µg loading onto CIMac PrimaS.

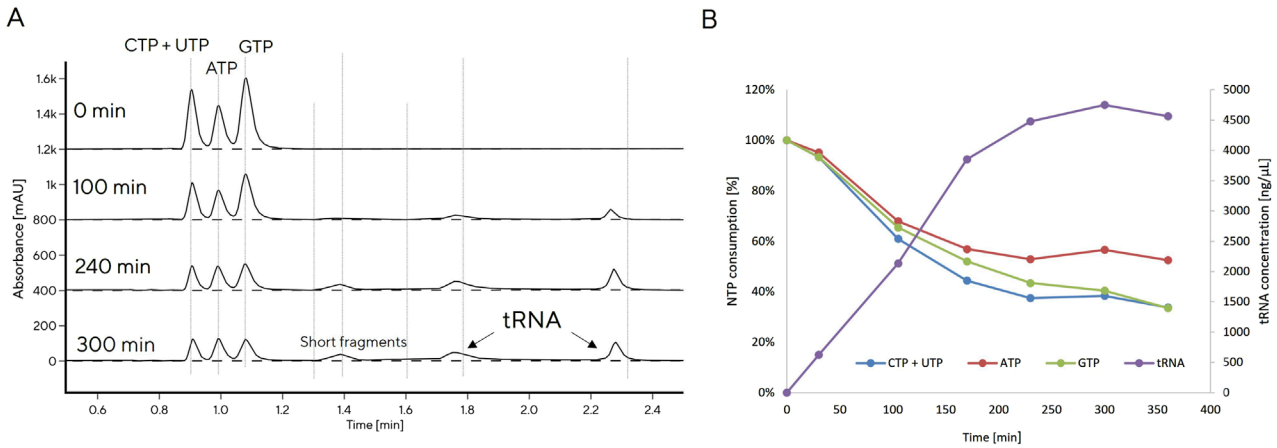

FIGURE 2
CIMac PrimaS monitoring of tRNA production with *in vitro* transcription (IVT 6) reaction **(A)**, tRNA production and NTPs consumption monitored at-line with CIMac PrimaS **(B)**.

We tested our optimized IVT protocol on two variant elongator tRNAs ($tRNA^{AsnE2}_{CAU}$, ELO2, and $tRNA^{AsnE3}_{CAU}$, ELO3, Supplementary Table S1). These variant tRNAs bind to elongation factor thermo unstable (EF-Tu) during translation with different affinities and allow incorporation of some unnatural amino acids to occur with higher yields (Iwane et al., 2021). IVT protocol optimized on INI resulted in a more modest increase in yield to 2.5 g/L for two other tRNA constructs (ELO2, ELO3) with different AUCG content (Supplementary Table S1), while reference protocol resulted in a comparable yield to INI (1.8 g/L; Supplementary Figure S2). It is notable that ELO2 and ELO3 share high sequence homology to each other, but differ in AUCG content from INI.

TABLE 2 Optimization of IVT parameters for production of tRNA.

Entry	Batch (B)/Fed-batch (FB)	ATP (mM)	GTP (mM)	GMP (mM)	CTP and UTP (mM, each)	$MgCl_2$ (mM)	DNA (ng/μL)	T7 (U/mL)	tRNA yield after 4 h (g/L)	tRNA yield overnight (g/L)
Reference (IVT 1)	B	3.75	3.75	—	3.75	22.50	4.3	10	1.5	—
IVT 2	B	6.00	6.00	—	6.00	25.00	4.0	10	1.8	—
IVT 3	B	4.00	5.50	—	4.00	22.50	8.0	10	2.9	—
IVT 4	B	6.00	12.00	—	6.00	27.00	3.0	10	4.1	4.5
IVT 5	B	4.50	12.00	—	5.00	23.90	3.0	10	4.0	4.2
IVT 6	B	6.00	12.00	—	6.00	27.00	5.0	12	4.7	4.8
IVT 7	FB	8.00	8.00[b]	—	8.00	30.00	5.0	10	3.2	4.7
IVT 8	FB	6.00[a]	10.00[b]	—	6.00[c]	30.00	5.6	10	3.5	4.4
IVT 9	B	6.00	6.00	5.00	6.00	25.00	4.0	10	1.5	—

[a]Feed additions of ATPs are marked with a.
[b]Feed additions of GTP are marked with b.
[c]Feed additions of CTP and UTP are marked with c.

10.3389/fmolb.2024.1443917

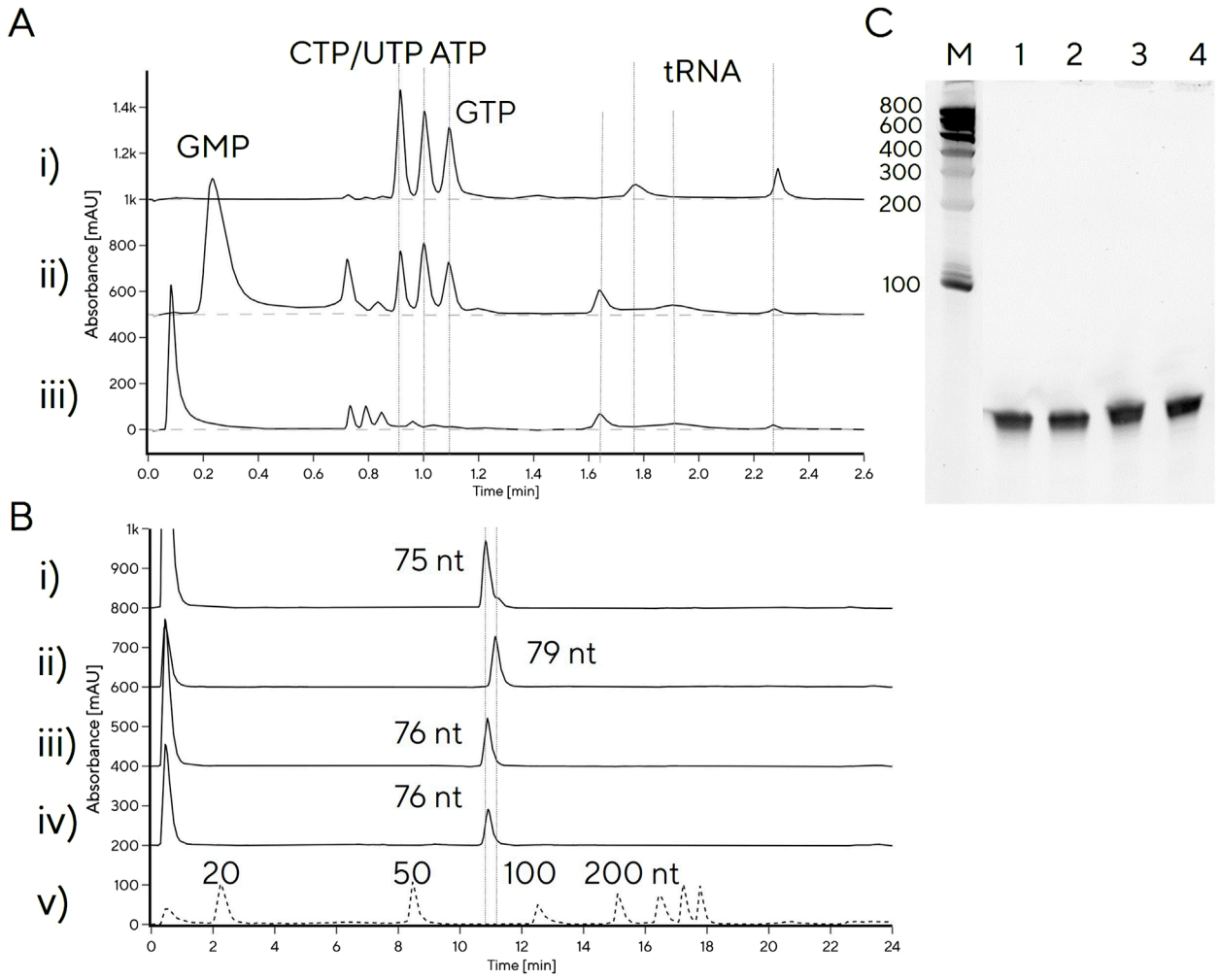

FIGURE 3
Analytical profiling of tRNA with variable 5′-phosphorylation status. **(A)** CIMac PrimaS HPLC analytical profiles of **(i)** tRNA produced with NTPs only; ii) tRNA produced with GMP, iii) tRNA produced with NTPs and treated with 5′-phosphatase. **(B)** CIMac SDVB RP-HPLC profiles of **(i)** IVT with GMP, ii) IVT without GMP, iii) IVT without GMP, treated with 5′-phosphatase (without purification); iv) tRNA produced without GMP, purified by Swiper and treated with 5′-phosphatase. **(C)** PAGE gel of 1) IVT treated with phosphatase, 2) Swiper-purified tRNA treated with phosphatase, 3) IVT without GMP, 4) IVT with GMP.

In IVT reactions for ELO2/3, CIMac PrimaS detected an increase in area of chromatographic peak at 1.4 min (Supplementary Figure S3A), which increased with a higher rate compared to tRNA peak (2.3 min; Supplementary Figure S3B). We increased sample loading to CIMac PrimaS to isolate fractions (Supplementary Figure S3C) and confirmed that the peak corresponds to RNA fragment of 20–40 nt (Supplementary Figure S3D–F), suggesting that ELO2/ELO3 constructs under 'high yield IVT conditions' led to a higher amount of aborted transcripts. We can conclude that IVT conditions to optimize tRNA yield may be construct-specific, at least for sequences with significantly different AUCG content, underscoring the importance of IVT monitoring when optimizing reactions to distinguish between full-length and abortive transcripts.

As most tRNA IVT protocols still include GMP (Goto et al., 2011a; Korenčić et al., 2002; Milligan and Uhlenbeck, 1989), we also investigated what effect addition of GMP would have on reaction yield. Adding GMP to reaction conditions of IVT 9 yielded 1.5 g/L tRNA compared to 1.8 g/L with NTPs only, likely due to competition with GTP for initiation of transcription. We noticed that the tRNA produced with GMP (IVT 9) exhibited a different chromatographic profile on CIMac PrimaS compared to tRNA produced without GMP, suggesting that retention times of the tRNA peaks depend on 5′-phosphorylation status. To verify this, tRNA was treated with 5′-phosphatase, which converts a 5′-triphosphate to a 5′-monophosphate. tRNA produced with GMP or treated with phosphatase exhibited a broader peak between 1.9 min, instead of the characteristic tRNA peak at 2.2 min (Figure 3A). It was surprising to observe that a difference in 5′-phosphorylation leads to observable differences in elution profile and suggests that 5′-phosphorylation state plays a significant role in binding to the stationary phase. This could potentially be exploited further for determination of 5′-phosphorylation status of tRNA,

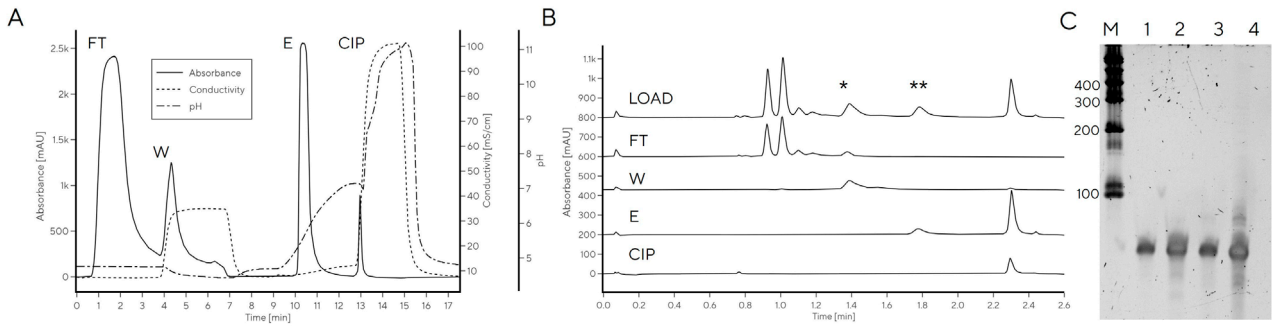

FIGURE 4
(A) Purification of tRNA from IVT with CIMmultus Swiper. Purification was performed as described in the material and methods **(B)** CIMac PrimaS analytics of fractions collected from tRNA purification on CIMmultus Swiper. **(C)** 8% Urea PAGE. FT: Flow-through. W: Wash. E: Elution. CIP: cleaning in place. M: Low range RNA ruler. 1–2: Gel-purified tRNA (50 and 250 pmol, respectively). 3–4: Swiper-purified tRNA (50 and 250 pmol, respectively).

in combination with IP-RP, which also distinguished between 5′-mono- and triphosphate tRNA. In IP-RP analytical chromatograms, the 5′-monophosphate tRNA eluted earlier than 5′-triphosphate tRNA (Figure 3B), the GMP-tRNA peak contained a shoulder at a higher retention time, indicating incomplete 5′-monophosphate incorporation. Denaturing PAGE electrophoretic mobility of all three tRNAs were indistinguishable (Figure 3C), consistent with unchanged tRNA length.

tRNA purification

We next investigated whether HPLC separation observed with analytical PrimaS method could be extended to a chromatographic purification method to avoid the slow and inefficient gel purifications that are commonly used for tRNA purification. A larger mass of tRNA could not be applied to PrimaS operated with a pyrophosphate gradient, as used for analytical separation, without losing resolution between peaks (e.g., Figure 1B). Use of a non-pyrophosphate buffer system was also unfeasible as pH > 10.5 would be required for RNA elution from PrimaS as previously reported (Megušar et al., 2023). Non-affinity purification of RNA of different sizes can be performed with multimodal monolith weak anion-exchanging properties and an isoelectric point of 5.3 (CIM Swiper) under near-neutral conditions (Miklavčič et al., 2023) — the IVT mixture is loaded in 50 mM Na-citrate, pH 5.0, to achieve selective binding of DNA and RNA (NTPs and other IVT components elute in flow-through). In agreement with previously reported work on mRNA, a peak with CIMac PrimaS profile consistent with the DNA template or short RNA fragments was detected in the 0.4 M NaCl wash (pH 5.0). The tRNA eluted when the pH was increased to 7.5 (Figures 4A, B). However, the overall purity was lower than observed for gel-excised tRNA; residual RNA fragments could be detected in the elution fraction when separated on a PAGE gel, particularly at higher loadings (Figure 4C).

In order to remove low-level contamination of the elution fraction, the Swiper wash step could potentially be further optimized (e.g., wash salt concentration increased). However, this risked decreasing the recovery of pure tRNA in the elution fraction [modulating wash concentration of NaCl on PrimaS (Megušar et al., 2023)]. Instead, we explored tRNA binding to weak anion exchange column (CIM DEAE) to increase selectivity between DNA and tRNA by virtue of stronger anion exchange character compared to Swiper. A head-to-head comparison of Swiper and DEAE revealed that the impurities which bound to Swiper and were partially removed in the wash step (e.g., characteristic CIMac PrimaS peak with RT 1.4 min, Figures 5A, C), did not bind to DEAE (Figures 5B, D)

While recovery of the main elution fraction was higher for Swiper (>90%) than DEAE (85%) (Supplementary Table S3), DEAE resulted in higher purity, presumably due to its stronger anion exchange character which can exploit minor charge differences between tRNA and fragments for separation (Figures 5E, F). In particular, PAGE gel indicated high purity of DEAE E1, and detected RNA fragments in fractions E2 and E3. The purity of DEAE E1 was confirmed by IP-RP HPLC which detected a single peak at target molecular size. In contrast to DEAE E1 elution, Swiper E1 elution contained shorter fragments detectable by IP-RP (peak at RT 0.5 min) and a smear observed in PAGE gel (Figure 5E, F).

Finally, the linear gradient elution on DEAE was converted to a three-step elution based on the conductivities required for elution of each target fraction (48, 54 and 86 mS/cm for E1, E2 and E3, respectively, Figures 6A, B). Due to the large differences in conductivity required for elution of each fraction, the separation was easily converted to a step elution with predicted purity profiles. Application of a step elution approach using an HPLC system was successful; the main tRNA fraction, E2, was pure and free of RNA fragments and DNA template which were removed in fraction E3 (Figure 6C), consistent with previous reports on Mono Q which showed DNA template elution after tRNA (Koubek et al., 2013). Binding capacity was determined from breakthrough curve and from elution, both resulting in binding capacity of 3.1 mg/mL (Supplementary Figure S4).

To facilitate tRNA purification in the absence of a HPLC system, the step elution method was transferred to spin purification columns containing a DEAE monolith disc. Centrifugal force was used for convective mass transfer of the tRNA-containing sample through the monolith stationary phase housed in conical tubes. The main elution (E2) contained highly pure tRNA (Figures 6D–F) with 90% recovery, as determined by UV. This is important, because it significantly

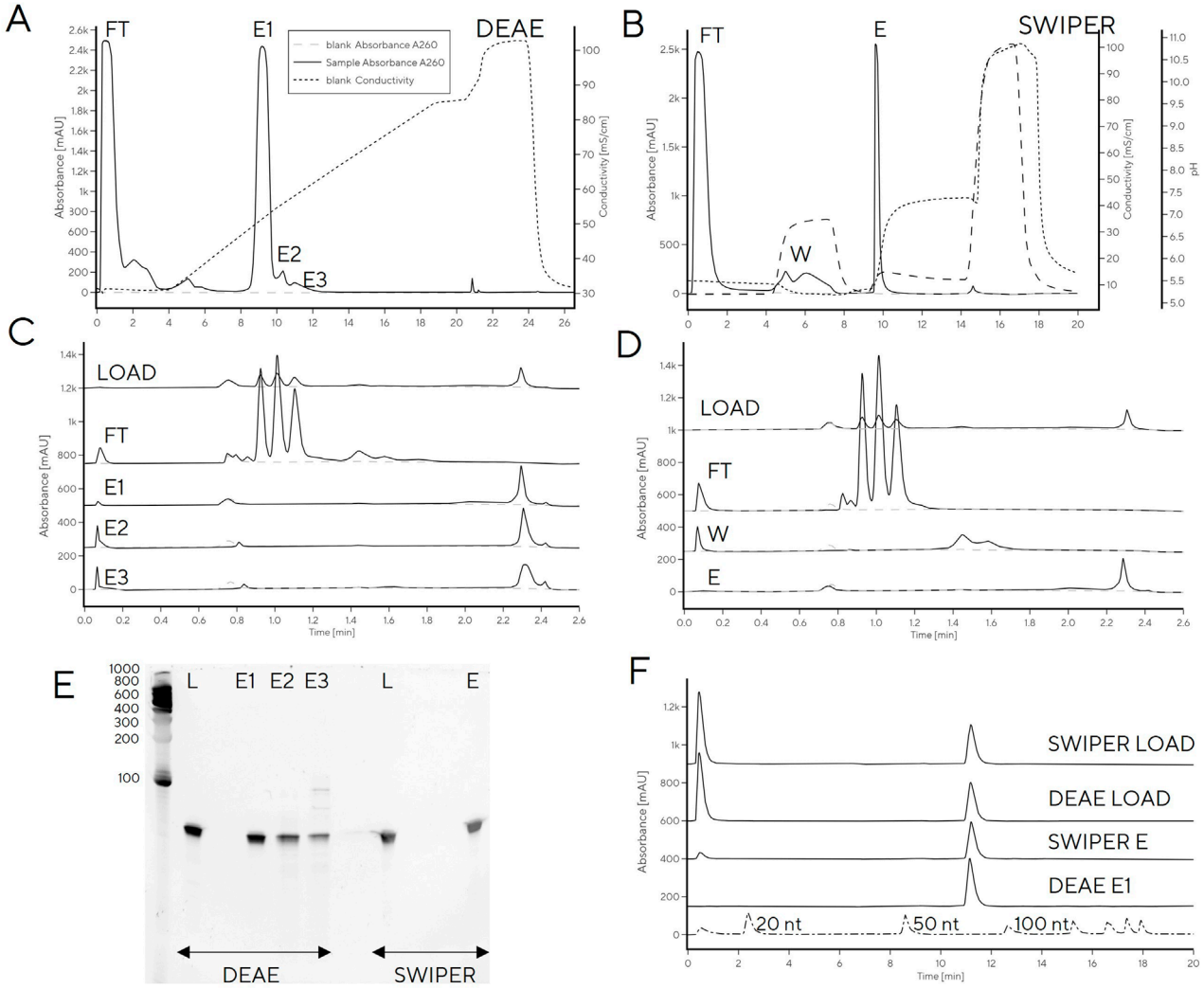

FIGURE 5
tRNA purification with **(A)** Swiper and **(B)** DEAE. CIMac PrimaS analytics of collected fractions from **(C)** Swiper: load, FT, Wash, Elution; and **(D)** Swiper: load, FT, E1, E2, and E3. **(E)** Fractions resolved on 10% TBE-Urea gel (left) and **(F)** IP-RP analysis of DEAE/Swiper elution fractions.

shortens the purification time required to obtain highly pure tRNA compared to traditional gel excision and avoids the need for using toxic denaturants (e.g., acrylamide in preparation of PAGE gels) without a loss in recovery.

Functional testing of synthetic tRNAs

tRNA constructs for all three tRNA tested (INI, ELO2 and ELO3) were all successfully synthesised using our optimized IVT protocol and purified with CIM DEAE using HPLC (Supplementary Figure S5). A second sample of INI was prepared and purified by SWIPER for comparison. Interestingly, DEAE elution peaks of ELO2 and ELO3, but not INI, contained a shoulder. These were identified as N+1/N+2 products by PAGE (Supplementary Figure S5D). Single nucleotide resolution of oligonucleotide mixtures has previously been shown on CIM DEAE (Podgornik et al., 1999), but not on construct sizes of >70 nucleotides, which we demonstrate here.

For use in codon reprogramming for mRNA display applications, it is necessary for the tRNA to be aminoacylated before addition to a cell-free translation system. One commonly used aminoacylation method is mediated by short RNA ribozymes called Flexizymes (Goto et al., 2011b; Murakami et al., 2003; Murakami et al., 2006; Niwa et al., 2009; Passioura and Suga, 2013). To demonstrate that the tRNA produced and purified under our optimised conditions could be aminoacylated and processed by the ribosome, we chose two unnatural amino acids to incorporate into a short peptide sequence. The initiator tRNA (INI) were loaded with *N*-biotinylated-L-phenylalanine, while the elongator tRNAs (ELO2, ELO3) were loaded with D-phenylalanine (Sako et al., 2008; Suga et al., 2011). By omitting methionine from the translation mixture and adding aminoacylated tRNAs, we were able to reprogram the initiator and elongator methionine codons to the noncanonical amino acids.

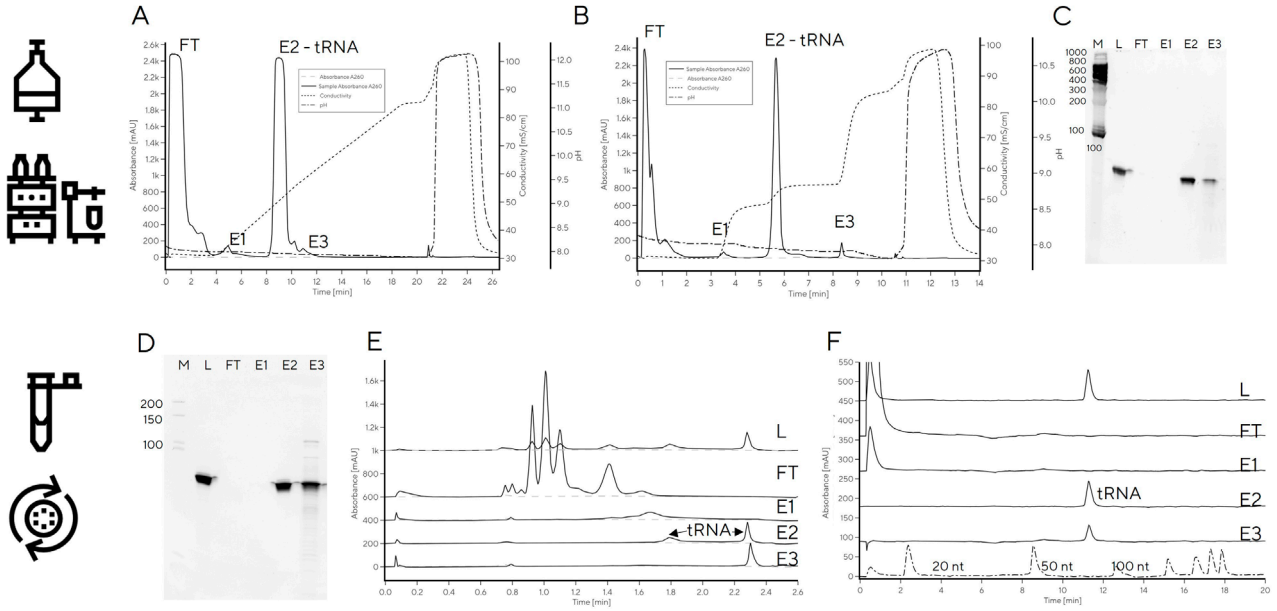

FIGURE 6
tRNA purification with step elution with CIM DEAE using HPLC **(A–C)** or centrifuge **(D–E)**. **(A)** Linear salt gradient elution of IVT mixture containing tRNA on CIM DEAE operated with HPLC; **(B)** step elution of IVT mixture containing tRNA on CIM DEAE operated with HPLC. **(C)** PAGE gel of step elution fractions FT, E1-E3. **(D)** PAGE gel of step elution fractions of IVT mixture containing tRNA on CIM DEAE operated with centrifuge. **(E)** CIMac PrimaS analytics of CIM DEAE spin column elution fractions (LOAD, FT, E1, E2, and E3). **(F)** RP-IP analysis of CIM DEAE spin column elution fractions.

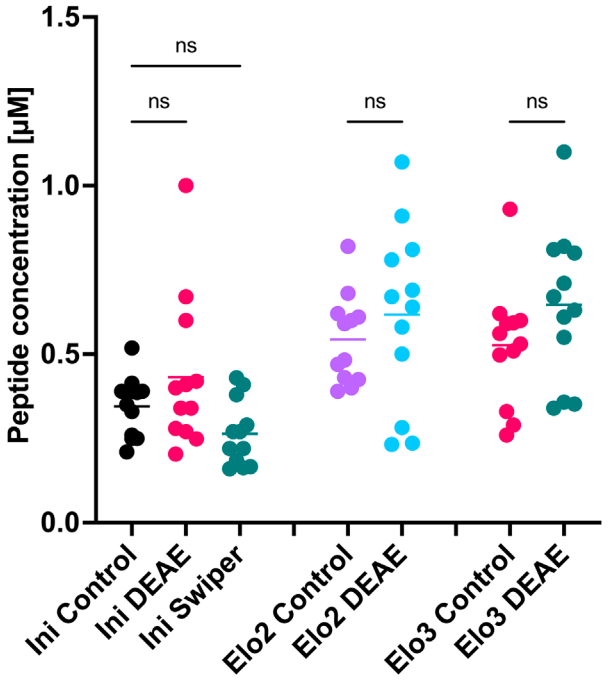

FIGURE 7
Comparison of tRNA aminoacylation and *in vitro* translation efficiencies. Assay performed as technical triplicates within independent triplicates. Ordinary one-way ANOVA followed by Šídák's multiple comparisons test was performed using GraphPad Prism version 10.2.3 for MacOS, GraphPad Software, Boston, Massachusetts USA, www.graphpad.com.

To compare the different batches of tRNA, we carried out cell-free *in vitro* translation of an mRNA template encoding a HiBit sequence. Translated peptides can be characterised through MALDI-TOF mass spectroscopy and quantified using a HiBit luminescence assay (Chan et al., 2023; Sato et al., 2022). MALDI-TOF MS confirmed that the correct sequence had been translated and the ribosome had incorporated the unnatural amino acids, loaded onto the tRNA, into the peptide sequence suggesting our synthetic tRNAs were functional (Supplementary Figure S6). Comparison of translation yields by HiBit assay showed no statistically significant variation in the yields from translations using tRNAs prepared by the different methods (Figure 7). This demonstrates that the tRNAs produced and purified through our optimised conditions can be aminoacylated and are functionally indistinguishable to the ribosome from those produced with GMP and purified on PAGE gel.

Conclusion

Through at-line HPLC monitoring of IVT reactions, we first optimized tRNA production method to achieve the highest reported tRNA yield (4.5 g/L), primarily by increasing GTP concentration which we showed to be the limiting factor. tRNA was produced in <4.5 h, while incubation overnight led to a minor increase in yield (10% for high-producing reactions). An efficient purification of tRNA was achieved with CIM DEAE, either coupled to a chromatography system operated in linear gradient or step elution mode or with a spin column, both achieving 90% recovery.

The whole process of production and purification of tRNA was shortened from approximately a day and a half to 6 h. tRNAs produced by the optimized IVT procedure were shown to be functionally indistinguishable from tRNA produced by a traditional method employing GMP in test *in vitro* translation reactions.

This study demonstrated how at-line HPLC monitoring can be used to monitor, and improve, production yields of IVT-derived tRNAs. Though the IVT monitoring approach is now widely used for mRNA applications, we show that adjustments in HPLC peak interpretation are required to apply the methodology to tRNA. With the advent of CRISPR-Cas technologies, which require both mRNA and guide RNAs of different lengths, the ability of at-line monitoring techniques to adapt to target RNA length will be of great importance. Furthermore, we show that multimodal purification optimized for mRNA and saRNA are applicable but surpassed in resolution and purity by traditional weak AEX monolith ligands (DEAE) with binding capacity comparable to mRNA (3 mg/mL). Due to a significantly lower overall negative charge of tRNA compared to mRNA due to shorter length, recovery from AEX is high while its high resolution is particularly useful for tRNA when separation of N+1/N+2 products is required. To our knowledge, this is the first reported use of spin columns for rapid isolation of tRNA, which can significantly ease efforts to produce tRNA for laboratory, pre-clinical and potentially clinical use. We foresee the use of this methodology for production of tRNA for *in vitro* translation studies, pre-clinical development of tRNA therapies, as well as for structural studies (NMR, X-ray, cryo-EM) of other short RNA molecules produced by IVT, including riboswitches, ribozymes and pre-micro RNAs.

Data availability statement

The raw data supporting the conclusions of this article will be made available by the authors, without undue reservation.

Author contributions

PM: Conceptualization, Data curation, Investigation, Visualization, Writing–original draft, Writing–review and editing. EC: Conceptualization, Data curation, Investigation, Methodology, Visualization, Writing–original draft, Writing–review and editing. TV: Data curation, Formal Analysis, Investigation, Writing–review and editing. SL: Formal Analysis, Methodology, Writing–review and editing. LW: Conceptualization, Project administration, Resources, Supervision, Writing–original draft, Writing–review and editing. RS: Conceptualization, Project administration, Resources, Supervision, Writing–original draft, Writing–review and editing.

Funding

The author(s) declare that financial support was received for the research, authorship, and/or publication of this article. This work was supported by funding from the UKRI [grant number EP/X020878/1 to LJW]. This work was also supported by the Francis Crick Institute which receives its core funding from Cancer Research UK (CC2030), the UK Medical Research Council (CC2030), and the Wellcome Trust (CC2030).

Conflict of interest

Authors PM, TV, SL, and RS were employed by Sartorius BIA Separations d.o.o.

The remaining authors declare that the research was conducted in the absence of any commercial or financial relationships that could be construed as a potential conflict of interest.

Publisher's note

Supplementary material

The Supplementary Material for this article can be found online at: https://www.frontiersin.org/articles/10.3389/fmolb.2024.1443917/full#supplementary-material

References

Albers, S., Allen, E. C., Bharti, N., Davyt, M., Joshi, D., Perez-Garcia, C. G., et al. (2023). Engineered tRNAs suppress nonsense mutations in cells and *in vivo*. *Nature* 618, 842–848. doi:10.1038/s41586-023-06133-1

Anastassiadis, T., and Köhrer, C. (2023). Ushering in the era of tRNA medicines. *J. Biol. Chem.* 299, 105246. doi:10.1016/j.jbc.2023.105246

Avcilar-Kucukgoze, I., Gamper, H., Hou, Y.-M., and Kashina, A. (2020). Purification and use of tRNA for enzymatic post-translational addition of amino acids to proteins. *Star. Protoc.* 1, 100207. doi:10.1016/j.xpro.2020.100207

Berg, M. D., and Brandl, C. J. (2021). Transfer RNAs: diversity in form and function. *RNA Biol.* 18, 316–339. doi:10.1080/15476286.2020.1809197

Cayama, E., Yépez, A., Rotondo, F., Bandeira, E., Ferreras, A. C., and Triana-Alonso, F. J. (2000). New chromatographic and biochemical strategies for quick preparative isolation of tRNA. *Nucleic Acids Res.* 28, e64. doi:10.1093/nar/28.12.e64

Chan, A. I., Sawant, M. S., Burdick, D. J., Tom, J., Song, A., and Cunningham, C. N. (2023). Evaluating translational efficiency of noncanonical amino acids to inform the design of druglike peptide libraries. *ACS Chem. Biol.* 18, 81–90. doi:10.1021/acschembio.2c00712

Coller, J., and Ignatova, Z. (2023). tRNA therapeutics for genetic diseases. *Nat. Rev. Drug Discov.* 23, 108–125. doi:10.1038/s41573-023-00829-9

Dunkak, K. S., Otto, M. R., and Beechem, J. M. (1996). Real-time fluorescence assay system for gene transcription: simultaneous observation of protein/DNA binding, localized DNA melting, and mRNA production. *Anal. Biochem.* 243, 234–244. doi:10.1006/abio.1996.0511

Easton, L. E., Shibata, Y., and Lukavsky, P. J. (2010). Rapid, nondenaturing RNA purification using weak anion-exchange fast performance liquid chromatography. *RNA* 16, 647–653. doi:10.1261/rna.1862210

Fechter, P., Rudinger, J., Giegé, R., and Théobald-Dietrich, A. (1998). Ribozyme processed tRNA transcripts with unfriendly internal promoter for T7 RNA polymerase: production and activity. *FEBS Lett.* 436, 99–103. doi:10.1016/s0014-5793(98)01096-5

Forster, A. C., Tan, Z., Nalam, M. N. L., Lin, H., Qu, H., Cornish, V. W., et al. (2003). Programming peptidomimetic syntheses by translating genetic codes designed *de novo*. *Proc. Natl. Acad. Sci.* 100, 6353–6357. doi:10.1073/pnas.1132122100

Goto, Y., Goto, Y., Katoh, T., and Suga, H. (2011a). *Preparation of materials for flexizyme reactions and genetic code reprogramming*. Protocol Exchange. Available at: https://experiments.springernature.com/articles/10.1038/nprot.2011.331.

Goto, Y., Katoh, T., and Suga, H. (2011b). Flexizymes for genetic code reprogramming. *Nat. Protoc.* 6, 779–790. doi:10.1038/nprot.2011.331

Guenther, R. H., Hara Gopal, D., and Agris, P. F. (1988). Purification of transfer RNA species by single-step ion-exchange high-performance liquid chromatography. *J. Chromatogr. A* 444, 79–87. doi:10.1016/s0021-9673(01)94010-5

Heckler, T. G., Chang, L. H., Zama, Y., Naka, T., and Hecht, S. M. (1984). Preparation of '2,('3)-O-Acyl-pCpA derivatives as substrates for T4 RNA ligase-mediated "chemical aminoacylation.". *Tetrahedron* 40, 87–94. doi:10.1016/0040-4020(84)85106-6

Höfer, K., Langejürgen, L. V., and Jäschke, A. (2013). Universal aptamer-based real-time monitoring of enzymatic RNA synthesis. *J. Am. Chem. Soc.* 135, 13692–13694. doi:10.1021/ja407142f

Huang, Y., Wiedmann, M. M., and Suga, H. (2019). RNA display methods for the discovery of bioactive macrocycles. *Chem. Rev.* 119, 10360–10391. doi:10.1021/acs.chemrev.8b00430

Iwane, Y., Kimura, H., Katoh, T., and Suga, H. (2021). Uniform affinity-tuning of N-methyl-aminoacyl-tRNAs to EF-Tu enhances their multiple incorporation. *Nucleic Acids Res.* 49, 10807–10817. doi:10.1093/nar/gkab288

Josephson, K., Hartman, M. C. T., and Szostak, J. W. (2005). Ribosomal synthesis of unnatural peptides. *J. Am. Chem. Soc.* 127, 11727–11735. doi:10.1021/ja0515809

Kartje, Z. J., Janis, H. I., Mukhopadhyay, S., and Gagnon, K. T. (2021). Revisiting T7 RNA polymerase transcription *in vitro* with the Broccoli RNA aptamer as a simplified real-time fluorescent reporter. *J. Biol. Chem.* 296, 100175. doi:10.1074/jbc.RA120.014553

Korenčić, D., Söll, D., and Ambrogelly, A. (2002). A one-step method for *in vitro* production of tRNA transcripts. *Nucleic Acids Res.* 30, e105. doi:10.1093/nar/gnf104

Koubek, J., Lin, K. F., Chen, Y. R., Cheng, R. P., and Huang, J. J. T. (2013). Strong anion-exchange fast performance liquid chromatography as a versatile tool for preparation and purification of RNA produced by *in vitro* transcription. *RNA* 19, 1449–1459. doi:10.1261/rna.038117.113

Lee, K. H., Song, J., Kim, S., Han, S. R., and Lee, S.-W. (2023). Real-time monitoring strategies for optimization of *in vitro* transcription and quality control of RNA. *Front. Mol. Biosci.* 10, 1229246. doi:10.3389/fmolb.2023.1229246

McCutchan, T. F., Gilham, P. T., and Söll, D. (1975). An improved method for the purification of tRNA by chromatography on dihydroxyboryl substituted cellulose. *Nucleic Acids Res.* 2, 853–864. doi:10.1093/nar/2.6.853

Megušar, P., Miklavčič, R., Korenč, M., Ličen, J., Vodopivec, T., Černigoj, U., et al. (2023). Scalable multimodal weak anion exchange chromatographic purification for stable mRNA drug substance. *ELECTROPHORESIS* 44, 1978–1988. doi:10.1002/elps.202300106

Mesters, J. R., Vorstenbosch, E. L. H., de Boer, A. J., and Kraal, B. (1994). Complete purification of tRNA, charged or modified with hydrophobic groups, by reversed-phase high-performance liquid chromatography on a C4/C18 column system. *J. Chromatogr. A* 679, 93–98. doi:10.1016/0021-9673(94)80314-5

Miklavčič, R., Megušar, P., Kodermac, Š. M., Bakalar, B., Dolenc, D., Sekirnik, R., et al. (2023). High recovery chromatographic purification of mRNA at room temperature and neutral pH. *Int. J. Mol. Sci.* 24, 14267. doi:10.3390/ijms241814267

Milligan, J. F., Groebe, D. R., Witherell, G. W., and Uhlenbeck, O. C. (1987). Oligoribonucleotide synthesis using T7 RNA polymerase and synthetic DNA templates. *Nucleic Acids Res.* 15, 8783–8798. doi:10.1093/nar/15.21.8783

Milligan, J. F., and Uhlenbeck, O. C. (1989). Synthesis of small RNAs using T7 RNA polymerase. *Methods Enzym.* 180, 51–62. doi:10.1016/0076-6879(89)80091-6Available at: https://www.sciencedirect.com/science/article/pii/0076687989800916.

Murakami, H., Ohta, A., Ashigai, H., and Suga, H. (2006). A highly flexible tRNA acylation method for non-natural polypeptide synthesis. *Nat. Methods* 3, 357–359. doi:10.1038/nmeth877

Murakami, H., Saito, H., and Suga, H. (2003). A versatile tRNA aminoacylation catalyst based on RNA. *Chem. and Biol.* 10, 655–662. doi:10.1016/s1074-5521(03)00145-5

Niwa, N., Yamagishi, Y., Murakami, H., and Suga, H. (2009). A flexizyme that selectively charges amino acids activated by a water-friendly leaving group. *Bioorg Med. Chem. Lett.* 19, 3892–3894. doi:10.1016/j.bmcl.2009.03.114

Ohta, A., Tanada, M., Shinohara, S., Morita, Y., Nakano, K., Yamagishi, Y., et al. (2023). Validation of a new methodology to create oral drugs beyond the rule of 5 for intracellular tough targets. *J. Am. Chem. Soc.* 145, 24035–24051. doi:10.1021/jacs.3c07145

Passioura, T., and Suga, H. (2013). Flexizyme-mediated genetic reprogramming as a tool for noncanonical peptide synthesis and drug discovery. *Chem. – A Eur. J.* 19, 6530–6536. doi:10.1002/chem.201300247

Perona, J. J., Swanson, R., Steitz, T. A., and Söll, D. (1988). Overproduction and purification of *Escherichia coli* tRNA(2Gln) and its use in crystallization of the glutaminyl-tRNA synthetase-tRNA(Gln) complex. *J. Mol. Biol.* 202, 121–126. doi:10.1016/0022-2836(88)90524-4

Pikovskaya, O., Serganov, A. A., Polonskaia, A., Serganov, A., and Patel, D. J. (2009). "Preparation and crystallization of riboswitch–ligand complexes," in *Riboswitches: methods and protocols*. Editor A. Serganov (Totowa, NJ: Humana Press), 115–128. doi:10.1007/978-1-59745-558-9_9

Podgornik, A., Barut, M., Jančar, J., and Štrancar, A. (1999). Isocratic separations on thin glycidyl methacrylate–ethylenedimethacrylate monoliths. *J. Chromatogr. A* 848, 51–60. doi:10.1016/s0021-9673(99)00472-0

Podgornik, A., Yamamoto, S., Peterka, M., and Krajnc, N. L. (2013). Fast separation of large biomolecules using short monolithic columns. *J. Chromatogr. B* 927, 80–89. doi:10.1016/j.jchromb.2013.02.004

Pregeljc, D., Skok, J., Vodopivec, T., Mencin, N., Krušič, A., Ličen, J., et al. (2023). Increasing yield of *in vitro* transcription reaction with at-line high pressure liquid chromatography monitoring. *Biotechnol. Bioeng.* 120, 737–747. doi:10.1002/bit.28299

Rosa, S. S., Prazeres, D. M. F., Azevedo, A. M., and Marques, M. P. C. (2021). mRNA vaccines manufacturing: challenges and bottlenecks. *Vaccine* 39, 2190–2200. doi:10.1016/j.vaccine.2021.03.038

Sako, Y., Morimoto, J., Murakami, H., and Suga, H. (2008). Ribosomal synthesis of bicyclic peptides via two orthogonal inter-side-chain reactions. *J. Am. Chem. Soc.* 130, 7232–7234. doi:10.1021/ja800953c

Sampson, J. R., and Uhlenbeck, O. C. (1998). Biochemical and physical characterization of an unmodified yeast phenylalanine transfer RNA transcribed *in vitro*. Available at: https://www.pnas.org/doi/10.1073/pnas.85.4.1033.

Sato, W., Rasmussen, M., Deich, C., Engelhart, A. E., and Adamala, K. P. (2022). Expanding luciferase reporter systems for cell-free protein expression. *Sci. Rep.* 12, 11489. doi:10.1038/s41598-022-15624-6

Sigal, M., Matsumoto, S., Beattie, A., Katoh, T., and Suga, H. (2024). Engineering tRNAs for the ribosomal translation of non-proteinogenic monomers. *Chem. Rev.* 124, 6444–6500. doi:10.1021/acs.chemrev.3c00894

Skok, J., Megušar, P., Vodopivec, T., Pregeljc, D., Mencin, N., Korenč, M., et al. (2022). Gram-scale mRNA production using a 250-mL single-use bioreactor. *Chem. Ing. Tech.* 94, 1928–1935. doi:10.1002/cite.202200133

Sprinzl, M., and Graeser, E. (1980). Role of the 5'-terminal phosphate of tRNA for its function during protein biosynthesis elongation cycle. *Nucleic Acids Res.* 8, 4737–4744. doi:10.1093/nar/8.20.4737

Suga, H., Hayashi, G., and Terasaka, N. (2011). The RNA origin of transfer RNA aminoacylation and beyond. *Philos. Trans. R. Soc. Lond B Biol. Sci.* 366, 2959–2964. doi:10.1098/rstb.2011.0137

Valentini, P., Pierattini, B., Zacco, E., Mangoni, D., Espinoza, S., Webster, N. A., et al. (2022). Towards SINEUP-based therapeutics: design of an *in vitro* synthesized SINEUP RNA. *Mol. Ther. Nucleic Acids* 27, 1092–1102. doi:10.1016/j.omtn.2022.01.021

Welbourne, E. N., Loveday, K. A., Nair, A., Nourafkan, E., Qu, J., Cook, K., et al. (2024). Anion exchange HPLC monitoring of mRNA *in vitro* transcription reactions to support mRNA manufacturing process development. *Front. Mol. Biosci.* 11, 1250833. doi:10.3389/fmolb.2024.1250833

Yamagishi, Y., Shoji, I., Miyagawa, S., Kawakami, T., Katoh, T., Goto, Y., et al. (2011). Natural product-like macrocyclic N-methyl-peptide inhibitors against a ubiquitin ligase uncovered from a ribosome-expressed *de novo* library. *Chem. Biol.* 18, 1562–1570. doi:10.1016/j.chembiol.2011.09.013

Yamamoto, S., Nakamura, M., Tarmann, C., and Jungbauer, A. (2007). Retention studies of DNA on anion-exchange monolith chromatography: binding site and elution behavior. *J. Chromatogr. A* 1144, 155–160. doi:10.1016/j.chroma.2007.01.025

Yamamoto, S., Yoshimoto, N., Tarmann, C., and Jungbauer, A. (2009). Binding site and elution behavior of DNA and other large biomolecules in monolithic anion-exchange chromatography. *J. Chromatogr. A* 1216, 2616–2620. 3rd Summer School on Monolith Technology for Biochromatography, Bioconversion and Solid-Phase Synthesis. doi:10.1016/j.chroma.2009.01.060

Yin, Y., and Carter, C. W., Jr (1996). Incomplete factorial and response surface methods in experimental design: yield optimization of tRNATrp from *in vitro* T7 RNA polymerase transcription. *Nucleic Acids Res.* 24, 1279–1286. doi:10.1093/nar/24.7.1279

Zhou, K. Z. Q., and Obexer, R. (2024). Non-canonical amino acids for engineering peptides and proteins with new functions. *Israel J. Chem.*, e202400006. doi:10.1002/ijch.202400006

10.3389/fmolb.2024.1443917

Glossary

Abbreviations

AGE	Agarose gel electrophoresis
BSA	Bovine serum albumin
BTP	Bis-tris propane
CAPS	N-cyclohexyl-3-aminopropanesulfonic acid
CIM	Convective Interaction Media
CIP	Cleaning-in-place
circRNA	Circular RNA
CMC	Chemistry, manufacturing and control
CoG	Cost of Goods
CV	Column volume
DS	Drug Substance
FLD	Fluorescence detection
FPLC	Fast protein liquid chromatography
Gu-HCl	Guanidine hydrochloride
HSW	High-salt wash
IVT	*in vitro* transcription
LNP	Lipid nanoparticles
mAb	Monoclonal antibody
MP	Mobile phase
mRNA	Messenger ribonucleic acid
MWCO	Molecular weight cut-off
NTP	Nucleotide triphosphate
Oligo dT	Oligo deoxythymidylic acid
polyA	Poly-adenine
pDNA	Plasmid DNA
RT	Retention time
saRNA	Self amplifying RNA
ssRNA	Single-stranded RNA
TFF	Tangential flow filtration
TEAA	Triethylammonium acetate

frontiers | Frontiers in Molecular Biosciences

TYPE Correction
PUBLISHED 22 October 2024
DOI 10.3389/fmolb.2024.1507191

OPEN ACCESS

EDITED AND REVIEWED BY
Alessio Branchini,
University of Ferrara, Italy

*CORRESPONDENCE
Louise J. Walport,
l.walport@imperial.ac.uk
Rok Sekirnik,
rok.sekirnik@biaseparations.com

†These authors have contributed equally to this work

RECEIVED 07 October 2024
ACCEPTED 14 October 2024
PUBLISHED 22 October 2024

CITATION
Megušar P, Calder EDD, Vodopivec Seravalli T, Lebar S, Walport LJ and Sekirnik R (2024) Corrigendum: HPLC for at-line reaction monitoring and purification improves yield and purity of tRNA.
Front. Mol. Biosci. 11:1507191.
doi: 10.3389/fmolb.2024.1507191

Corrigendum: HPLC for at-line reaction monitoring and purification improves yield and purity of tRNA

Polona Megušar[1†], Ewen D. D. Calder[2,3†], Tina Vodopivec Seravalli[1], Sergeja Lebar[1], Louise J. Walport[2,3*] and Rok Sekirnik[1*]

[1]Sartorius BIA Separations d.o.o., Ajdovščina, Slovenia, [2]Department of Chemistry, Molecular Sciences Research Hub, Imperial College London, London, United Kingdom, [3]Protein-Protein Interaction Laboratory, The Francis Crick Institute, London, United Kingdom

KEYWORDS

tRNA, *in vitro* transcription, HPLC, chromatography, anion exchange

A Corrigendum on
HPLC for at-line reaction monitoring and purification improves yield and purity of tRNA

by Megušar P, Calder EDD, Vodopivec Seravalli T, Lebar S, Walport LJ and Sekirnik R (2024). Front. Mol. Biosci. 11:1443917. doi: 10.3389/fmolb.2024.1443917

In the published article, there was an error. Incorrect chromatographic system supplier was named in the Methods section.

A correction has been made to **Materials and methods**, *Purification development*, Paragraph 1. This sentence previously stated:

"Chromatographic purification was performed on an HPLC system (Knauer, Berlin, DE) with four pumps and a multiwavelength UV-Vis detector (10 mm flow cell path length). Patfix software (Sartorius BIA Separations) was used for instrument control and data acquisition."

The corrected sentence appears below:

"Chromatographic purification was performed using PATfix system (Sartorius BIA Separations, Slovenia) equipped with quaternary pump and a multiwavelength UV-Vis detector (10 mm flow cell path length). PATfix 2.0 software (Sartorius BIA Separations) was used for instrument control and data acquisition."

The authors apologize for this error and state that this does not change the scientific conclusions of the article in any way. The original article has been updated.

Publisher's note

All claims expressed in this article are solely those of the authors and do not necessarily represent those of their affiliated organizations, or those of the publisher, the editors and the reviewers. Any product that may be evaluated in this article, or claim that may be made by its manufacturer, is not guaranteed or endorsed by the publisher.

frontiers | Frontiers in Molecular Biosciences

TYPE Review
PUBLISHED 21 November 2024
DOI 10.3389/fmolb.2024.1504876

OPEN ACCESS

EDITED BY
Xinli Liu,
University of Houston, United States

REVIEWED BY
Venkata Raman Kallakunta,
Bayer, United States
Na Xu,
Maastricht University, Netherlands

*CORRESPONDENCE
Zoltán Kis,
z.kis@sheffield.ac.uk

RECEIVED 01 October 2024
ACCEPTED 08 November 2024
PUBLISHED 21 November 2024

CITATION
Nair A and Kis Z (2024) Bacteriophage RNA polymerases: catalysts for mRNA vaccines and therapeutics.
Front. Mol. Biosci. 11:1504876.
doi: 10.3389/fmolb.2024.1504876

Bacteriophage RNA polymerases: catalysts for mRNA vaccines and therapeutics

Adithya Nair[1] and Zoltán Kis[1,2]*

[1]School of Chemical, Materials and Biological Engineering, University of Sheffield, Sheffield, United Kingdom, [2]Department of Chemical Engineering, Imperial College London, London, United Kingdom

Decades of research on bacteriophage-derived RNA polymerases (RNAPs) were vital for synthesizing mRNA using the *in vitro* transcription (IVT) reaction for vaccines during the COVID-19 pandemic. The future success of mRNA-based products relies on the efficiency of its manufacturing process. mRNA manufacturing is a platform technology that complements the quality by design (QbD) paradigm. We applied the QbD framework in combination with key mechanistic insights on RNAP to assess the impact of IVT-associated critical process parameters (CPPs) and critical material attributes (CMAs) on the critical quality attributes (CQAs) of the mRNA drug substance and on manufacturing key performance indicators (KPIs). We also summarize the structure-function relationship of T7 RNAP and its engineered mutants aimed at enhancing the critical production of low-immunogenic mRNA therapeutics. Alternatives to the current set of standard RNAPs in large-scale IVTs are also discussed based on a phylogenetic background. Finally, the review dives into the economic implications of improving mRNA manufacturing based on the main enzyme, T7 RNAP, used to synthesize the mRNA drug substance. The review concludes by mapping the relationship between various CMAs and CPPs with different phases of the IVT reaction from a QbD perspective.

KEYWORDS

bacteriophage RNA polymerase, T7 RNA polymerase, T7 RNA polymerase mutants, RNA polymerase engineering, *in vitro* transcription, mRNA vaccines and therapeutics, mRNA manufacturing, quality by design

1 Introduction

Bacteriophage-derived DNA-dependent RNA polymerases (RNAPs) have been instrumental in cell-free *in vitro* synthesis of RNA. These polymerases play a central role in the *in vitro* transcription reaction (IVT), enabling the production of RNA vaccines and therapeutics from nanograms to the kilogram scale (Krieg and Melton, 1984; Milligan et al., 1987; Yisraeli and Melton, 1989; Dias et al., 2018; Skok et al., 2022a). The transition of phage polymerases from an enzyme for producing small-scale RNA for research purposes to a significant component in the large-scale manufacturing of mRNA vaccines and therapeutics occurred during the COVID-19 pandemic (Kis et al., 2020b; Kis et al., 2020a; Szabó et al., 2022). The synthesis of all regulatory-approved mRNA vaccines utilized the IVT reaction that used the bacteriophage T7-derived RNA polymerase. This transformative mRNA platform technology is advancing the development of a rapidly growing number (already in hundreds) of vaccines and therapeutics against a

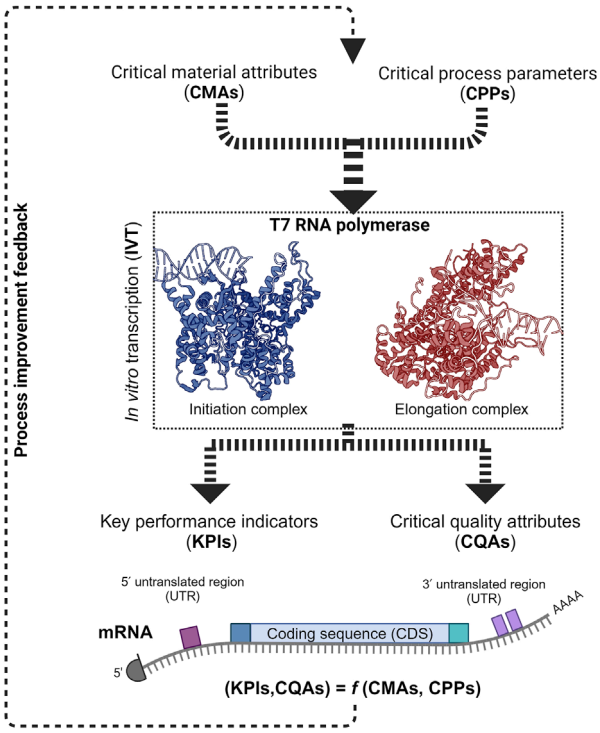

GRAPHICAL ABSTRACT

wide range of diseases, including infectious diseases, cancers, immune disorders, rare diseases, cardiovascular diseases and much more (Kumar et al., 2022; Qin et al., 2022; Whitley et al., 2022). Apart from the conventional type of non-replicating mRNA (used in both the approved SARS-CoV2 vaccines), there is significant interest in developing vaccines and therapeutics based on self-amplifying mRNA (saRNA) and circular mRNA (circRNA) (Bloom et al., 2020; Pisignano et al., 2023; Qi et al., 2023; Jones et al., 2024). Next-generation products based on saRNA and circRNA promise lower dosage, better stability, and longer duration *in vivo* expression. saRNA codes for a viral RNA-dependent RNA polymerase (usually derived from alphaviruses) along with the gene of interest; this coded polymerase is responsible for the *in vivo* amplification of the drug substance (Comes et al., 2023). circRNA forms covalently closed loop structures compared to linear RNA, which are resistant to exoribonuclease digestion and provide better stability (Greene et al., 2017; Bai et al., 2023). Regardless of the type of mRNA, IVT is the choice of synthesis, and bacteriophage-derived RNA polymerases remain the enzymes used for this polymerization reaction.

1.1 Discovery and early application

The history of the IVT reaction that enables large-scale mRNA synthesis is intertwined with the discovery and characterization of RNAPs. The discovery of mRNA as the intermediary between DNA and protein in the late 1950s to early 1960s prompted the search for the enzyme responsible for mRNA synthesis. This, in turn, led to the discovery of mammalian/bacterial RNAPs in the 1960s and bacteriophage RNAPs later in the 1970s (Weiss and Gladstone, 1959; Hurwitz et al., 1960; Stevens, 1960; Chamberlin et al., 1970; Hurwitz, 2005). The single-subunit RNAPs (ss-RNAPs) from bacteriophages T7, T3, and SP6 were among the first to be discovered, isolated, characterized and synthesized (Chamberlin et al., 1970; Gelfand and Hayashi, 1970; Dunn et al., 1971; Chakraborty et al., 1973; Niles et al., 1974; Butler and Chamberlin, 1982; Kassavetis et al., 1982; Davanloo et al., 1984; Morris et al., 1986; Kotani et al., 1987). RNAPs from T-odd phages (T7 and T3) were the first to be extensively investigated due to research on phage-infected bacteria and their associated gene expression (Summers and Siegel, 1970; Lillehaug et al., 1973; Dunn et al., 1977). These phage polymerases, their corresponding interactions with their specific promoters, and the IVT reaction parameters were studied throughout the 1970s (Dunn et al., 1971; Chamberlin and Ring, 1973a; Bautz et al., 1974; Oakley et al., 1975; Oakley and Coleman, 1977). The extensive research on these phage RNAPs led to the development of an efficient expression system (Davanloo et al., 1984; Moffatt et al., 1984; Tabor and Richardson, 1985; Studier and Moffatt, 1986) and subsequent large-scale *in vitro* mRNA synthesis. Different phases within the IVT reaction are shown in Figure 1.

Early sequence elucidation of the T7 RNAP, its promoters, and the development of T7-based expression systems made it the gold standard for the current *in vitro* industrial scale production of mRNA and *in vivo* gene expression systems. Even after sharing similarities with the T3 RNAP (83% amino acid sequence similarity), early adoption, high promoter specificity and processivity led to T7 being preferred over other homologous

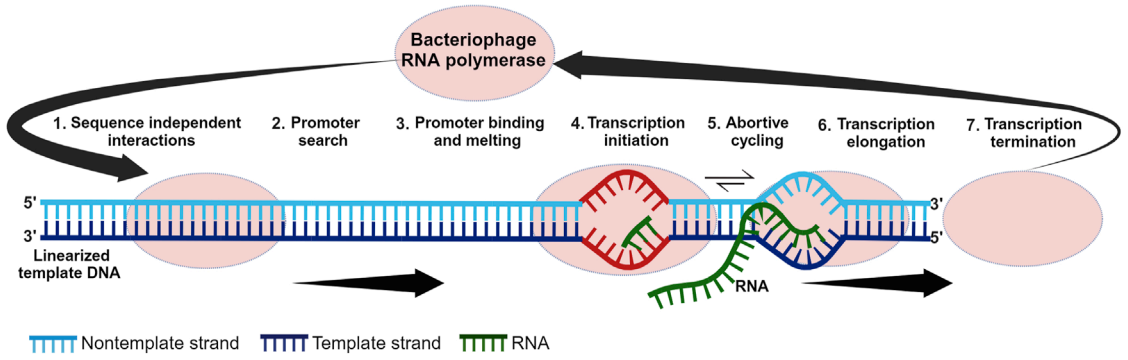

FIGURE 1
Different phases within the *in vitro* transcription reaction. In step one, the polymerase scans the template DNA for the promoter sequence. Once the promoter is found, it is melted in step three. Transcription is initiated in step four and this is followed by abortive cycling in step five. Promoter escape and transition to elongation occur in step six which is followed by termination in step seven.

phage polymerases (T3 and SP6) (Eun, 1996). Moreover, for *in vitro* applications with high ribonucleotide (rNTP) concentrations (>20 mM), T7 has proven much more effective than SP6 RNAP (CustomBiotech, 2023). Surprisingly, it was an SP6 RNAP-based IVT (Krieg and Melton, 1984), credited with being first used for synthesizing large quantities of eukaryotic mRNA. Structural and phylogenetic analysis have shown the extensively used T7, T3 and SP6 RNAPs to be related to each other along with other bacteriophage and mitochondrial RNAPs (nuclear gene-encoded and linear mitochondrial plasmid-encoded RNAPs) (Joho et al., 1990; Klement et al., 1990; Jorgensen et al., 1991; McAllister and Raskin, 1993; Cermakian et al., 1997). Similar to the RNAPs, their associated promoters have conserved sequences, suggesting an evolutionary relationship. A timeline of significant events, from the discovery of the first bacteriophage-derived RNAPs to their current large-scale application, is given in Figure 2.

1.2 Single-subunit vs. multi-subunit RNAPs

ss-RNAPs are recognized for their structural simplicity, high promoter specificity, and processivity; these properties have made the bacteriophage RNAPs the ideal choice for various research and manufacturing-related applications. Multi-subunit RNAPs (ms-RNAPs), found in eukaryotes, bacteria, archaea, and some viruses, in contrast, are structurally complex (consists of catalytic subunit aided by several accessory subunits) and have lower processivity compared to ss-RNAPs (Chamberlin and Ryan, 1982; Eun, 1996; Sousa and Mukherjee, 2003). Additionally, these ms-RNAPs require specific transcription factors for their function. *Escherichia coli* RNAP (a well-characterized ms-RNAP) consists of 5 subunits (α_2 $\beta\beta'\omega$) and additional transcription factors (σ), and this complex is around four times bigger than the common ss-RNAPs (T7, T3 and SP6). The multi-subunit bacterial RNAPs are less complex than their eukaryotic counterparts; unlike bacterial RNAPs, there is a broader diversity within the eukaryotic RNAPs used for the synthesis of different types of RNAs (Chamberlin, 1974; Helmann and Chamberlin, 1988; Saltzman and Weinmann, 1989; Horwitz and Loeb, 1990; Woychik and Young, 1990; Eun, 1996).

The eukaryotic RNAPs tend to have more subunits (10–14 subunits for RNAP II) compared to bacterial RNAPs and are 5–7 times bigger than the previously mentioned phage polymerases. Regarding transcription rate, the single-subunit RNAPs are faster, usually 100–200 nucleotide/second (nt/sec) than the multi-subunit RNAPs (usually around 20–50 nt/s) (Eun, 1996; Sousa and Mukherjee, 2003). Furthermore, the promoters for single-subunit RNAPs also tend to be a single continuous block of sequences, unlike those for multi-subunit RNAPs, which tend to have multiple regulatory elements. A disadvantage of the structural and functional simplicity associated with single-subunit RNAPs is reflected in its lack of proofreading mechanisms, which is not observed among its muti-subunit counterparts (Sydow and Cramer, 2009). An interesting difference between single-subunit and multi-subunit RNAPs pertains to the latter's sensitivity towards antibiotics such as rifamycins (binds to β subunit, prevents transcription elongation) and fidaxomycins (inhibits transcription initiation), making bacterial RNAPs an ideal drug target. Antibiotics that specifically target eukaryotic RNAPs were also screened based on this logic, anti-cancer drug α-amanitin targets RNAP II by preventing translocation of the enzyme and disrupting nucleotide addition in the elongation phase (Chamberlin and Ring, 1972; Chamberlin and Ring, 1973b; Küpper et al., 1973; Ma et al., 2016; Mosaei and Harbottle, 2019; Kirsch et al., 2022). Sensitivity to elevated concentrations of salts is also another difference between single-subunit and multi-subunit RNAPs; while the activity of the former is inhibited, the latter is stimulated/tolerant in the presence of excess salt concentrations (Chamberlin and Ring, 1973b).

1.3 Elucidation of transcription mechanisms

Once the amino acid and nucleotide sequences (Moffatt et al., 1984; Mcgraw et al., 1985; Kotani et al., 1987; Dietz et al., 1990) of bacteriophage-related RNAPs were deciphered, these enzymes were overexpressed (Davanloo et al., 1984; Morris et al., 1986) and used extensively in *in vitro* studies to reveal the various mechanistic properties of the transcription reaction. Early studies

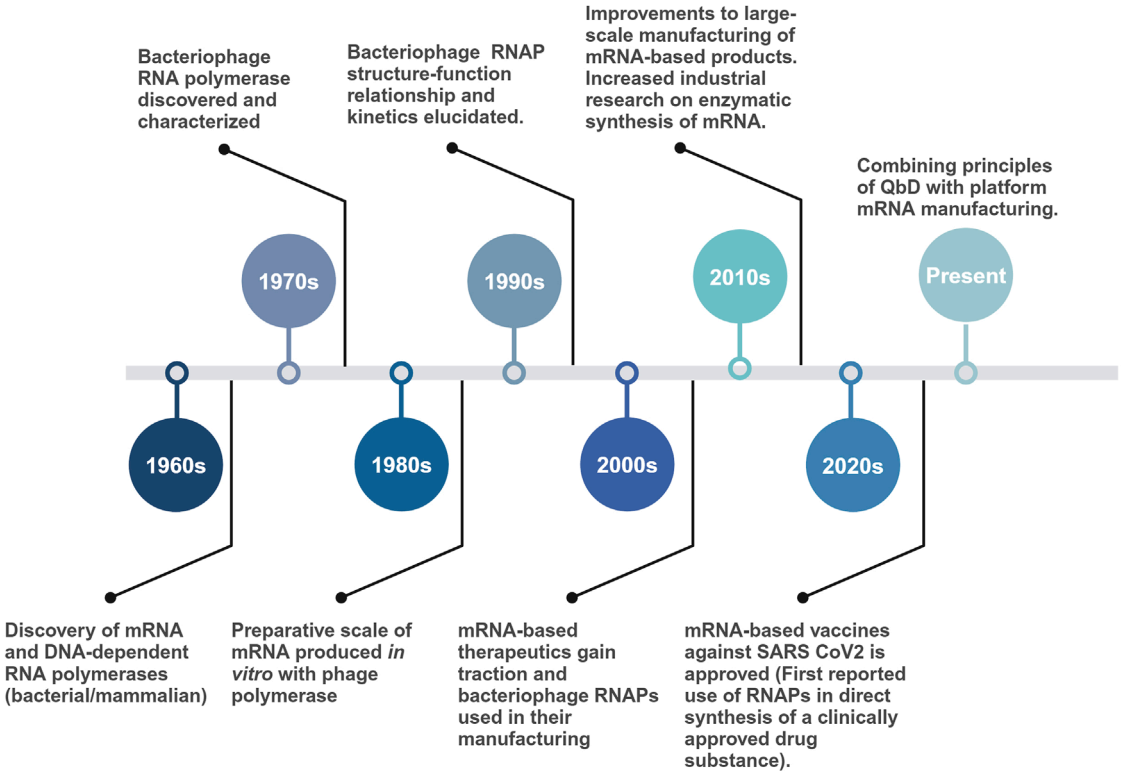

FIGURE 2
Timeline of major events starting with the discovery of bacteriophage-derived RNAPs to their use in large-scale production of mRNA-based vaccine drug substance. More than five decades of fundamental research on single-subunit RNAPs enabled the rapid manufacturing of mRNA-based vaccines during the COVID-19 pandemic.

gave insights into promoter binding, initial template melting and transcription initiation (Bautz et al., 1974; Oakley et al., 1975; Oakley et al., 1979; Bishayee et al., 1976; Martin and Coleman, 1987; Muller et al., 1988). Reaction kinetics were studied to elucidate binding affinity and subsequent reaction rate with Michaelis constant (K_m) for enzyme-promoter binding in the presence of different ions, the initiating nucleotide and subsequent nucleotides (Martin and Coleman, 1987; Martin et al., 1988; Maslak and Martin, 1994). Structure-function studies revealed the role of various domains of the enzyme and their interactions with i) template DNA (based on DNA footprinting studies), ii) the ribonucleotides, iii) the divalent metal ion co-factor (Mg^{2+}), iv) nascent RNA, v) RNA-DNA hybrid (within the transcription bubble), vi) growing single-stranded RNA and vii) terminator sequences (Oakley et al., 1975; Ikeda and Richardson, 1986a; Muller et al., 1988; Muller et al., 1989; Basu et al., 1989; Martin and Coleman, 1989). The difference between the initiation complex (IC) and elongation complex (EC) was elucidated, and the processivity of the RNAP in the elongation phase was determined (Martin et al., 1988; Muller et al., 1988). The structure-function analysis also identified which domains of the enzyme were responsible for the major events in each phase during the transcription reaction (Sousa, 1996; Sousa, 1997; Brieba and Sousa, 2000; Brieba and Sousa, 2001; Yin and Steitz, 2002). Moreover, the stoichiometry of the IVT reaction was improved based on the mechanistic and structure-function studies (Maslak and Martin, 1994). These early works also revealed the drawbacks of phage RNAP-assisted IVT reactions. Several product-related impurities, including but not limited to short abortive transcripts, "run-on"/"read-through" transcripts, and double-stranded RNA (dsRNA), were discovered (Milligan et al., 1987; Krupp, 1988; Triana-Alonso et al., 1995). The exact mechanism of generating some of these byproducts (abortive transcripts, dsRNA) has been deciphered, but ambiguity remains for impurities such as run-on transcripts.

1.4 T7 RNAP (the mRNA vaccine production gold standard)

T7 bacteriophage-derived RNAP is most often used for *in vitro* synthesis of mRNA-based products; this enzyme has practically served as a model for understanding single-subunit RNAPs as well as the transcription reaction in general (McAllister, 1993; Eun, 1996; Yin and Steitz, 2002; Sousa, 2013). T7 RNAP has been successful in its industrial applications, and extensive knowledge of its structure and structure-function relationship has made it the ideal candidate for IVT optimization. The enzyme characterization began shortly after its discovery in the 1970s (Chamberlin and Ring, 1973a); studies on T7 RNAP inhibition and its interactions with the T7 promoter were among the initial findings (Chamberlin and Ring, 1973b; Chamberlin and Ryan, 1982). Elucidation of the T7

RNAP transcription mechanism began with studies on promoter binding and transcription initiation; the interactions between T7 RNAP and its corresponding Class II and III promoters were also studied (this helped optimize IVT parameters such as ionic strength and reaction temperature) (Mcallister and Carter, 1980; Carter and McAllister, 1981). The structural simplicity of the T7 RNAP was also responsible for its extensive use in studying the transition of RNAPs from initiation to elongation complex (Jia and Patel, 1997; Yin and Steitz, 2002; Skinner et al., 2004; Tang et al., 2009; Koh et al., 2018). Sequence-dependent and independent transcription termination mechanisms were also elucidated to give a better mechanistic understanding of transcription (Macdonald et al., 1994; Lyakhov et al., 1998). Decades of structural studies from the late 1980s revealed the 3D structure and the structure-function properties of T7 RNAP. The enzyme is broadly split into its amino-terminal domain (N-terminal domain, NTD) and carboxyl-terminal domain (C-terminal domain, CTD); the latter is further divided into "fingers," "palm," and "thumb" subdomains (Sousa, 1996; Sousa, 1997; Cheetham et al., 1999; Yin and Steitz, 2002; Yin and Steitz, 2004). CTD is the main polymerase domain of the enzyme, and the function of each subdomain has been elucidated with structure-function studies. Moreover, these studies have also been used for phylogenetic analysis to reveal homology with closely related RNAPs and structural similarities with distantly related RNAPs, pointing to the convergent evolution of RNAPs. The NTD is among the "accessory" modules along with the promoter recognition loop (inserted within the CTD), the C-terminal loop, and the 4-helix bundle (Sousa and Mukherjee, 2003; Sousa, 2013). T7 RNAPs were also subjected to extensive kinetic studies; although these were initially done to understand the different mechanisms involved in the transcription reaction, the insights derived from these studies lay the foundation for large-scale synthesis of *in vitro* transcribed mRNA (Young et al., 1997; Rosa et al., 2022; Samnuan et al., 2022). Various computation models simulating the IVT reaction resulted from these extensive studies on T7 RNAP-enabled IVT reaction (Akama et al., 2012; van de Berg et al., 2021; Stover et al., 2024). T7 RNAP structure in the IC is shown in Figure 3.

1.5 Drawbacks associated with phage RNAPs

As mentioned, the product-related impurities generated during the IVT reaction can be traced back to specific RNAP mechanisms. Once mRNA-based vaccines and therapeutics gained traction, these impurities and their impact on patient safety were scrutinized (Mu et al., 2018; Lenk et al., 2024). Even though these impurities can be removed with various downstream purification techniques, the associated costs pose a significant hurdle (Kis et al., 2020a). RNAPs during IVT produce impurities such as dsRNA, abortive transcripts (product of abortive cycling), and run-on transcripts. Additionally, the mRNA-based products may require the incorporation of modified nucleotides into the transcript; this could lower the activity of wild-type RNAPs used to synthesize the drug substance (Nelson et al., 2020; Chen et al., 2022). The single-subunit RNAPs also lack the capabilities of 5′ modifications (5′ cap); this is offset by either post-transcriptional capping or co-transcriptional capping using cap analogs such as ARCA (dinucleotide) or CleanCap® (GAG trinucleotides) (Hogrefe et al., 2017; Roy and Ong, 2021). Post-transcriptional enzymatic capping is an effective method but requires additional purification after the initial synthesis and an additional enzymatic reaction. There is ongoing work to optimize a "co-transcriptional" one-pot IVT and enzymatic capping reaction (Nwokeoji et al., 2023), including the use of fusion proteins between the T7 RNAP and capping enzymes. Co-transcriptional analog-based capping is hindered by the lower capping efficiency seen in the case of ARCA or cost burdens due to proprietary CleanCap® technology. Regardless, a one-step synthesis stage can be more attractive in terms of process productivity and manufacturing costs (Wang et al., 2017; Chan et al., 2023). The limitations of bacteriophage-derived RNAPs in the context of product-related impurities have led to the development of solutions that include mutant T7 RNAPs and RNAPs derived from less commonly used bacteriophages. A summary of such mutants and alternative RNAPs is given in Tables 1, 2, respectively. These solutions claim to reduce the generation of product-related impurities and improve the quality of the drug substance at the synthesis stage. However, thorough analysis and validation is required before they can replace the current standard RNAPs.

1.6 Mutant T7 RNAPs

As T7 RNAP was characterized extensively, its structure and structure-related functions were modified to make mutant RNAPs with a reduced product-related impurity footprint. The wild-type T7 RNAP also has limited capabilities in synthesizing transcripts containing modified nucleotides. These substrate modifications could include 2′ modified ribose, base modifications (Ψ Uridine, N1-methyl-Psuedouridine) or 5′ cap analogs (ARCA, GAG) (Siegmund et al., 2012; Meyer et al., 2015; Chen et al., 2022; Miller et al., 2024). Modifications to amino acid sequence in the T7 RNAP finger subdomain, responsible for interactions with the substrate, are widely employed for incorporating substrates other than wild-type ribonucleotides. The palm subdomain is also modified to incorporate alternative substrates. A solution to reduce the synthesis of immunogenic dsRNA is the use of RNAPs at higher reaction temperatures (>45°C) (Wu et al., 2020; Wu et al., 2021; Roy and Robb, 2022). This was achieved with modifications to the amino acid sequence throughout the T7 RNAP; in most cases, the CTD was modified. Apart from thermostability, properties such as structural stability were also considered, such that the enzymes do not form homodimers and reduce the overall enzymatic activity. Modifications to NTD, specifically the linker between NTD and CTD, have been targeted to make mutant T7 RNAPs that generate fewer abortive transcripts by facilitating an easier transition to EC from the IC (Wu et al., 2021; Dousis et al., 2023; Rabideau et al., 2019). The C-helix within the NTD is also targeted to achieve the same IC to EC transition. Additions to the end of CTD were previously observed to be detrimental to the enzyme's function (Mookhtiar et al., 1991; Gardner et al., 1997), but newer studies have found CTD insertional mutants to be functional and effective in the reduction of run-on transcripts (Dousis et al., 2023).

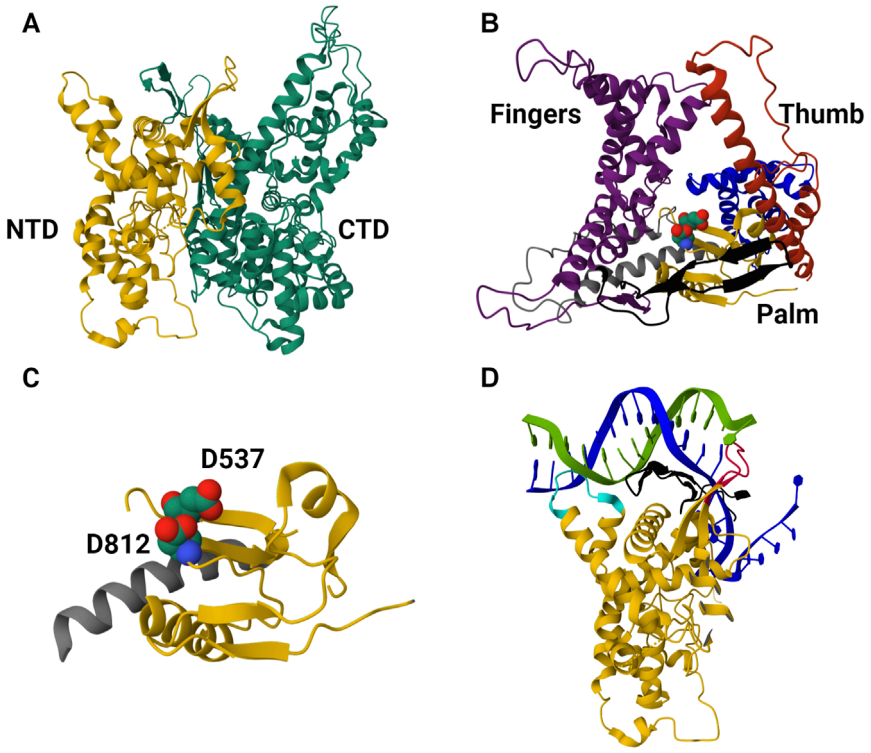

FIGURE 3
The 3D protein structure of the T7 RNAP in the initiation complex. **(A)** Structure of T7 RNAP in the initiation complex (IC) derived from PDB-1QLN. It is divided into the N-terminal domain (NTD, colored in yellow) and the C-terminal domain (CTD, colored in green). NTD amino acid residues range from 1 to 312, while CTD ranges from 313 to 883. **(B)** Structure of the CTD. The CTD is the catalytic domain (structured like a cupped right hand) of the enzyme with three subdomains, namely, i) "fingers" (colored purple, residues 541 to 737 and 771–778), ii) "palm" (colored yellow, residues 411 to 448, 532 to 540 and 788–838) and iii) "thumb" (colored red, residues 330–410). **(C)** The palm subdomain of the CTD. Residues D537 and D812 in space-filling representation (close to the C-terminal loop). These residues coordinate with the co-factor (Mg^{2+}) and facilitate phosphodiester bond formation between ribonucleotides. **(D)** The NTD binding to the promoter region of the template DNA. The NTD and promoter recognition loop bind to the promoter region of the double-stranded template DNA and open it up to start transcription initiation. Positively charged residues from 91 to 103 within the NTD (colored cyan) interact with the minor groove of the promoter (from –17 to –13 bp). An intercalating loop (colored red) formed by residues 232 to 242 opens the DNA duplex and stabilizes the upstream edge of the bubble. The promoter recognition loop formed by residues 739 to 770 (colored black, antiparallel β ribbon) interacts with the major groove in a sequence-specific manner.

1.7 Alternatives to T7 RNAP

Apart from modifications to the well-characterized bacteriophage RNAPs, other lesser-known phage RNAPs and modified DNA polymerases are also being considered for industrial-scale production of mRNA. These RNAPs are assumed to provide certain advantages over the current industry standards by producing fewer product-related impurities. Most of these belong to the *Autographiviridae* family of viruses (Zhu et al., 2014; Lu et al., 2019; Xu et al., 2020; Xia et al., 2022; Streit et al., 2023; Curry et al., 2024). The search for alternative phage RNAPs other than T7, T3, SP6 and K11 for IVT is reflected in the increasing number of research articles and patent applications (summarized in Table 2); although these new RNAPs are touted as a solution to the current standards, their extensive characterization and effectiveness is yet to be established. Similar to the development of mutant T7 RNAPs, mutants of these new alternative RNAPs are also being explored for improved activity and wider substrate type utilization (Zhu et al., 2015). Mutated DNAPs from extremophiles (e.g., *Thermococcus gorgonarius*) are also reported to be helpful in the synthesis of mRNA using IVT, especially at elevated incubation temperatures (>45°C) (Wang et al., 2017).

1.8 IVT improvement strategies

Immobilized RNAP and template DNA in an IVT reaction are also explored to reduce the synthesis of product-related impurities. The proximity of RNAP and template DNA, along with IVT process parameters such as high ionic strength, is used to reduce the rebinding of RNAP onto the synthesized mRNA, thus mitigating the RNA-dependent RNA polymerase activity (Cavac et al., 2021; MalagodaPathiranage et al., 2023). Immobilized RNAPs, commonly done with streptavidin, have been previously employed for single-molecule analysis to elucidate the transcription kinetics (Skinner et al., 2004). Apart from the benefits of reducing product-related impurities, immobilization also helps reduce manufacturing costs by potentially aiding the reuse of the RNAP (Malag et al., 2024). Raw materials for mRNA synthesis are the highest manufacturing cost contributors; a significant

TABLE 1 List of T7 RNAP mutants and their improved functions.

Source	Type of modification	Residue location	Domain position	Application
Ikeda (1995)	Substitution	E222K	NTD	Modified promoter recognition
Sousa and Jendrisak (2000)	Substitution	Y639F	Fingers	2′-fluoro-nucleoside incorporation
Sugiyama et al. (2009)	Substitution	S430P, N433T, S633P, F849I, F880Y	Fingers, Palm	Thermostability
Padilla and Sousa (2002)	Substitution	Y639F, H784A	Fingers, Palm	2′-fluoro-nucleoside incorporation
Chelliserrykattil and Ellington (2004)	Substitution	E593G, Y639V, V685A, H784G	Fingers, Palm	2′-O-methyl-nucleoside incorporation
Chelliserrykattil and Ellington (2004)	Substitution	G542V, H772R, H784S	Fingers, Palm	2′-fluoro-nucleoside incorporation
Guilleres et al. (2005), Guilleres et al. (2004)	Substitution	P266L	NTD	Reduced 8 nt abortive transcription
Siegmund et al. (2012)	Substitution	I119V, G225S, K333N, D366N, F400L, Y639V, S661G, H784G, F880Y	NTD, Fingers, Palm, Thumb	2-Se-methyl-UTP and 2′-O-methyl-UTP incorporation
Brakmann and Ibach (2015)	Substitution	R425C	Palm	2′-O-methyl-nucleoside incorporation
Meyer et al. (2015)	Substitution	S430P, N433T, E593G, S633P, Y639V, V685A, H784G, F849I, F880Y	Fingers, Palm	2′-modified-nucleoside incorporation, improved activity
Ellington and Meyer (2018)	Substitution	S430P, N433T, G542V, S633P, H772R, H784S, F849I, F880Y	Fingers, Palm	2′-modified-nucleoside incorporation
Sobek et al. (2016)	Substitution	V426L, A702V, V795I	Fingers, Palm	Thermostability
Greif et al. (2017)	Substitution	C723S	Fingers	Stability (reduced homodimers)
Martin and Ramirez-Tapia (2015)	Insertion	G-ins-E252, G-ins-G259, G-ins-P266	NTD	Reduced abortive transcripts
Ong et al. (2019)	Substitution	T75Q, A83K, I109L, H205S, K206P, I281P, A327P, T375K, D388E, L446F, C510Q, L534V, V567P, G618Q, K642R, M832F, D834E, S856T, A863P, A866K	NTD, Fingers, Palm, Thumb	Thermostability
Jain (2021)	Substitution	I320L, I396L, F546W, S684A, G788A	Fingers, Palm, Thumb	Thermostability, reduced dsRNA
Miller et al. (2022)	Substitution	P664W	Fingers	Cap analog incorporation
Thompson et al. (2022)	Substitution	P266L, K378R, S430P, N433T, S633P, Y639L, H784A, F849I, F880Y	NTD, Fingers, Palm, Thumb	2′-modified-nucleoside incorporation, thermostability
Oe et al. (2013)	Substitution	K179, V685A, Q768	NTD, Fingers	Thermostability
Rabideau et al. (2019)	Insertion, Substitution	S43A, G47A, R257A G-ins-844	NTD, C-terminal	Reduced dsRNA
Wu et al. (2021)	Substitution	S43Y	NTD	Reduced dsRNA

TABLE 2 List of commonly used and alternative bacteriophage RNAPs.

Source	Name	Promoter	Total number of amino acid residues	Genbank accession number
Xu et al. (2020)	*Yersinia* phage phiR8-01	TCGACCCTATTAAAC	810	CCI88411.2
	Aeromonas phage phiAS7	TTGATTCGGTACGCCTAA	816	YP_007007815.1
	Caulobacter phage Percy	ACATTCTCGCTACACCAA	805	YP_009225265.1
	Burkholderia phage Bp AMP4	TTTCGGTCGCCTTACCGACAC	831	CDL65264.1
	Pseudomonas phage Andromeda	CCACTATAGCAACA	803	YP_009279548.1
	Proteus phage vB_PmiP Pm5460	TAATTAGAGACCACTATA	875	YP_009209198.1
	Delftia phage IME-DE1	GTTAGCCCACACCATT	859	YP_009191807.1
	Vibrio phage N4	AATTAACCCACACTATA	883	YP_003347903.1
	Morganella phage vB_MmoP MP2	ACATTTGTGGCACTATA	883	YP_009291533.1
	Xanthomonas phage f30-Xaj	TTGGTACACCTATA	836	YP_009276314.1
	Escherichia phage T7	TTAATACGACTCACTATA	883	QZB83517.1
	Pantoea phage LIMElight	TGACGTTATAGAGAGACAAC	818	YP_007002889.1
	Salmonella virus SP6	ATTTAGGTGACACTATA	874	NP_853568.1
	Escherichia phage ECBP5	TAGGCACTACAATA	877	YP_009146377.1
	Kluyvera phage Kvpl	AATACGACTCACTATT	882	YP_002308386.1
	Klebsiella phage KP32	ATTAGGGCACACTATAG	906	YP_003347522.1
	Stenotrophomonas phage IME15	TTAATACGACTCACTATAGGGAGA	883	YP_006990207.1
	Enterobacteria phage T3	AATTAACCCTCACTAAAGGG	884	NP_523301.1
Lu et al. (2019)	*Klebsiella* phage KP34	TAATGTTACAGGAGTA	822	YP_003347629.1
Zhu et al. (2014)	Cyanophage Syn5	ATTGGGCACCCGTAA	779	YP_001285424.1
Xia et al. (2022)	Psychrophilic phage VSW-3	TTAATTGGGCCACCTATA	798	YP_009596173.1
Streit et al. (2023)	Phage_EMG_100,139,454	TCAGAAGTCACACTATAA	816	UVM79537.1

fraction comes from the RNAP costs. The benefits of enzyme immobilization become much more apparent while transitioning from a batch to a flow-based continuous manufacturing mode (Wochner et al., 2015; Kis et al., 2020b).

1.9 Quality by design to improve IVT

As phage RNAP is a central element of the IVT reaction, it directly affects the mRNA's critical quality attributes (CQAs). Product-related impurities synthesized as byproducts, along with the intended transcripts, affect the purity of the drug substance (DS) (Lenk et al., 2024; Popova et al., 2024). The IVT process parameters can also influence the fidelity of the RNAP and may cause errors in the transcripts that would cause a decrease in the effectivity of the DS *in vivo* or even safety issues. The integrity (intactness of the transcript) is also affected by the IVT process parameters due to their effect on the RNAP and the transcription complex. Therefore, the critical process parameters (CPPs) and critical material attributes (CMAs) that affect the RNAP activity must be identified, mapped

and optimized to synthesize the intended transcript with the target CQAs under efficient manufacturing conditions. Understanding the effect of CPPs and CMAs on the RNAP activity at different phases of transcription reaction becomes essential in implementing the quality by design (QbD) approach in manufacturing mRNA-based products (Daniel et al., 2022; Nair et al., 2024). QbD implementation also has the added advantage of efficiently using prior knowledge and assisting with subsequent approvals as long as the reported design space is maintained. mRNA manufacturing also has the unique advantage of using similar unit operations for the production of multiple products by only changing the transcript encoding template DNA; this property makes it a platform technology and the manufacturing knowledge from one product is easily transferable to another. Pharmaceutical manufacturing is increasingly moving towards the QbD paradigm and mRNA manufacturing, with its "platformability", complements this approach.

2 RNAP mechanisms in *in vitro* transcription

The discovery of single-subunit RNAPs from bacteriophages significantly helped elucidate the transcription reaction. Steps like template scanning, promoter binding, transcription initiation, abortive cycling, processive elongation and termination have been studied in detail and the reaction parameters that influence these steps have been determined. The following sections will look at these distinct phases in the context of *in vitro* transcription and their corresponding RNAP mechanisms.

2.1 Promoter search

Before the RNAP binds to the promoter region and initiates the transcription, it searches/scans for it on the template DNA with intermittent weak interactions in a sequence-independent manner (Skinner et al., 2004; Kim and Larson, 2007). This phenomenon is often explained using diffusion processes (driven by thermal fluctuations) and has been studied extensively for single and multi-subunit RNAPs (Park et al., 1982; Guthold et al., 1999). Studies on protein-nucleic acid interactions have suggested four mechanisms (Berg et al., 1981) for the translocation of polymerases on nucleic acids; these are macroscopic dissociation-reassociation, microscopic dissociation-reassociation (hopping), intersegment transfer and sliding (one-dimensional diffusion); these mechanisms are depicted in Figure 4. The sequence-independent interaction of RNAPs with DNA has been studied further with single-molecule assays in combination with fluorescence microscopy, total internal reflection fluorescence (TIRF) with optical trapping and atomic force microscopy (AFM) (Guthold et al., 1999; Harada et al., 1999; Lee and Myong, 2021). The results from the assays mentioned above suggest a linear motion of RNAP on the template during promoter search; a more complex grove-tracking motion was also suggested, considering the double-helical structure of the DNA (Harada et al., 2001). The outcome of all these studies has led to the consensus that facilitated diffusion helps with promoter search (Bai et al., 2006). For the T7 RNAP, the NTD was observed to be responsible for nonspecific polynucleotide interactions, and the nicking/extensive proteolysis of this domain shows reduced interaction of the RNAP with nonspecific DNA (Muller et al., 1988). The property of RNAPs to interact with nonspecific DNA segments as in the case of searching for the promoter site, is sometimes adapted to sequester/quench RNAP activity (useful for single-round transcription studies or minimizing RNA-dependent RNA polymerase activity by competing with synthesized transcripts) (Chamberlin and Ring, 1973a; Chamberlin, 1974; Gholamalipour et al., 2019). In theory, CMAs such as template DNA length, could be optimized to reduce the nonspecific DNA interactions that the RNAP encounters in an IVT reaction. Linearized plasmid DNA amplified using bacterial fermentation contains a considerable amount of sequences (e.g., antibiotic resistance genes that act as selectable markers, origins of replication, multiple cloning sites, copy number control elements, etc.) not relevant for the final product. These could be reduced by using cell-free enzymatically prepared templates such as PCR products or proprietary templates based on dbDNA™, oeDNA™ or opDNA™ technology (Adie et al., 2022; Barreira et al., 2022; Cameron, 2024; Dhir et al., 2024).

2.2 Promoter binding and melting

RNAP-promoter binding follows a two-step mechanism, and initial interactions are like any other weak nonspecific RNAP-template DNA interactions. Once the RNAP recognizes the promoter site, it binds to it and forms the closed initiation complex (Újvári and Martin, 1996; Bandwar and Patel, 2002; Tang and Patel, 2006a). It has been observed with footprinting assays that RNAPs recognize one face of the DNA duplex (Oakley et al., 1979; Strothkamp et al., 1980). The NTD and the promoter recognition loop recognize the promoter region in bacteriophage-derived RNAPs. For the T7 RNAP, amino acid residues 93–101 in the NTD bind to the promoter's upstream −13 to −17 AT-rich region (Sousa and Mukherjee, 2003). The promoter recognition loop (residues from 739–770) in the T7 RNAP is an insertion within the polymerase domain that recognizes the −12 to −8 promoter identity region (PIR) within the T7 promoter, and it is this interaction that confers specificity between the homologous T3 and T7 RNAPs with their corresponding promoters (Bailey et al., 1983; Li et al., 1996; Cheetham and Steitz, 1999). The nucleotide at positions −11, −10 and −12 were determined to be the main specificity determinants between T3 and T7, while it was −9 and −8 for SP6 and T7 (Klement et al., 1990; Jorgensen et al., 1991). Mutations in the specificity loop and changes to the sequence within the PIR have been done to confirm the promoter recognition capabilities of the standard bacteriophage-derived RNAPs (T7, T3 and SP6) (Rong et al., 1998a). The entire consensus promoter can be divided into two regions: the upstream recognition/binding element (−17 to −5) and the downstream initiation element with melting/unwinding region from −4 to −1 (usually AT-rich, a TATA box in case of class III T7 promoter) and the initial transcription region from +1 to +4 (Carter and McAllister, 1981; Chapman and Burgess, 1987; Imburgio et al., 2000). Extensive studies on the promoter sequences have revealed the relevance of each domain within the consensus promoter and its interactions with the corresponding bacteriophage RNAPs (Chapman and Burgess, 1987; Li et al., 1996).

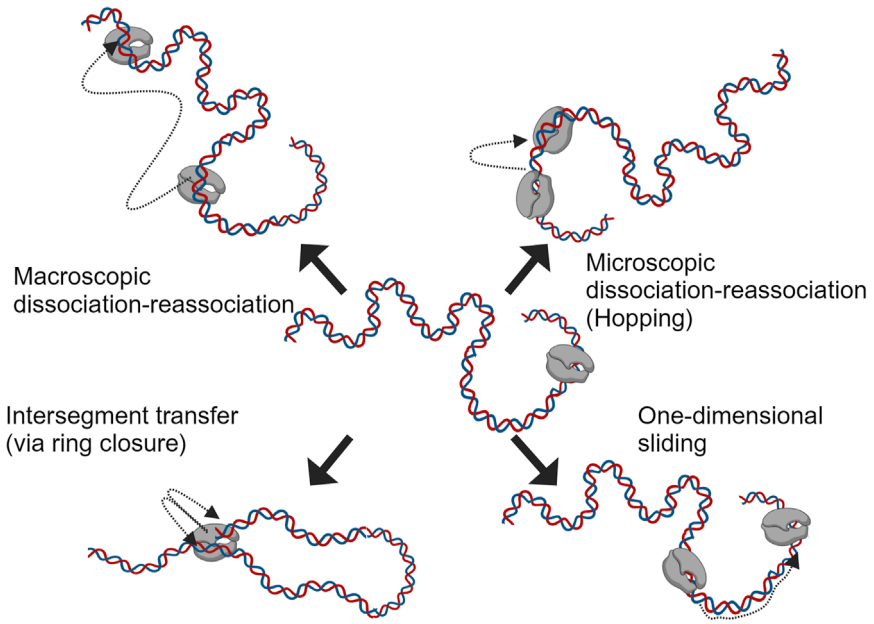

FIGURE 4
Different mechanisms speculated in aiding facilitated diffusion during promoter search by RNAP on template DNA (adapted from Berg et al., 1981).

The elements upstream of −5 are required in the double-stranded form, while the nontemplate strand from the −4 position can be removed without hindering the transcription reaction (Maslak and Martin, 1993). A comparison of promoters from commonly used bacteriophage RNAPs is given in Figure 5. Studies with partially single-stranded/nicked promoters (downstream of −5) have shown improved binding kinetics without hindering promoter recognition. Substitutions in the recognition regions have shown greater effects on RNAP binding (K_m) with little effects on the catalytic activity (k_{cat}). In contrast, substitutions in the melting and initiation regions have shown a greater impact on initiation than on binding (Ikeda and Richardson, 1986a; Újvári and Martin, 1997; Weston et al., 1997; Imburgio et al., 2000). It should be noted that for the T7 RNAP, the promoter recognition is very specific but surprisingly weak (Villemain et al., 1997). The T7 class II promoters are weaker than class III promoters and show higher sensitivity to IVT parameters such as temperature and ionic strength (Mcallister and Carter, 1980).

The impact of different types of anions and cations, along with additional reagents like polyamines (spermidine) have suggested optimum levels of these components to improve the key performance indicators (KPIs) for the IVT reaction and CQAs of the transcribed mRNA (Maslak and Martin, 1994). The effect of acetate, chloride and glutamate ions along with their counter ions (Na^+ or K^+) on the binding kinetics were explored and have led to unprecedented improvements in the IVT reactions (Boman et al., 2024). It is theorized that these ions compete with the binding of the phosphate backbone of the template DNA, as most of the initial interactions are electrostatic in nature. Acetate and glutamate anions interact less with the RNAP binding site, as evidenced by the higher tolerance of these anions by the RNAP. Moreover, as binding is a diffusion-led phenomenon, the reaction temperature acts as a CPP for this step. Optimization of this CPP based on the temperature tolerance of the RNAP is also reported; 37°C is considered optimal for standard wild-type RNAPs (Maslak and Martin, 1994).

2.3 Transcription initiation

Following the binding process, the RNAP melts the promoter to form the open initiation complex (this isomerization is achieved by conformational changes in the RNAP and the template DNA). Thereby, in the case of T7 RNAP-promoter complex, the template is melted from the −4 to +3 position with respect to the transcription initiation site (Cheetham et al., 1999; Újvári and Martin, 2000; Tang and Patel, 2006b; Tang and Patel, 2006a). Rapid promoter opening is synchronized with promoter binding, and it is assumed that the closed and open complexes remain in a state of equilibrium, with closed complexes favored until the initiating nucleotide stabilizes the open complex. The conformational changes associated with transcription initiation include an approximately 90° bend of the downstream template DNA around the −1 site. After the initiating NTP along with the +2 NTP stabilizes the open complex and the first phosphodiester bond is formed to produce a ribonucleotide dimer, this process is repeated until a trimer is formed without any changes in the initial transcription bubble (−4 to +3) (Kuzmine and Martin, 2001; Stano et al., 2002; Tang and Patel, 2006a; Tang and Patel, 2006b; Tang et al., 2009). The rate constant of making a the 2 nt dimer is approximately 2 s^{-1}, this decreases as the length of the transcript increases and gets maintained at 0.8 s^{-1} in the elongation phase (Tang et al., 2009). In theory, using dinucleotide or trinucleotide cap analogs skips the first phosphodiester catalysis and may provide better open complex stabilization and initiation of transcription. Most of the energy required for melting/opening

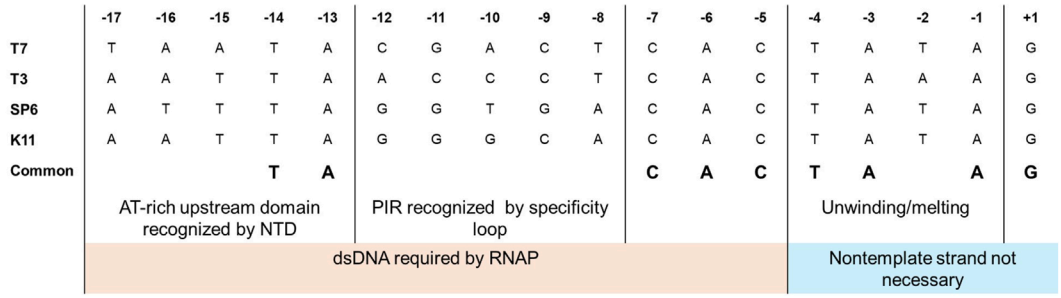

FIGURE 5
Comparison of promoters for commonly used bacteriophage RNAPs. A two-domain structure can be observed for the promoters, with upstream elements from −17 to −5 involved in recognition/binding and initiation elements from −4 to +3 (adapted from Imburgio et al., 2000; Sousa and Mukherjee, 2003).

of the promoter comes from the binding of the RNAP with the upstream duplex element of the promoter (−17 to −5) (Újvári and Martin, 1996; Bandwar and Patel, 2002; Bandwar et al., 2002). The melting is further facilitated by the interaction of the template strand with the active site cleft and the insertion of the β-hairpin formed by the residues 232–243 in the RNAP between the template and nontemplate strands (Cheetham et al., 1999; Stano and Patel, 2002; Sousa, 2013). The upstream edge of the bubble is stabilized by V237 stacking on the promoter's −5 bp (Brieba and Sousa, 2001; Liu and Martin, 2001).

For T7 RNAP, the initiating nucleotide is mostly GTP, and its binding to the active site is facilitated by the base pairing with the template strand along with Hoogesteen pairing of N-6 and O-6 of the guanine base with either R425 or R632 and interactions with H784 (Kuzmine et al., 2003). It should be noted that the K_m for the initiating nucleotide is much higher than the rest of the nucleotides and that the second nucleotide is recruited first during synthesis of the first phosphodiester bond (Martin and Coleman, 1989; Jia and Patel, 1997; Stano et al., 2002). The initiating NTP has its triphosphate group intact, while the second NTP recruited to the transcription site loses a pyrophosphate (PPi) group during the bond formation. There are some ambiguities regarding the opening of the promoter being a rate-limiting step; initial experiments with partially single-stranded promoters (no nontemplate strand downstream of −5) and double-stranded promoters did not suggest any drastic difference for the initiation rates and K_m for binding. However, later studies have proved improved stability and binding while using partially single-stranded promoters (Jia et al., 1996; Újvári and Martin, 1996; Jia and Patel, 1997; Villemain et al., 1997). The inherent instability of the open complex, which is a function of the promoter sequence in the melting and initiation region along with its interaction with the RNAP, acts as a kinetic mechanism for promoter specificity (Villemain et al., 1997). CMAs such as the sequence of template DNA, presence of nontemplate DNA (double-stranded vs. partially single-stranded DNA) at the melting and initiation region, along with CPPs such as concentration of +1 and +2 NTPs or cap analogs (either dinucleotide or trinucleotide) that helps with stabilization of the open complex should be considered for optimization of the IVT reaction. Additionally, metal ions and polyamines such as Mg^{2+} and spermidine and their interaction with the template DNA have also been reported to stabilize the open complex, thereby adding their concentrations to the list of potential CPPs that impact this phase of the IVT reaction.

2.4 Abortive cycling

The initial transcription bubble can accommodate up to a trimer of the nascent mRNA before additional conformational changes are required to extend the ribonucleotide polymer. The downstream boundary of the transcription bubble expands downstream from +4 to +8 while still maintaining contact with the promoter (the upstream edge of the bubble remains fixed) (Cheetham and Steitz, 1999; Liu and Martin, 2002; Gong et al., 2004). This initial stage of polymerization, called abortive cycling, is a rate-limiting step before the enzyme transitions to a processive elongation phase. Essentially, the template DNA is "scrunched" within the transcription bubble until the nascent mRNA reaches a minimal length of 8 nt (Cheetham and Steitz, 1999). The promoter release phenomenon as a function of growing nascent RNA (RNA:DNA hybrid) is well documented with exonuclease digestion and fluorescent studies by using promoters with fluorescent base analogs (Liu and Martin, 2002; Gong et al., 2004). The transcription bubble expansion proceeds after each nucleotide incorporation as the RNAP translocates on the template DNA.

The phenomenon of initial transcription proceeding without losing the upstream promoter complex induces template DNA bending and rotation of the NTD of the RNAP. It has been shown that the template DNA is bent almost 90° in the IC compared to a much-relaxed angle close to 40° in the EC (Tang et al., 2008). The conformational changes in the RNAP result from the growing RNA:DNA hybrid bumping against the NTD, causing its rotation by 40°, which ends with a large 220° rotation of the same domain during the transition to EC (Yin and Steitz, 2002; Bandwar et al., 2007; Durniak et al., 2008; Tang et al., 2008; Vahia and Martin, 2011). This rotation of the NTD helps with the abrogation of promoter contact and clears the RNAP to a processive elongation phase. During the abortive cycling, a reciprocal pushback by the NTD on the RNA:DNA hybrid causes the release of the nascent mRNA. Multiple rounds of this back and forth between RNAP and the growing RNA:DNA hybrid is necessary before the promoter clearance (Koh et al., 2018). The length of the RNA:DNA hybrid

at 8 bp provides a topological lock and stabilizes the transcription bubble, which is the same topological lock that provides stability to the transcription bubble in the EC (Liu and Martin, 2009). RNAP undergoes additional conformational changes, including bending of the thumb subdomain, while the nascent RNA reaches a length of 5–6 nt. Abortive cycling can lead to the RNAP either reinitiating the transcription on the same template (RNAP recycling) or starting it on a new one (RNAP exchange) (Koh et al., 2018). The reinitiations were observed to depend on the RNAP concentration or the initiating nucleotide (GTP) for RNAP exchange and RNAP recycling, respectively. At high GTP concentrations, RNAP recycling was preferred. Abortive cycling ends with a transition to EC following the NTD rearrangement; RNAPs lose the promoter specificity and begin sequence-independent processive elongation. Moreover, the T7 RNAP's H-subdomain within the NTD is rearranged to form the RNA exit channel (Yin and Steitz, 2002; Tang et al., 2008). The chemical energy from phosphodiester bond formation during the nascent RNA synthesis is converted to mechanical energy during the NTD rotation. It acts as a piston for the RNAP to overcome promoter contact and transition to EC. Abortive cycling is observed in all RNAPs and some have suggested an evolutionary prerogative for its presence. It is assumed that the short nucleotide released during abortive cycling acts as primers for polymerases that do not have *de-novo* synthesis capabilities (DNA polymerases) (Matsumoto, 1994).

As abortive cycling introduces byproducts that impact the quality of the drug substance, CMAs and CPPs that affect this phase need to be optimized. CMAs affecting abortive transcription include a sequence of the initially transcribed RNA (>8 nt). It has been shown that the presence of U in this sequence can lead to higher rates of abortive transcription (based on single nucleotide substitutions) (Imburgio et al., 2000). However, newer data with multiple base substitutions in the initially transcribed sequence (ITS) have highlighted cross-talk between the bases from +4 to +8, and the inclusion of AT-rich regions here has been reported to improve IVT productivity and a reduction in product-related impurities arising from abortive transcription (Conrad et al., 2020; Sari et al., 2024). The structure of the promoter is also reported to be an important influencing factor for abortive cycling, it has been shown that partially single-stranded (duplex promoter and only template strand) or nicked promoters (in the nontemplate strand) reduce the generation of abortive transcripts. It is proposed these modified promoters induce less stress in the transcription bubble by reducing the degree of template DNA scrunching (Gong and Martin, 2006).

CMAs pertaining to the RNAPs have also been extensively studied and used to reduce the abortive cycling phase. Initially, the promoter binding affinity was attributed to be the main factor in preventing the transition to the elongation phase; this was supported by studies based on a T7 RNAP mutant with P266L substitution (Guilleres et al., 2005; Guilleres et al., 2004). Later, it was proved that the binding affinity for the wild-type and the mutant were not significantly different and that the mutant synthesized longer abortive transcripts than the wild-type RNAP. Based on the NTD pushback theory, multiple mutant RNAPs have been engineered to reduce the abortive transcription by easing this phenomenon (Ramírez-Tapia and Martin, 2012; Tang et al., 2014). Substitutions, insertions and deletions in the C-helix of NTD and the linker region between NTD and CTD are reported to reduce the abortive transcripts (Martin and Ramirez-Tapia, 2015). Abortive cycling has been of great interest for IVT optimization studies as it acts as a rate-limiting step before the RNAP transitions to the processive elongation phase, and the byproduct from this mechanism is a product-related impurity that affects the KPI of the IVT reaction and the CQAs of the transcribed drug substance. CMAs, such as template sequences, has been optimized to reduce abortive cycling.

2.5 Processive elongation

The transition from the initiation phase through abortive cycling to the processive elongation phase happens after structural changes to both the RNAP and the template DNA. Although the transition to EC proceeds after promoter clearance and the synthesis of >8 nt RNA, the highly processive and stable EC (mature EC) does not form until 12–14 nt RNA is synthesized (Mentesana et al., 2000). Bacteriophage-derived RNAPs catalyze the synthesis of the RNA polymer close to 200 nt/s in this elongation phase (Golomb and Chamberlin, 1974). The transcription bubble stability in the elongation phase is maintained by an almost 8 bp long RNA:DNA hybrid (based on the topological lock) and interactions of the nontemplate strand with the RNAP (Sousa and Mukherjee, 2003; Theis et al., 2004; Liu and Martin, 2009). In one of the main conformational changes to the RNAP in the EC, the specificity loop is displaced from the position in the IC and forms part (lid) of the RNA exit channel. The changes in the NTD are also well characterized; the promoter binding domain (PBD) undergoes a rigid body rotation of 220° along with changes to the C-helix (transition from loop to helix) and H domain (becomes part of the RNA exit channel) (Yin and Steitz, 2002; Steitz, 2009).

The Brownian ratchet mechanism explains the process of nucleotide addition; the catalysis itself proceeds via a two-metal ion mechanism (divalent metal ions such as Mg^{2+} facilitate this step) (Sosunov et al., 2005; Guo and Sousa, 2006). Apart from the RNAP, the template DNA also undergoes specific changes after transitioning to EC. The downstream DNA is less bent and positioned differently in the EC, for the T7 RNAP, residues K711, K713 and K714 maintain the orientation of the downstream DNA (Nayak et al., 2007). The role of the thumb subdomain in the stability of the elongation complex is also explored. It is theorized that this motif acts such as a sliding clamp once bound to the template DNA and interacts with the growing RNA via positively charged residues (Mukherjee et al., 2002).

The translocation of RNAP along the DNA during RNA synthesis proceeds via the following two steps. In the first step, after the phosphodiester bond formation and release of PPi, the EC is in a "pre-translocated" position. In this state, the RNA still occupies the position in which the incoming NTP should bind to extend the transcript. In the second step, conformational changes that lead to the extension come after the PPi released from the phosphodiester bond interacts with the finger subdomain (open state) and O-helix interacts with incoming NTP (closed state). This step, called the "post-translocated" position, achieves the transfer of the substrate to the insertion site, translocation of RNA:DNA duplex (function of Y639 displacement in T7 RNAP), opening of the downstream DNA (by 1 bp) and closing/reannealing of upstream DNA. These

open and closed states drive the translocation of the EC along the DNA (Yin and Steitz, 2002; Temiakov et al., 2004; Steitz, 2009). The template sequence also affects the forward translocation, and it has been reported that the K_m for the elongating NTP is affected by the ease or hindrance to forward translocation (Thomen et al., 2008). Fidelity of this highly processive state can be owed to the base pair interactions the incoming NTP has with the nucleotide on the template strand; these tend to be fast and the right base pairing increases the residence time for interactions. A factor that might increase the residence time for these incoming nucleotides may decrease the fidelity (use of divalent metal ions with stronger coordination than Mg^{2+}) (Pezo and Wain-Hobson, 1997).

CMAs relating to template DNA and the RNAP affect the EC's processivity. As mentioned above, the template DNA sequence regulates nucleotide incorporation speed. The structural stability of the RNAP also impacts the EC; early purification strategies for T7 RNAP after overexpression in bacterial cells resulted in structural damage of the NTD due to nicking between residues K172 to K179 (Muller et al., 1988). Studies of the processivity of this nicked enzyme and RNAP with extensively degraded NTD have shown either highly reduced processivity or complete dissociation in the elongation phase. Structural studies have shown that this nicked region of the RNAP forms a part of the RNA exit channel, and the disruption in the interaction of the growing RNA strand with the exit channel affects the processivity of the EC (Yin and Steitz, 2002; Koh et al., 2018). CPPs related to IVT reactions, such as nucleotide concentration, RNAP concentration (instability from enzyme bumping), co-factor concentration, and reaction temperature, also affect the EC and its processivity. The inherent stability of the EC or the RNAP conformation in the EC may also result in the synthesis of product-related impurities such as dsRNA (Dousis et al., 2023). As mentioned above, the conformational changes in the RNAP during elongation catalyze the RNA polymerization in a sequence-independent manner; the RNAP binds to 3′looped RNA and proceeds with its extension without requiring promoter recognition (Gholamalipour et al., 2018). Indeed, newer T7 RNAP (G47A) mutants showing less dsRNA generation indicate stabilizing IC relative to the EC (Dousis et al., 2023; Rabideau et al., 2019). This hypothesis requires further studies and comparison of run-off vs. terminator sequence-dependent termination.

2.6 Transcription termination

The highly processive elongation phase ends once the EC encounters specific terminator sequences or simple dissociation from the lack of downstream DNA (linearized DNA). In hyper-forward translocation, the RNAP is pushed forward by secondary structures (hairpin loop) and a stretch of downstream U residues in the synthesized RNA (Lyakhov et al., 1998; Zhou et al., 2007; You et al., 2023). Sequences with a high degree of base complementarity and base pairing strength drive the formation of these structures in the RNA; this, along with a weaker base pairing of U (in RNA) with A (in template strand), facilitates the opening of the hybrid topological lock (Zhou et al., 2007). The T7 RNAP has a corresponding terminator sequence found in the phage genome; this sequence is inherently weak at termination, with reported efficiency between 60%–80% (Calvopina-Chavez et al., 2022). Sequence-dependent terminators can be divided into structured class I (hairpin-forming) and unstructured class II sequences. The former achieves termination by inducing hyper-translocation (3′OH group of the RNA is removed from the active site, ending the catalytic cycle). At the same time, the latter is theorized to collapse the transcription bubble that leads to DNA unbending and translocation from restraining interaction with upstream DNA (Macdonald et al., 1994). Regardless of the mechanism, the outcome unthreads the RNA from the topological lock with the template strand. Class I terminators for phage polymerases have a more stable stem and longer U-run than similar termination structures for bacterial polymerases. Novel hairpin structure coding terminator sequences with at least 12 internal base pairs and 60% GC content have been proposed to offer better termination efficiencies (Striedner and Wittwer, 2019). Secondary structure stabilization can be estimated by Gibbs-energy (ΔG); higher stability pertains to lower ΔG (Mairhofer et al., 2015). It was shown that structures with stems greater than 9 bp, even after decreasing the ΔG, did not improve termination efficiency (for bacterial terminator sequences).

In contrast to the mechanism of class I terminators, where RNA structure is responsible for termination, class II terminators do not form these structures; this suggests a fundamental difference in the termination mechanism between these two sequences. Class II terminators were originally isolated from the human prepro-parathyroid hormone (PTH) gene (He et al., 1998). Later, similar terminators were found in the concatemer junction (CJ) of bacteriophage DNA, *E.coli* rrn BT1 terminator and cDNA copy of vesicular stomatitis virus (VSV). As it is not the RNA structure that drives termination in a class II sequence, the overall mechanism was more complex to decipher. It was shown that class II terminators must be present as a duplex and that the nontemplate strand was crucial in its functioning; base changes within the PTH terminator were shown to reduce the terminator efficiency. The conserved class II sequence was determined to be the 7 bp ATCTGTT (ATCTGTTTT for T7 RNAP); the upstream sequence, although important, is not absolutely required. A U-run downstream of the main sequence is a standard feature for both class I and II terminators. Moreover, shortening of the four U residues or their substitution prevents termination by class II sequences (He et al., 1998). Class II terminators have been found to be better suited for IVT application, but newer terminator sequences based on the combination of class I and II terminator sequences have proven to be highly efficient in both *in vitro* and *in vivo* applications. These constructs have shown more than 90% termination efficiency (Mairhofer et al., 2015; Striedner and Wittwer, 2019; Calvopina-Chavez et al., 2022).

Run-off transcription using a linearized template DNA is a hallmark of the IVT reaction. This mechanism partly gives the IVT reaction its high turnover. The enzyme elongates on the template DNA until the end of the template DNA, e.g., obtained by plasmid linearization, and the T7 RNAP slides off. The forward hyper translocation of the RNAP is favoured in run-off transcription as the regulation from melting the downstream DNA is absent at the end of the template, which, combined with reannealing of the template and nontemplate strand, results in the collapse of the transcription bubble and dissociation of the RNA:DNA hybrid. The productivity (from high turnover) in a run-off transcription is much higher

compared to one in which internal dissociation terminates the elongation phase. It presents its own challenges as the EC becomes very unstable at the end of the template and adds nucleotides to the 3′end of the intended transcript. 3′heterogeneity is a major problem and leads to "nontemplated" nucleotide addition (N+ *x* additions; here, N is the intended transcript length). Recent results have shown that these additions depend on the template-dependent (cis-primed extension of 3'looped back RNA) (Gholamalipour et al., 2018).

The termination phase of transcription by bacteriophage-derived RNAPs might be the least studied in optimizing the IVT reaction. As mentioned above, several product-related byproducts are generated due to improper termination of the processive elongation phase; the characteristics that make IVT productive could potentially be responsible for such an outcome. CMA improvements related to template DNA that facilitate sequence-dependent termination, linearization (of plasmid DNA) without 3'overhangs (Rong et al., 1998b), and transcript sequence optimization for reducing complementarity to prevent 3'loop back could be one area for overall process optimization. CMAs related to the RNAP have also been extensively explored. Mutant RNAPs that give much better 3'homogeneity compared to wild-type T7 (Wu et al., 2021; Dousis et al., 2023) RNAP are documented. Thermostable mutant RNAPs (Ong et al., 2022; Roy and Robb, 2022) that take advantage of higher process temperature to disrupt loopback formations in the synthesized RNA and alternative bacteriophage RNAPs, such as those derived from cyanophage Syn5 (Zhu et al., 2013), have been reported to give much better 3'homogeneity compared to the current standard wild-type T7 RNAP. Any approach that can revert the RNAP to IC without proceeding to an RNA-dependent RNA polymerization after termination and dissociation could help lower the generation of dsRNA byproducts. CPPs associated with IVT that directly influence termination need to be assessed; this includes process temperature, concentration of RNAP, concentration of non-canonical nucleotides, presence of ions such as Mg^{2+} or arginine (in case of class II terminators) and the presence of chaotropic agents that disrupt secondary structure (in case of class I terminators).

3 Mutant T7 RNAPs and alternatives based on structure-function relationship

An insight into the structure-function relationship was given in the previous section; it touched upon some important residues within the T7 RNAP that were the key enablers of the transcription phase-associated functions. Since there is considerable homology between the standard bacteriophage RNAPs used for manufacturing applications, the insights from one can be extrapolated to a certain degree onto the others (Cermakian et al., 1997). As T7 RNAP is the most characterized, this section will focus on it; crystal structures of T7 enzyme during the various phases of a transcription reaction are well documented (Sousa et al., 1989; Sousa et al., 1993; Sousa, 1997; Cheetham and Steitz, 1999; Yin and Steitz, 2002). The same structures have played a crucial role in understanding the underlying mechanisms of the transcription reaction. The T7 RNAP can be broadly divided into the NTD and CTD. NTD extends from residues 1 to 312, while CTD extends from 313 to 883 (Sousa and Mukherjee, 2003; Sousa, 2013). The CTD is also synonymous with the polymerase domain; this can be further subdivided into the fingers (residues 541 to 737 and 771–778), palm (residues 411 to 448, 532 to 540, 788–838) and thumb (residues 330–410) subdomains (refer Figure 2). Apart from the CTD polymerase domain, which resembles the shape of a cupped right hand, there are accessory modules that are present in the T7 RNAP; these include the NTD, the promoter recognition loop (739–770), C-terminal loop (residues 820–883) and extra 4-helix bundle (residues 449–531). These modules enable promoter recognition, duplex opening, RNA binding and displacement and transcription regulation (Sousa and Mukherjee, 2003). An extensive list of mutant T7 RNAPs (from patent documents and research articles) based on proposed improvements to structure-function relationships is given in Table 1. Although these mutant T7 RNAPs provide extended capabilities for non-canonical substrate utilization and reduction in product-related impurities, they require extensive characterization. Properties such as fidelity requires further investigation before they can be used in large-scale manufacturing of mRNA-based products.

3.1 Amino-terminal domain (NTD)

The NTD has four motifs that perform crucial roles; these include: i) promoter binding domain (PBD), a six-helix subdomain (residues 72–150 and 191–267) that interacts with the AT-rich upstream region of the promoter; ii) H domain, a two-helix subdomain (residues 151–190) that forms part of the RNA exit channel; iii) C-helix (residues 28–71), responsible for active site enlargement and iv) C-linker (residues 251–296), facilitates transition from IC to EC by providing structural flexibility (Sousa and Mukherjee, 2003; Martin and Ramirez-Tapia, 2015; Dousis et al., 2023). The NTD undergoes drastic conformational changes during the transition from IC to EC, facilitating the high processivity of the T7 RNAP seen during the elongation phase. Positively charged residues (93–101) of the PBD interact with the minor grove of the promoter (−17 to −13 bp) and the intercalating loop (residues 232–242) with V237 facilitates the opening of the duplex by stacking on the −5 bp and stabilizing the upstream edge of the open complex (Brieba and Sousa, 2001; Yin and Steitz, 2002; Tang et al., 2008; Tang et al., 2009). The H subdomain shows significant movement during the transition from IC to EC. It moves towards the active site and becomes part of the RNA exit channel and the other accessory module (promoter recognition loop) (Tang et al., 2009). Studies on nicked T7 RNAP (in the H subdomain) have shown decreased activity in the elongation phase, and this could be attributed to the disruption in the RNA exit channel, which is partly formed by the H subdomain (Muller et al., 1988). C-linker and C-helix also have an active role in the transition of IC to EC; the former facilitates the enlargement of the active site during the initial transcription, especially for the accommodation of the template DNA from scrunching. Conversely, C-linker helps with the structural flexibility of the NTD and facilitates its movement (Sousa and Mukherjee, 2003; Dousis et al., 2023). The NTD of T7 RNAP has been subjected to various mutations to improve the industrial application. As is evident from Table 1, thermostability-conferring mutations are the most common when it comes to NTD mutations. The mutations to C-linker and C-helix have also been employed to reduce the

synthesis of abortive transcripts or reduce the RNA-dependent RNA polymerase activity of the enzyme. It has been speculated that stabilization of EC to IC after termination/dissociation might be the key to reducing product-related impurities such as dsRNA and 3′heterogeneous products. Regardless, NTD modifications can reduce product-related impurities passively by relying on increased process temperatures or actively by reducing cryptic promoter-independent RNA-dependent RNA polymerase activity.

3.2 Carboxyl-terminal domain (CTD)

The polymerase domain is the larger entity within the T7 RNAP and structurally looks like a cupped right hand. It is responsible for the catalysis of NTPs to the RNA polymer. The subdomains are named finger, palm, and thumb, respectively, each responsible for a particular function during the transcription.

3.2.1 Fingers subdomain

The finger subdomain interacts with the incoming NTP and the template strand downstream of the templating base. The O-helix, part of a five-helix motif within the finger subdomain, interacts with the incoming NTPs using K631 and R627 (positive residues interact with the triphosphate group of the incoming NTP) (Temiakov et al., 2004; Steitz, 2009). Y639 at the tip of the O-helix plays the role of nucleotide insertion to the active site, and the same residue is responsible for substrate discrimination (ribose vs. deoxyribose) based on Mg^{2+} mediated interaction with 2′OH group on the ribose sugar (Brieba et al., 2002; Temiakov et al., 2004). It should be noted that H784 and G542 also play a role in substrate discrimination between ribonucleotides and deoxyribonucleotides (Temiakov et al., 2004; Steitz, 2009). G542 provides less steric clash with 2′OH group, while H784 makes hydrogen bonds with 2′OH of the ribonucleotide. These residues are highly conserved in all phage-like DNA-dependent RNA polymerases. In DNA polymerases, G542 will be replaced with a bulkier residue such as glutamic acid (Cheetham and Steitz, 1999). The movement of the finger domain facilitates the translocation of the RNAP on the template DNA; Y639 pushes the RNA:DNA hybrid, while F644 coordinates the downstream template motion (Da et al., 2017). Moreover, as this domain is responsible for substrate binding and incorporation in the active site, it regulates the fidelity of the RNAP. Multiple modifications have been done to the finger subdomain as it is relevant in substrate incorporation, fidelity, and to an extent the processivity of the RNAP. The earliest T7 mutants were designed to incorporate non-canonical NTPs to the RNA polymer, including 2′-fluoro, 2′-O-methyl base incorporations (refer Table 1). Recently, the incorporation of modified NTPs for better *in vivo* activity has gained traction, especially for specialized therapeutics (Zhu et al., 2022). In such a scenario, mutant T7 RNAPs capable of such synthesis at scale will become more relevant. Increasing the specificity for cap analogs used in co-transcriptional capping is also another area where mutant T7 RNAPs can be specifically useful. Proprietary co-transcriptional cap analogs are the main raw material cost contributors; moreover, their poor utilization further increases the associated manufacturing costs. T7 mutants capable of higher specificity for these cap analogs will reduce the manufacturing cost due to less raw material requirement (Miller et al., 2022). Apart from this, modifications to the finger subdomain have also provided better thermostability to the enzyme. Another interesting modification (C723S) in the finger subdomain has provided better stability of the enzyme, reduced the formation of homodimers due to the disulfide bridge between cysteine residues, and improved the overall enzymatic activity (Greif et al., 2017).

3.2.2 Palm subdomain

The palm subdomain houses the active site of the RNAP, and the highly conserved aspartate residues at D537 and D812 facilitate the formation of phosphodiester bonds (Woody et al., 1996). These residues coordinate with 2 Mg^{2+} ions that stabilize the pentacoordinate phosphorous intermediate and facilitate nucleophilic attack of the 3′-OH on the RNA terminal nucleotide by the α phosphate of the substrate NTP (two-metal ion mechanism) (Yang et al., 2006). PPi released as a result of this reaction coordinate with the finger subdomain to drive the translocation of the polymers (Steitz, 2009). Although T7 RNAP is a highly helical enzyme, the RNA and DNA facing side of the palm subdomain is composed of β sheets (Cheetham and Steitz, 1999). The residues responsible for catalysis are highly conserved and any changes here are detrimental to the activity of the RNAP; however, T7 mutants with thermostable properties are engineered by changes in the palm subdomain (most of the time in combination with changes in the finger subdomain). The palm subdomain also remains conserved across various RNA and DNA polymerases.

3.2.3 Thumb subdomain

The thumb subdomain is vital for the stabilization of the EC, it wraps around the DNA to form a clamp which would prevent dissociation of the complex during translocation on the DNA. The growing RNA:DNA hybrid interacts with positively charged residues on the thumb subdomain and facilitates its stabilization (Durniak et al., 2008). Mutations in the thumb subdomain to neutral residues increase the dissociation of RNA. Like mutants derived for the palm subdomains, thumb subdomain mutations result in thermostable properties.

3.2.4 Accessory modules

Apart from changes in the main subdomains, mutations in the accessory modules (apart from NTD) are quite rare; in our assessment, we did not find any mutant with changes to the promoter recognition loop (anti-parallel β ribbon). Changes to the C terminal loop are also rare, as it was previously reported that any changes in this motif are detrimental to the enzyme's activity. F882 provides a binding site to the elongating NTP, and any changes to the F880, A881, F882 and F883 affect the catalytic efficiency (Gardner et al., 1997). Insertional mutants with smaller residues after F883 were found to be still active and based on this, a G884 mutant was engineered that showed better 3′homogeneity of the transcripts compared to wild-type T7 RNAP (Dousis et al., 2023; Rabideau et al., 2019). The extra 4-helix bundle is yet to be characterized for its function; so far, we have found only one mutant that confers thermostability to the enzyme from changes in this accessory module.

3.3 Phylogeny and alternatives to T7 RNAP

The T7 RNAP shows structural similarity with other RNAPs and DNAPs as well as limited similarity with the polymerase domain of reverse transcriptase. T7 RNAP is a member of the single-subunit RNAPs, which includes other bacteriophage RNAPs, nuclear gene-coded mitochondrial RNAPs and chloroplast RNAPs (Cermakian et al., 1997). The accessory modules described in the previous section provide the most significant variation between these related enzymes. Similarities with DNAPs have prompted using mutants capable of incorporating rNTPs as a possible alternative for bacteriophage-derived RNAPs. Mostly, these alternatives are isolated from extremophiles, which gives the added advantage of thermostability (Wang et al., 2017). Structural similarity between T7 RNAP and Pol I class of DNAPs suggests they come from a common ancestor. However, the cellular multi-subunit RNAPs lie outside this superfamily. Based on the phylogenetic analysis, T7 RNAP alternatives could be used to meet specific industrial applications. The product-related impurities generated by the wild-type T7 RNAP could be avoided with alternatives derived from other bacteriophages or extremophile bacteria. A few of the newly characterized alternatives include RNAPs derived from *Klebsiella* phage (KP34), Cyanophage (Syn5), and *Pseudomonas* phage (VSW-3) (Zhu et al., 2013; Lu et al., 2019; Xia et al., 2022). The RNAPs from the alternatives provide several advantages over the wild-type T7 RNAP, including higher processivity (useful for the synthesis of longer RNA constructs such as self-amplifying mRNA), reduced 3′heterogeneity, reduced dsRNA generation and improved incorporation of modified NTPs. We have summarized a list derived from patent applications and research articles of potential T7 RNAP alternatives that may have industrial usefulness in Table 2 and showed the phylogenetic relationship between these alternatives using a neighbor-joining phylogenetic tree in Figure 6. Apart from using mutant T7 RNAP and alternative bacteriophage-derived RNAPs, a new solution for mRNA-based products comes from fusion proteins; here, T7 or related RNAPs are fused with another enzyme capable of activities such as 5′capping (Chan et al., 2023). Such a solution for producing capped mRNA can have significant manufacturing cost benefits. Currently, enzymatic capping is resource intensive as mRNA produced from the IVT process needs to be purified before the capping reaction is done using another enzymatic reaction (usually done with vaccinia or faustovirus capping enzymes). Fused enzymes with polymerase and capping activity can reduce/circumvent the dependence on proprietary capping reagents and reduce the raw material costs and operating costs, as fused enzymes grant a one-pot synthesis and capping reaction.

3.4 Methods for RNAP engineering

The review has highlighted many mutants that are useful for specific industrial applications; therefore, another question that arises is how these mutants are screened and engineered; this could be broadly divided into directed evolution and rational design. While the former does not require information about structure-function properties, the latter heavily relies on the sequence and structure-function relationship and aims to introduce changes via methods such as site-directed mutagenesis (Reetz et al., 2023). Directed evolution introduces random mutations via methods like error-prone PCR or DNA shuffling; continuous directed evolution and phage-assisted continuous evolution (PACE) are newer iterations of this method (Packer and Liu, 2015; Miller et al., 2020). The mutants highlighted in the table were engineered via rational design and directed evolution methods such as PACE. The cost and time associated with screening and engineering of useful mutant enzymes can be substantial; however, strategies such as adaptive machine learning are reducing this burden and helping screen mutants with fewer evaluations (Hie and Yang, 2022). Apart from screening of mutants, improvements in phylogenetic analysis have also helped with the identification of potential alternatives for commonly used T7 RNAP; regardless of whether screening for mutants or T7 alternatives, computational methods assist with high throughput screening while reducing overall resource utilization and associated costs.

4 QbD and economics of mRNA manufacturing

As mRNA-based products are gaining traction and newer varieties like self-amplifying and circular mRNA are being considered for use in prophylactic and therapeutic applications, optimizing the process that enables manufacturing these drug substances becomes crucial. Implementing the quality by design (QbD) paradigm for mRNA manufacturing is being discussed extensively, and this approach complements the 'platformability' inherent to mRNA manufacturing (Daniel et al., 2022; Whitley et al., 2022; Nair et al., 2024). Throughout this review, we focused on a central component of this manufacturing process, the enzyme that enables the production of the drug substance. From a QbD perspective, the CMAs and CPPs that affect the CQAs and KPIs do so by influencing the functionality of the RNAP. Moreover, it can also be seen that different CMAs and CPPs affect the CQAs by influencing the enzyme in its various phases during the IVT reaction. As noted, the CPPs, such as ionic strength, have more relevance at the initiation than at the transcription reaction's elongation or termination phase. Substrate concentration, co-factor concentration, type of buffering agent, type of template DNA, sequence of template DNA, pH, reaction time and temperature are some of the few CMAs and CPPs that affect this process. Mapping the relationship between CMAs/CPPs and CQAs is essential in the QbD paradigm. This could be improved further by understanding the fundamental mechanisms involved in the process. Traceability and reagent quality used in manufacturing are other crucial aspects to consider when establishing a stable and capable process; often, this is achieved with good manufacturing practice (GMP) compliance. This approach also facilitates troubleshooting in case of quality failures and maintains consistency in the quality of the final product. GMP-graded reagents increase the overall production costs, but adapting them at the early stage of development can aid in entering clinical trials and reaching regulatory approvals faster. Importantly, GMP-graded reagents do not always have higher-quality than reagents sold for research and development purposes. However, GMP-grade reagents are: 1) produced using production processes validated to ensure consistency and reproducibility, 2)

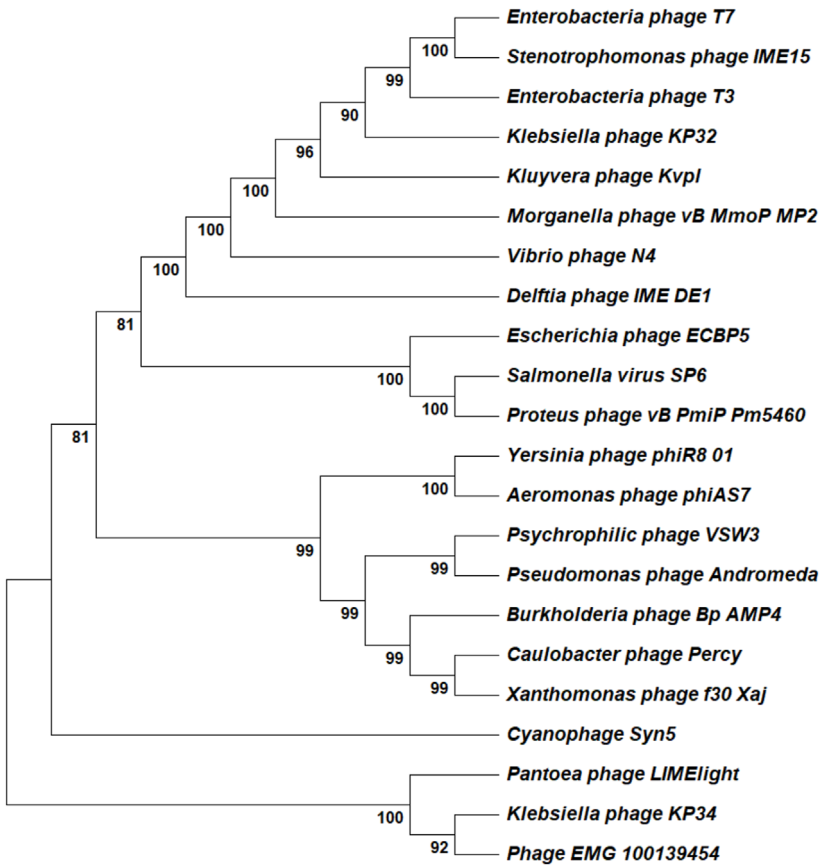

FIGURE 6
Phylogenetic analysis of T7 RNAP alternatives. All the reported alternatives are single-subunit RNAPs and the analysis was done using a simple neighbor-joining tree. The analyzed RNAPs belong to the *Autographiviridae* family.

undergo stringent quality control and testing, 3) include thorough documentation, offering traceability of raw materials, batch records, testing results, and certificates of analyses. RNAPs used in mRNA manufacturing are manufactured and formulated like any other reagents; therefore, GMP compliance that ensures consistent functioning should be followed. Certificates of analysis with enzyme activity and purity and a list of ancillary materials should be provided. Moreover, these criteria may change depending on any additional modifications to the RNAP, including changes to the expression host (e.g., *Escherichia coli*) and plasmid vector containing the RNAP gene sequence.

The development of computational models for better process monitoring and control is the next step in process optimization/improvement; these models can either be data-driven or mechanistic models (based on reaction kinetic or mass balance) (Hengelbrock et al., 2023). Data-driven models are black boxes that solely rely on process data and are robust within the model input-output variable space (capable of mostly interpolation). On the other hand, mechanistic models are robust and can be capable of extrapolation, but they are relatively more difficult to develop and computationally complex. Hybrid models that combine the advantages of both these models could be an ideal solution, but this will require better process characterization (Nair et al., 2024). Looking at the IVT reaction based on the influence of CMAs/CPPs on the RNAP and the CQA of the synthesized process output will undoubtedly benefit better process and quality control. Furthermore, the transition to bioprocess 4.0 will also require adopting digital tools such as soft sensors and digital twins that rely on process data and a robust computational model derived from a well-characterized process (Isoko et al., 2024).

In the end, the efficiency of the manufacturing process determines the economic viability of the drug product and if the manufacturing costs associated with a drug modality are high, its wider adoption is severely hindered. As mRNA-based vaccines have proven their effectiveness, more and more products are being designed with this technology for both prophylactic and therapeutic applications. Currently, mRNA manufacturing is expensive, with raw material costs dominating the operating expenditure; most of this can be attributed to the use of proprietary reagents such as cap analogs used in the co-transcriptional capping of mRNA. As mentioned in the previous sections, strategies that can reduce the amount of these reagents or circumvent them completely can drastically reduce production costs (Kis et al., 2020b). Moreover, product-related impurities, such as immunogenic dsRNA, need to be separated from the drug substance before it can be formulated into the drug product. Downstream purification processes are another major cost contributor to the overall manufacturing process (Kis et al., 2020b). If the generation of unwanted byproducts can

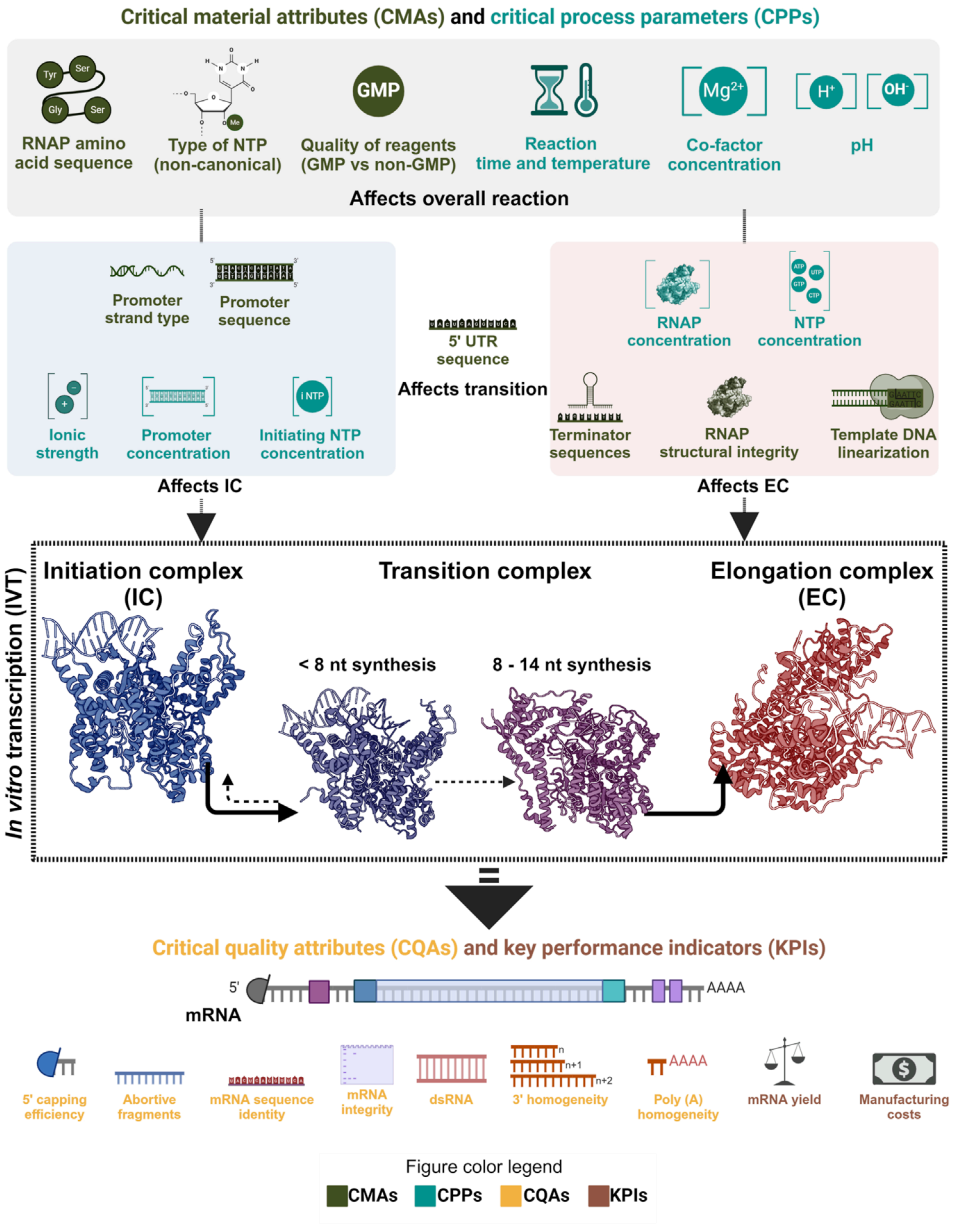

FIGURE 7
Effect of CPPs and CMAs on the T7 RNAP during the IVT reaction. CPPs and CMAs that affect the overall reaction are grouped in the grey box, the ones that affect the IC are grouped in the blue box and the ones that affect the EC are grouped in the red box. QbD implementation based on the insights gained from these interactions would serve to optimize the CQAs and KPIs of the final product and manufacturing process, respectively. Initiation complex with synthesis up to 3 nucleotides is depicted by PDB-1QLN. The transition complexes with the synthesis of RNA up to 8-nt is depicted by PDB-3E3J and the synthesis of 8–14-nt is depicted by PDB-1MSW. The elongation complex is depicted by PDB-1S76.

be reduced, it can have huge implications for the costs associated with downstream processes. Some of the product-related impurities are very challenging to remove even with advanced purification strategies; this reduces the effective yield from the IVT process and the downstream purification processes. Indeed, modifications to the T7 RNAP, as previously described, aim to reduce the overall manufacturing costs. The RNAP is also a significant contributor to the cost of raw materials, and therefore, strategies to reduce this should be seriously considered. Simple strategies can be effective, such as optimizing RNAP concentration in the IVT reaction to avoid reagent excess. More complex strategies could involve a change in the mode of operation for the IVT reaction; recently, a shift from batch mode of operation to fed-batch was suggested to produce large quantities of mRNA all the while using relatively less amount of RNAP (Elich et al., 2020; Skok et al., 2022a; Pregeljc et al., 2023; Boman et al., 2024; Guo et al., 2024). Enzyme reuse/recycling could be another method for cost reduction. Immobilized T7 RNAP is reported to be reused in multiple cycles of IVT reaction. Moreover, some modifications with immobilized T7 RNAP have also been suggested to reduce the synthesis of product-related impurities,

thus reducing downstream process-related costs. If we look at the IVT reaction closely, we can see that optimizing the catalyst can be the solution to making mRNA manufacturing more cost-competitive. There have been multiple studies done to optimize the large-scale IVT reaction, but these have yet to include a fundamental understanding of how RNAPs influence the final quality of the product. As summarized, there are CMAs and CPPs that do not directly influence the final product; they influence the RNAP that synthesizes the mRNA and improving its functionality may hold the key to the success of this drug substance. Figure 7 summarizes the effect of CPPs and CMAs on the T7 RNAP during the IVT reaction as discussed.

5 Conclusion

In this review, we assessed the role of bacteriophage-derived RNAPs in the IVT reaction from a QbD perspective, as these enzymes are at the center of the IVT reaction that has enabled the synthesis of a drug substance class that has gained significant traction ever since the success of mRNA vaccines during the SARS CoV2 pandemic. Decades of fundamental research have enabled extensive characterization of the RNAPs used for large-scale mRNA synthesis. Combining this wealth of knowledge with the QbD approach can improve the manufacturing process and make it highly efficient. We provided a historical background to the discovery and initial characterization of the most used bacteriophage-derived RNAPs and used T7 RNAP to represent industrially applicable single-subunit RNAPs to explain the various phases of the transcription reaction. The influence of CMAs and CPPs involved with the IVT reaction and their direct influence on the RNAP was also considered; this should help implement the QbD approach from a mechanistic perspective. Moreover, we tried to combine the structure-function relationship and industrial applicability of the T7 RNAP and several of its mutants. Alternatives to T7 RNAP were also discussed, although it should be noted that industrial use of any of the less characterized alternatives will likely have significant regulatory hurdles. An advantage of wild-type T7 RNAP is its extensive characterization, which lowers risks and increases the likelihood of faster regulatory approvals. We concluded the review by emphasizing the influence of RNAP on the economics of the mRNA manufacturing process. Considerable improvements to the production costs can be achieved by the use of RNAPs that reduce raw material utilization (pertaining to cap analogs) or circumvent the use of proprietary reagents altogether (single-pot synthesis and enzymatic capping). The reuse/recycling of RNAPs can also reduce manufacturing costs and improve the overall sustainability of the manufacturing process.

Author contributions

AN: Conceptualization, Writing–original draft, Writing–review and editing. ZK: Funding acquisition, Supervision, Writing–original draft, Writing–review and editing.

Funding

The author(s) declare that financial support was received for the research, authorship, and/or publication of this article. This research is funded by the Department of Health and Social Care using United Kingdom Aid funding and is managed by the EPSRC. This study was co-funded by Wellcome Leap R3 Program. This funder played no role in study design, data collection, analysis and interpretation of data, or the writing of this manuscript. Open access publication was supported by the University of Sheffield Institutional Open Access Fund.

Conflict of interest

The authors declare that the research was conducted in the absence of any commercial or financial relationships that could be construed as a potential conflict of interest.

Generative AI statement

The author(s) declare that no Generative AI was used in the creation of this manuscript.

Publisher's note

All claims expressed in this article are solely those of the authors and do not necessarily represent those of their affiliated organizations, or those of the publisher, the editors and the reviewers. Any product that may be evaluated in this article, or claim that may be made by its manufacturer, is not guaranteed or endorsed by the publisher.

Author disclaimer

The views expressed in this publication are those of the author(s) and not necessarily those of the Department of Health and Social Care.

References

Adie, T., Orefo, I., Kysh, D., Kondas, K., Thapa, S., Extance, J., et al. (2022). dbDNA™: an advanced platform for genetic medicines. *Drug Discov. Today* 27, 374–377. doi:10.1016/J.DRUDIS.2021.09.018

Akama, S., Yamamura, M., and Kigawa, T. (2012). A multiphysics model of *in vitro* transcription coupling enzymatic reaction and precipitation formation. *Biophys. J.* 102, 221–230. doi:10.1016/j.bpj.2011.12.014

Bai, L., Santangelo, T. J., and Wang, M. D. (2006). Single-molecule analysis of RNA polymerase transcription. *Annu. Rev. Biophys. Biomol. Struct.* 35, 343–360. doi:10.1146/ANNUREV.BIOPHYS.35.010406.150153

Bai, Y., Liu, D., He, Q., Liu, J., Mao, Q., and Liang, Z. (2023). Research progress on circular RNA vaccines. *Front. Immunol.* 13, 1091797. doi:10.3389/fimmu.2022.1091797

Bailey, J. N., Klement, J. F., and McAllister, W. T. (1983). Relationship between promoter structure and template specificities exhibited by the bacteriophage T3 and T7 RNA polymerases. *Proc. Natl. Acad. Sci.* 80, 2814–2818. doi:10.1073/PNAS.80.10.2814

Bandwar, R. P., Jia, Y., Stano, N. M., and Patel, S. S. (2002). Kinetic and thermodynamic basis of promoter strength: multiple steps of transcription initiation by T7 RNA polymerase are modulated by the promoter sequence. *Biochemistry* 41, 3586–3595. doi:10.1021/BI0158472

Bandwar, R. P., Ma, N., Emanuel, S. A., Anikin, M., Vassylyev, D. G., Patel, S. S., et al. (2007). The transition to an elongation complex by T7 RNA polymerase is a multistep process. *J. Biol. Chem.* 282, 22879–22886. doi:10.1074/JBC.M702589200

Bandwar, R. P., and Patel, S. S. (2002). The energetics of consensus promoter opening by T7 RNA polymerase. *J. Mol. Biol.* 324, 63–72. doi:10.1016/S0022-2836(02)01034-3

Barreira, M., Kerridge, C., Jorda, S., Olofsson, D., Neumann, A., Horton, H., et al. (2022). Enzymatically amplified linear dbDNATM as a rapid and scalable solution to industrial lentiviral vector manufacturing. *Gene Ther.* 30 (1 30), 122–131. doi:10.1038/s41434-022-00343-4

Basu, S., Maitra, U., Ikeda, R. A., and Richardson, C. C. (1989). T7 RNA Polymerase Interacts with its Promoter from One Side of the DNA the interactions of T7 RNA polymerase with its promoter DNA have been previously probed in footprinting experiments with either DNase I or (methidiumpropyl-EDTA)-Fe(II) to cleave unprotected DNA. Available at: https://pubs.acs.org/sharingguidelines.

Bautz, E. K., McAllister, W. T., Küpper, H., Beck, E., and Bautz, F. A. (1974). Initiation of transcription by RNA polymerases of *E. coli* and phage T3. *Adv. Exp. Med. Biol.* 44, 7–21. doi:10.1007/978-1-4684-3246-6_2

Berg, O. G., Winter, R. B., and von Hippel, P. H. (1981). Diffusion-driven mechanisms of protein translocation on nucleic acids. 1. Models and theory. *Biochemistry* 20, 6929–6948. doi:10.1021/bi00527a028

Bishayee, S., Yudelevich, A., and Maitra, U. (1976). Specificity of RNA chain initiation by bacteriophage T7-induced RNA polymerase. *Biochem. Biophys. Res. Commun.* 68, 626–633. doi:10.1016/0006-291X(76)91191-8

Bloom, K., van den Berg, F., and Arbuthnot, P. (2020). Self-amplifying RNA vaccines for infectious diseases. *Gene Ther.* 28 (3 28), 117–129. doi:10.1038/s41434-020-00204-y

Boman, J., Marušič, T., Seravalli, T. V., Skok, J., Pettersson, F., Nemec, K. Š., et al. (2024). Quality by design approach to improve quality and decrease cost of *in vitro* transcription of mRNA using design of experiments. *Biotechnol. Bioeng.* 121, 3415–3427. doi:10.1002/BIT.28806

Brakmann, S., and Ibach, J. (2015). T7 RNA polymerase variants and methods of using the same.

Brieba, L. G., Padilla, R., and Sousa, R. (2002). Role of T7 RNA polymerase His784 in start site selection and initial transcription. *Biochemistry* 41, 5144–5149. doi:10.1021/BI016057V

Brieba, L. G., and Sousa, R. (2000). Roles of histidine 784 and tyrosine 639 in ribose discrimination by T7 RNA polymerase. *Biochemistry*, 39, 919, 923. doi:10.1021/bi992324+

Brieba, L. G., and Sousa, R. (2001). The T7 RNA polymerase intercalating hairpin is important for promoter opening during initiation but not for RNA displacement or transcription bubble stability during elongation. *Biochemistry* 40, 3882–3890. doi:10.1021/BI002716C

Butler, E. T., and Chamberlin, M. J. (1982). Bacteriophage SP6-specific RNA polymerase. I. Isolation and characterization of the enzyme. *J. Biol. Chem.* 257, 5772–5778. doi:10.1016/s0021-9258(19)83846-2

Calvopina-Chavez, D. G., Gardner, M. A., and Griffitts, J. S. (2022). Engineering efficient termination of bacteriophage T7 RNA polymerase transcription. *Genes.|Genomes|Genetics* G3, jkac070. doi:10.1093/G3JOURNAL/JKAC070

Cameron, I. (2024). 4basebio: unlocking the potential of synthetic DNA. *Glob. Pharma, NA-NA*. Available at: https://go.gale.com/ps/i.do?p=HRCA&sw=w&issn=&v=2.1&it=r&id=GALE%7CA780334827&sid=googleScholar&linkaccess=fulltext (Accessed September 21, 2024).

Carter, A. D., and McAllister, W. T. (1981). Sequences of three class II promoters for the bacteriophage T7 RNA polymerase. *J. Mol. Biol.* 153, 825–830. doi:10.1016/0022-2836(81)90421-6

Cavac, E., Ramírez-Tapia, L. E., and Martin, C. T. (2021). High-salt transcription of DNA cotethered with T7 RNA polymerase to beads generates increased yields of highly pure RNA. *J. Biol. Chem.* 297, 100999. doi:10.1016/J.JBC.2021.100999

Cermakian, N., Ikeda, T. M., Miramontes, P., Lang, B. F., Gray, M. W., and Cedergren, R. (1997). On the evolution of the single-subunit RNA polymerases. *J. Mol. Evol.* 45, 671–681. doi:10.1007/PL00006271

Chakraborty, P. R., Sarkar, P., Huang, H. H., and Maitra, U. (1973). Studies on T3-induced ribonucleic acid polymerase: III. Purification and characterization of the T3-INDUCED ribonucleic acid polymerase from bacteriophage T3-INFECTED ESCHERICHIA coli cells. *J. Biol. Chem.* 248, 6637–6646. doi:10.1016/S0021-9258(19)43401-7

Chamberlin, M., Mcgrath, J., and Waskell, L. (1970). New RNA polymerase from *Escherichia coli* infected with bacteriophage T7. *Nature* 228, 227–231. doi:10.1038/228227A0

Chamberlin, M., and Ring, J. (1973a). Characterization of T7-specific ribonucleic acid polymerase: I. General properties of the enzymatic reaction and the template specificity of the enzyme. *J. Biol. Chem.* 248, 2235–2244. doi:10.1016/S0021-9258(19)44211-7

Chamberlin, M., and Ring, J. (1973b). Characterization of T7-specific ribonucleic acid polymerase: II. Inhibitors of the enzyme and their application to the study of the enzymatic reaction. *J. Biol. Chem.* 248, 2245–2250. doi:10.1016/S0021-9258(19)44212-9

Chamberlin, M., and Ryan, T. (1982). 4 bacteriophage DNA-dependent RNA polymerases. *Enzym. Ess.* 15, 87–108. doi:10.1016/S1874-6047(08)60276-0

Chamberlin, M. J. (1974). The selectivity of transcription. *Annu. Rev. Biochem.* 43, 721–775. doi:10.1146/annurev.bi.43.070174.003445

Chamberlin, M. J., and Ring, J. (1972). Characterization of T7 specific RNA polymerase. 3. Inhibition by derivatives of rifamycin SV. *Biochem. Biophys. Res. Commun.* 49, 1129–1136. doi:10.1016/0006-291X(72)90330-0

Chan, S. H., Tirole, L., Kneller, D., Kelley, T. M., Dai, N., and Robb, G. B. (2023). Co-transcriptional capping using an RNA capping enzyme-T7 RNA polymerase fusion protein. *bioRxiv*, 2023. doi:10.1101/2023.10.28.564488

Chapman, K. A., and Burgess, R. R. (1987). Construction of bacteriophage T7 late promoters with point mutations and characterization by *in vitro* transcription properties. *Nucleic Acids Res.* 15, 5413–5432. doi:10.1093/NAR/15.13.5413

Cheetham, G. M. T., Jeruzalmi, D., and Steltz, T. A. (1999). Structural basis for initiation of transcription from an RNA polymerase-promoter complex. *Nature* 399, 80–83. doi:10.1038/19999

Cheetham, G. M. T., and Steitz, T. A. (1999). Structure of a transcribing T7 RNA polymerase initiation complex. *Science* 286, 2305–2309. doi:10.1126/SCIENCE.286.5448.2305

Chelliserrykattil, J., and Ellington, A. D. (2004). Evolution of a T7 RNA polymerase variant that transcribes 2'-O-methyl RNA. *Nat. Biotechnol.* 22, 1155–1160. doi:10.1038/NBT1001

Chen, T. H., Potapov, V., Dai, N., Ong, J. L., and Roy, B. (2022). N1-methyl-pseudouridine is incorporated with higher fidelity than pseudouridine in synthetic RNAs. *Sci. Rep.* 12, 13017. doi:10.1038/S41598-022-17249-1

Comes, J. D. G., Pijlman, G. P., and Hick, T. A. H. (2023). Rise of the RNA machines – self-amplification in mRNA vaccine design. *Trends Biotechnol.* 41, 1–8. doi:10.1016/j.tibtech.2023.05.007

Conrad, T., Plumbom, I., Alcobendas, M., Vidal, R., and Sauer, S. (2020). Maximizing transcription of nucleic acids with efficient T7 promoters. *Commun. Biol.* 3 (1 3), 439–448. doi:10.1038/s42003-020-01167-x

Curry, E., Sedelnikova, S., Rafferty, J., Hulley, M., Pohle, M., Muir, G., et al. (2024). Expanding the RNA polymerase biocatalyst solution space for mRNA manufacture. *Biotechnol. J.* 19, 2400012. doi:10.1002/BIOT.202400012

CustomBiotech (2023). Starting guidelines for the use of SP6 RNA Polymerase for mRNA synthesis. Available at: https://custombiotech.roche.com/global/en/products/cb/sp6-rna-polymerase-rec-gmp-grade-pid00000520.html?gclid=CjwKCAjwl6-3BhBWEiwApN6_ko2YZhHRb8gTlsdVkWmEQJ5eoMhzDDXW0W3-kFIU9PbWHTGdHq6ydhoCvNQQAvD_BwE&s_kwcid=AL!13333!3!664918111647!p!!g!!sp6%20polymerase (Accessed September 20, 2024).

Da, L. T., Chao, E., Shuai, Y., Wu, S., Su, X. D., and Yu, J. (2017). T7 RNA polymerase translocation is facilitated by a helix opening on the fingers domain that may also prevent backtracking. *Nucleic Acids Res.* 45, 7909–7921. doi:10.1093/NAR/GKX495

Daniel, S., Kis, Z., Kontoravdi, C., and Shah, N. (2022). Quality by Design for enabling RNA platform production processes. *Trends Biotechnol.* 40, 1213–1228. doi:10.1016/J.TIBTECH.2022.03.012

Davanloo, P., Rosenberg, A. H., Dunn, J. J., and Studier, F. W. (1984). Cloning and expression of the gene for bacteriophage T7 RNA polymerase. *Proc. Natl. Acad. Sci.* 81, 2035–2039. doi:10.1073/PNAS.81.7.2035

Dhir, A., Winckler, C., Mañas, C., Lal, C., Whiffen, Z., Picher, Á., et al. (2024). Synthetic, enzymatically produced dna for gene therapy and vaccine applications. *Cytotherapy* 26, S133–S134. doi:10.1016/J.JCYT.2024.03.255

Dias, A., Crawford, D., DeRosa, F., Abysalh, J., and Heartlein, M. (2018). inventors; Translate Bio, Inc, assignee; Large scale synthesis of messenger RNA. United States patent application US 2018/0258423 A1.

Dietz, A., Weisser, H. J., Kössel, H., and Hausmann, R. (1990). The gene for Klebsiella bacteriophage K11 RNA polymerase: sequence and comparison with the homologous genes of phages T7, T3, and SP6. *Mol. Gen. Genet.* 221, 283–286. doi:10.1007/BF00261733

Dousis, A., Ravichandran, K., Hobert, E. M., Moore, M. J., and Rabideau, A. E. (2023). An engineered T7 RNA polymerase that produces mRNA free of immunostimulatory byproducts. *Nat. Biotechnol.* 41, 560–568. doi:10.1038/s41587-022-01525-6

Dunn, J. J., Anderson, C. W., Atkins, J. F., Bartelt, D. C., and Crockett, W. C. (1977). Bacteriophages T7 and T3 as model systems for RNA synthesis and processing. *Prog. Nucleic Acid. Res. Mol. Biol.* 19, 263–273. doi:10.1016/S0079-6603(08)60924-1

Dunn, J. J., Bautz, F. A., and Bautz, E. K. F. (1971). Different template specificities of phage T3 and T7 RNA polymerases. *Nat. New Biol.* 230 (11 230), 94–96. doi:10.1038/newbio230094a0

Durniak, K. J., Bailey, S., and Steitz, T. A. (2008). The structure of a transcribing T7 RNA polymerase in transition from initiation to elongation. *Science* 322, 553–557. doi:10.1126/science.1163433

Elich, J., Rabideau, A., Shamashkin, M., Philpot, R., Fritz, B., and Wojciechowski, P. (2020). inventors; ModernaTX, Inc, assignee; Fed-batch *in vitro* transcription process. *WO 2020/185811 A1*.

Ellington, A. D., and Meyer, A. J. (2018). inventors; the Board of Regents of the University of Texas System, assignee; T7 RNA polymerase variants with expanded substrate range and enhanced transcriptional yield. *U. S. Pat.*, 9988612.

Eun, H.-M. (1996). RNA polymerases, *Biochemistry*, 491–565. doi:10.1016/B978-012243740-3/50010-7

Gardner, L. P., Mookhtiar, K. A., and Coleman, J. E. (1997). Initiation, elongation, and processivity of carboxyl-terminal mutants of T7 RNA polymerase. *Biochemistry* 36, 2908–2918. doi:10.1021/BI962397I

Gelfand, D. H., and Hayashi, M. (1970). *In vitro* synthesis of a DNA dependent RNA polymerase coded on coliphage T7 genome. *Nature* 228 (5277 228), 1162–1165. doi:10.1038/2281162a0

Gholamalipour, Y., Johnson, W. C., and Martin, C. T. (2019). Efficient inhibition of RNA self-primed extension by addition of competing 3′-capture DNA-improved RNA synthesis by T7 RNA polymerase. *Nucleic Acids Res.* 47, e118. doi:10.1093/NAR/GKZ700

Gholamalipour, Y., Karunanayake Mudiyanselage, A., and Martin, C. T. (2018). 3′ end additions by T7 RNA polymerase are RNA self-templated, distributive and diverse in character—RNA-Seq analyses. *Nucleic Acids Res.* 46, 9253–9263. doi:10.1093/NAR/GKY796

Golomb, M., and Chamberlin, M. (1974). Characterization of T7-specific ribonucleic acid polymerase: IV. Resolution of the major *in vitro* transcripts by gel electrophoresis. *J. Biol. Chem.* 249, 2858–2863. doi:10.1016/S0021-9258(19)42709-9

Gong, P., Esposito, E. A., and Martin, C. T. (2004). Initial bubble collapse plays a key role in the transition to elongation in T7 RNA polymerase. *J. Biol. Chem.* 279, 44277–44285. doi:10.1074/JBC.M409118200

Gong, P., and Martin, C. T. (2006). Mechanism of instability in abortive cycling by T7 RNA polymerase. *J. Biol. Chem.* 281, 23533–23544. doi:10.1074/JBC.M604023200

Greene, J., Baird, A. M., Brady, L., Lim, M., Gray, S. G., McDermott, R., et al. (2017). Circular RNAs: biogenesis, function and role in human diseases. *Front. Mol. Biosci.* 4, 38. doi:10.3389/fmolb.2017.00038

Greif, M., Rudolph, C., Schmidt, M., Sobek, H., and Thalhofer, J.-P. (2017). *T7 RNA polymerase variants with cysteine-serine substitutions*. US patent 9663769 B2. Basel, Switzerland: Roche Diagnostics International. assignee.

Guilleres, J., Lopez, P. J., Proux, F., Launay, H., and Dreyfus, M. (2005). A mutation in T7 RNA polymerase that facilitates promoter clearance. *Proc. Natl. Acad. Sci. U. S. A.* 102, 5958–5963. doi:10.1073/PNAS.0407141102

Guillerez, J., Lopez, P., and Dreyfus, M. (2004). inventors; Centre National de la Recherche Scientifique, assignee; Polypeptides derived from RNA polymerases and use thereof. *U. S. Pat. Appl. U. S. 2004/0091854A1*.

Guo, L., Liu, Z., Song, S., Yao, W., Yang, M., and Chen, G. (2024). Maximizing the mRNA productivity for *in vitro* transcription by optimization of fed-batch strategy. *Biochem. Eng. J.* 210, 109412. doi:10.1016/J.BEJ.2024.109412

Guo, Q., and Sousa, R. (2006). Translocation by T7 RNA polymerase: a sensitively poised Brownian ratchet. *J. Mol. Biol.* 358, 241–254. doi:10.1016/J.JMB.2006.02.001

Guthold, M., Zhu, X., Rivetti, C., Yang, G., Thomson, N. H., Kasas, S., et al. (1999). Direct observation of one-dimensional diffusion and transcription by *Escherichia coli* RNA polymerase. *Biophys. J.* 77, 2284–2294. doi:10.1016/S0006-3495(99)77067-0

Harada, Y., Funatsu, T., Murakami, K., Nonoyama, Y., Ishihama, A., and Yanagida, T. (1999). Single-molecule imaging of RNA polymerase-DNA interactions in real time. *Biophys. J.* 76, 709–715. doi:10.1016/S0006-3495(99)77237-1

Harada, Y., Ohara, O., Takatsuki, A., Itoh, H., Shimamoto, N., and Kinosita, K. (2001). Direct observation of DNA rotation during transcription by *Escherichia coli* RNA polymerase. *Nature* 409, 113–115. doi:10.1038/35051126

He, B., Kukarin, A., Temiakov, D., Chin-Bow, S. T., Lyakhov, D. L., Rong, M., et al. (1998). Characterization of an unusual, sequence-specific termination signal for T7 RNA polymerase. *J. Biol. Chem.* 273, 18802–18811. doi:10.1074/jbc.273.30.18802

Helmann, J. D., and Chamberlin, M. J. (1988). Structure and function of bacterial sigma factors. *Annu. Rev. Biochem.* 57, 839–872. doi:10.1146/annurev.bi.57.070188.004203

Hengelbrock, A., Schmidt, A., and Strube, J. (2023). Digital twin fundamentals of mRNA *in vitro* transcription in variable scale toward autonomous operation. *ACS Omega* 9, 8204–8220. doi:10.1021/acsomega.3c08732

Hie, B. L., and Yang, K. K. (2022). Adaptive machine learning for protein engineering. *Curr. Opin. Struct. Biol.* 72, 145–152. doi:10.1016/J.SBI.2021.11.002

Hogrefe, R., Lebedev, A., Mccaffrey, A., and Shin, D. (2017). Compositions and methods for synthesizing 5′- capped RNAs .

Horwitz, M. S. Z., and Loeb, L. A. (1990). Structure—function relationships in *Escherichia coli* promoter DNA. *Prog. Nucleic Acid. Res. Mol. Biol.* 38, 137–164. doi:10.1016/S0079-6603(08)60710-2

Hurwitz, J. (2005). The discovery of RNA polymerase. *J. Biol. Chem.* 280, 42477–42485. doi:10.1074/jbc.X500006200

Hurwitz, J., Bresler, A., and Diringer, R. (1960). The enzymic incorporation of ribonucleotides into polyribonucleotides and the effect of DNA. *Biochem. Biophys. Res. Commun.* 3, 15–19. doi:10.1016/0006-291X(60)90094-2

Ikeda, R. A. (1995). *Mutant T7 RNA polymerase GP1(lys22) exhibiting altered promoter recognition*. US patent 5385834. Atlanta, GA, United States: Georgia Tech Research Corporation, assignee.

Ikeda, R. A., and Richardson, C. C. (1986a). Interactions of the RNA polymerase of bacteriophage T7 with its promoter during binding and initiation of transcription. *Proc. Natl. Acad. Sci. U. S. A.* 83, 3614–3618. doi:10.1073/PNAS.83.11.3614

Imburgio, D., Rong, M., Ma, K., and McAllister, W. T. (2000). Studies of promoter recognition and start site selection by T7 RNA polymerase using a comprehensive collection of promoter variants. *Biochemistry* 39, 10419–10430. doi:10.1021/BI000365W

Isoko, K., Cordiner, J. L., Kis, Z., and Moghadam, P. Z. (2024). Bioprocessing 4.0: a pragmatic review and future perspectives. *Digit. Discov.* 3, 1662–1681. doi:10.1039/D4DD00127C

Jain, R. (2021). inventors; GreenLight Biosciences, Inc, assignee; T7 RNA polymerase variants. United States patent application US 2021/0180034 A1.

Jia, Y., Kumar, A., and Patel, S. S. (1996). Equilibrium and stopped-flow kinetic studies of interaction between T7 RNA polymerase and its promoters measured by protein and 2-aminopurine fluorescence changes. *J. Biol. Chem.* 271, 30451–30458. doi:10.1074/JBC.271.48.30451

Jia, Y., and Patel, S. S. (1997). Kinetic mechanism of transcription initiation by bacteriophage T7 RNA polymerase. *Biochemistry* 36, 4223–4232. doi:10.1021/BI9630467

Joho, K. E., Gross, L. B., McGraw, N. J., Raskin, C., and McAllister, W. T. (1990). Identification of a region of the bacteriophage T3 and T7 RNA polymerases that determines promoter specificity. *J. Mol. Biol.* 215, 31–39. doi:10.1016/S0022-2836(05)80092-0

Jones, C. H., Androsavich, J. R., So, N., Jenkins, M. P., MacCormack, D., Prigodich, A., et al. (2024). Breaking the mold with RNA—a "RNAissance" of life science. *NPJ Genom Med.* 9, 2. doi:10.1038/S41525-023-00387-4

Jorgensen, E. D., Durbin, R. K., Risman, S. S., and McAllister, W. T. (1991). Specific contacts between the bacteriophage T3, T7, and SP6 RNA polymerases and their promoters. *J. Biol. Chem.* 266, 645–651. doi:10.1016/s0021-9258(18)52483-2

Kassavetis, G. A., Butler, E. T., Roulland, D., and Chamberlin, M. J. (1982). Bacteriophage SP6-specific RNA polymerase. II. Mapping of SP6 DNA and selective *in vitro* transcription. *J. Biol. Chem.* 257, 5779–5788. doi:10.1016/S0021-9258(19)83847-4

Kim, J. H., and Larson, R. G. (2007). Single-molecule analysis of 1D diffusion and transcription elongation of T7 RNA polymerase along individual stretched DNA molecules. *Nucleic Acids Res.* 35, 3848–3858. doi:10.1093/NAR/GKM332

Kirsch, S. H., Haeckl, F. P. J., and Müller, R. (2022). Beyond the approved: target sites and inhibitors of bacterial RNA polymerase from bacteria and fungi. *Nat. Prod. Rep.* 39, 1226–1263. doi:10.1039/D1NP00067E

Kis, Z., Kontoravdi, C., Dey, A. K., Shattock, R., and Shah, N. (2020a). Rapid development and deployment of high-volume vaccines for pandemic response. *J. Adv. Manuf. Process* 2, e10060. doi:10.1002/AMP2.10060

Kis, Z., Kontoravdi, C., Shattock, R., and Shah, N. (2020b). Resources, production scales and time required for producing RNA vaccines for the global pandemic demand. *Vaccines* 9, 3–9. doi:10.3390/VACCINES9010003

Klement, J. F., Moorefiedl, M. B., Jorgensen, E., Brown, J. E., Risman, S., and McAllister, W. T. (1990). Discrimination between bacteriophage T3 and T7 promoters by the T3 and T7 RNA polymerases depends primarily upon a three base-pair region located 10 to 12 base-pairs upstream from the start site. *J. Mol. Biol.* 215, 21–29. doi:10.1016/S0022-2836(05)80091-9

Koh, H. R., Roy, R., Sorokina, M., Tang, G. Q., Nandakumar, D., Patel, S. S., et al. (2018). Correlating transcription initiation and conformational changes by a single-subunit RNA polymerase with near base-pair resolution. *Mol. Cell.* 70, 695–706. doi:10.1016/J.MOLCEL.2018.04.018

Kotani, H., Ishizaki, Y., Hiraoka, N., and Obayashi, A. (1987). Nucleotide sequence and expression of the cloned gene of bacteriophage SP6 RNA polymerase. *Nucleic Acids Res.* 15, 2653–2664. doi:10.1093/nar/15.6.2653

Krieg, P. A., and Melton, D. A. (1984). Functional messenger RNAs are produced by SP6 *in vitro* transcription of cloned cDNAs. *Nucleic Acids Res.* 12, 7057–7070. doi:10.1093/NAR/12.18.7057

Krupp, G. (1988). RNA synthesis: strategies for the use of bacteriophage RNA polymerases. *Gene* 72, 75–89. doi:10.1016/0378-1119(88)90129-1

Kumar, A., Blum, J., Thanh Le, T., Havelange, N., Magini, D., and Yoon, I. K. (2022). The mRNA vaccine development landscape for infectious diseases. *Nat. Rev. Drug Discov.* 21, 333–334. doi:10.1038/D41573-022-00035-Z

Küpper, H. A., McAllister, W. T., and Bautz, E. K. F. (1973). Comparison of *Escherichia coli* and T3 RNA polymerases. Differential inhibition of transcription by various drugs. *Eur. J. Biochem.* 38, 581–586. doi:10.1111/J.1432-1033.1973.TB03093.X

Kuzmine, I., Gottlieb, P. A., and Martin, C. T. (2003). Binding of the priming nucleotide in the initiation of transcription by T7 RNA polymerase. *J. Biol. Chem.* 278, 2819–2823. doi:10.1074/JBC.M208405200

Kuzmine, I., and Martin, C. T. (2001). Pre-steady-state kinetics of initiation of transcription by T7 RNA polymerase: a new kinetic model. *J. Mol. Biol.* 305, 559–566. doi:10.1006/JMBI.2000.4316

Lee, C. Y., and Myong, S. (2021). Probing steps in DNA transcription using single-molecule methods. *J. Biol. Chem.* 297, 101086–101300. doi:10.1016/j.jbc.2021.101086

Lenk, R., Kleindienst, W., Szabó, G. T., Baiersdörfer, M., Boros, G., Keller, J. M., et al. (2024). Understanding the impact of *in vitro* transcription byproducts and contaminants. *Front. Mol. Biosci.* 11, 1426129. doi:10.3389/fmolb.2024.1426129

Li, T., Ho, H. H., Maslak, M., Schick, C., and Martin, C. T. (1996). Major groove recognition elements in the middle of the T7 RNA polymerase promoter. *Biochemistry* 35, 3722–3727. doi:10.1021/BI9524373

Lillehaug, J. R., Helland, D., and Sjöberg, N. O. (1973). *In vivo* and *in vitro* transcription of T7 early genes by T7 RNA polymerase. *FEBS Lett.* 33, 335–338. doi:10.1016/0014-5793(73)80224-8

Liu, C., and Martin, C. T. (2001). Fluorescence characterization of the transcription bubble in elongation complexes of T7 RNA polymerase. *J. Mol. Biol.* 308, 465–475. doi:10.1006/JMBI.2001.4601

Liu, C., and Martin, C. T. (2002). Promoter clearance by T7 RNA polymerase. Initial bubble collapse and transcript dissociation monitored by base analog fluorescence. *J. Biol. Chem.* 277, 2725–2731. doi:10.1074/jbc.M108856200

Liu, X., and Martin, C. T. (2009). Transcription elongation complex stability: the topological lock. *J. Biol. Chem.* 284, 36262–36270. doi:10.1074/JBC.M109.056820

Lu, X., Wu, H., Xia, H., Huang, F., Yan, Y., Yu, B., et al. (2019). Klebsiella phage KP34 RNA polymerase and its use in RNA synthesis. *Front. Microbiol.* 10, 2487. doi:10.3389/fmicb.2019.02487

Lyakhov, D. L., He, B., Zhang, X., Studier, F. W., Dunn, J. J., and McAllister, W. T. (1998). Pausing and termination by bacteriophage T7 RNA polymerase. *J. Mol. Biol.* 280, 201–213. doi:10.1006/JMBI.1998.1854

Ma, C., Yang, X., and Lewis, P. J. (2016). Bacterial transcription as a target for antibacterial drug development. *Microbiol. Mol. Biol. Rev.* 80, 139–160. doi:10.1128/MMBR.00055-15

Macdonald, L. E., Durbin, R. K., Dunn, J. J., and McAllister, W. T. (1994). Characterization of two types of termination signal for bacteriophage T7 RNA polymerase. *J. Mol. Biol.* 238, 145–158. doi:10.1006/JMBI.1994.1277

Mairhofer, J., Wittwer, A., Cserjan-Puschmann, M., and Striedner, G. (2015). Preventing T7 RNA polymerase read-through transcription-A synthetic termination signal capable of improving bioprocess stability. *ACS Synth. Biol.* 4, 265–273. doi:10.1021/sb5000115

Malag, K., Banerjee, R., Aig, C., and Mar, T. (2024). A new approach to RNA synthesis: immobilization of stably and functionally co-tethered promoter DNA and T7 RNA polymerase. *Nucleic Acids Res.* 2024, 1–12. doi:10.1093/NAR/GKAE599

MalagodaPathiranage, K., Cavac, E., Chen, T.-H., Roy, B., and Martin, C. T. (2023). High-salt transcription from enzymatically gapped promoters nets higher yields and purity of transcribed RNAs. *Nucleic Acids Res.* 51, e36. doi:10.1093/NAR/GKAD027

Martin, C. T., and Coleman, J. E. (1987). Kinetic analysis of T7 RNA polymerase-promoter interactions with small synthetic promoters. *Biochemistry* 26, 2690–2696. doi:10.1021/bi00384a006

Martin, C. T., and Coleman, J. E. (1989). T7 RNA polymerase does not interact with the 5'-phosphate of the initiating nucleotide. *Biochemistry* 28, 2760–2762. doi:10.1021/BI00433A002

Martin, C. T., Muller, D. K., and Coleman, J. E. (1988). Processivity in early stages of transcription by T7 RNA polymerase. *Biochemistry* 27, 3966–3974. doi:10.1021/BI00411A012

Martin, C. T., and Ramirez-Tapia, L. (2015). inventors; University of Massachusetts, assignee; Modified T7-related RNA polymerases and methods of use thereof. *U. S. Pat. 9045740 B2*.

Maslak, M., and Martin, C. T. (1993). Kinetic analysis of T7 RNA polymerase transcription initiation from promoters containing single-stranded regions. *Biochemistry* 32, 4281–4285. doi:10.1021/BI00067A017

Maslak, M., and Martin, C. T. (1994). Effects of solution conditions on the steady-state kinetics of initiation of transcription by T7 RNA polymerase. *Biochemistry* 33, 6918–6924. doi:10.1021/BI00188A022

Matsumoto, J. (1994). Evolutionary role of abortive transcript as a primer for DNA replication. *J. Mol. Evol.* 39, 620–624. doi:10.1007/BF00160407

McAllister, W. T. (1993). Structure and function of the bacteriophage T7 RNA polymerase (or, the virtues of simplicity). *Cell. Mol. Biol. Res.* 39, 385–391.

Mcallister, W. T., and Carter, A. D. (1980). Regulation of promoter selection by the bacteriophage T7 RNA polymerase *in vitro*. *Nucleic Acids Res.* 8, 4821–4837. doi:10.1093/NAR/8.20.4821

McAllister, W. T., and Raskin, C. A. (1993). The phage RNA polymerases are related to DNA polymerases and reverse transcriptases. *Mol. Microbiol.* 10, 1–6. doi:10.1111/J.1365-2958.1993.TB00897.X

Mcgraw, N. J., Bailey, J. N., Cleaves, G. R., Dembinski, D. R., Gocke, C. R., Joliffe, L. K., et al. (1985). Sequence and analysis of the gene for bacteriophage T3 RNA polymerase. *Nucleic Acids Res.* 13, 6753–6766. doi:10.1093/NAR/13.18.6753

Mentesana, P. E., Chin-Bow, S. T., Sousa, R., and McAllister, W. T. (2000). Characterization of halted T7 RNA polymerase elongation complexes reveals multiple factors that contribute to stability. *J. Mol. Biol.* 302, 1049–1062. doi:10.1006/JMBI.2000.4114

Meyer, A. J., Garry, D. J., Hall, B., Byrom, M. M., McDonald, H. G., Yang, X., et al. (2015). Transcription yield of fully 2′-modified RNA can be increased by the addition of thermostabilizing mutations to T7 RNA polymerase mutants. *Nucleic Acids Res.* 43, 7480–7488. doi:10.1093/NAR/GKV734

Miller, M., Alvizo, O., Baskerville, S., Chinthala, A., Chng, C., Dassie, J., et al. (2024). An engineered T7 RNA polymerase for efficient co-transcriptional capping with reduced dsRNA byproducts in mRNA synthesis. *Faraday Discuss.* 252, 431–449. doi:10.1039/D4FD00023D

Miller, M. G., Chng, C., Alvizo, O., Mayo, M. A., Riggins, J. N., Yi, X., et al. (2022). inventors; Codexis, Inc, assignee; T7 RNA polymerase variants. US patent 11236312 B2.

Miller, S. M., Wang, T., and Liu, D. R. (2020). Phage-assisted continuous and non-continuous evolution. *Nat. Protoc.* 15 (12 15), 4101–4127. doi:10.1038/s41596-020-00410-3

Milligan, J. F., Groebe, D. R., Whherell, G. W., and Uhlenbeck, O. C. (1987). Oligoribonucleotide synthesis using T7 RNA polymerase and synthetic DNA templates. *Nucleic Acids Res.* 15, 8783–8798. doi:10.1093/nar/15.21.8783

Moffatt, B. A., Dunn, J. J., and Studier, F. W. (1984). Nucleotide sequence of the gene for bacteriophage T7 RNA polymerase. *J. Mol. Biol.* 173, 265–269. doi:10.1016/0022-2836(84)90194-3

Mookhtiar, K. A., Peluso, P. S., Coleman, J. E., Muller, D. K., and Dunn, J. J. (1991). Processivity of T7 RNA polymerase requires the C-terminal phe882-ala883-COO- or "foot.". *Biochemistry* 30, 6305–6313. doi:10.1021/bi00239a032

Morris, C. E., Klement, J. F., and McAllister, W. T. (1986). Cloning and expression of the bacteriophage T3 RNA polymerase gene. *Gene* 41, 193–200. doi:10.1016/0378-1119(86)90098-3

Mosaei, H., and Harbottle, J. (2019). Mechanisms of antibiotics inhibiting bacterial RNA polymerase. *Biochem. Soc. Trans.* 47, 339–350. doi:10.1042/BST20180499

Mu, X., Greenwald, E., Ahmad, S., and Hur, S. (2018). An origin of the immunogenicity of *in vitro* transcribed RNA. *Nucleic Acids Res.* 46, 5239–5249. doi:10.1093/nar/gky177

Mukherjee, S., Brieba, L. G., and Sousa, R. (2002). Structural transitions mediating transcription initiation by T7 RNA polymerase. *Cell.* 110, 81–91. doi:10.1016/S0092-8674(02)00815-2

Muller, D. K., Martin, C. T., and Coleman, J. E. (1988). Processivity of proteolytically modified forms of T7 RNA Polymerase1. Available at: https://pubs.acs.org/sharingguidelines.

Muller, D. K., Martin, C. T., and Coleman, J. E. (1989). T7 RNA polymerase interacts with its promoter from one side of the DNA helix. *Biochemistry* 28, 3306–3313. doi:10.1021/BI00434A028

Nair, A., Loveday, K. A., Kenyon, C., Qu, J., and Kis, Z. (2024). Quality by digital design for developing platform RNA vaccine and therapeutic manufacturing processes. *Methods Mol. Biol.* 2786, 339–364. doi:10.1007/978-1-0716-3770-8_16

Nayak, D., Guo, Q., and Sousa, R. (2007). Functional architecture of T7 RNA polymerase transcription complexes. *J. Mol. Biol.* 371, 490–500. doi:10.1016/j.jmb.2007.05.070

Nelson, J., Sorensen, E. W., Mintri, S., Rabideau, A. E., Zheng, W., Besin, G., et al. (2020). Impact of mRNA chemistry and manufacturing process on innate immune activation. *Sci. Adv.* 6, eaaz6893. doi:10.1126/SCIADV.AAZ6893

Niles, E. G., Conlon, S. W., and Summers, W. C. (1974). Purification and physical characterization of T7 RNA polymerase from T7-infected escherichia coli B. *Biochemistry* 13, 3904–3912. doi:10.1021/bi00716a014

Nwokeoji, A. O., Chou, T., and Nwokeoji, E. A. (2023). Low resource integrated platform for production and analysis of capped mRNA. *ACS Synth. Biol.* 12, 329–339. doi:10.1021/acssynbio.2c00609

Oakley, J. I., Strothkamp, R. E., Sarris, A. H., and Coleman, J. E. (1979). T7 RNA polymerase: promoter structure and polymerase binding. *Biochemistry* 18, 528–537. doi:10.1021/BI00570A023

Oakley, J. L., and Coleman, J. E. (1977). Structure of a promoter for T7 RNA polymerase. *Proc. Natl. Acad. Sci. U. S. A.* 74, 4266–4270. doi:10.1073/pnas.74.10.4266

Oakley, J. L., Pascale, J. A., and Coleman, J. E. (1975). T7 RNA polymerase: conformation, functional groups, and promotor binding. *Biochemistry* 14, 4684–4691. doi:10.1021/BI00692A019

Oe, S., Sato, H., and Ide, T. (2013). RNA polymerase mutant with improved functions.

Ong, J., Potapov, V., Hung, K.-C., Asahara, H., Chong, S., and Tzertzinis, G. (2019). Inventors; new england biolabs, inc, assignee; thermostable variants of T7 RNA polymerase. US patent 10519431 B2.

Ong, J., Potapov, V., Hung, K.-C., Asahara, H., Chong, S., and Tzertzinis, G. (2022). Inventors; new england biolabs, inc, assignee; thermostable variants of T7 RNA polymerase. *U. S. Pat. Appl. U. S. 2022/0275352 A1*.

Packer, M. S., and Liu, D. R. (2015). Methods for the directed evolution of proteins. *Nat. Rev. Genet.* 16, 379–394. doi:10.1038/nrg3927

Padilla, R., and Sousa, R. (2002). A Y639F/H784A T7 RNA polymerase double mutant displays superior properties for synthesizing RNAs with non-canonical NTPs. *Nucleic Acids Res.* 30, e138. doi:10.1093/NAR/GNF138

Park, C. S., Wu, F. Y., and Wu, C. W. (1982). Molecular mechanism of promoter selection in gene transcription. II. Kinetic evidence for promoter search by a one-dimensional diffusion of RNA polymerase molecule along the DNA template. *J. Biol. Chem.* 257, 6950–6956. doi:10.1016/s0021-9258(18)34522-8

Pezo, V., and Wain-Hobson, S. (1997). Hypermutagenic *in vitro* transcription employing biased NTP pools and manganese cations. *Gene* 186, 67–72. doi:10.1016/S0378-1119(96)00682-8

Pisignano, G., Michael, D. C., Visal, T. H., Pirlog, R., Ladomery, M., and Calin, G. A. (2023). Going circular: history, present, and future of circRNAs in cancer. *Oncogene* 42 (38 42), 2783–2800. doi:10.1038/s41388-023-02780-w

Popova, P. G., Lagace, M. A., Tang, G., and Blakney, A. K. (2024). Effect of *in vitro* transcription conditions on yield of high quality messenger and self-amplifying RNA. *Eur. J. Pharm. Biopharm.* 198, 114247. doi:10.1016/J.EJPB.2024.114247

Pregeljc, D., Skok, J., Vodopivec, T., Mencin, N., Krušič, A., Ličen, J., et al. (2023). Increasing yield of *in vitro* transcription reaction with at-line high pressure liquid chromatography monitoring. *Biotechnol. Bioeng.* 120, 737–747. doi:10.1002/bit.28299

Qi, D., Ke, R., Huang, J. H., and Wu, E. (2023). Forging the future of circRNA therapeutics: unleashing synthetic potential and conquering challenges. *Mol. Ther. Nucleic Acids* 33, 42–43. doi:10.1016/j.omtn.2023.06.002

Qin, S., Tang, X., Chen, Y., Chen, K., Fan, N., Xiao, W., et al. (2022). mRNA-based therapeutics: powerful and versatile tools to combat diseases. *Signal Transduct. Target. Ther.* 7 (1 7), 166–235. doi:10.1038/s41392-022-01007-w

Rabideau, A. E., Dousis, A., Ravichandran, K., and Hobert, E. (2019). inventors; ModernaTX, assignee; RNA polymerase variants. WO 2019/036682 A1.

Ramírez-Tapia, L. E., and Martin, C. T. (2012). New insights into the mechanism of initial transcription: the T7 RNA polymerase mutant P266L transitions to elongation at longer RNA lengths than wild type. *J. Biol. Chem.* 287, 37352–37361. doi:10.1074/JBC.M112.370643

Reetz, M. T., Sun, Z., and Qu, G. (2023). Introduction to directed evolution and rational design as protein engineering techniques. *Enzyme Eng.*, 1–28. doi:10.1002/9783527836895.CH1

Rong, M., Biao, H., Mcallister, W. T., and Durbin, R. K. (1998a). Promoter specificity determinants of T7 RNA polymerase. *Proc. Natl. Acad. Sci. U. S. A.* 95, 515–519. doi:10.1073/PNAS.95.2.515

Rong, M., Durbin, R. K., and McAllister, W. T. (1998b). Template strand switching by T7 RNA polymerase. *J. Biol. Chem.* 273, 10253–10260. doi:10.1074/JBC.273.17.10253

Rosa, S. S., Nunes, D., Antunes, L., Prazeres, D. M. F., Marques, M. P. C., and Azevedo, A. M. (2022). Maximizing mRNA vaccine production with Bayesian optimization. *Biotechnol. Bioeng.* 119, 3127–3139. doi:10.1002/BIT.28216

Roy, B., and Ong, J. (2021). inventors; New England Biolabs, Inc, assignee; Methods and compositions for increasing capping efficiency of transcribed RNA. US patent 11072808 B2.

Roy, B., and Robb, B. (2022). Inventors; new england biolabs, inc, assignee; use of thermostable RNA polymerases to produce RNAs having reduced immunogenicity. *United Sates Pat. Appl. U. S. 2022/0288240 A1*.

Saltzman, A. G., and Weinmann, R. (1989). Promoter specificity and modulation of RNA polymerase II transcription. *FASEB J.* 3, 1723–1733. doi:10.1096/FASEBJ.3.6.2649403

Samnuan, K., Blakney, A. K., McKay, P. F., and Shattock, R. J. (2022). Design-of-experiments *in vitro* transcription yield optimization of self-amplifying RNA. *F1000Res* 11, 333. doi:10.12688/f1000research.75677.1

Sari, Y., Sousa Rosa, S., Jeffries, J., and Marques, M. P. C. (2024). Comprehensive evaluation of T7 promoter for enhanced yield and quality in mRNA production. *Sci. Rep.* 14 (1 14), 9655–9712. doi:10.1038/s41598-024-59978-5

Siegmund, V., Santner, T., Micura, R., and Marx, A. (2012). Screening mutant libraries of T7 RNA polymerase for candidates with increased acceptance of 2′-modified nucleotides. *Chem. Commun.* 48, 9870–9872. doi:10.1039/C2CC35028A

Skinner, G. M., Baumann, C. G., Quinn, D. M., Molloy, J. E., and Hoggett, J. G. (2004). Promoter binding, initiation, and elongation by bacteriophage T7 RNA polymerase: a single-molecule view of the transcription cycle. *J. Biol. Chem.* 279, 3239–3244. doi:10.1074/jbc.M310471200

Skok, J., Megušar, P., Vodopivec, T., Pregeljc, D., Mencin, N., Korenč, M., et al. (2022a). Gram-scale mRNA production using a 250-mL single-use bioreactor. *Chem. Ing. Tech.* 94, 1928–1935. doi:10.1002/cite.202200133

Sobek, H., Thalhofer, J.-P., Mueller, R., Schmidt, M., Greif, M., Ruf, A., et al. (2016). inventors; Roche Diagnostics Operations, Inc. assignee; T7 RNA polymerase variants with enhanced thermostability. *U. S. Pat. Appl. U. S. 2016/0032261 A1*.

Sosunov, V., Zorov, S., Sosunova, E., Nikolaev, A., Zakeyeva, I., Bass, I., et al. (2005). The involvement of the aspartate triad of the active center in all catalytic activities of multisubunit RNA polymerase. *Nucleic Acids Res.* 33, 4202–4211. doi:10.1093/nar/gki688

Sousa, R. (1996). Structural and mechanistic relationships between nucleic acid polymerases. *Trends Biochem. Sci.* 21, 186–190. doi:10.1016/S0968-0004(96)10023-2

Sousa, R. (1997). Fundamental aspects of T7 RNA polymerase structure and mechanism. *Nucleic Acids Mol. Biol.* 1–14, 1–14. doi:10.1007/978-3-642-60691-5_1

Sousa, R. (2013). "T7 RNA polymerase," in *Encyclopedia of biological chemistry*. Second Edition (Elsevier Inc.), 355–359. doi:10.1016/B978-0-12-378630-2.00267-X

Sousa, R., Chung, Y. J., Rose, J. P., and Wang, B. C. (1993). Crystal structure of bacteriophage T7 RNA polymerase at 3.3 A resolution. *Nature* 364, 593–599. doi:10.1038/364593A0

Sousa, R., and Jendrisak, J. J. (2000). *Methods for using mutant RNA polymerases with reduced discrimination between non-canonical and canonical nucleoside triphosphates*. US patent 6107037. Madison, WI, United States: Epicentre Technologies Corporation, assignee.

Sousa, R., and Mukherjee, S. (2003). T7 RNA polymerase. *Prog. Nucleic Acid. Res. Mol. Biol.* 73, 1–41. doi:10.1016/S0079-6603(03)01001-8

Sousa, R., Rose, J. P., Je Chung, Y., Lafer, E. M., and Wang, B.-C. (1989). Single crystals of bacteriophage T7 RNA polymerase. *Proteins* 5, 266–270. doi:10.1002/PROT.340050403

Stano, N. M., Levin, M. K., and Patel, S. S. (2002). The +2 NTP binding drives open complex formation in T7 RNA polymerase. *J. Biol. Chem.* 277, 37292–37300. doi:10.1074/jbc.M201600200

Stano, N. M., and Patel, S. S. (2002). The intercalating beta-hairpin of T7 RNA polymerase plays a role in promoter DNA melting and in stabilizing the melted DNA for efficient RNA synthesis. *J. Mol. Biol.* 315, 1009–1025. doi:10.1006/jmbi.2001.5313

Steitz, T. A. (2009). The structural changes of T7 RNA polymerase from transcription initiation to elongation. *Curr. Opin. Struct. Biol.* 19, 683–690. doi:10.1016/J.SBI.2009.09.001

Stevens, A. (1960). Incorporation of the adenine ribonucleotide into RNA by cell fractions from *E. coli* B. *Biochem. Biophys. Res. Commun.* 3, 92–96. doi:10.1016/0006-291X(60)90110-8

Stover, N. M., Ganko, K., and Braatz, R. D. (2024). Mechanistic modeling of *in vitro* transcription incorporating effects of magnesium pyrophosphate crystallization. *Biotechnol. Bioeng.* 121, 2636–2647. doi:10.1002/BIT.28699

Streit, W., Han, Y., and Kinfu, B. (2023). inventors; Universität Hamburg, assignee; Novel single-subunit RNA polymerase. *Eur. Pat. Appl. EP 4 265 718 A1*.

Striedner, G., and Wittwer, A. (2019). inventors; Boehringer Ingelheim RCV GmbH and Co KG, assignee; Transcription terminator sequences. US patent 9745588 B2.

Strothkamp, R. E., Oakley, J. L., and Coleman, J. E. (1980). Promoter melting by T7 ribonucleic acid polymerase as detected by single-stranded endonuclease digestion. *Biochemistry* 19, 1074–1080. doi:10.1021/bi00547a005

Studier, F. W., and Moffatt, B. A. (1986). Use of bacteriophage T7 RNA polymerase to direct selective high-level expression of cloned genes. *J. Mol. Biol.* 189, 113–130. doi:10.1016/0022-2836(86)90385-2

Sugiyama, A., Nishiya, Y., Kawakami, B., and bioMerieus, B. V. (2009). assignee; RNA polymerase mutants with increased thermostability. US patent 7507567 B2.

Summers, W. C., and Siegel, R. B. (1970). Transcription of late phage RNA by T7 RNA polymerase. *Nature* 228 (5277 228), 1160–1162. doi:10.1038/2281160a0

Sydow, J. F., and Cramer, P. (2009). RNA polymerase fidelity and transcriptional proofreading. *Curr. Opin. Struct. Biol.* 19, 732–739. doi:10.1016/J.SBI.2009.10.009

Szabó, G. T., Mahiny, A. J., and Vlatkovic, I. (2022). COVID-19 mRNA vaccines: platforms and current developments. *Mol. Ther.* 30, 1850–1868. doi:10.1016/J.YMTHE.2022.02.016

Tabor, S., and Richardson, C. C. (1985). A bacteriophage T7 RNA polymerase/promoter system for controlled exclusive expression of specific genes. *Proc. Natl. Acad. Sci. U. S. A.* 82, 1074–1078. doi:10.1073/PNAS.82.4.1074

Tang, G. Q., Nandakumar, D., Bandwar, R. P., Lee, K. S., Roy, R., Ha, T., et al. (2014). Relaxed rotational and scrunching changes in P266L mutant of T7 RNA polymerase reduce short abortive RNAs while delaying transition into elongation. *PLoS One* 9, e91859. doi:10.1371/JOURNAL.PONE.0091859

Tang, G. Q., and Patel, S. S. (2006a). Rapid binding of T7 RNA polymerase is followed by simultaneous bending and opening of the promoter DNA. *Biochemistry* 45, 4947–4956. doi:10.1021/bi052292s

Tang, G. Q., and Patel, S. S. (2006b). T7 RNA polymerase-induced bending of promoter DNA is coupled to DNA opening. *Biochemistry* 45, 4936–4946. doi:10.1021/BI0522910

Tang, G. Q., Roy, R., Bandwar, R. P., Ha, T., and Patel, S. S. (2009). Real-time observation of the transition from transcription initiation to elongation of the RNA polymerase. *Proc. Natl. Acad. Sci. U. S. A.* 106, 22175–22180. doi:10.1073/pnas.0906979106

Tang, G. Q., Roy, R., Ha, T., and Patel, S. S. (2008). Transcription initiation in a single-subunit RNA polymerase proceeds through DNA scrunching and rotation of the N-terminal subdomains. *Mol. Cell.* 30, 567–577. doi:10.1016/J.MOLCEL.2008.04.003

Temiakov, D., Patlan, V., Anikin, M., McAllister, W. T., Yokoyama, S., and Vassylyev, D. G. (2004). Structural basis for substrate selection by T7 RNA polymerase. *Cell.* 116, 381–391. doi:10.1016/S0092-8674(04)00059-5

Theis, K., Gong, P., and Martin, C. T. (2004). Topological and conformational analysis of the initiation and elongation complex of t7 RNA polymerase suggests a new twist. *Biochemistry* 43, 12709–12715. doi:10.1021/BI0486987

Thomen, P., Lopez, P. J., Bockelmann, U., Guillerez, J., Dreyfus, M., and Heslot, F. (2008). T7 RNA polymerase studied by force measurements varying cofactor concentration. *Biophys. J.* 95, 2423–2433. doi:10.1529/BIOPHYSJ.107.125096

Thompson, K., Wang, Y., and Zhu, S. (2022). RNA polymerase for synthesis of modified RNA.

Triana-Alonso, F. J., Dabrowski, M., Wadzack, J., and Nierhaus, K. H. (1995). Self-coded 3′-extension of run-off transcripts produces aberrant products during *in vitro* transcription with T7 RNA polymerase. *J. Biol. Chem.* 270, 6298–6307. doi:10.1074/JBC.270.11.6298

Újvári, A., and Martin, C. T. (1996). Thermodynamic and kinetic measurements of promoter binding by T7 RNA polymerase. *Biochemistry* 35, 14574–14582. doi:10.1021/BI961165G

Újvári, A., and Martin, C. T. (1997). Identification of a minimal binding element within the T7 RNA polymerase promoter. *J. Mol. Biol.* 273, 775–781. doi:10.1006/JMBI.1997.1350

Újvári, A., and Martin, C. T. (2000). Evidence for DNA bending at the T7 RNA polymerase promoter. *J. Mol. Biol.* 295, 1173–1184. doi:10.1006/JMBI.1999.3418

Vahia, A. V., and Martin, C. T. (2011). Direct tests of the energetic basis of abortive cycling in transcription. *Biochemistry* 50, 7015–7022. doi:10.1021/BI200620Q

van de Berg, D., Kis, Z., Behmer, C. F., Samnuan, K., Blakney, A. K., Kontoravdi, C., et al. (2021). Quality by design modelling to support rapid RNA vaccine production against emerging infectious diseases. *npj Vaccines* 6 (1 6), 65–10. doi:10.1038/s41541-021-00322-7

Villemain, J., Guajardo, R., and Sousa, R. (1997). Role of open complex instability in kinetic promoter selection by bacteriophage T7 RNA polymerase. *J. Mol. Biol.* 273, 958–977. doi:10.1006/JMBI.1997.1358

Wang, Y., Ramakrishnan, D., De Fougerolles, A., and Whoriskey, S. (2017). inventors; ModernaTX, Inc. assignee; Enzymes and polymerases for the synthesis of RNA. US patent 9790531 B2.

Weiss, S. B., and Gladstone, L. (1959). A mammalian system for the incorporation of cytidine triphosphate into ribonucleic acid. *J. Am. Chem. Soc.* 81, 4118–4119. doi:10.1021/ja01524a087

Weston, B. F., Kuzmine, I., and Martin, C. T. (1997). Positioning of the start site in the initiation of transcription by bacteriophage T7 RNA polymerase. *J. Mol. Biol.* 272, 21–30. doi:10.1006/JMBI.1997.1199

Whitley, J., Zwolinski, C., Denis, C., Maughan, M., Hayles, L., Clarke, D., et al. (2022). Development of mRNA manufacturing for vaccines and therapeutics: mRNA platform requirements and development of a scalable production process to support early phase clinical trials. *Transl. Res.* 242, 38–55. doi:10.1016/J.TRSL.2021.11.009

Wochner, A., Roos, T., Ketterer, T. inventors, and CureVac, A. G. (2015). assignee; Methods and means for enhancing RNA production. *WO 2015/188933 Al.*

Woody, A. Y. M., Eaton, S. S., Osumi-Davis, P. A., and Woody, R. W. (1996). Asp537 and Asp812 in bacteriophage T7 RNA polymerase as metal ion-binding sites studied by EPR, flow-dialysis, and transcription. *Biochemistry* 35, 144–152. doi:10.1021/BI952037F

Woychik, N. A., and Young, R. A. (1990). RNA polymerase II: subunit structure and function. *Trends Biochem. Sci.* 15, 347–351. doi:10.1016/0968-0004(90)90074-L

Wu, H., Wei, T., Yu, B., Cheng, R., Huang, F., Lu, X., et al. (2021). A single mutation attenuates both the transcription termination and RNA-dependent RNA polymerase activity of T7 RNA polymerase. *RNA Biol.* 18, 451–466. doi:10.1080/15476286.2021.1954808

Wu, M. Z., Asahara, H., Tzertzinis, G., and Roy, B. (2020). Synthesis of low immunogenicity RNA with high-temperature *in vitro* transcription. *RNA* 26, 345–360. doi:10.1261/RNA.073858.119

Xia, H., Yu, B., Jiang, Y., Cheng, R., Lu, X., Wu, H., et al. (2022). Psychrophilic phage VSW-3 RNA polymerase reduces both terminal and full-length dsRNA byproducts in *in vitro* transcription. *RNA Biol.* 19, 1130–1142. doi:10.1080/15476286.2022.2139113

Xu, D. K., Tung, K. C., Baffert, S., Greener, A., and Zieler, H. (2020). inventors; Primordial Genetics, Inc, assignee; Methods and compositions for manufacturing polynucleotides. WO 2020/243026 A1.

Yang, W., Lee, J. Y., and Nowotny, M. (2006). Making and breaking nucleic acids: two-Mg2+-ion catalysis and substrate specificity. *Mol. Cell.* 22, 5–13. doi:10.1016/J.MOLCEL.2006.03.013

Yin, Y. W., and Steitz, T. A. (2002). Structural basis for the transition from initiation to elongation transcription in T7 RNA polymerase. *Science* 298, 1387–1395. doi:10.1126/science.1077464

Yin, Y. W., and Steitz, T. A. (2004). The structural mechanism of translocation and helicase activity in T7 RNA polymerase. *Cell.* 116, 393–404. doi:10.1016/S0092-8674(04)00120-5

Yisraeli, J. K., and Melton, D. A. (1989). Synthesis of long, capped transcripts *in vitro* by SP6 and T7 RNA polymerases. *Methods Enzymol.* 180, 42–50. doi:10.1016/0076-6879(89)80090-4

You, L., Omollo, E. O., Yu, C., Mooney, R. A., Shi, J., Shen, L., et al. (2023). Structural basis for intrinsic transcription termination. *Nature* 613, 783–789. doi:10.1038/s41586-022-05604-1

Young, J. S., Ramirez, W. F., and Davis, R. H. (1997). Modeling and optimization of a batch process for *in vitro* RNA production. *Biotechnol. Bioeng.* 56, 210–220. doi:10.1002/(SICI)1097-0290(19971020)56:2<210::AID-BIT10>3.0.CO;2-K

Zhou, Y., Navaroli, D. M., Enuameh, M. S., and Martin, C. T. (2007). Dissociation of halted T7 RNA polymerase elongation complexes proceeds via a forward-translocation mechanism. *Proc. Natl. Acad. Sci. U. S. A.* 104, 10352–10357. doi:10.1073/pnas.0606306104

Zhu, B., Hernandez, A., Tan, M., Wollenhaupt, J., Tabor, S., and Richardson, C. C. (2015). Synthesis of 2′-fluoro RNA by Syn5 RNA polymerase. *Nucleic Acids Res.* 43, e94. doi:10.1093/NAR/GKV367

Zhu, B., Tabor, S., Raytcheva, D. A., Hernandez, A., King, J. A., and Richardson, C. C. (2013). The RNA polymerase of marine cyanophage Syn5. *J. Biol. Chem.* 288, 3545–3552. doi:10.1074/JBC.M112.442350

Zhu, B., Tabor, S., and Richardson, C. C. (2014). Syn5 RNA polymerase synthesizes precise run-off RNA products. *Nucleic Acids Res.* 42, e33. doi:10.1093/NAR/GKT1193

Zhu, Y., Zhu, L., Wang, X., and Jin, H. (2022). RNA-based therapeutics: an overview and prospectus. *Cell. Death and Dis.* 13 (7 13), 644–715. doi:10.1038/s41419-022-05075-2

Frontiers in
Molecular Biosciences

Explores biological processes in living organisms on a molecular scale

Focuses on the molecular mechanisms underpinning and regulating biological processes in organisms across all branches of life.

Discover the latest Research Topics

See more →

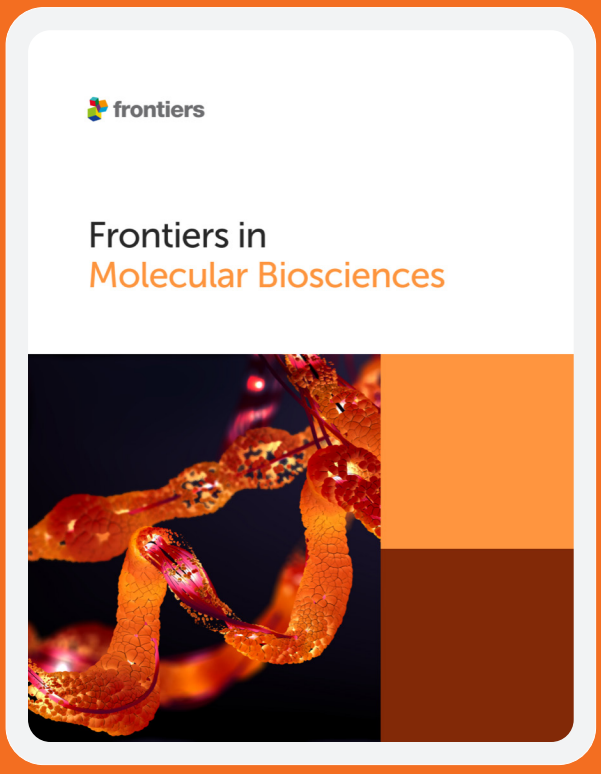

Frontiers

Avenue du Tribunal-Fédéral 34
1005 Lausanne, Switzerland
frontiersin.org

Contact us

+41 (0)21 510 17 00
frontiersin.org/about/contact